Quantum computation: quantum process and characterization

Xiao Xue

QuTech, Delft University of Technology, Lorentzweg 1, 2628 CJ Delft, Netherlands

Quantum computers look like…

AMO

Solid-state

From google

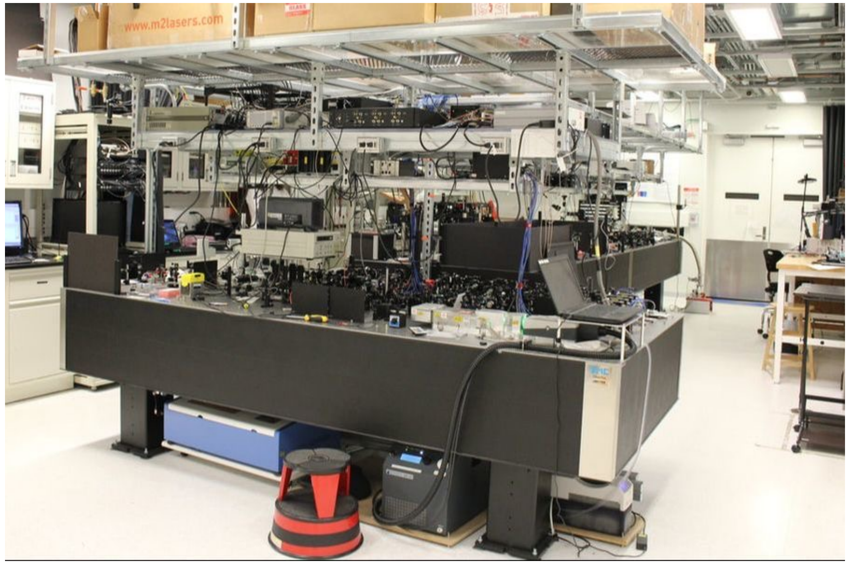

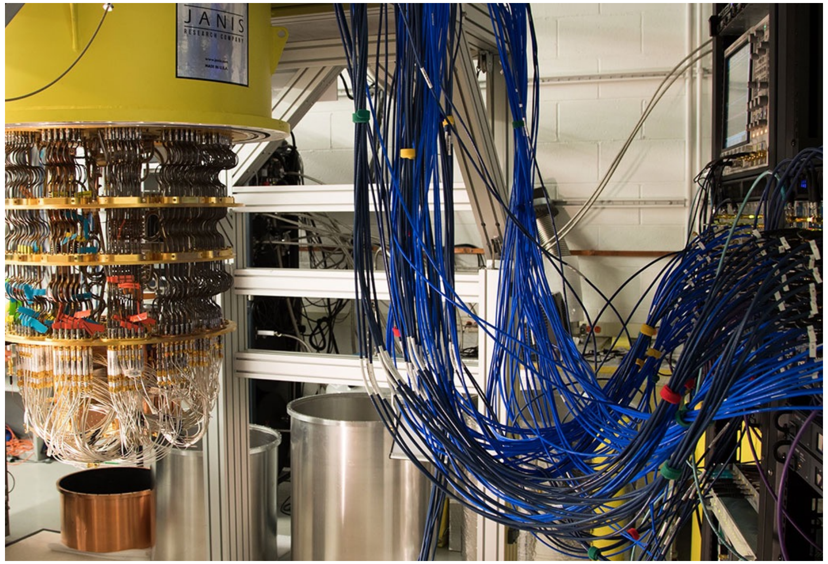

Quantum bit

Spin

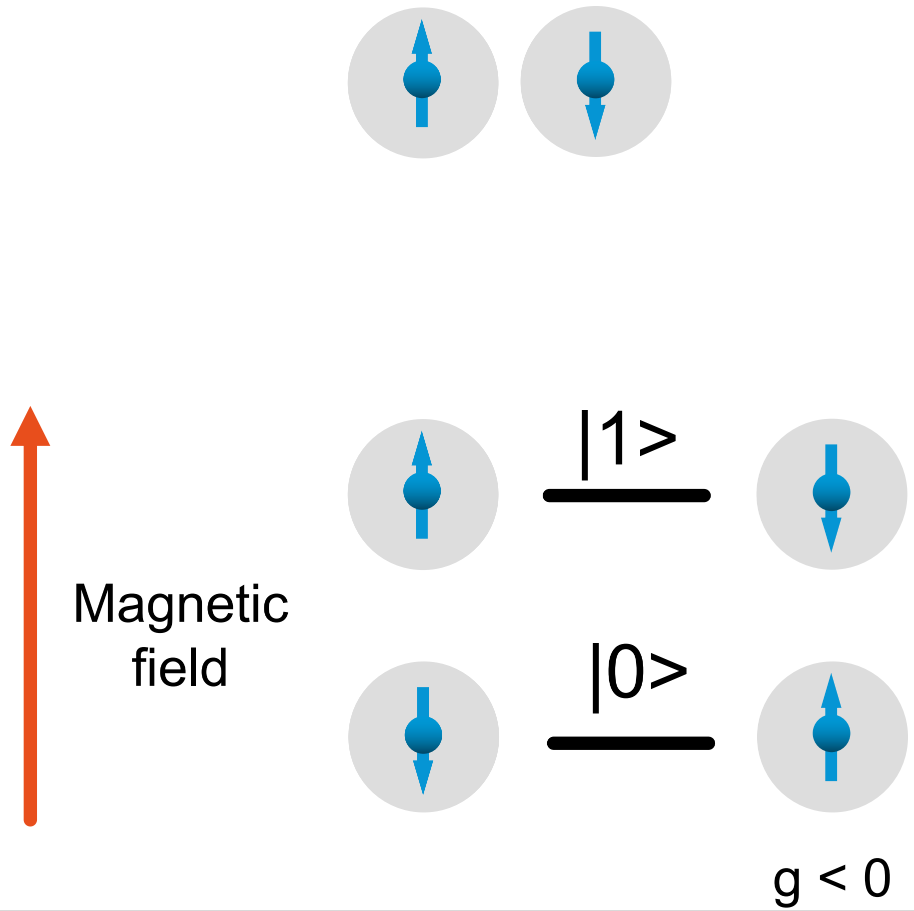

Oscillator

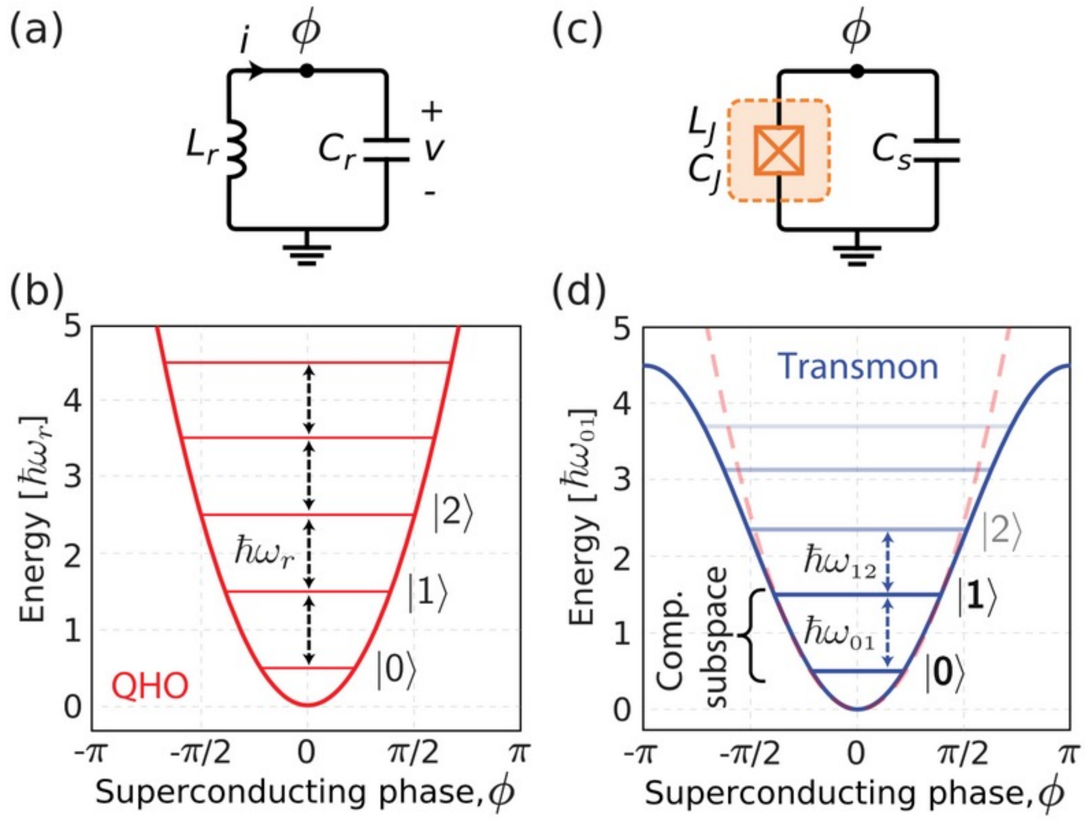

QuTech

Pure state and mixed state

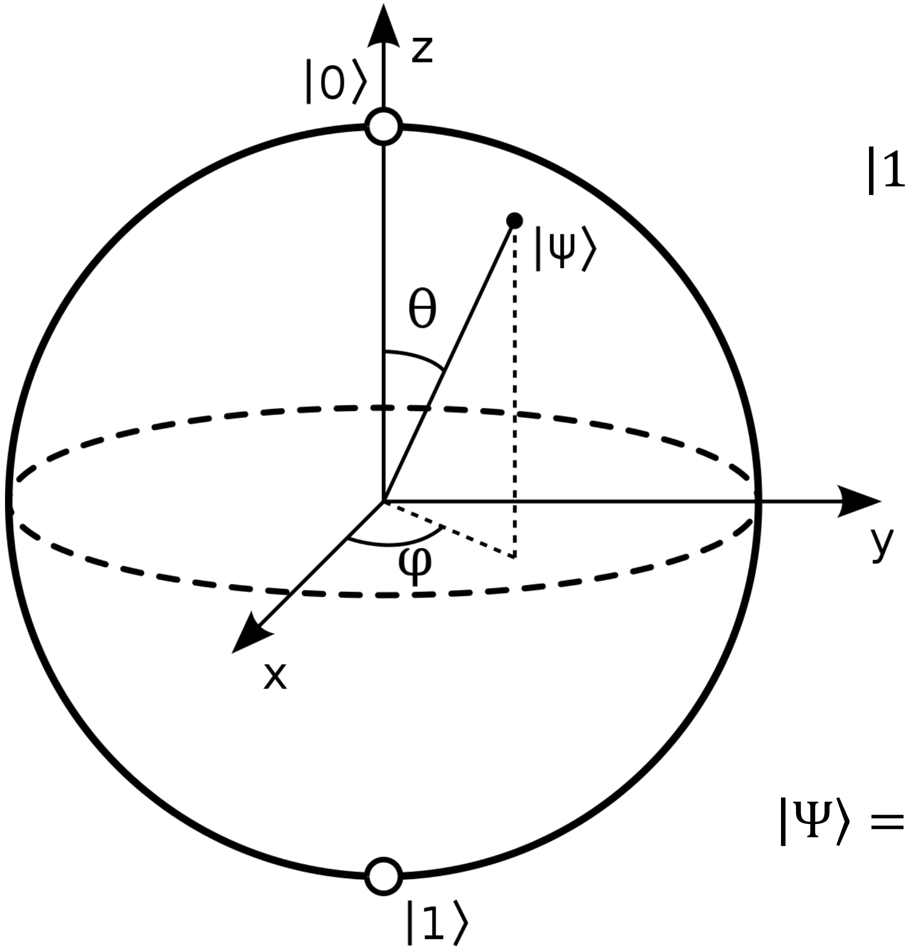

$$|0\rangle = \begin{pmatrix} 1 \\ 0 \end{pmatrix} \qquad \langle 0| = (1\ 0) \qquad \rho_0 = |0\rangle\langle 0| = \begin{pmatrix} 1 & 0 \\ 0 & 0 \end{pmatrix}$$

$$|1\rangle = \begin{pmatrix} 0 \\ 1 \end{pmatrix} \qquad \langle 1| = (0\ 1) \qquad \rho_1 = |1\rangle\langle 1| = \begin{pmatrix} 0 & 0 \\ 0 & 1 \end{pmatrix}$$

$$|+x\rangle = \frac{|0\rangle + |1\rangle}{\sqrt{2}} = \frac{1}{\sqrt{2}}\begin{pmatrix} 1 \\ 1 \end{pmatrix} \qquad \rho_{+x} = |+x\rangle\langle +x| = \frac{1}{2}\begin{pmatrix} 1 & 1 \\ 1 & 1 \end{pmatrix}$$

$$|\Psi\rangle = \cos\theta\,|0\rangle + \sin\theta\, e^{i\varphi}|1\rangle = a|0\rangle + b|1\rangle \qquad \rho_\Psi = |\Psi\rangle\langle\Psi| = \begin{pmatrix} a^2 & ab^* \\ a^*b & b^2 \end{pmatrix}$$

QuTech

Pure state and mixed state

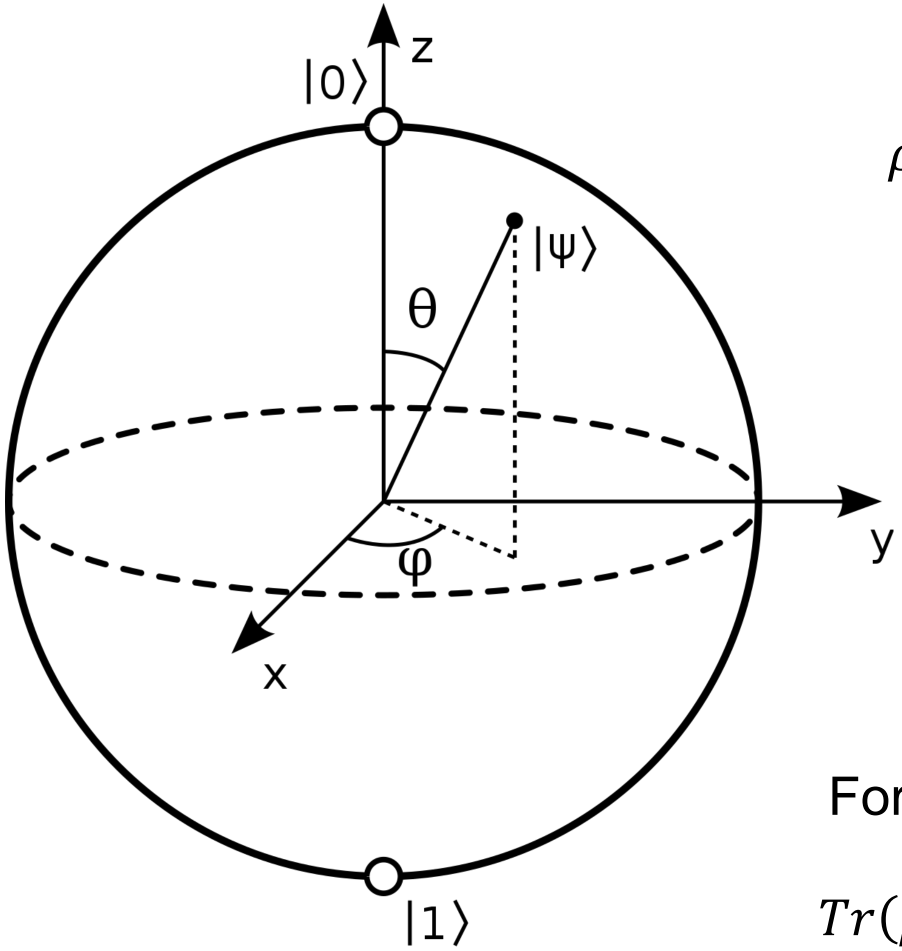

$$\rho_\Psi = |\Psi\rangle\langle\Psi| = \begin{pmatrix} a^2 & ab^* \\ a^*b & b^2 \end{pmatrix}$$

$$\rho_{\Psi'} = \begin{pmatrix} a^2 & 0 \\ 0 & b^2 \end{pmatrix} \qquad \rho_{max-mixed} = \frac{|0\rangle\langle 0| + |1\rangle\langle 1|}{2} = \frac{1}{2}\begin{pmatrix} 1 & 0 \\ 0 & 1 \end{pmatrix}$$

For any ρ:

$$Tr(\rho) = a^2 + b^2 \equiv 1$$

For a pure state ρ: $Tr(\rho^2) = 1$

For a mixed state ρ: $Tr(\rho^2) < 1$

QuTech

Relaxation and dephasing

Figure: Nielsen & Chuang

$$\rho_\Psi = |\Psi\rangle\langle\Psi| = \begin{pmatrix} a^2 & ab^* \\ a^* b & b^2 \end{pmatrix}$$

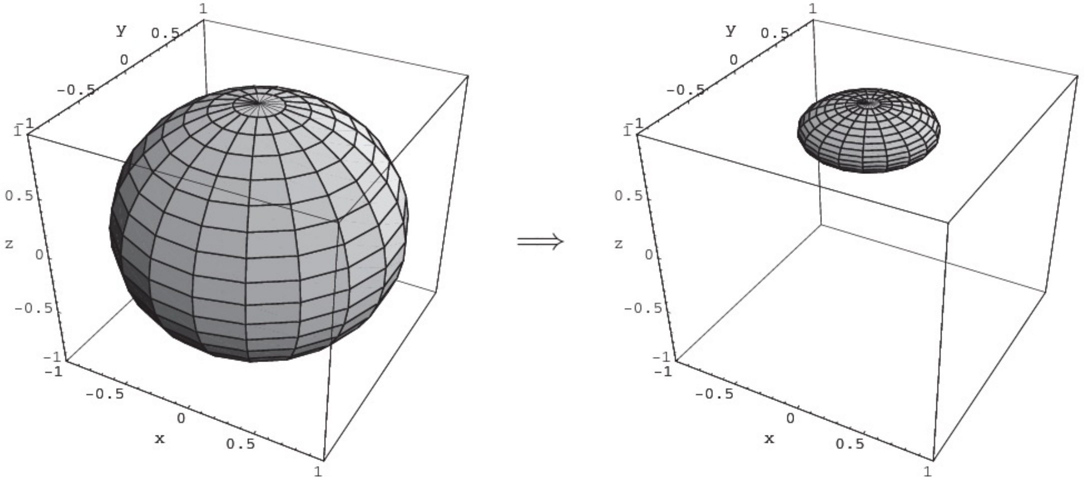

Relaxation:

$$\rho_{\Psi'} = \begin{pmatrix} 1 - e^{-\frac{t}{T_1}}(1 - a^2) & e^{-\frac{t}{2T_1}} ab^* \\ e^{-\frac{t}{2T_1}} a^* b & e^{-\frac{t}{T_1}} b^2 \end{pmatrix} \rightarrow \begin{pmatrix} 1 & 0 \\ 0 & 0 \end{pmatrix}$$

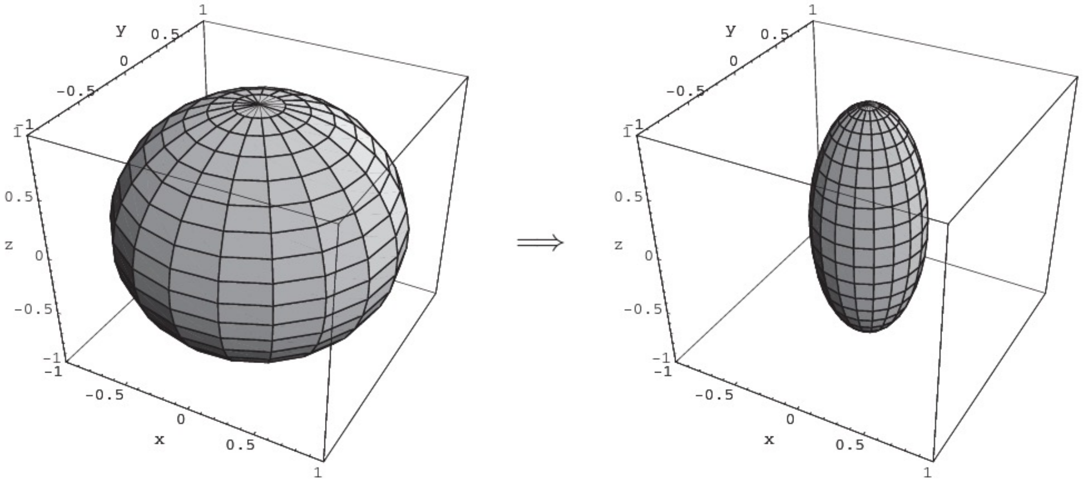

Dephasing:

$$\rho_{\Psi'} = \begin{pmatrix} a^2 & e^{-\left(\frac{t}{T_2}\right)^{(2)}} ab^* \\ e^{-\left(\frac{t}{T_2}\right)^{(2)}} a^* b & b^2 \end{pmatrix} \rightarrow \begin{pmatrix} a^2 & 0 \\ 0 & b^2 \end{pmatrix}$$

Depolarizing process

$$\rho_\Psi = |\Psi\rangle\langle\Psi| = \begin{pmatrix} a^2 & ab^* \\ a^*b & b^2 \end{pmatrix}$$

Figure: Nielsen & Chuang

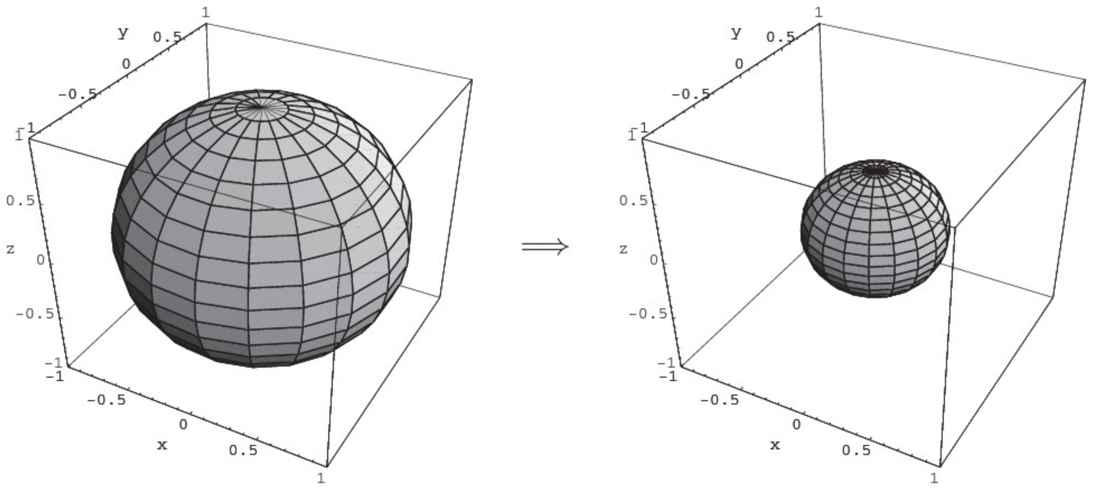

Depolarizing:

$$\rho_{\Psi'} = \begin{pmatrix} \frac{1}{2} - e^{-\frac{t}{T_d}}(\frac{1}{2} - a^2) & e^{-\frac{t}{T_d}} ab^* \\ e^{-\frac{t}{T_d}} a^*b & \frac{1}{2} - e^{-\frac{t}{T_d}}(\frac{1}{2} - b^2) \end{pmatrix} \to \begin{pmatrix} \frac{1}{2} & 0 \\ 0 & \frac{1}{2} \end{pmatrix}$$

QuTech

State Fidelity

$$F = Tr(\rho_{mea}\rho_{ref})$$

Consider $\rho_{ref} = |\alpha\rangle\langle\alpha|$ as a pure state

$$F = Tr(\rho_{mea}\rho_{ref}) = \langle\alpha|\rho_{mea}|\alpha\rangle$$

Recap:

For a pure state ρ: $Tr(\rho^2) = 1$

For a mixed state ρ: $Tr(\rho^2) < 1$

Measurement fidelity

Let's think about it a bit further…

$$F = Tr(\rho_{mea}\rho_{ref}) = \langle\alpha|\rho_{mea}|\alpha\rangle$$

Consider ρ_{mea} as known, but $\rho_{ref} = |\alpha\rangle\langle\alpha|$ is unknown…
F gives "measurement fidelity".

Faulty measurement: $\rho_{ref} = p_\alpha|\alpha\rangle\langle\alpha| + p_\beta|\beta\rangle\langle\beta|$

$$F = Tr\left(\rho_{mea}\rho_{ref}\right) = p_\alpha\langle\alpha|\rho_{mea}|\alpha\rangle + p_\beta\langle\beta|\rho_{mea}|\beta\rangle$$

Positive operator-valued measurement

For an ideal POVM, $E_m = |\psi_m\rangle\langle\psi_m|$, with $|\psi_m\rangle$ often chosen to be the eigenstates.

Outcome: $P_m = Tr(|\psi\rangle\langle\psi| E_m)$

Single qubit: $\{E_0 = |0\rangle\langle 0|,\ E_1 = |1\rangle\langle 1|\}$

Measurement error:

$$\{E_0^e = (1-\epsilon_0)|0\rangle\langle 0| + \epsilon_1 |1\rangle\langle 1|,\ E_1^e = \epsilon_0 |0\rangle\langle 0| + (1-\epsilon_1)|1\rangle\langle 1|\}$$

ϵ_0 and ϵ_1 are the readout errors of $|0\rangle$ and $|1\rangle$ states

Measurement fidelity:

$$F_0 = Tr(E_0^e E_0) = Tr(E_0^e |0\rangle\langle 0|) = 1 - \epsilon_0$$
$$F_1 = Tr(E_1^e E_1) = Tr(E_1^e |1\rangle\langle 1|) = 1 - \epsilon_1$$

Quantum operation/channel

Consider a state

$$\rho = |\alpha\rangle\langle\alpha|$$

$$\rho = p_\alpha|\alpha\rangle\langle\alpha| + p_\beta|\beta\rangle\langle\beta|$$

Define a quantum operation/channel

$$\Lambda(\rho) = K|\alpha\rangle\langle\alpha|K^\dagger$$

$$\Lambda(\rho) = p_\alpha K|\alpha\rangle\langle\alpha|K^\dagger + p_\beta K|\beta\rangle\langle\beta|K^\dagger$$

Sometimes the channel is a statistical mixture of multiple operators

$$\Lambda(\rho) = K_1\rho K_1^\dagger + K_2\rho K_2^\dagger + \cdots$$

$$K_1^\dagger K_1 + K_2^\dagger K_2 + \cdots = I$$

defined as Kraus operators

Dephasing channel

$$\rho = \begin{pmatrix} a & c^* \\ c & b \end{pmatrix}$$

If ρ completely loses its phase information:

$$\mathcal{K}_{dephase_{max}}(\rho) = \frac{\rho + Z\rho Z}{2} = a|0\rangle\langle 0| + b|1\rangle\langle 1|$$

The Kraus operators are $I/\sqrt{2}$ and $Z/\sqrt{2}$.

Often ρ loses its phase with probability (error rate) $1 - p$

$$\mathcal{K}_{dephase}(\rho) = p\rho + \frac{1-p}{2}(\rho + Z\rho Z) = \frac{1+p}{2}\rho + \frac{1-p}{2}Z\rho Z$$

with the Kraus operators $\sqrt{(1+p)/2}I$ and $\sqrt{(1-p)/2}Z$.

Depolarizing channel

If ρ completely loses its information in all directions:

$$\rho = \begin{pmatrix} a & c^* \\ c & b \end{pmatrix}$$

$$\mathcal{K}_{dep_{max}}(\rho) = \frac{\rho + X\rho X + Y\rho Y + Z\rho Z}{4} = I$$

The Kraus operators of the maximum-depolarizing channel $\mathcal{K}_{dep_{max}}$ are $I/2$, $X/2$, $Y/2$, and $Z/2$.

Often ρ loses its information with probability (error rate) $1-p$:

$$\begin{aligned} \mathcal{K}_{dep}(\rho) &= p\rho + (1-p)I/2 \\ &= \frac{1+3p}{4}\rho + \frac{1-p}{4}(X\rho X + Y\rho Y + Z\rho Z) \end{aligned}$$

Here, the Kraus operators are $\sqrt{1+3p}I/2$, $\sqrt{1-p}X/2$, $\sqrt{1-p}Y/2$, and $\sqrt{1-p}Z/2$.

Recurring $\mathcal{K}_{dep}$ will finally fully depolarize the state:

$$\lim_{N\to\infty} \mathcal{K}_{dep}{}^{N}(\rho) = \mathcal{K}_{dep_{max}}(\rho) = I.$$

QuTech

Kraus operator in Pauli basis: χ-matrix

$$P_0 = I$$
$$P_1 = X$$
$$P_2 = Y$$
$$P_3 = Z$$

$$\Lambda(\rho) = K_1 \rho K_1^\dagger + K_2 \rho K_2^\dagger + \cdots$$

$$K_i = \sum_{j=1}^{d^2} a_{ij} P_j$$

$$= \sum_{j,k=1}^{d^2} \chi_{jk} P_j \rho P_k$$

Single qubit case:

$$K_i = a_{i0} I + a_{i1} X + a_{i2} Y + a_{i3} Z$$

$$\chi_{jk} = \sum_i a_{ij} a_{ik}^*$$

χ-matrix is a $d^2 \times d^2$ dimensional complex matrix

Examples of χ-matrices

$$\mathcal{K}_{dephase}(\rho) = p\rho + \frac{1-p}{2}(\rho + Z\rho Z) = \frac{1+p}{2}\rho + \frac{1-p}{2}Z\rho Z$$

$$\mathcal{K}_{dep}(\rho) = p\rho + (1-p)I = \frac{1+3p}{4}\rho + \frac{1-p}{4}(X\rho X + Y\rho Y + Z\rho Z)$$

$$\chi_{dephasing} = \begin{array}{cc} \begin{array}{cccc} I & X & Y & Z \end{array} & \\ \begin{pmatrix} \frac{1+p}{2} & 0 & 0 & 0 \\ 0 & 0 & 0 & 0 \\ 0 & 0 & 0 & 0 \\ 0 & 0 & 0 & \frac{1-p}{2} \end{pmatrix} & \begin{array}{c} I \\ X \\ Y \\ Z \end{array} \end{array}$$

$$\chi_{dep} = \begin{pmatrix} \frac{1+3p}{4} & 0 & 0 & 0 \\ 0 & \frac{1-p}{4} & 0 & 0 \\ 0 & 0 & \frac{1-p}{4} & 0 \\ 0 & 0 & 0 & \frac{1-p}{4} \end{pmatrix}$$

- χ-matrix is a matrix of coefficients.
- It's always symmetric.

QuTech

Examples of χ-matrices

It's difficult to use χ-matrix for multiple operations

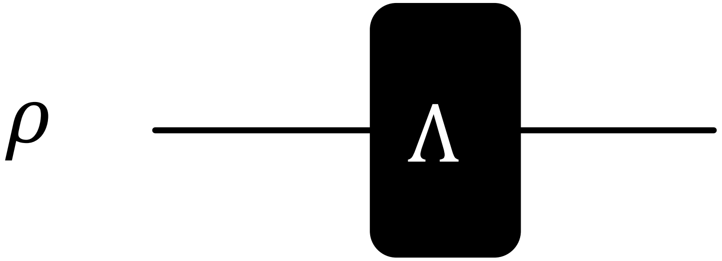

$$\Lambda(\rho) = \sum_{j,k=1}^{d^2} \chi_{jk} P_j \rho P_k$$

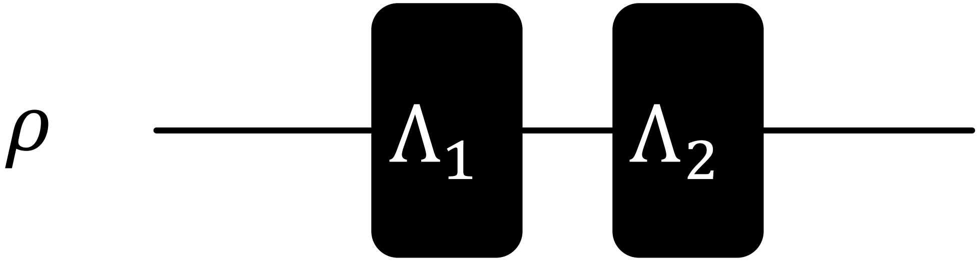

$$\Lambda_2(\Lambda_1(\rho)) = \sum_{p,q=1}^{d^2} \chi^2_{pq} P_p \Big(\sum_{j,k=1}^{d^2} \chi^1_{jk} P_j \rho P_k \Big) P_q$$

Superoperators

Revision of state fidelity

Operators can be decomposed into Paulis

$$K_i = a_{i0}I + a_{i1}X + a_{i2}Y + a_{i3}Z$$

Same for density matrices (density operators)

$$\rho = \frac{1}{2}(I + r_x X + r_y Y + r_z Z)$$

Now let's imagine performing POVM:

On the x-axis: $F = Tr(\rho X) = r_x$

On the y-axis: $F = Tr(\rho Y) = r_y$

On the z-axis: $F = Tr(\rho Z) = r_z$

$$Tr(IX) = 0$$
$$Tr(YX) = 0$$
$$Tr(ZX) = 0$$
$$Tr(XX) = 1$$

Quantum state tomography

How to perform POVM along the x-axis?

$$X = \begin{pmatrix} 0 & 1 \\ 1 & 0 \end{pmatrix} = \frac{1}{2}\begin{pmatrix} 1 & 1 \\ 1 & 1 \end{pmatrix} - \frac{1}{2}\begin{pmatrix} 1 & -1 \\ -1 & 1 \end{pmatrix}$$

$$= \frac{1}{2}(|0\rangle + |1\rangle)(\langle 0| + \langle 1|) - \frac{1}{2}(|0\rangle - |1\rangle)(\langle 0| - \langle 1|)$$

$$r_x = Tr(\rho X) = Tr(\rho \rho_{0+1}) - Tr(\rho \rho_{0-1})$$

$$r_y = Tr(\rho Y) = Tr(\rho \rho_{0+i1}) - Tr(\rho \rho_{0-i1})$$

$$r_z = Tr(\rho Z) = Tr(\rho \rho_0) - Tr(\rho \rho_1)$$

$$F = Tr(\rho \rho_{ref})$$

- ρ_{ref} must be a physical state (not necessarily a pure state), with $Tr(\rho_{ref}) = 1$.
- Pauli matrices cannot be prepared as they are not density matrices of any physical state.

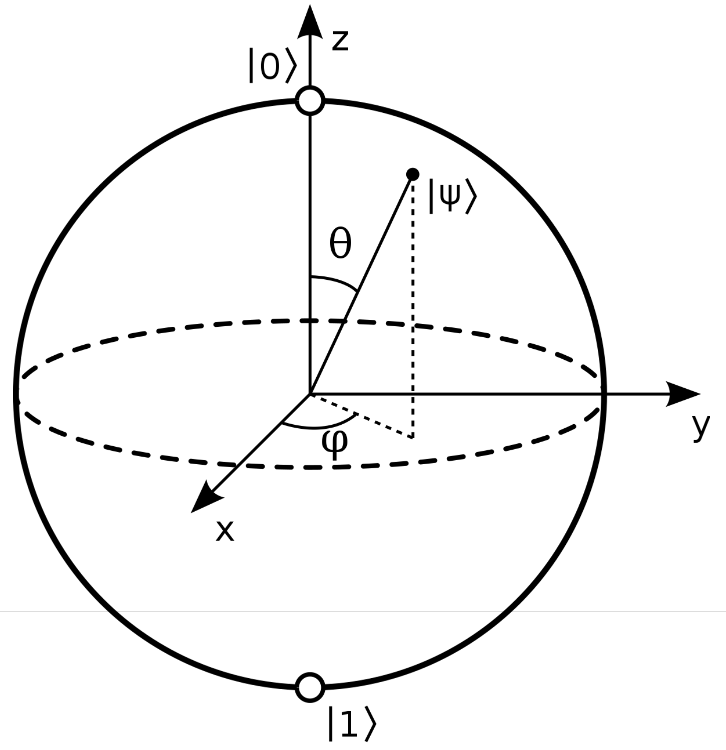

QuTech

Super-operator and Pauli transfer matrix

$$\rho = \frac{1}{2}(I + r_x X + r_y Y + r_z Z) \stackrel{\text{def}}{=} \begin{pmatrix} Tr(\rho I) \\ Tr(\rho X) \\ Tr(\rho Y) \\ Tr(\rho Z) \end{pmatrix} = \begin{pmatrix} 1 \\ r_x \\ r_y \\ r_z \end{pmatrix}$$

- A $d \times d$ dimensional density matrix can be represented now as a d^2 dimensional vector.
- The first entry is always 1 : Trace preserving (TP).
- The other entries correspond to the projection onto x/y/z axes in Bloch sphere.

QuTech

Pauli transfer matrix (quantum channel)

$$\Lambda_{ij}^{\mathcal{K}} = \frac{1}{d} Tr[P_i \mathcal{K}(P_j)]$$

$$\rho = \frac{1}{2}(I + r_x X + r_y Y + r_z Z) \stackrel{\text{def}}{=} \begin{pmatrix} 1 \\ r_x \\ r_y \\ r_z \end{pmatrix}$$

PTM is expressed in the Pauli operator basis, meaning it can be directly applied to a state vector in the super-operator format

$$|\rho\rangle\rangle = \frac{1}{\sqrt{2}} \begin{pmatrix} Tr(\rho I) \\ Tr(\rho X) \\ Tr(\rho Y) \\ Tr(\rho Z) \end{pmatrix} = \frac{1}{\sqrt{2}} \begin{pmatrix} 1 \\ r_x \\ r_y \\ r_z \end{pmatrix}$$

$$\{I/\sqrt{d},\ X/\sqrt{d},\ Y/\sqrt{d},\ Z/\sqrt{d}\}$$

$$\langle\langle E| = \frac{1}{\sqrt{2}}(1, Tr(EX), Tr(EY), Tr(EZ))$$

State/measurement fidelity:

$$Tr[E\rho] = \langle\langle E|\rho\rangle\rangle$$

QuTech

Examples of PTMs

$$\mathcal{K}_{dephase}(\rho) = p\rho + \frac{1-p}{2}(\rho + Z\rho Z)$$
$$= \frac{1+p}{2}\rho + \frac{1-p}{2} Z\rho Z$$

$$\mathcal{K}_{dep}(\rho) = p\rho + (1-p)I$$
$$= \frac{1+3p}{4}\rho + \frac{1-p}{4}(X\rho X + Y\rho Y + Z\rho Z)$$

Output density operator

$$\Lambda_{dephasing} = \begin{array}{cc} \begin{pmatrix} 1 & 0 & 0 & 0 \\ 0 & p & 0 & 0 \\ 0 & 0 & p & 0 \\ 0 & 0 & 0 & 1 \end{pmatrix} & \begin{array}{c} I \\ X \\ Y \\ Z \end{array} \\ \begin{array}{cccc} I & X & Y & Z \end{array} & \end{array}$$

Input density operator

$$\Lambda_{dep} = \begin{pmatrix} 1 & 0 & 0 & 0 \\ 0 & p & 0 & 0 \\ 0 & 0 & p & 0 \\ 0 & 0 & 0 & p \end{pmatrix}$$

- χ-matrix is a matrix of input-output.
- It's not always symmetric.

PTM Application

Density operator

$$\mathcal{K}_{dephase}(\rho) = p\rho + \frac{1-p}{2}(\rho + Z\rho Z)$$
$$= \frac{1+p}{2}\rho + \frac{1-p}{2}Z\rho Z$$

$$\rho = \frac{1}{2}\left(I + r_x X + r_y Y + r_z Z\right)$$

Output density operator

Super operator

$$\begin{array}{c|c} \Lambda_{dephasing} = \begin{pmatrix} 1 & 0 & 0 & 0 \\ 0 & p & 0 & 0 \\ 0 & 0 & p & 0 \\ 0 & 0 & 0 & 1 \end{pmatrix} & \begin{matrix} I \\ X \\ Y \\ Z \end{matrix} \\ \begin{matrix} \quad\quad\quad\quad I & X & Y & Z \end{matrix} & \end{array}$$

Input density operator

Directly multiply

$$|\rho\rangle\rangle = \frac{1}{\sqrt{2}}\begin{pmatrix} 1 \\ r_x \\ r_y \\ r_z \end{pmatrix}$$

Pauli transfer matrix

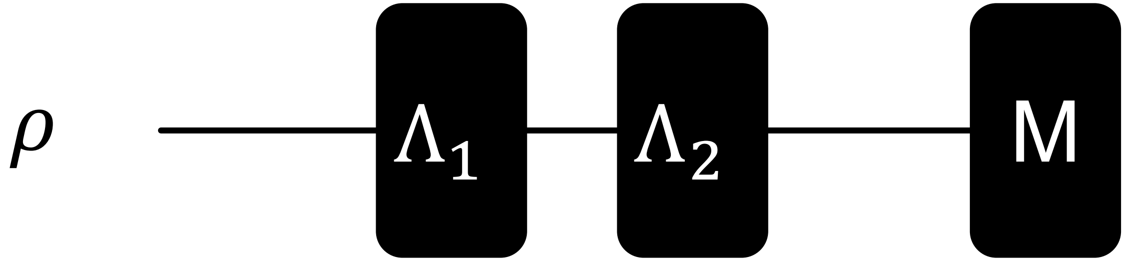

$$\Lambda_2(\Lambda_1(\rho)) = \sum_{p,q=1}^{d^2} \chi_{pq}^2 P_p \Big(\sum_{j,k=1}^{d^2} \chi_{jk}^1 P_j \rho P_k \Big) P_q$$

A complete circuit:

$$p_E = \langle\langle E | \mathcal{G}_N ... \mathcal{G}_2 \mathcal{G}_1 | \rho \rangle\rangle$$

where $\mathcal{G}_i$ is the PTM of the i-th gate.

$$\Lambda_2(\Lambda_1(\rho)) \Rightarrow G_2 G_1 | \rho \gg$$

G_i is the PTM of Λ_i

Average gate fidelity:

$$F_g = \frac{Tr[\mathcal{G}^{-1}\mathcal{G}^{ideal}] + d}{d(d+1)}$$

Example: controlled-Z gate

Red: +1
Blue: -1

Red: +1/4
Blue: -1/4

Pauli transfer matrix

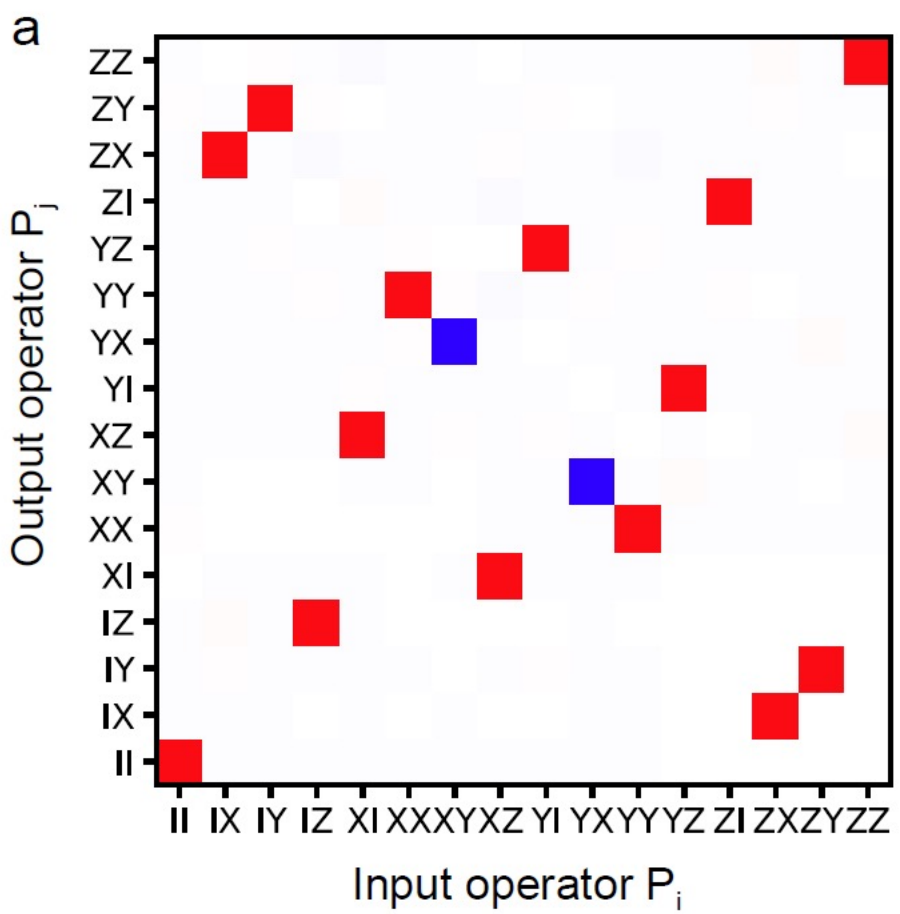

χ-matrix

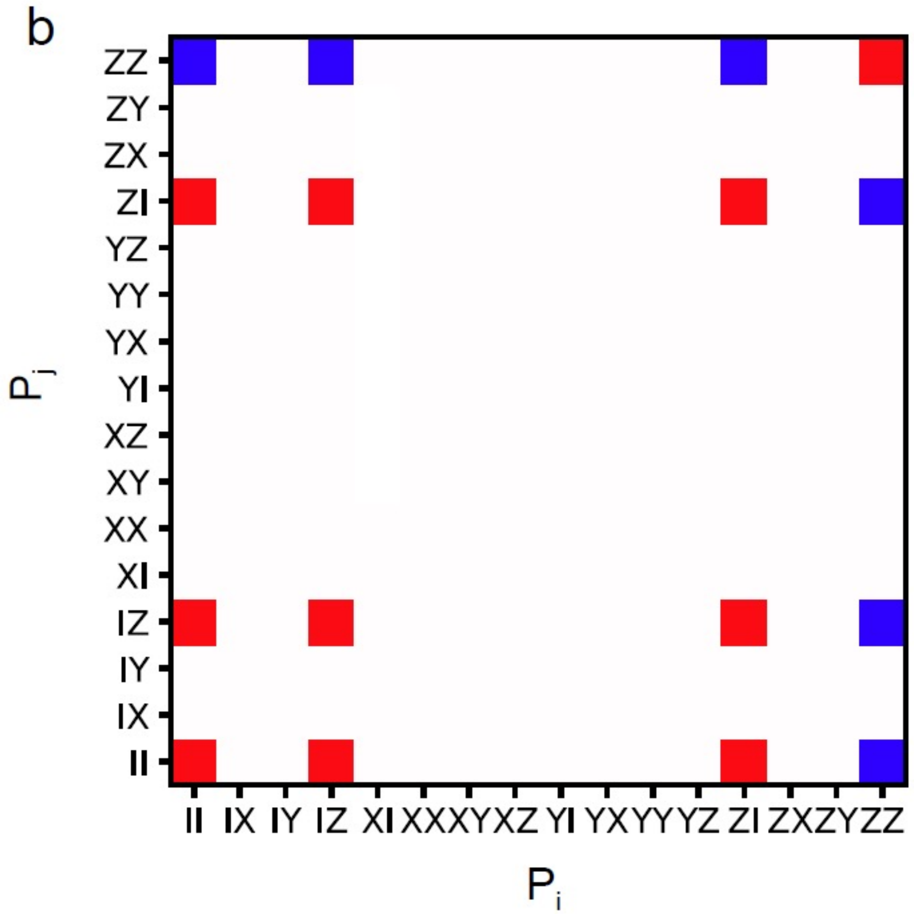

Characterize a quantum process

Quantum process tomography

Measure the complete input-output correlation.

Intuition: prepare different states in experiment, and apply the operator on them, followed by measurement of the outcome states.

This can be described in either χ-matrix or PTM, but PTM is easier.

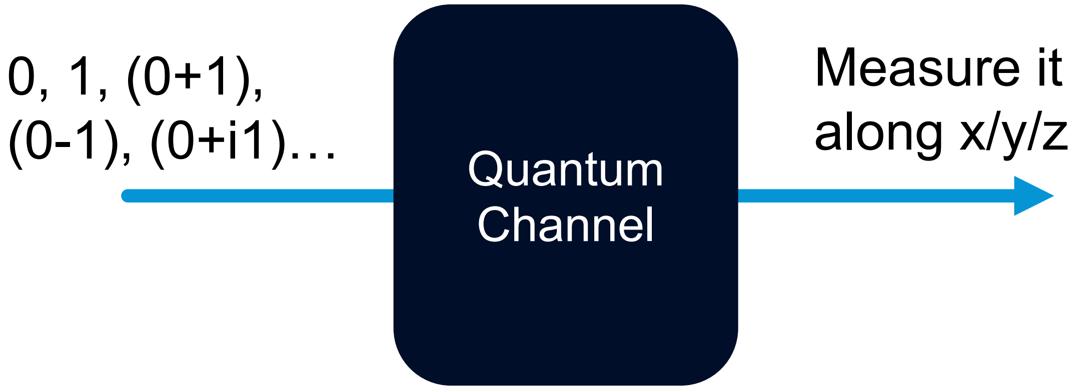

Quantum process tomography

Entry of a PTM

$$\mathcal{G}_{ij} = \langle\langle P_i|\mathcal{G}|P_j\rangle\rangle$$

$$\begin{aligned}\mathcal{G}_{13} &= \frac{1}{2}\langle\langle X|\mathcal{G}|Z\rangle\rangle \\ &= \frac{1}{2}\langle\langle \rho_{\hat{x}} - \rho_{-\hat{x}}|\mathcal{G}|\rho_0 - \rho_1\rangle\rangle\end{aligned}$$

$$\rho_{\pm\hat{x}} \longrightarrow \frac{1}{\sqrt{2}}(|0\rangle \pm |1\rangle)$$

$$\rho_{0/1} \longrightarrow |0\rangle \,/\, |1\rangle$$

Therefore, a PTM $\mathcal{G}$ can be fully reconstructed by preparing and measuring the state in all the basis states $\{\rho_0, \rho_1, \rho_{\hat{x}}, \rho_{-\hat{x}}, \rho_{\hat{y}}, \rho_{-\hat{y}}\}$ before and after the process respectively.

QuTech

Quantum process tomography

Entry of a PTM

$$\mathcal{G}_{ij} = \langle\langle P_i|\mathcal{G}|P_j\rangle\rangle$$

$$\begin{aligned}\mathcal{G}_{13} =& \frac{1}{2}\langle\langle X|\mathcal{G}|Z\rangle\rangle \\ =& \frac{1}{2}\langle\langle \rho_{\hat{x}} - \rho_{-\hat{x}}|\mathcal{G}|\rho_0 - \rho_1\rangle\rangle\end{aligned}$$

$$\rho_{\pm\hat{x}} \longrightarrow \frac{1}{\sqrt{2}}(|0\rangle \pm |1\rangle)$$

$$\rho_{0/1} \longrightarrow |0\rangle \,/\, |1\rangle$$

Limitation:

State Preparation and Measurement (SPAM) error

Solution:

- Gate set tomography
- Randomized benchmarking
- Others…

QuTech

Randomized benchmarking

Depolarizing error

$$F_g = \frac{Tr[\mathcal{G}^{-1}\mathcal{G}^{ideal}] + d}{d(d+1)}$$

$$\mathcal{G} = \Lambda\mathcal{G}^{ideal}$$

Error: Λ

$$Tr[\mathcal{G}^{-1}\mathcal{G}^{ideal}] = Tr[\Lambda^{-1}I]$$

Coherent error: rotation angle, rotation axis…
Incoherent error: dephasing, depolarizing, relaxation…

Assumptions:

1. The error of a gate does not depend on the previous gates (Markovian).
2. The error of different gates are the same (gate-independent).

(Imagine the error is decoherence and all gates are equally long)

Depolarizing error

"Twirling" a small error with unitary operators.

$$\Lambda_{dep} \approx \sum_i \mathcal{U}_i^\dagger \Lambda \mathcal{U}_i$$

In reality, we can use Clifford group to efficiently approximate the twirling process

$$\Lambda_{dep}(\rho) = \frac{1}{K} \sum_{k=1}^{K} \mathcal{C}_k^\dagger \Lambda \mathcal{C}_k |\rho\rangle\rangle$$

$$\Lambda_{dep}(\rho) = p\rho + (1-p)I/d$$

Fidelity of error Λ:

$$F_\Lambda = F_{\Lambda_{dep}}$$

$$F_\Lambda = Tr[\Lambda^{-1} I] = p + \frac{1-p}{d}$$

Clifford gates

Clifford stabilizes Paulis:

$$C_k P_i C_k^{\dagger} = P_j$$

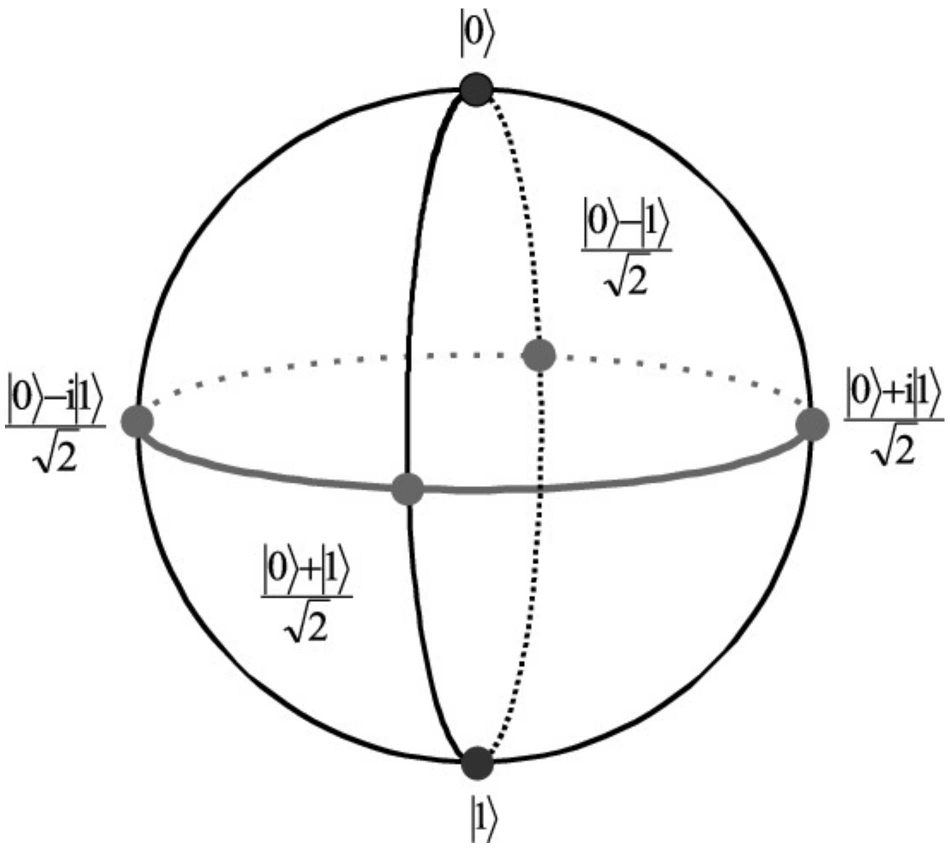

Single qubit Cliffords	
Paulis	I
	X
	Y
	Y, X
$2\pi/3$ rotations	X/2, Y/2
	X/2, -Y/2
	-X/2, Y/2
	-X/2, -Y/2
	Y/2, X/2
	Y/2, -X/2
	-Y/2, X/2
	-Y/2, -X/2
$\pi/2$ rotations	X/2
	-X/2
	Y/2
	-Y/2
	-X/2, Y/2, X/2
	-X/2, -Y/2, X/2
Hadamard-like	X, Y/2
	X, -Y/2
	Y, X/2
	Y, -X/2
	X/2, Y/2, X/2
	-X/2, Y/2, -X/2

QuTech

R. Barends et al., Nature 2014

Clifford gates

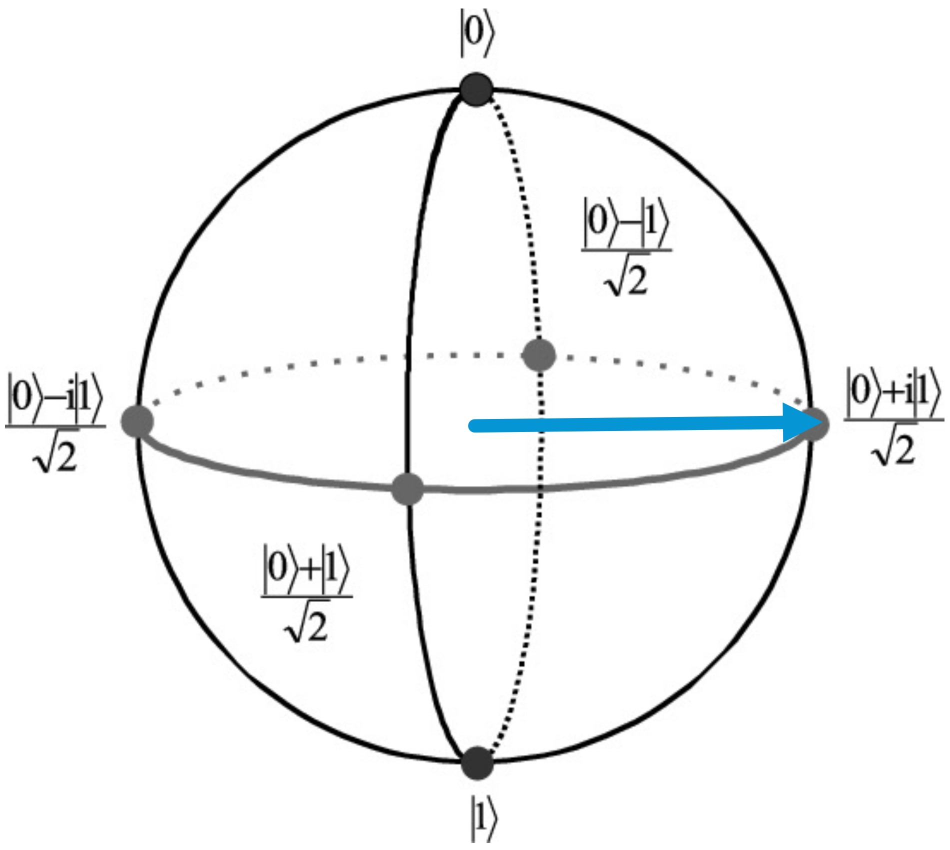

Single qubit Cliffords	
Paulis	I
	X
	Y
	Y, X
$2\pi/3$ rotations	X/2, Y/2
	X/2, -Y/2
	-X/2, Y/2
	-X/2, -Y/2
	Y/2, X/2
	Y/2, -X/2
	-Y/2, X/2
	-Y/2, -X/2
$\pi/2$ rotations	X/2
	-X/2
	Y/2
	-Y/2
	-X/2, Y/2, X/2
	-X/2, -Y/2, X/2
Hadamard-like	X, Y/2
	X, -Y/2
	Y, X/2
	Y, -X/2
	X/2, Y/2, X/2
	-X/2, Y/2, -X/2

Clifford gates

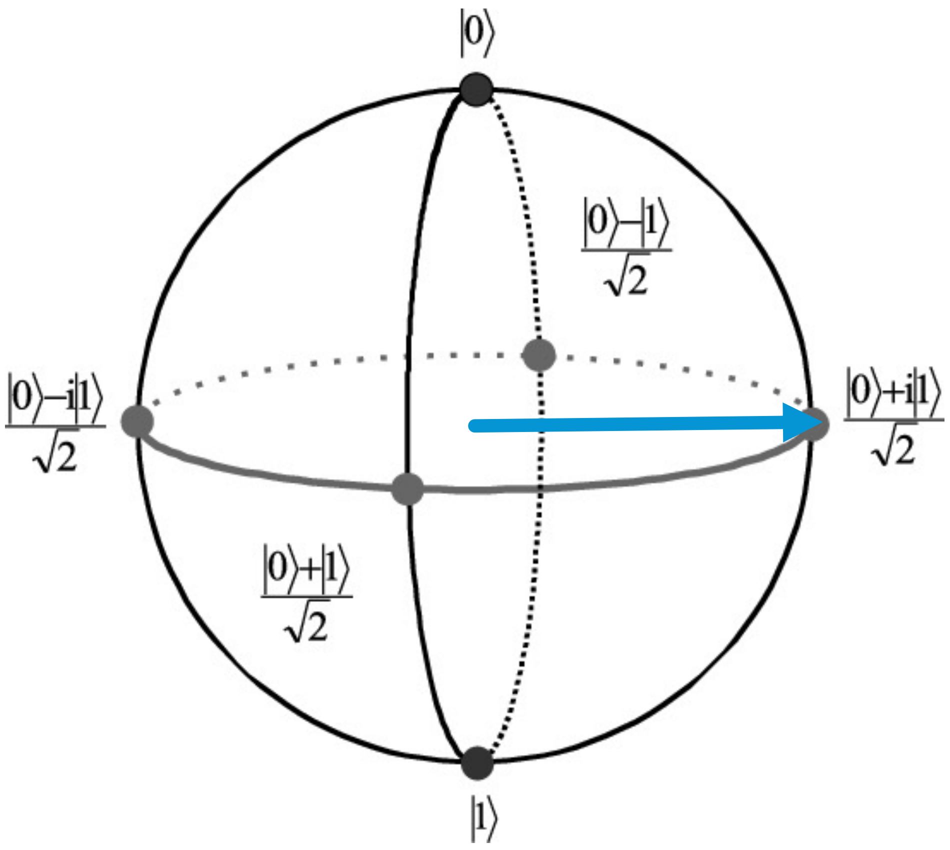

Single qubit Cliffords	
Paulis	I
	X
	Y
	Y, X
$2\pi/3$ rotations	X/2, Y/2
	X/2, -Y/2
	-X/2, Y/2
	-X/2, -Y/2
	Y/2, X/2
	Y/2, -X/2
	-Y/2, X/2
	-Y/2, -X/2
$\pi/2$ rotations	X/2
	-X/2
	Y/2
	-Y/2
	-X/2, Y/2, X/2
	-X/2, -Y/2, X/2
Hadamard-like	X, Y/2
	X, -Y/2
	Y, X/2
	Y, -X/2
	X/2, Y/2, X/2
	-X/2, Y/2, -X/2

Clifford gates

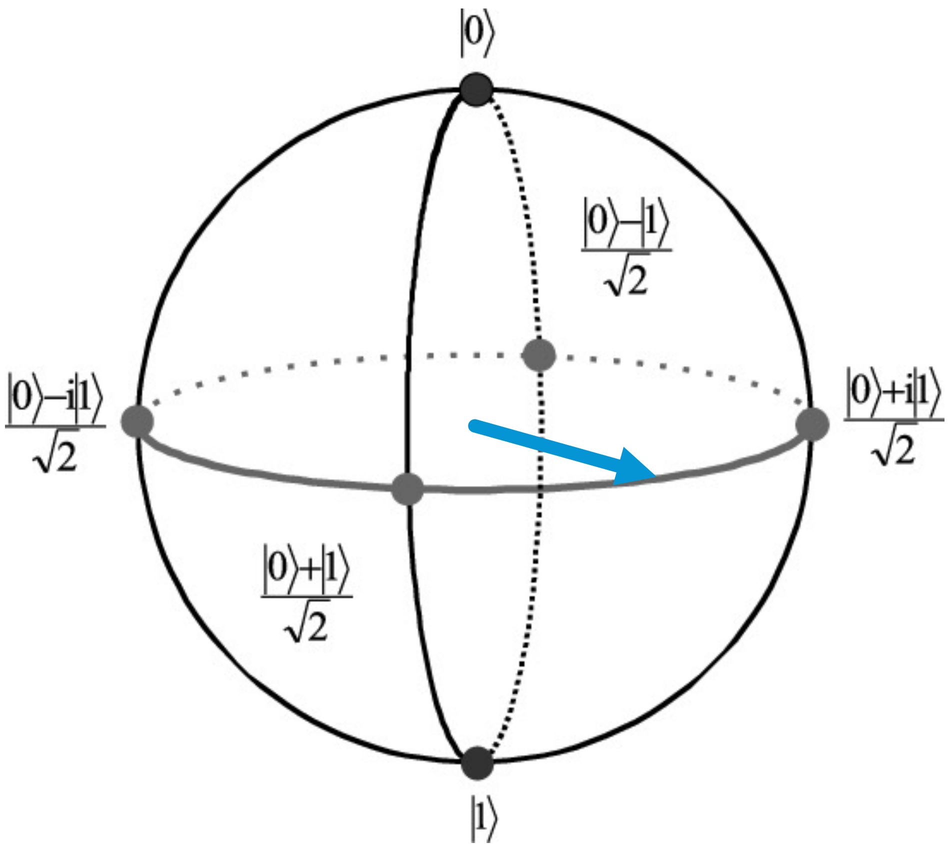

Single qubit Cliffords	
Paulis	I
	X
	Y
	Y, X
$2\pi/3$ rotations	X/2, Y/2
	X/2, -Y/2
	-X/2, Y/2
	-X/2, -Y/2
	Y/2, X/2
	Y/2, -X/2
	-Y/2, X/2
	-Y/2, -X/2
$\pi/2$ rotations	X/2
	-X/2
	Y/2
	-Y/2
	-X/2, Y/2, X/2
	-X/2, -Y/2, X/2
Hadamard-like	X, Y/2
	X, -Y/2
	Y, X/2
	Y, -X/2
	X/2, Y/2, X/2
	-X/2, Y/2, -X/2

Clifford gates

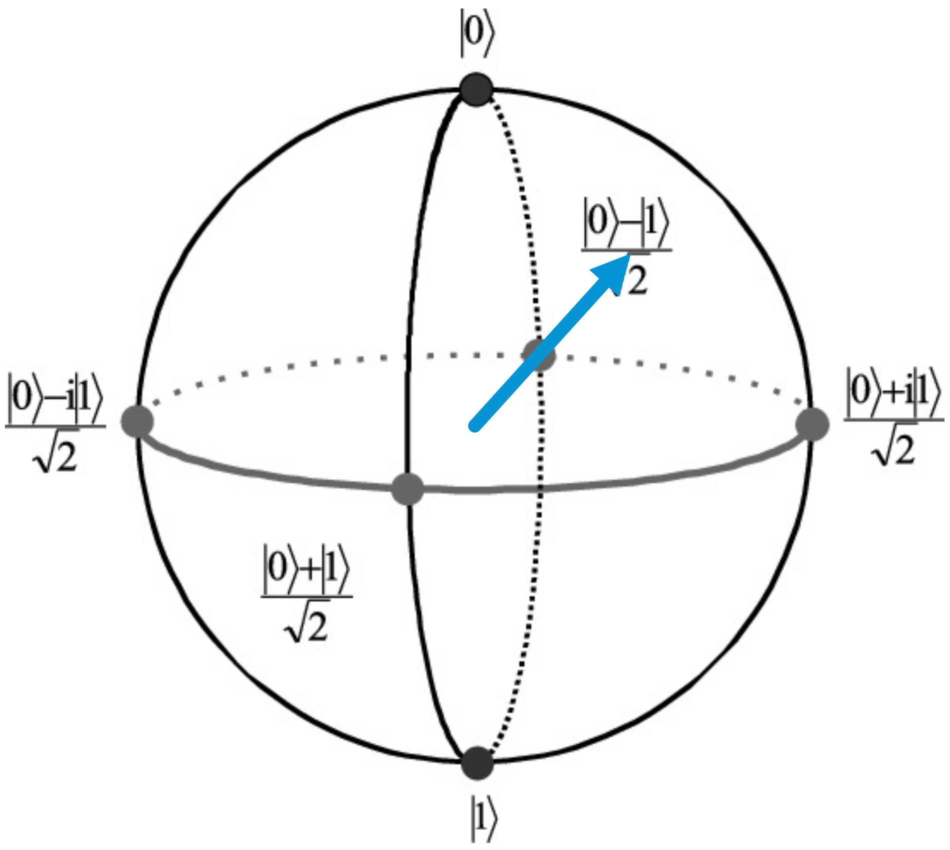

Single qubit Cliffords	
Paulis	I
	X
	Y
	Y, X
$2\pi/3$ rotations	X/2, Y/2
	X/2, -Y/2
	-X/2, Y/2
	-X/2, -Y/2
	Y/2, X/2
	Y/2, -X/2
	-Y/2, X/2
	-Y/2, -X/2
$\pi/2$ rotations	X/2
	-X/2
	Y/2
	-Y/2
	-X/2, Y/2, X/2
	-X/2, -Y/2, X/2
Hadamard-like	X, Y/2
	X, -Y/2
	Y, X/2
	Y, -X/2
	X/2, Y/2, X/2
	-X/2, Y/2, -X/2

Concatenated depolarizing channel

1-step depolarizing channel:

$$\Lambda_{dep}(\rho) = \frac{1}{K}\sum_{k=1}^{K} \mathcal{C}_k^\dagger \Lambda \mathcal{C}_k |\rho\rangle\rangle$$

Outcome state:

$$\Lambda_{dep}(\rho) = p\rho + (1-p)I/d$$

m-step depolarizing channel :

$$\Lambda_{dep}^m(\rho) = \int_{k_m,\ldots,k_2,k_1} \frac{1}{K^m} \mathcal{C}_{k_m}^\dagger \Lambda \mathcal{C}_{k_m} \ldots \mathcal{C}_{k_2}^\dagger \Lambda \mathcal{C}_{k_2} \mathcal{C}_{k_1}^\dagger \Lambda \mathcal{C}_{k_1} |\rho\rangle\rangle$$

Outcome state:

$$\Lambda_{dep}^m(\rho) = \Lambda_{dep_m} \ldots \Lambda_{dep_2} \Lambda_{dep_1} |\rho\rangle\rangle = p^m \rho + \frac{1-p^m}{d} I,$$

QuTech

Randomized benchmarking

Sequence fidelity:

$$\begin{aligned} F_{seq}(\rho_\psi) &= Tr[E_\psi \Lambda^m(\rho_\psi)] \\ &= Tr[E_\psi(\rho_\psi - \frac{I}{d})]p^m + Tr[E_\psi \frac{I}{d}] \\ &= Ap^m + B. \end{aligned}$$

Fidelity of error Λ:

$$F_\Lambda = Tr[\Lambda^{-1} I] = p + \frac{1-p}{d}$$

Randomized benchmarking

$$\Lambda_{dep}^{m}(\rho) = \int_{k_m,\dots,k_2,k_1} \frac{1}{K^m} \mathcal{C}_{k_m}^{\dagger} \Lambda \mathcal{C}_{k_m} \dots \mathcal{C}_{k_2}^{\dagger} \Lambda \mathcal{C}_{k_2} \mathcal{C}_{k_1}^{\dagger} \Lambda \mathcal{C}_{k_1} |\rho\rangle\rangle \longrightarrow \begin{aligned} \Lambda_{dep}^{m}(\rho) &= \Lambda_{dep_m} \dots \Lambda_{dep_2} \Lambda_{dep_1} |\rho\rangle\rangle \\ &= p^m \rho + \frac{1-p^m}{d} I, \end{aligned}$$

Now let $\mathcal{C}_{l_1} = \mathcal{C}_{k_1}, \mathcal{C}_{l_2} = \mathcal{C}_{k_2}\mathcal{C}_{k_1}^{\dagger}, \dots,$ and $\mathcal{C}_{l_m} = \mathcal{C}_{k_m}\mathcal{C}_{k_{m-1}}^{\dagger}$, and let $\mathcal{C}_{l_{m+1}} = \mathcal{C}_{k_m}^{\dagger} = (\mathcal{C}_{l_m} \dots \mathcal{C}_{l_2} \cdot \mathcal{C}_{l_1})^{\dagger}$, the sequence can be written as:

$$\Lambda_{dep}^{m}(\rho) = \int_{l_m,\dots,l_2,l_1} \frac{1}{K^m} \mathcal{C}_{l_{m+1}} \Lambda \mathcal{C}_{l_m} \dots \Lambda \mathcal{C}_{l_2} \Lambda \mathcal{C}_{l_1} |\rho\rangle\rangle.$$

Recall: $\mathcal{G} = \Lambda \mathcal{G}^{ideal}$

RB measures Clifford gate fidelity.

Randomized benchmarking

$$\Lambda_{dep}^{m}(\rho) = \int_{l_m,\ldots,l_2,l_1} \frac{1}{K^m} \mathcal{C}_{l_{m+1}} \Lambda \mathcal{C}_{l_m} \ldots \Lambda \mathcal{C}_{l_2} \Lambda \mathcal{C}_{l_1} |\rho\rangle\rangle.$$

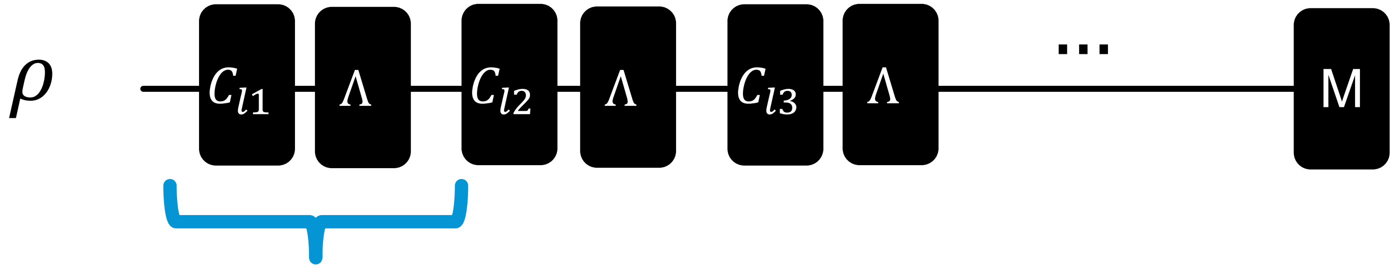

A real Clifford gate
with error

$$\begin{aligned}\Lambda_{dep}^{m}(\rho) &= \Lambda_{dep_m} \ldots \Lambda_{dep_2} \Lambda_{dep_1} |\rho\rangle\rangle \\ &= p^m \rho + \frac{1 - p^m}{d} I,\end{aligned}$$

$$F_\Lambda = Tr[\Lambda^{-1} I] = p + \frac{1-p}{d}$$

Randomized benchmarking

$$\Lambda_{dep}^{m}(\rho) = \int_{k_m,\ldots,k_2,k_1} \frac{1}{K^m} \mathcal{C}_{k_m}^{\dagger} \Lambda \mathcal{C}_{k_m} \ldots \mathcal{C}_{k_2}^{\dagger} \Lambda \mathcal{C}_{k_2} \mathcal{C}_{k_1}^{\dagger} \Lambda \mathcal{C}_{k_1} |\rho\rangle\rangle \longrightarrow$$

$$\begin{aligned}\Lambda_{dep}^{m}(\rho) &= \Lambda_{dep_m} \ldots \Lambda_{dep_2} \Lambda_{dep_1} |\rho\rangle\rangle \\ &= p^m \rho + \frac{1-p^m}{d} I,\end{aligned}$$

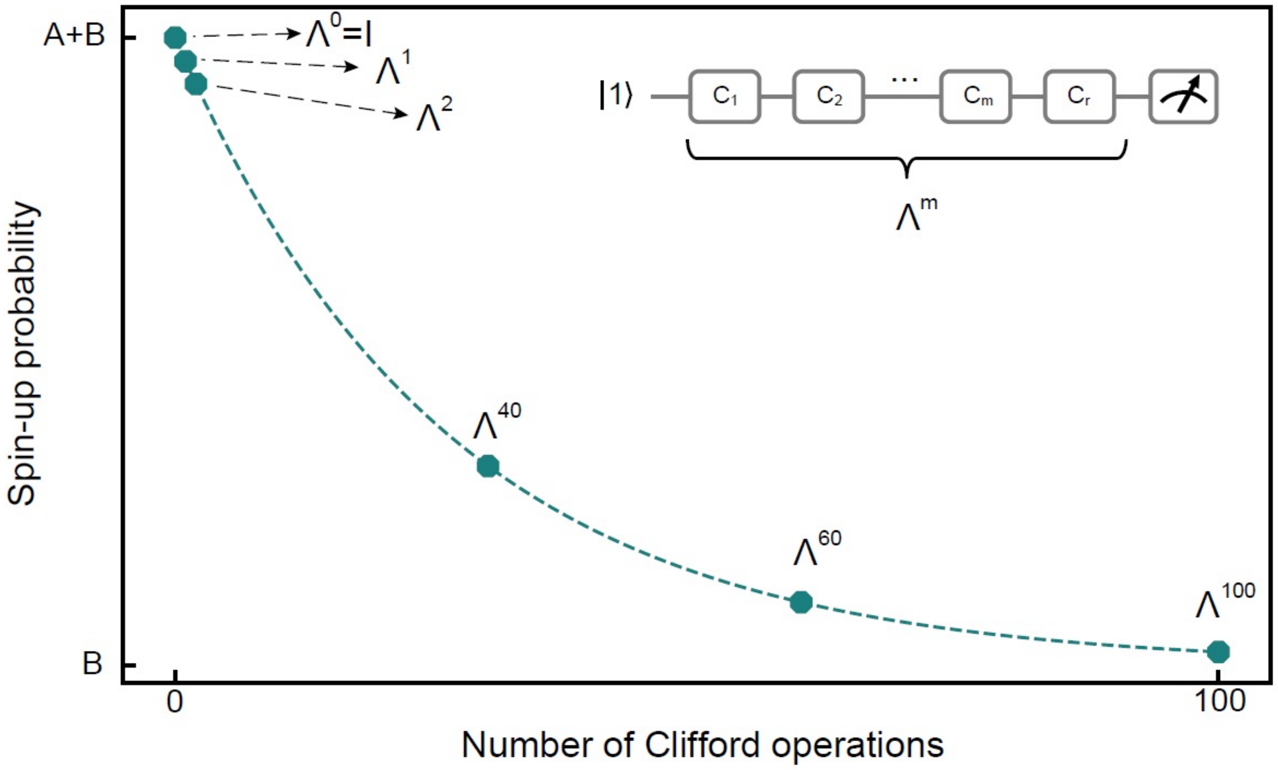

Single-qubit RB

Single exponential decay:

$$F_{\sigma_z} = Ap^m + B$$

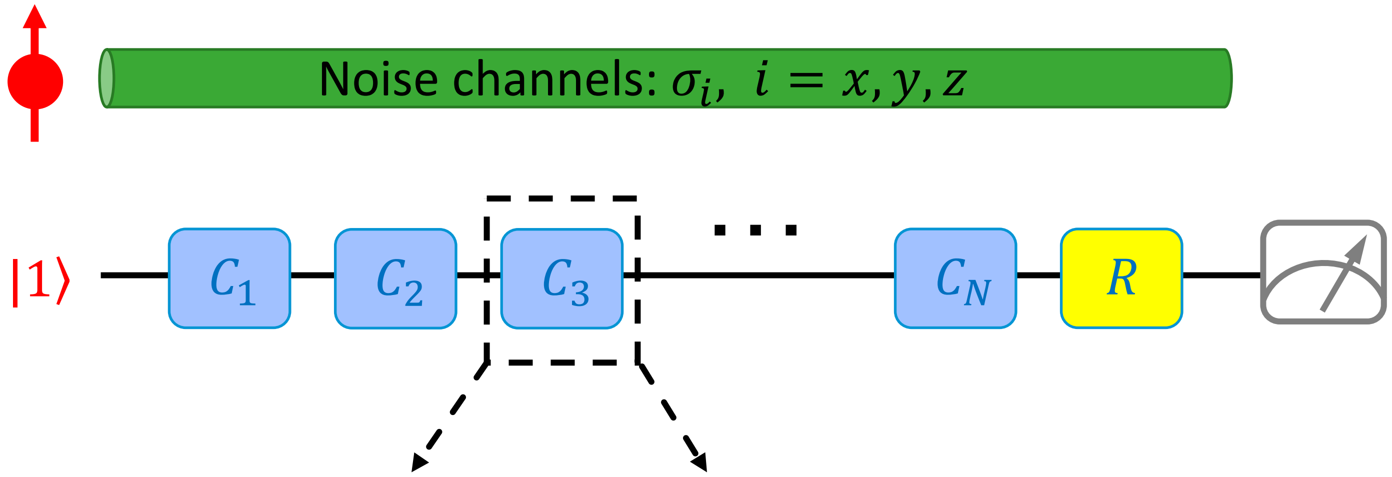

$$\begin{array}{c} \sigma_0 \\ \sigma_x \\ \sigma_y \\ \sigma_z \end{array} \begin{pmatrix} 1 & 0 & 0 & 0 \\ 0 & p & 0 & 0 \\ 0 & 0 & p & 0 \\ 0 & 0 & 0 & p \end{pmatrix} \Longrightarrow \begin{pmatrix} 1 & 0 \\ 0 & p\mathbf{I} \end{pmatrix} \begin{array}{c} \sigma_0 \\ \sigma_i \end{array} \quad i = x, y, z$$

Simplified notation

Two-qubit RB

Single exponential decay:

$$F_{\sigma_z \otimes \sigma_z} = Ap^m + B$$

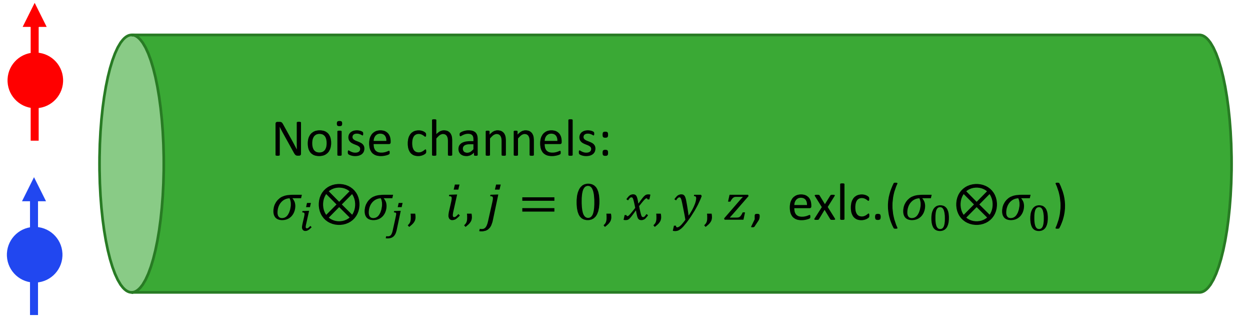

In total
11520 elements

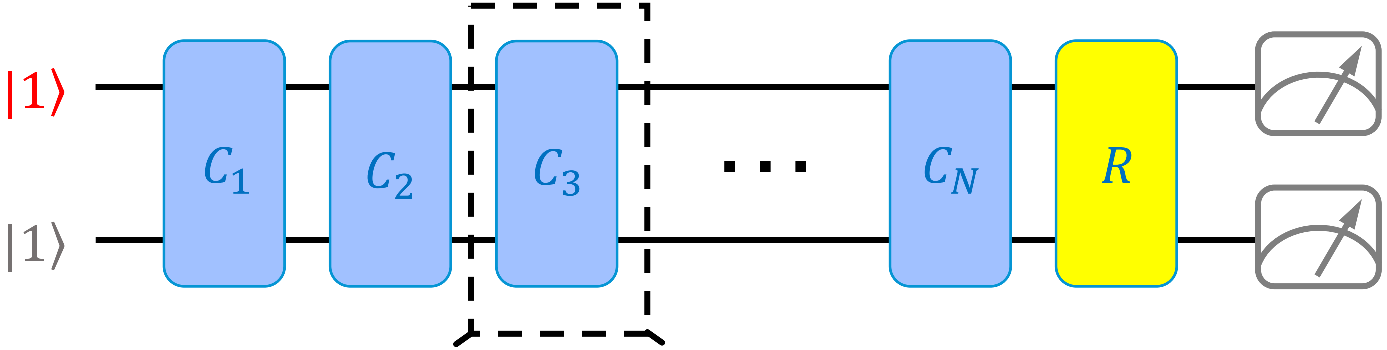

$$\begin{array}{cc} \begin{pmatrix} 1 & 0 & 0 & 0 \\ 0 & p\mathbf{I}_1 & 0 & 0 \\ 0 & 0 & p\mathbf{I}_2 & 0 \\ 0 & 0 & 0 & p\mathbf{I}_{12} \end{pmatrix} & \begin{array}{c} \sigma_0 \otimes \sigma_0 \\ \sigma_i \otimes \sigma_0 \\ \sigma_0 \otimes \sigma_j \\ \sigma_i \otimes \sigma_j \end{array} \end{array}$$

$i, j = x, y, z$

Simultaneous RB

Three-fold exponential decay:

$$F_{\sigma_z \otimes \sigma_z} = \mathrm{A}_1 p_1^m + \mathrm{A}_2 p_2^m + \mathrm{A}_{12} p_{12}^m + B$$

$$p_{eff} = \frac{3}{15}(p_1 + p_2) + \frac{9}{15} p_{12}$$

Sequence randomly sampled for each qubit

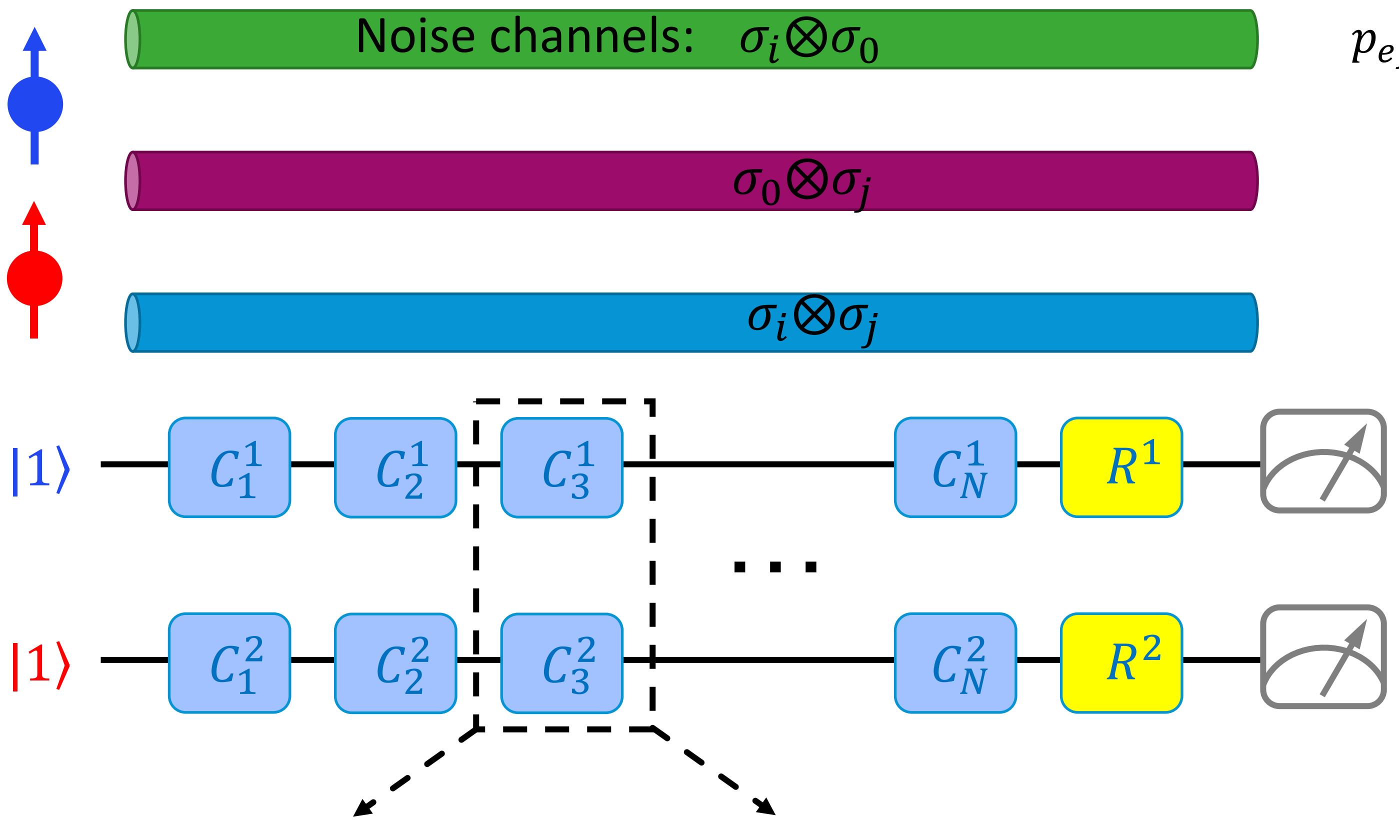

$$\begin{array}{cc} \begin{pmatrix} 1 & 0 & 0 & 0 \\ 0 & p_1 \mathbf{I}_1 & 0 & 0 \\ 0 & 0 & p_2 \mathbf{I}_2 & 0 \\ 0 & 0 & 0 & p_{12} \mathbf{I}_{12} \end{pmatrix} & \begin{array}{c} \sigma_0 \otimes \sigma_0 \\ \sigma_i \otimes \sigma_0 \\ \sigma_0 \otimes \sigma_j \\ \sigma_i \otimes \sigma_j \end{array} \end{array}$$

J.Helsen, **X.X.**, npj Quantum Info 2019
X.X., et al. PRX 2019
See also: J.M.Gambetta et al, PRL 2012

Simultaneous RB

Three-fold exponential decay:

$$F_{\sigma_z \otimes \sigma_z} = \mathrm{A}_1 p_1^m + \mathrm{A}_2 p_2^m + \mathrm{A}_{12} p_{12}^m + B$$

With correlated errors: $p_{12} \neq p_1 \cdot p_2$ $\Longrightarrow$ General case

$$p_{eff} = \frac{3}{15}(p_1 + p_2) + \frac{9}{15} p_{12}$$

No correlated errors: $p_{12} = p_1 \cdot p_2$ $\Longrightarrow$ $\Lambda_{dep}^{sim}(\rho) = \left(p_1 \rho^1 + \frac{1-p_1}{2} I\right) \otimes \left(p_2 \rho^2 + \frac{1-p_2}{2} I\right)$

Sequence randomly sampled for each qubit

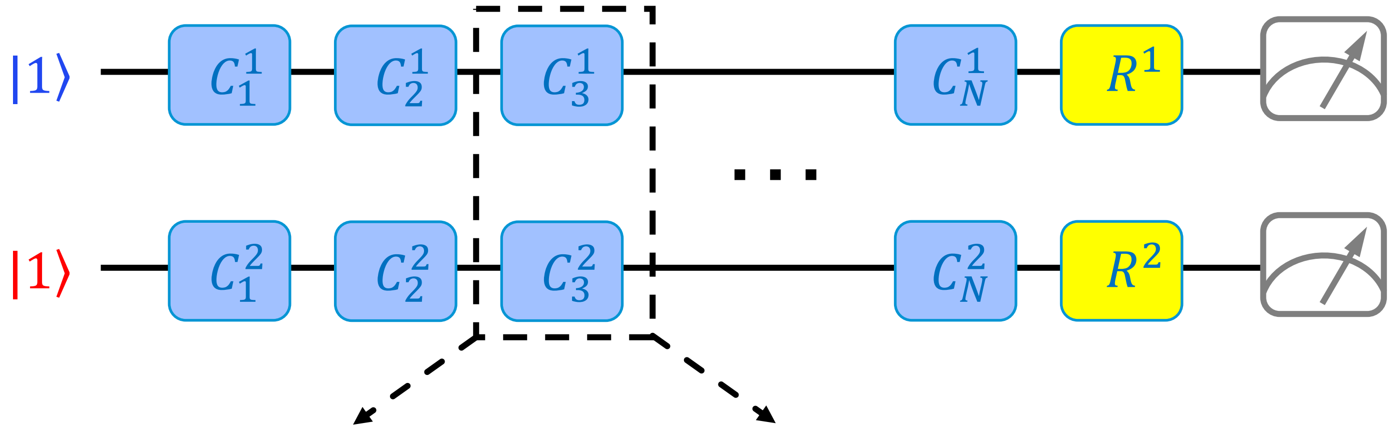

$$\begin{array}{c} \begin{pmatrix} 1 & 0 & 0 & 0 \\ 0 & p_1 \mathbf{I}_1 & 0 & 0 \\ 0 & 0 & p_2 \mathbf{I}_2 & 0 \\ 0 & 0 & 0 & p_{12} \mathbf{I}_{12} \end{pmatrix} \end{array} \begin{array}{c} \sigma_0 \otimes \sigma_0 \\ \sigma_i \otimes \sigma_0 \\ \sigma_0 \otimes \sigma_j \\ \sigma_i \otimes \sigma_j \end{array}$$

QuTech

J.Helsen, **X.X.**, npj Quantum Info 2019
X.X., et al. PRX 2019
See also: J.M.Gambetta et al, PRL 2012

Separating the three channels

Two-qubit space

$$\begin{array}{cc} \begin{pmatrix} 1 & 0 & 0 & 0 \\ 0 & p_1\mathbf{I}_1 & 0 & 0 \\ 0 & 0 & p_2\mathbf{I}_2 & 0 \\ 0 & 0 & 0 & p_{12}\mathbf{I}_{12} \end{pmatrix} & \begin{array}{c} \sigma_0\otimes\sigma_0 \\ \sigma_i\otimes\sigma_0 \\ \sigma_0\otimes\sigma_j \\ \sigma_i\otimes\sigma_j \end{array} \end{array}$$

$\mathbf{I}_1$ subspace

$$\begin{array}{cc} \begin{pmatrix} 1 & 0 & 0 & 0 \\ 0 & p_1 & 0 & 0 \\ 0 & 0 & p_1 & 0 \\ 0 & 0 & 0 & p_1 \end{pmatrix} & \begin{array}{c} \sigma_0\otimes\sigma_0 \\ \sigma_x\otimes\sigma_0 \\ \sigma_y\otimes\sigma_0 \\ \sigma_z\otimes\sigma_0 \end{array} \end{array}$$

Isolate the $\sigma_z\otimes\sigma_0$ term (SPAM bases)

Use additional two-qubit Pauli operators to flip the initial state ρ

$$\Lambda(\sigma_i\otimes\sigma_j\ \rho\ \sigma_i\otimes\sigma_j)$$

$$\Downarrow$$

$$\sum_{i,j} \chi_{\sigma_z\otimes\sigma_0}(\sigma_i\otimes\sigma_j)\cdot\Lambda(\sigma_i\otimes\sigma_j\ \rho\ \sigma_i\otimes\sigma_j)$$

$$\Downarrow$$

$$\begin{pmatrix} 1 & 0 & 0 & 0 \\ 0 & 0 & 0 & 0 \\ 0 & 0 & 0 & 0 \\ 0 & 0 & 0 & p_1 \end{pmatrix} (\rho)$$

$p_2\mathbf{I}_2$ and $p_{12}\mathbf{I}_{12}$ become all 0

Character function: $\chi_{\sigma_z\otimes\sigma_0}(\sigma_i\otimes\sigma_j)$

X.Xue., et al. PRX 2019

TABLE I. Values for the character function $\chi_P(\sigma)$ for $P \in \{(\sigma_z\otimes I), (I\otimes\sigma_z), (\sigma_z\otimes\sigma_z)\}$.

$P\backslash\sigma$	II	$\sigma_z I$	$I\sigma_z$	$\sigma_z\sigma_z$	$\sigma_x I$	$I\sigma_x$	$\sigma_x\sigma_x$	$\sigma_y I$	$I\sigma_y$	$\sigma_y\sigma_y$	$\sigma_z\sigma_x$	$\sigma_x\sigma_z$	$\sigma_z\sigma_y$	$\sigma_y\sigma_z$	$\sigma_x\sigma_y$	$\sigma_y\sigma_x$
$\sigma_z I$	1	1	1	1	−1	1	−1	−1	1	−1	1	−1	1	−1	−1	−1
$I\sigma_z$	1	1	1	1	1	−1	−1	1	−1	−1	−1	1	−1	1	−1	−1
$\sigma_z\sigma_z$	1	1	1	1	−1	−1	1	−1	−1	1	−1	−1	−1	−1	1	1

QuTech

Add Pauli operators at the beginning

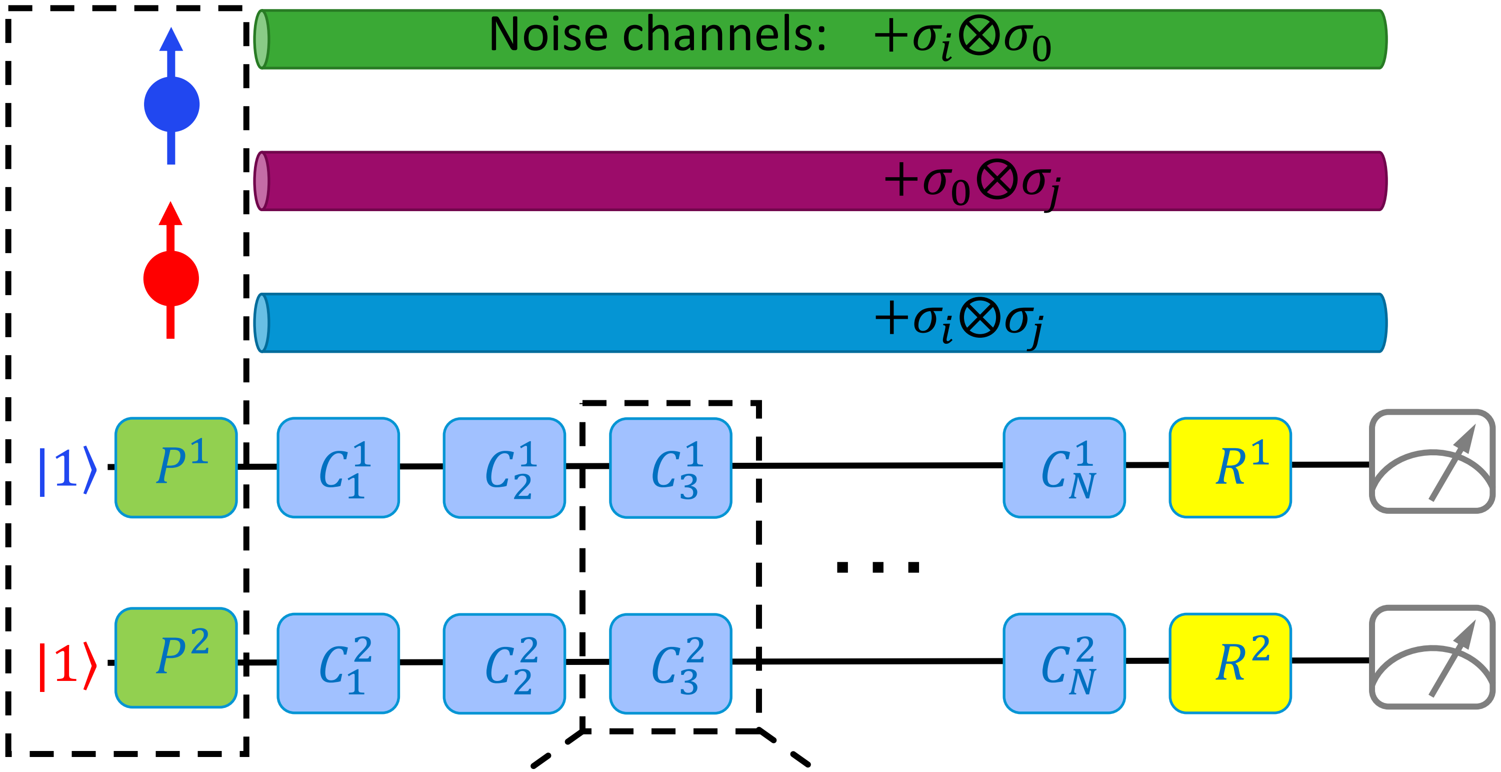

$\sigma_0 \otimes \sigma_0,\ \sigma_0 \otimes \sigma_z,$
$\sigma_z \otimes \sigma_0,\ \sigma_z \otimes \sigma_z$

Sequence randomly sampled for each qubit

$$\begin{pmatrix} 1 & 0 & 0 & 0 \\ 0 & p_1\mathbf{I}_1 & 0 & 0 \\ 0 & 0 & p_2\mathbf{I}_2 & 0 \\ 0 & 0 & 0 & p_{12}\mathbf{I}_{12} \end{pmatrix}$$

J.Helsen

QuTech

J.Helsen, **X.X.**, npj Quantum Info 2019
X.X., et al. PRX 2019

Character randomized benchmarking

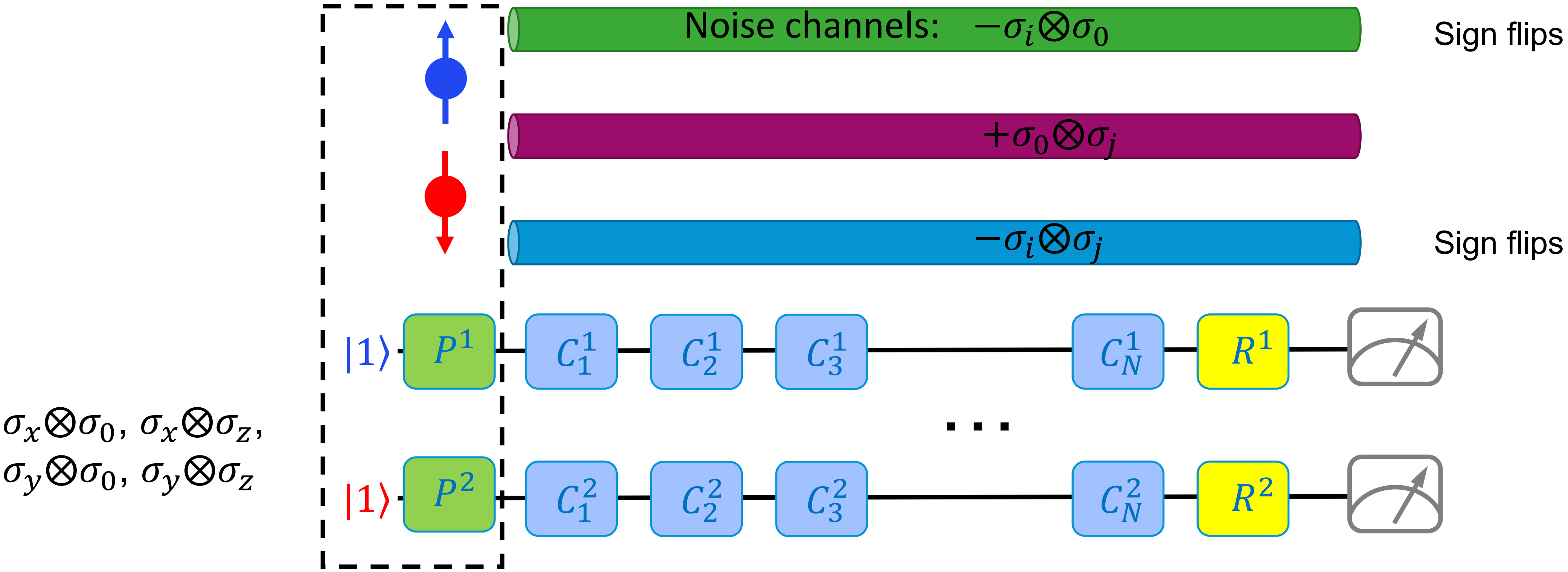

J.Helsen

QuTech

J.Helsen, **X.X.**, npj Quantum Info 2019
X.X., et al. PRX 2019

Quantum computation with spin qubits in semiconductor

Xiao Xue

QuTech, Delft University of Technology, Lorentzweg 1, 2628 CJ Delft, Netherlands

“Quantum phenomena do not occur in a Hilbert space.
They occur in a laboratory.”

-- Asher Peres

Future quantum computer

Linke, et al, PNAS 2017

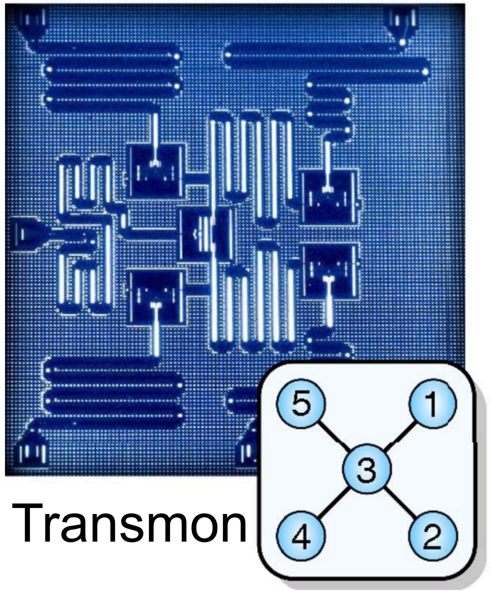

Transmon

Semiconducter (quantum dot, donor…)
- ❖ Scaling, high density;
- ❖ Coherence;
- ❖ "Hot" (cryo-electronics, easy wiring).

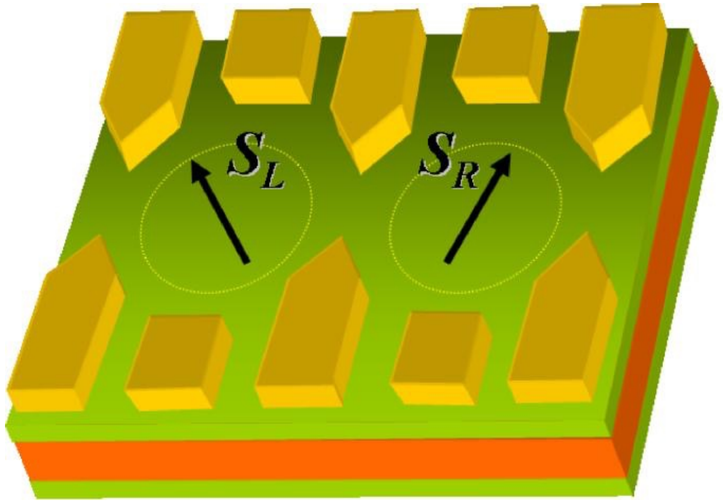

Loss, DiVincenzo, PRA 1998

Kane, Nature 1998

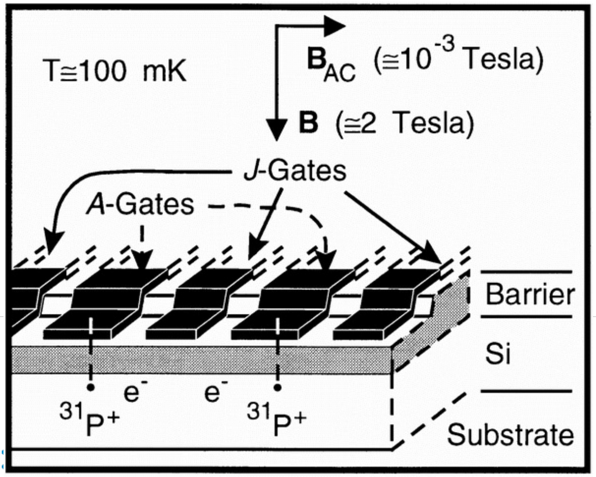

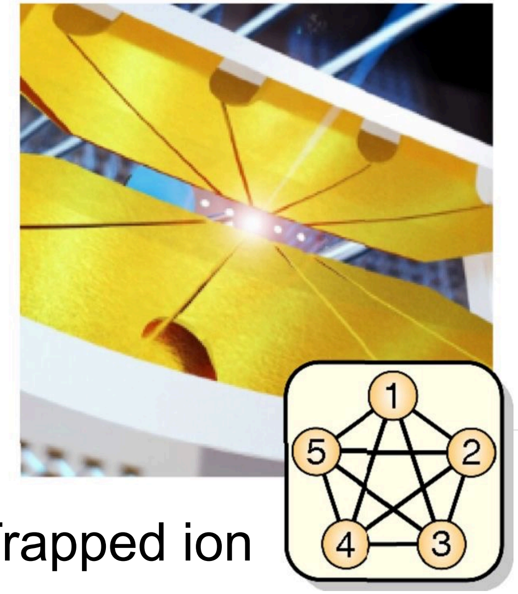

Trapped ion

1 billion qubits

Trapped ions

100 X 100 m^2

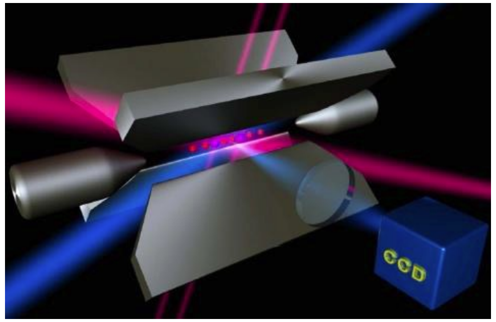

Much smaller for surface trap

Superconducting qubits

5 X 5 m^2

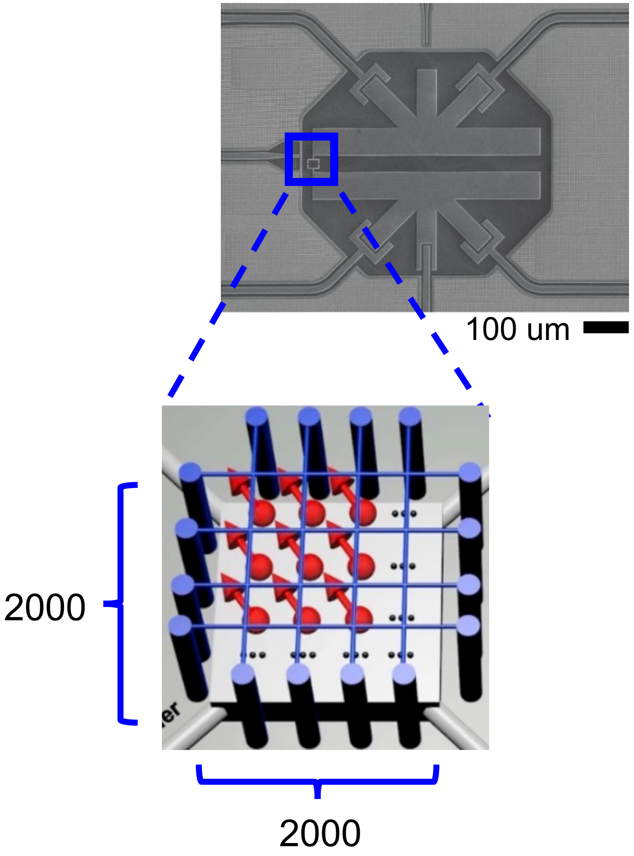

Spin qubits

5 X 5 mm^2

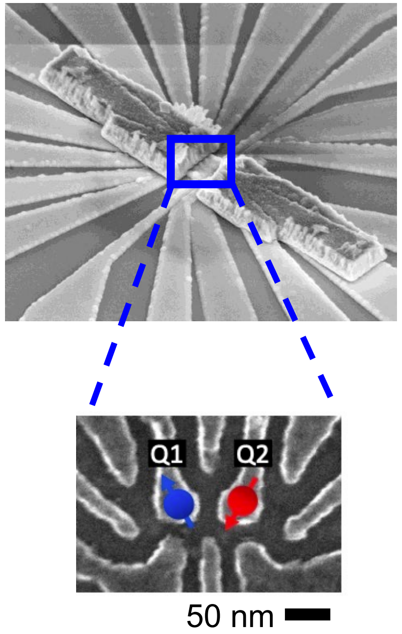

Transistor v.s. quantum dot

Transistor: 1 gate / 1 device

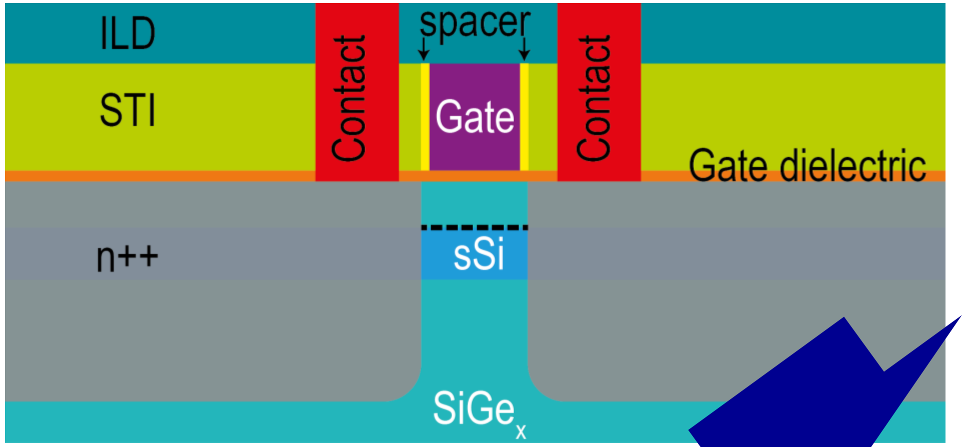

Loss and DiVincenzo, PRA 1998

All-electrical operation

- Tunable energy of electrons
- Tunable tunnel barriers
- Electrical contacts

QDots: 2*N*+3 gates / *N* devices

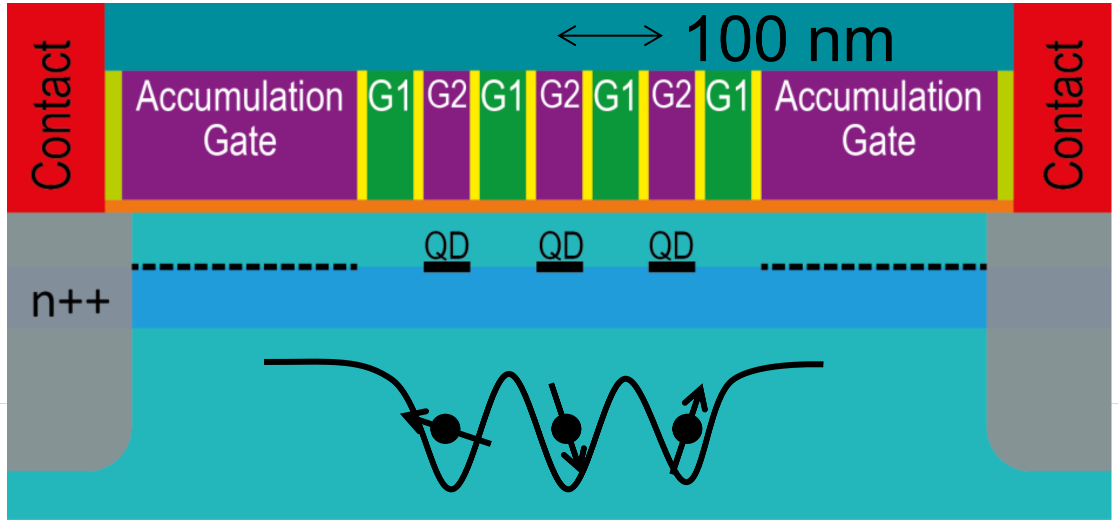

A good starting point
for scalability

QuTech

Maurand et al, Nature Nano 2016

Intel-QuTech collaboration

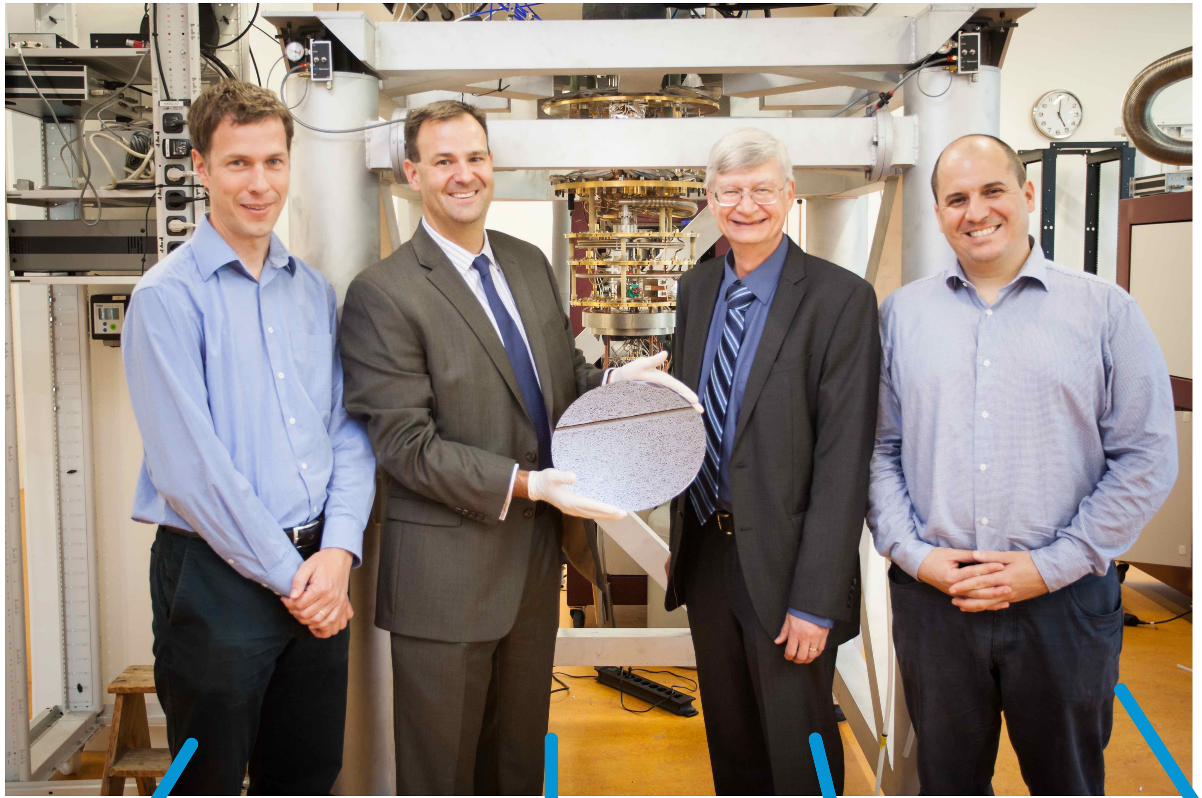

10 years, 50 M$

Silicon spin qubits
Transmon qubits

Architecture, Cryo-CMOS, interconnects

Lieven Vandersypen
Director of QuTech
PI of spin qubit group

Jim Clark
PI Intel Quantum group

Mike Mayberry
Vice president Intel

Leo DiCarlo
PI of SC qubit group

QuTech

Achievement: quantum dot arrays made @ Intel 300 mm cleanroom

Qubits made at Intel

L. M. K. Vandersypen, M. A. Eriksson.
Physics Today, 2019

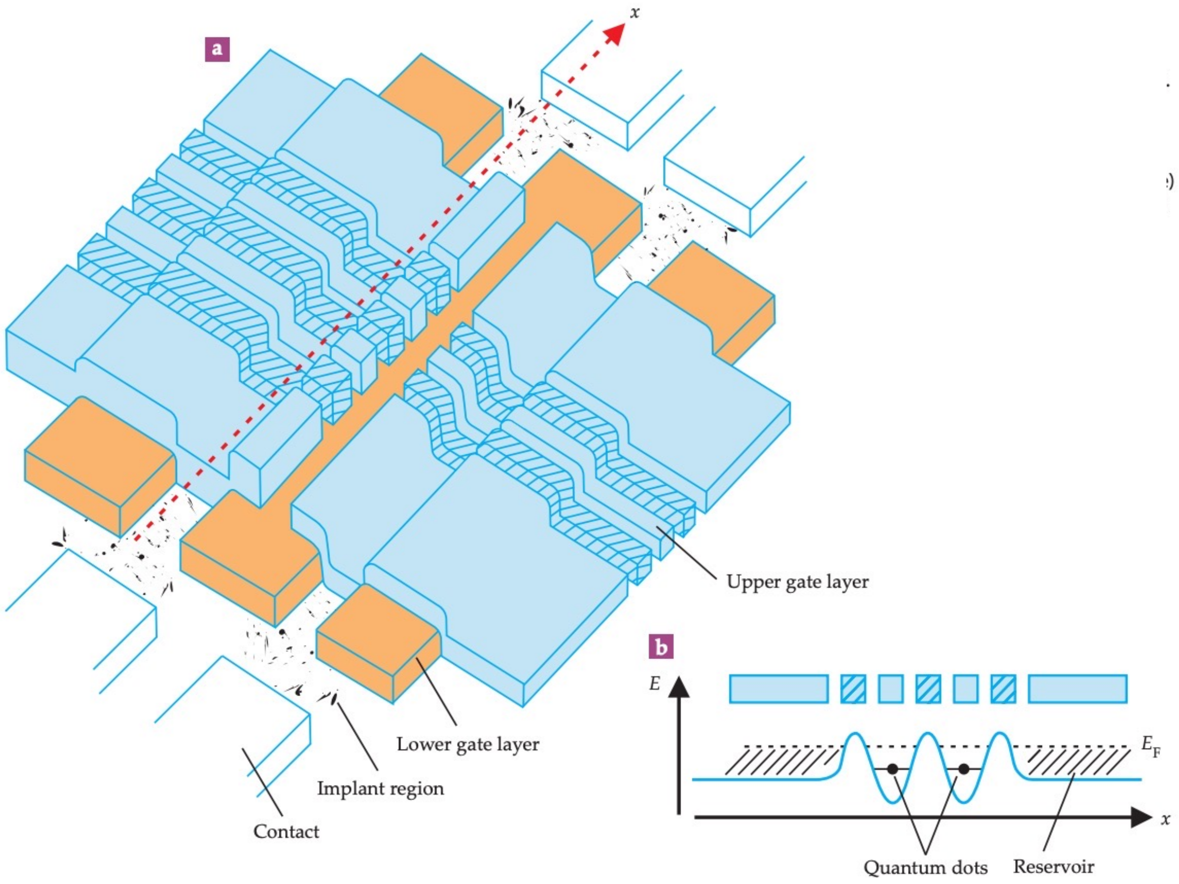

Spin qubits made in Intel Fin-FET

Zwerver et al., Nature Electronics 2022

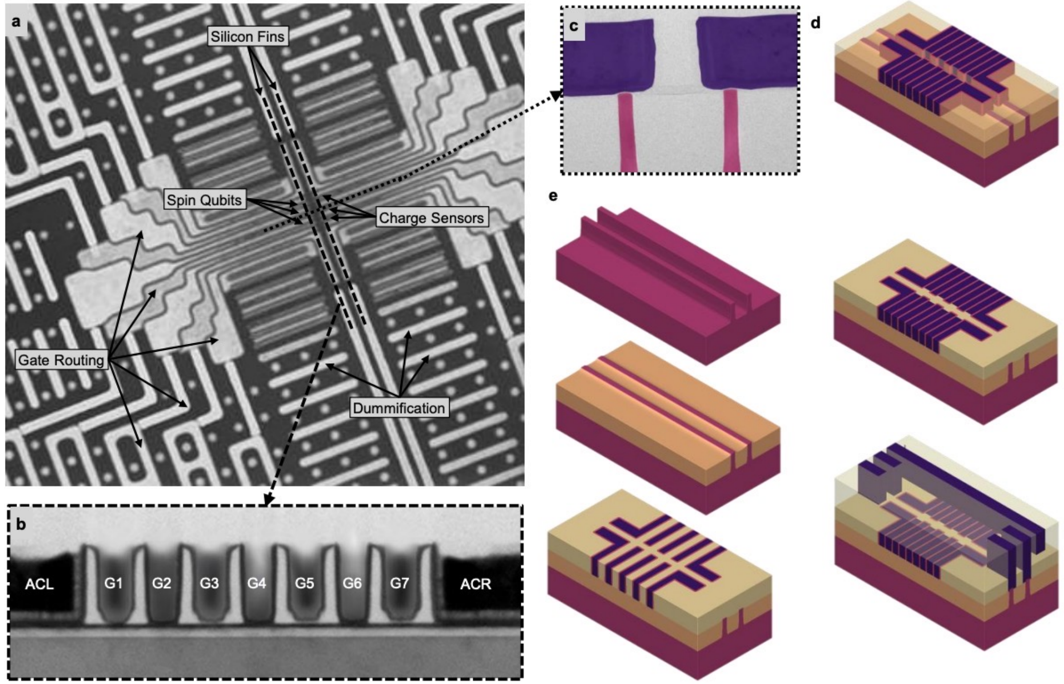

For comparison:

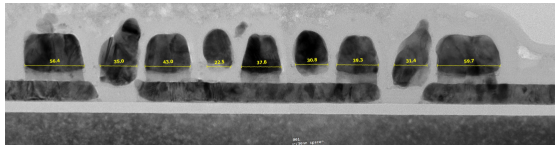

300mm fabrication

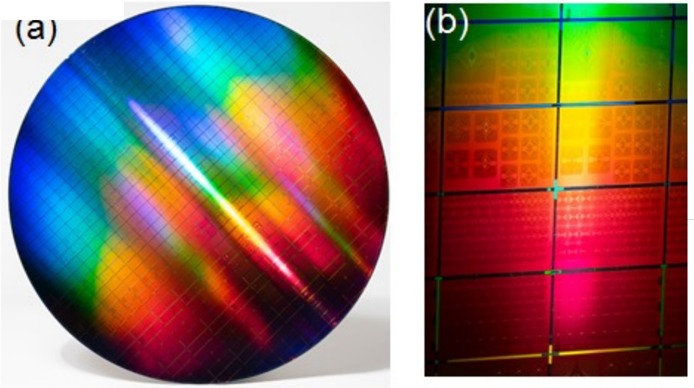

R. Pillarisetty, et al., IEDM 2019

Semiconductor heterostructure

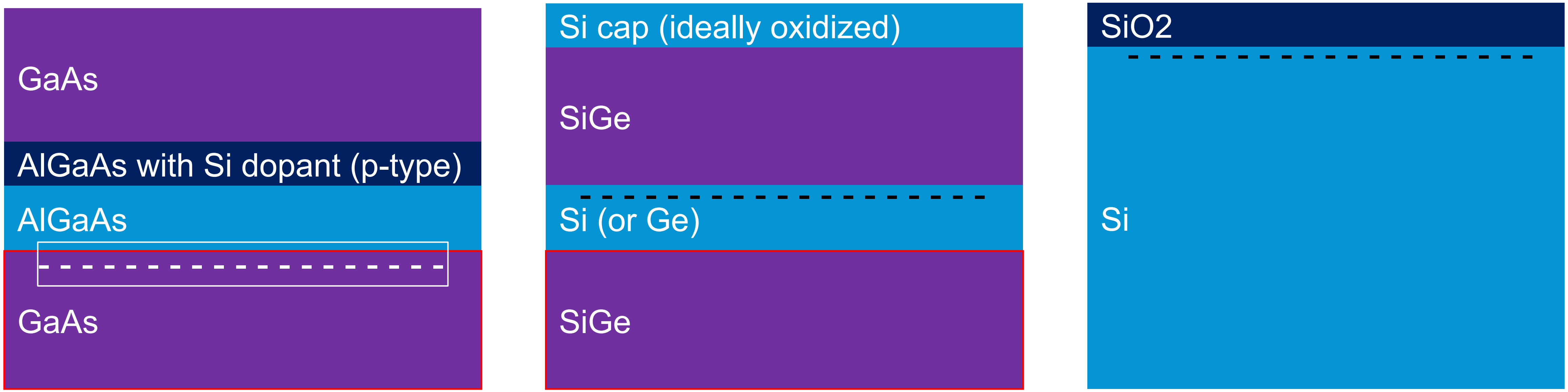

Argument: bury the electrons deeply

For Ge, the carriers are holes instead.

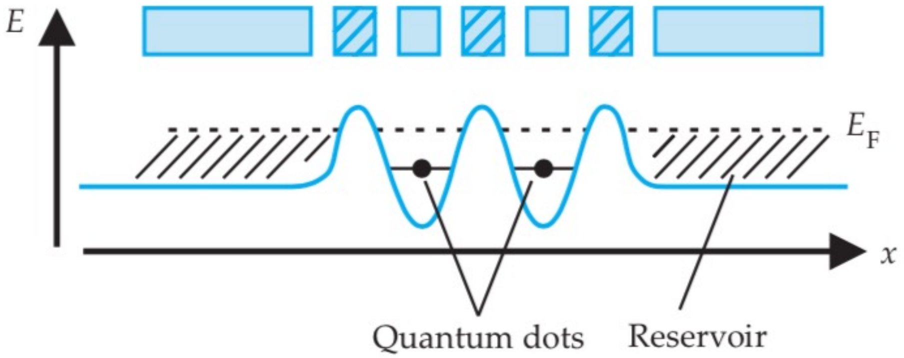

Semiconductor heterostructure

Argument: bury the electrons deeply

For Ge, the carriers are holes instead.

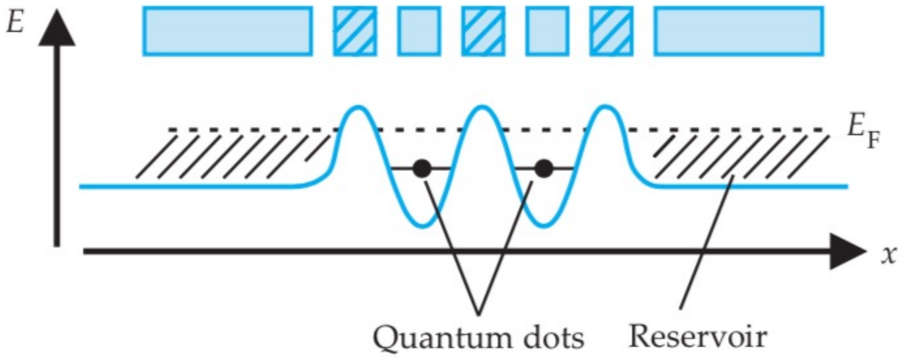

QuTech

Semiconductor heterostructure

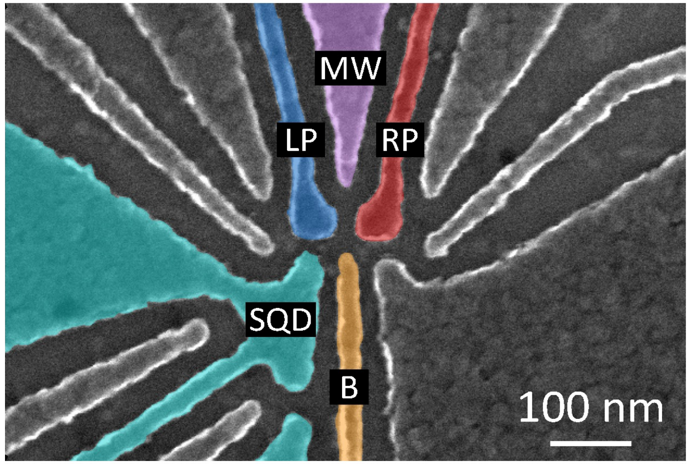

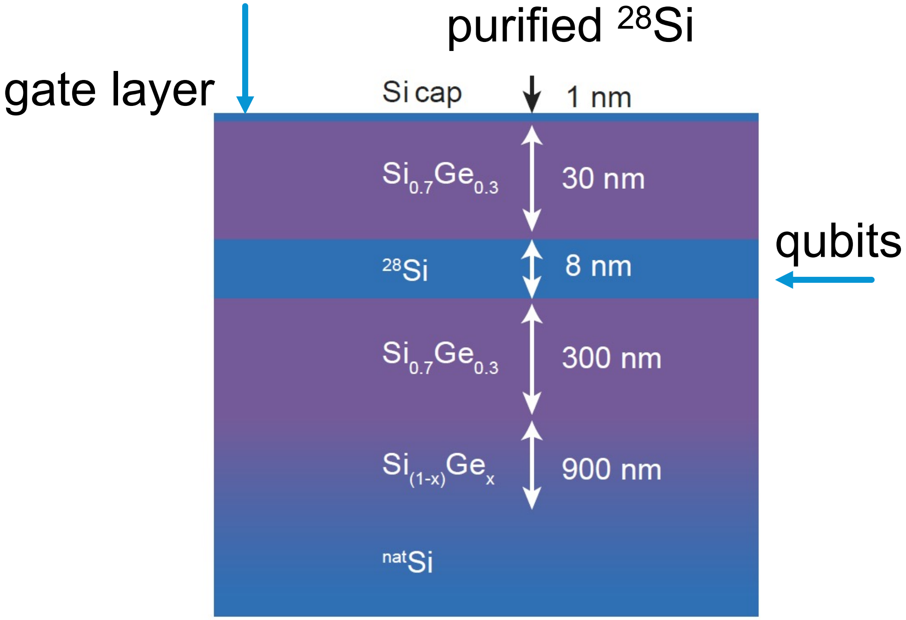

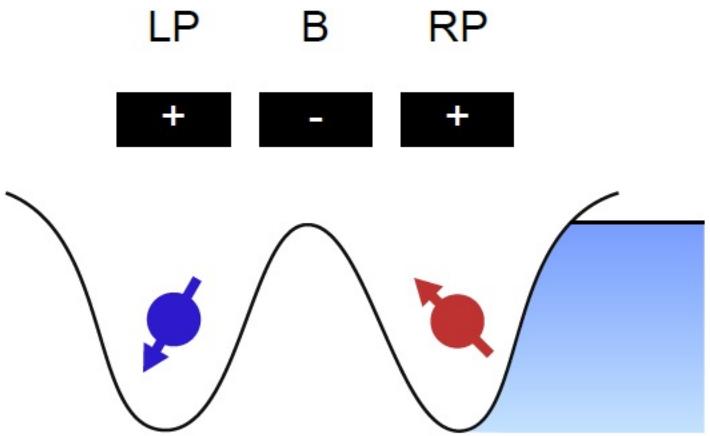

QuTech

Artificial atom

Single electron energy diagram
-> orbital energy

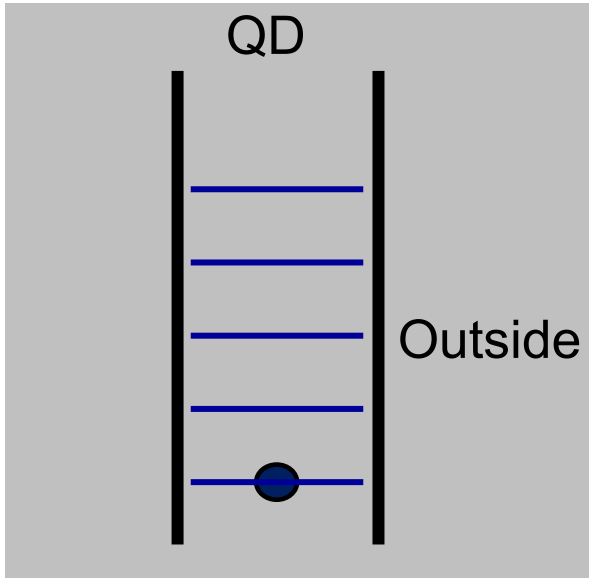

Multiple electron energy diagram
-> orbital energy + charging energy

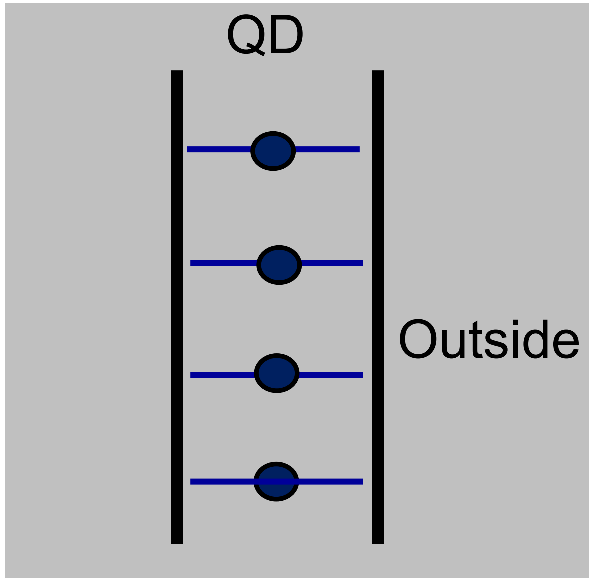

- Ideally, the dot is a quantum harmonic oscillator.
- In reality, there's always some deviation.
- For simplicity, we often plot it as a finite square potential well.

QuTech

R. Hanson et al., RMP 2007

Transport

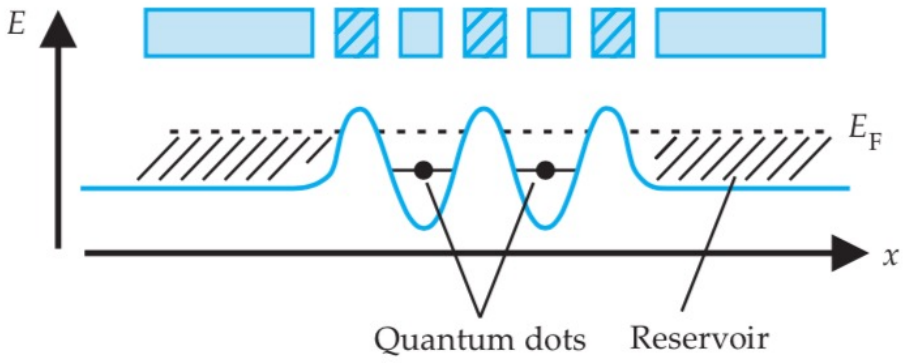

"Single electron transistor"

+

The energy levels are controlled via a metal gate on top

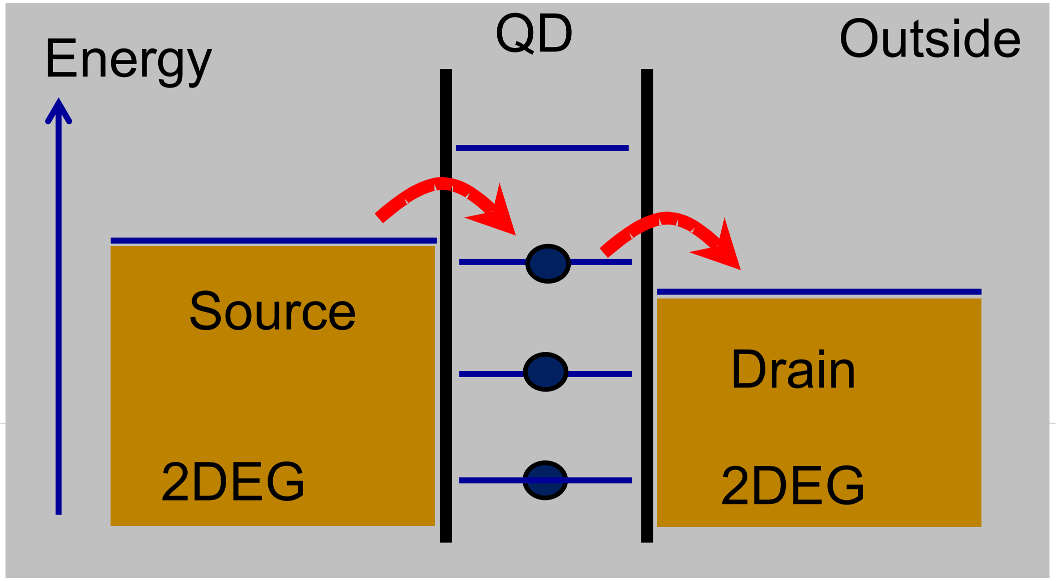

Coulomb peaks:

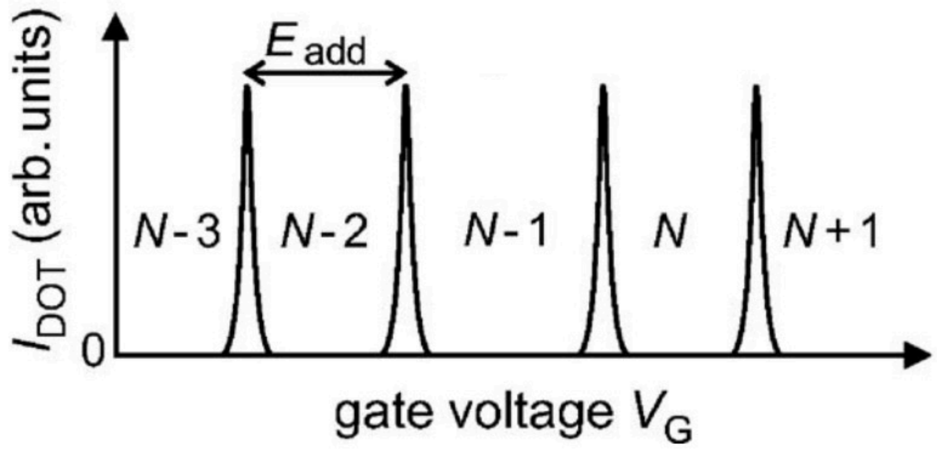

Single electron spin state

Last electron

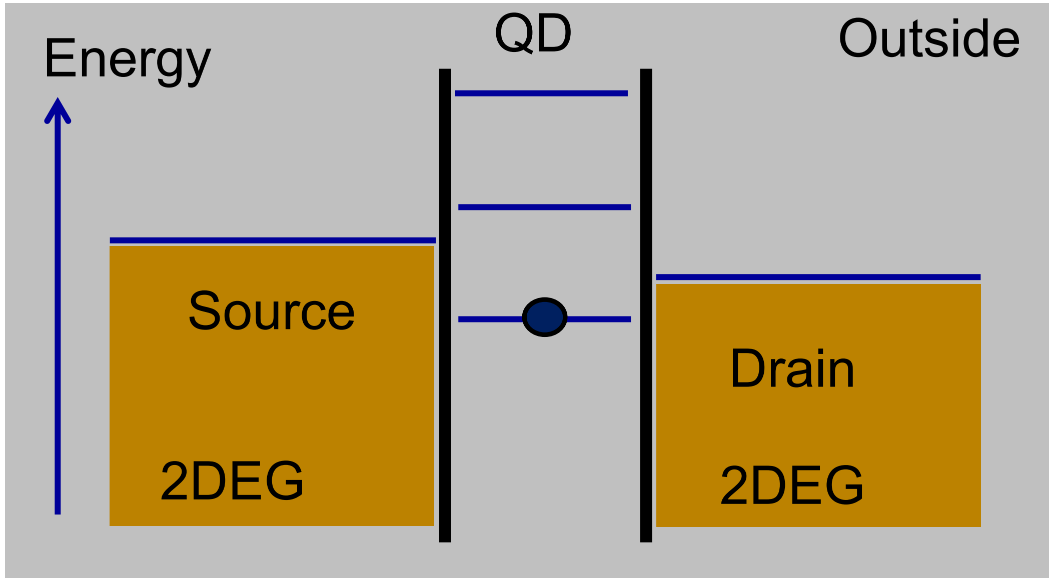

Apply a magnetic field

Zeeman splitting:

$$E_z = g\mu_B B_z$$

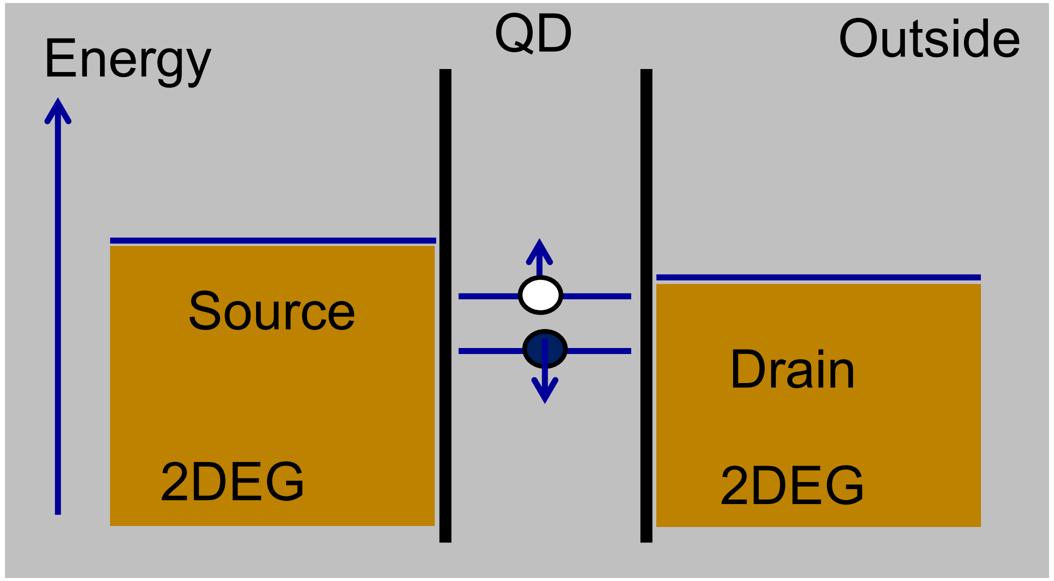

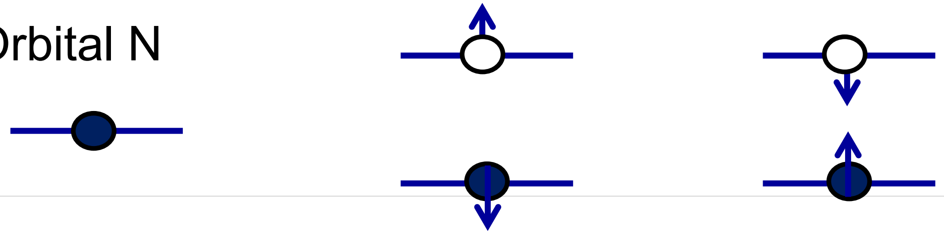

g > 0

g < 0

Spin-to-charge conversion

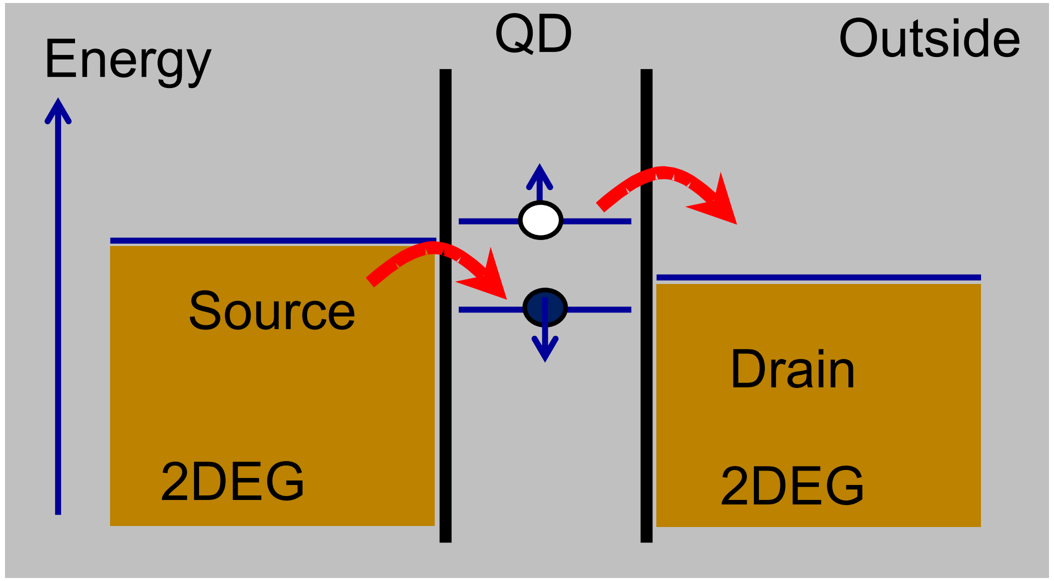

- Spin-up ---> 0 electron
- Spin-down ---> 1 electron

Two electrons in one dot

Orbital N=0

Orbital N

Orbital N

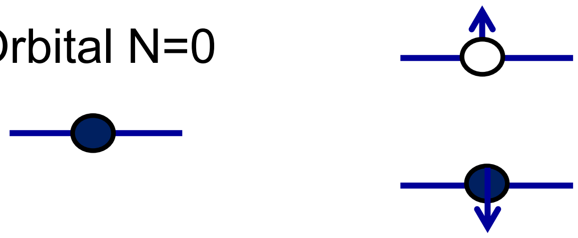

Orbital N=0

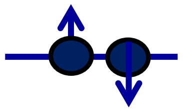

$(|{\downarrow\uparrow}\rangle - |{\uparrow\downarrow}\rangle)/\sqrt{2}$

Spin-singlet, with total spin 0.

They are not distinguishable.

Orbital 1

Orbital 0

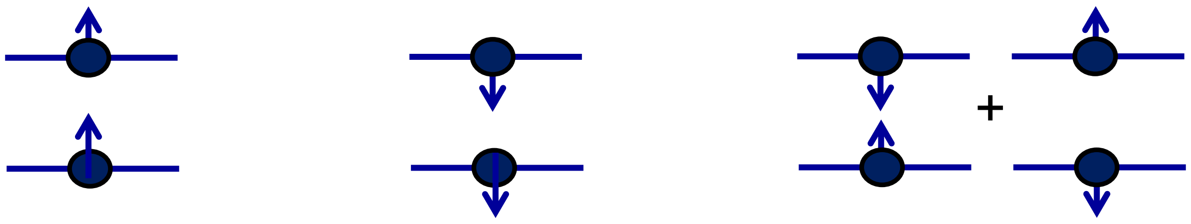

$|{\uparrow\uparrow}\rangle$ $|{\downarrow\downarrow}\rangle$ $(|{\downarrow\uparrow}\rangle + |{\uparrow\downarrow}\rangle)/\sqrt{2}$

Spin-triplet
Total spin1

QuTech

Charge sensor (SET)

A QD with one electron
Spin qubit

A QD with many electrons
Degenerate states-> spin doesn't matter

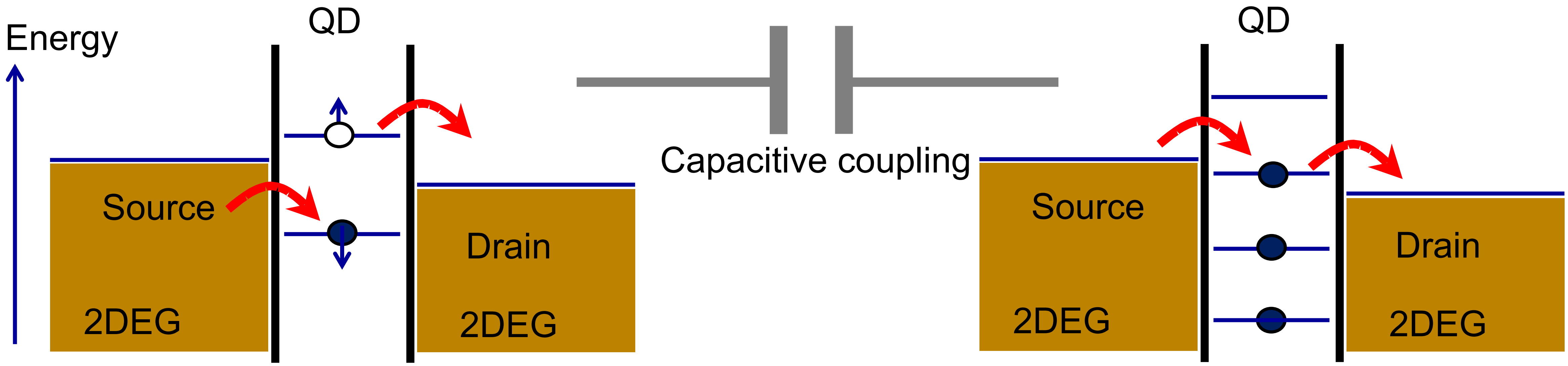

All peaks shifted

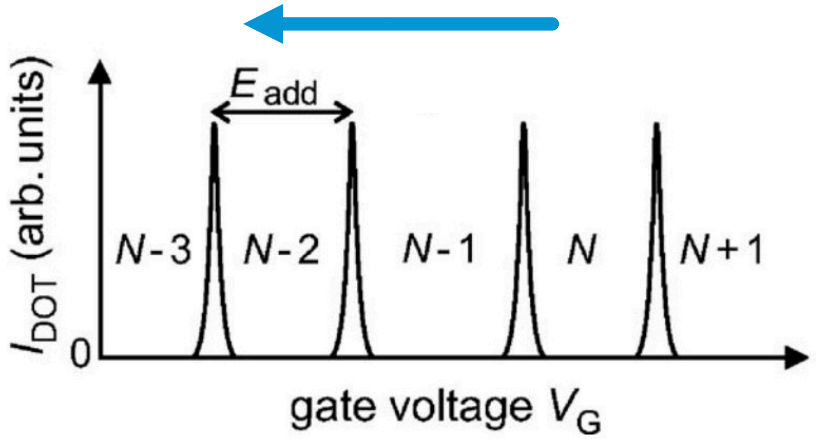

Charge sensor (SET)

Monitor the current through the sensor

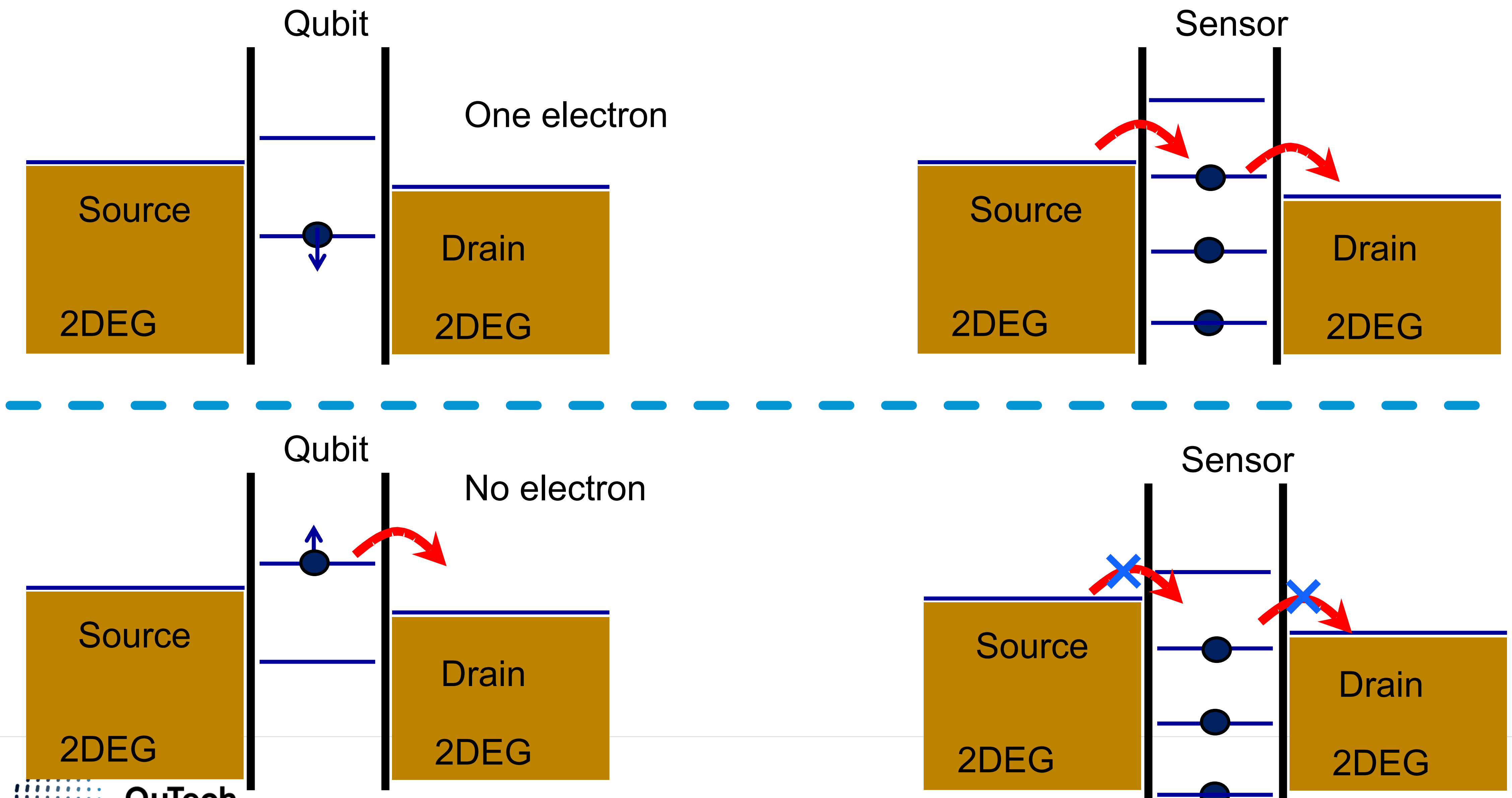

QuTech

Initialization-readout cycle

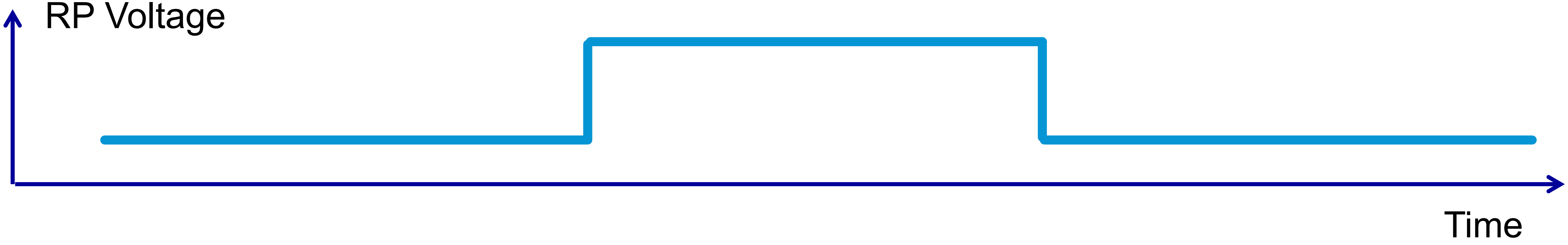

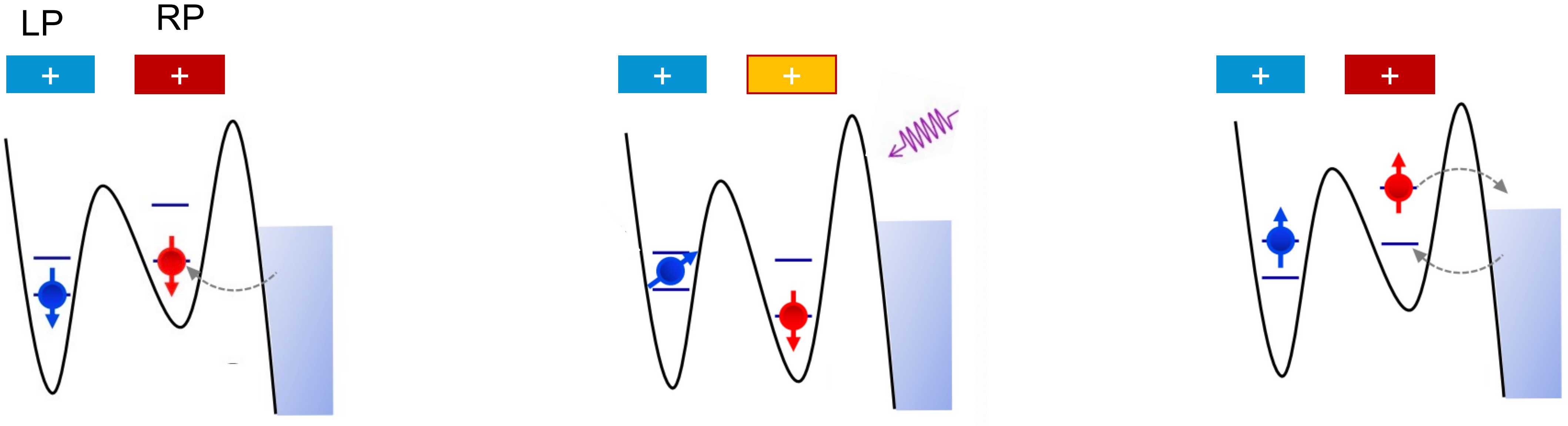

Step 1
Initialization

Step 2
Operation

Step 3
Readout

QuTech

Double quantum dot (DQD)

Fermi-Hubbard model

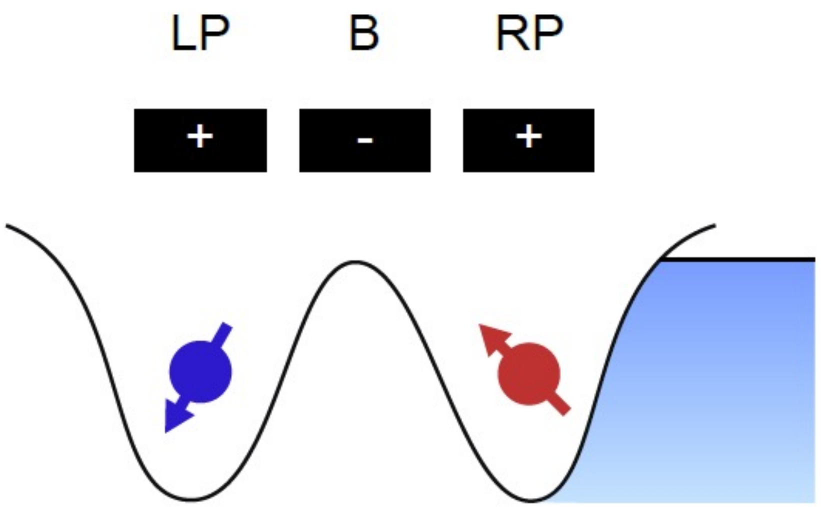

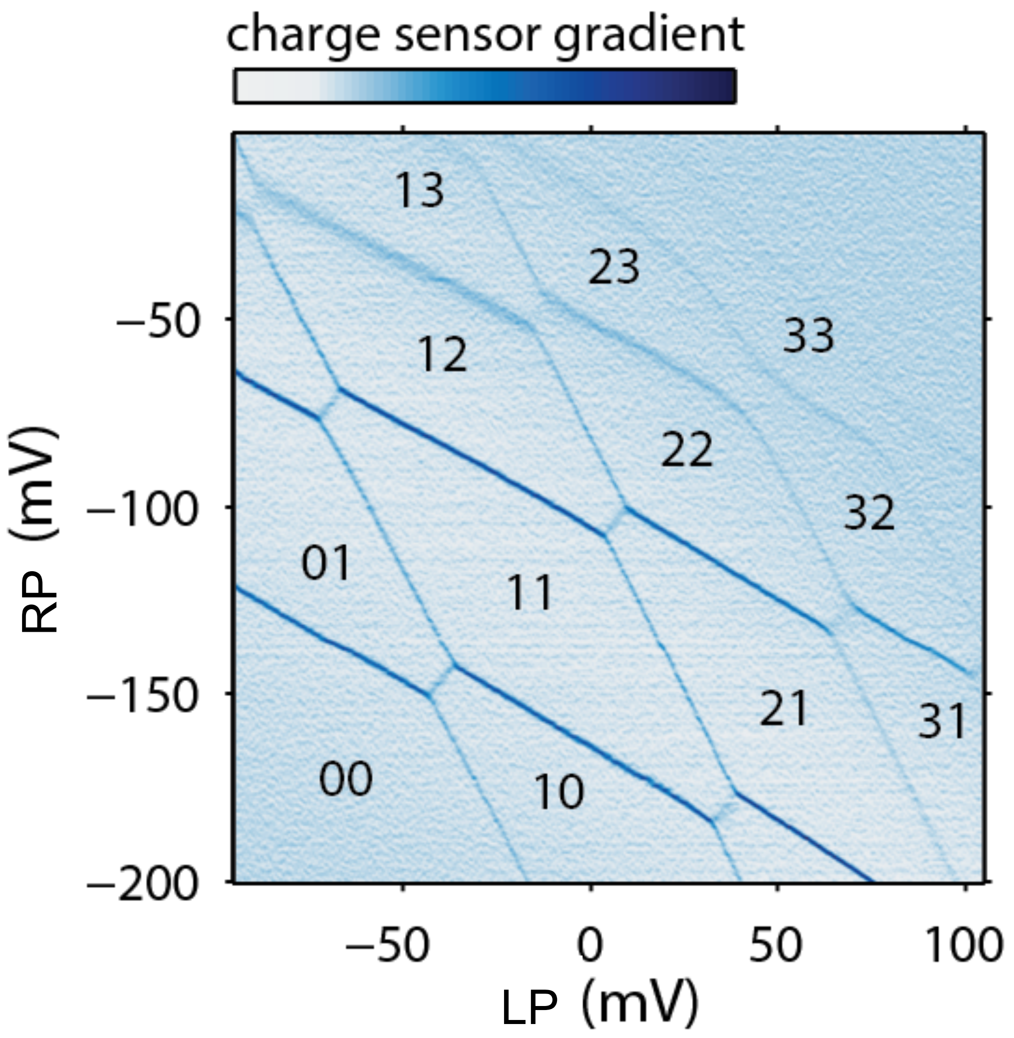

"Charge stability diagram"

Pauli spin blockade

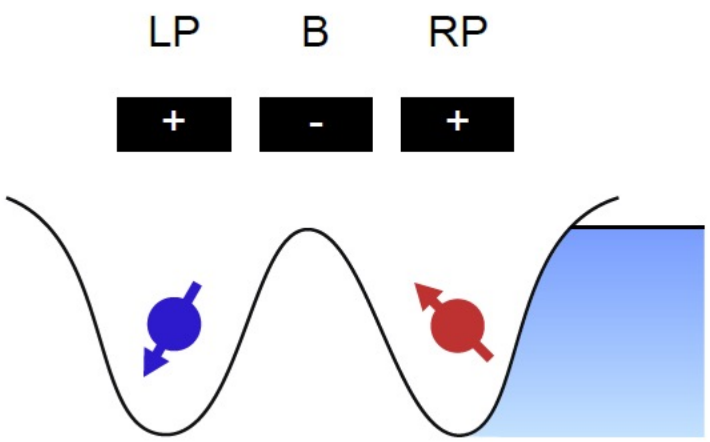

J off

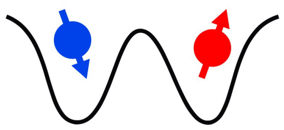

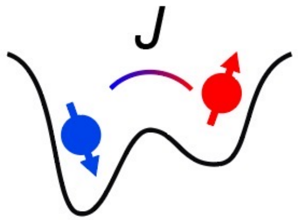

"Detuning"

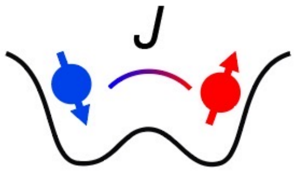

Open barrier

$(|\downarrow\uparrow\rangle - |\uparrow\downarrow\rangle)/\sqrt{2}$
allows tunneling

(0, 2) charge state

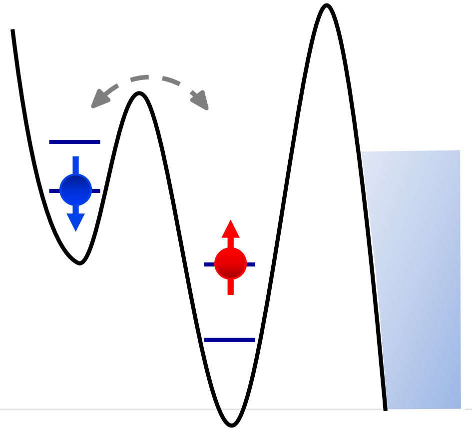

$|\uparrow\uparrow\rangle$ $|\downarrow\downarrow\rangle$

$(|\downarrow\uparrow\rangle + |\uparrow\downarrow\rangle)/\sqrt{2}$
forbids tunneling

(1, 1) charge state

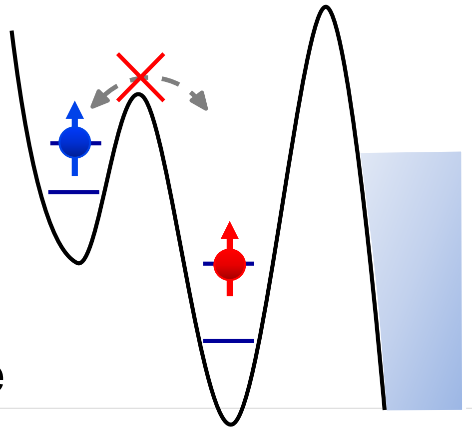

Two-spin energy diagram

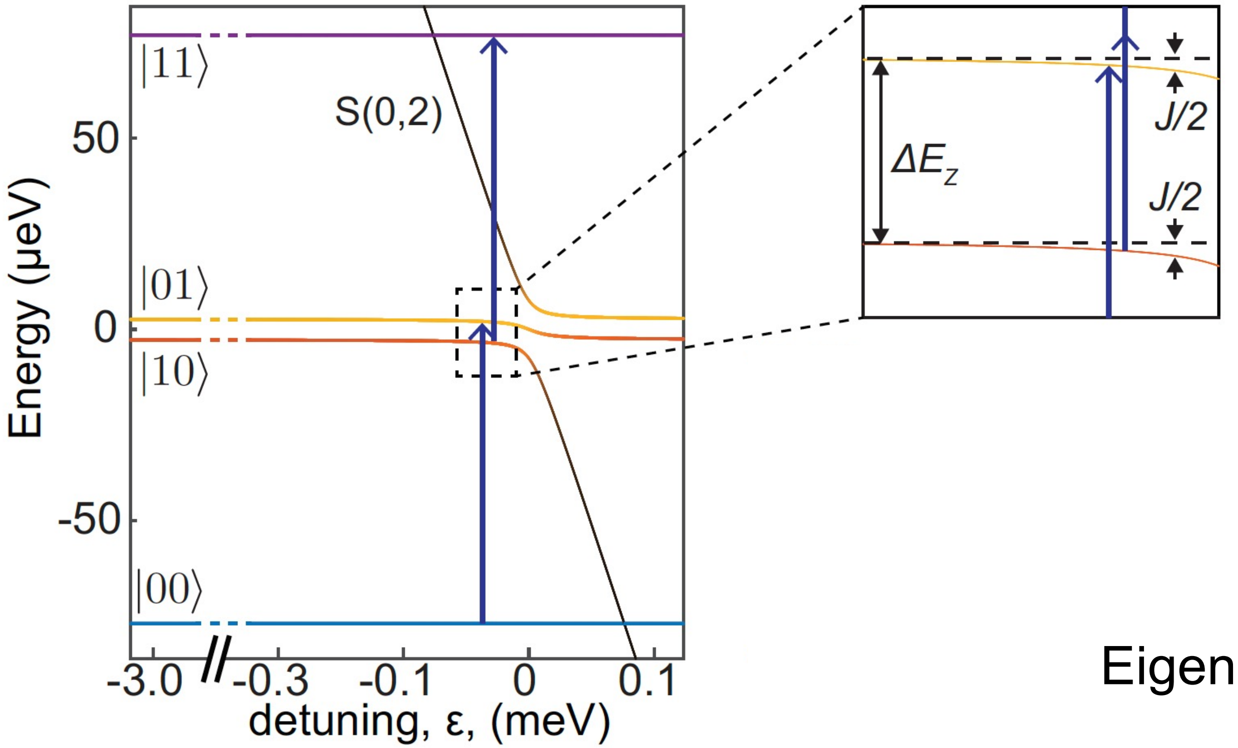

Zeeman energy difference:

- Non-uniform g-factor
- Different local B field

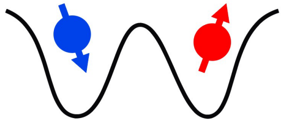

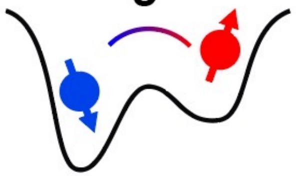

	J off		J
Eigenstates	$\lvert\uparrow\uparrow\rangle$		$\lvert\uparrow\uparrow\rangle$
	$\lvert\downarrow\uparrow\rangle$	Adiabatic transfer →	$(\lvert\downarrow\uparrow\rangle + \lvert\uparrow\downarrow\rangle)/\sqrt{2}$
	$\lvert\uparrow\downarrow\rangle$		$(\lvert\downarrow\uparrow\rangle - \lvert\uparrow\downarrow\rangle)/\sqrt{2}$
	$\lvert\downarrow\downarrow\rangle$		$\lvert\downarrow\downarrow\rangle$

Single-shot readout – spin-charge conversion

Spin-selective tunneling:

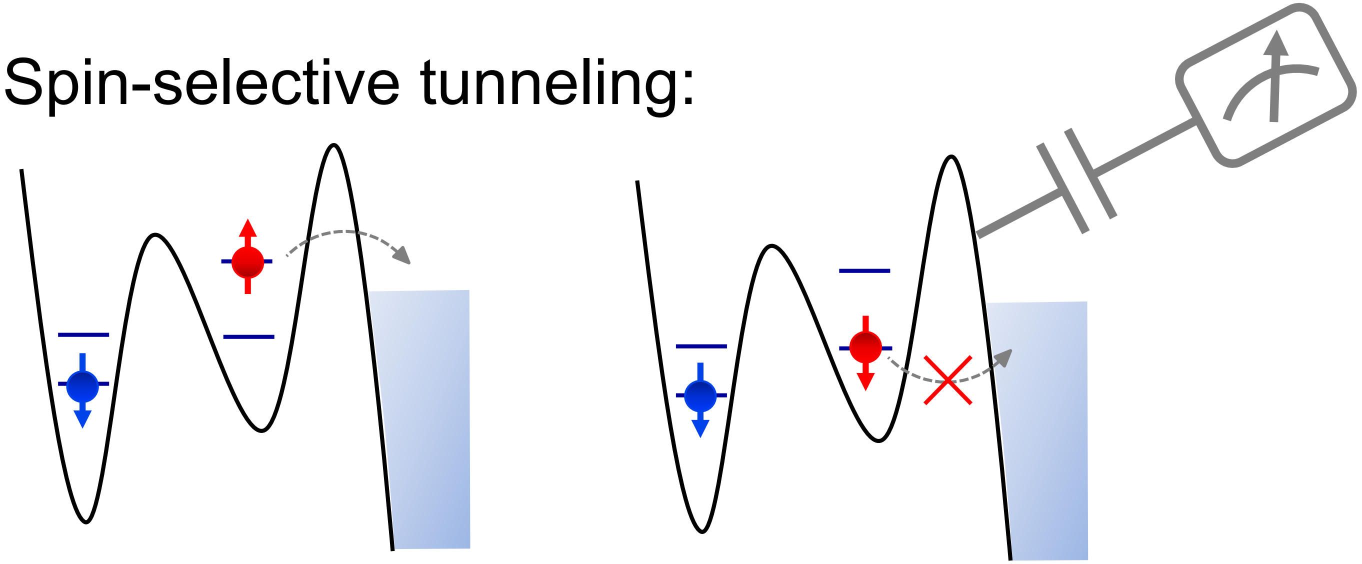

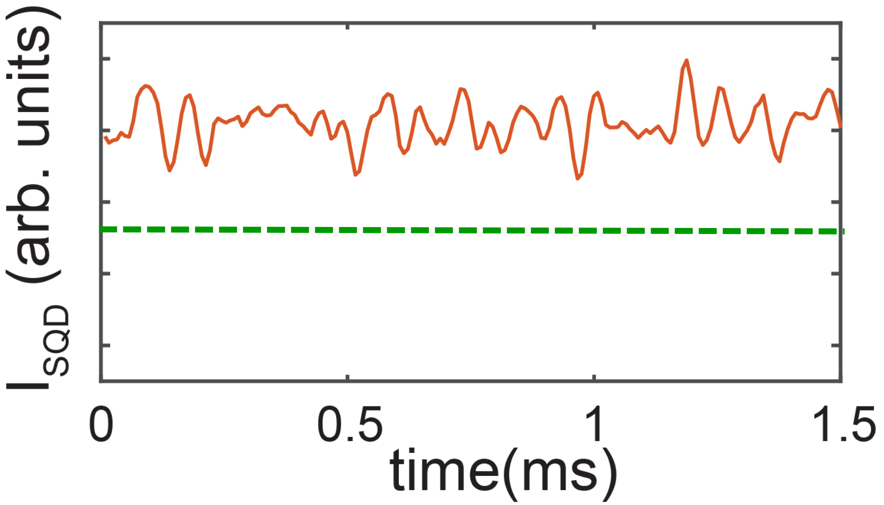

Pauli spin blockade:

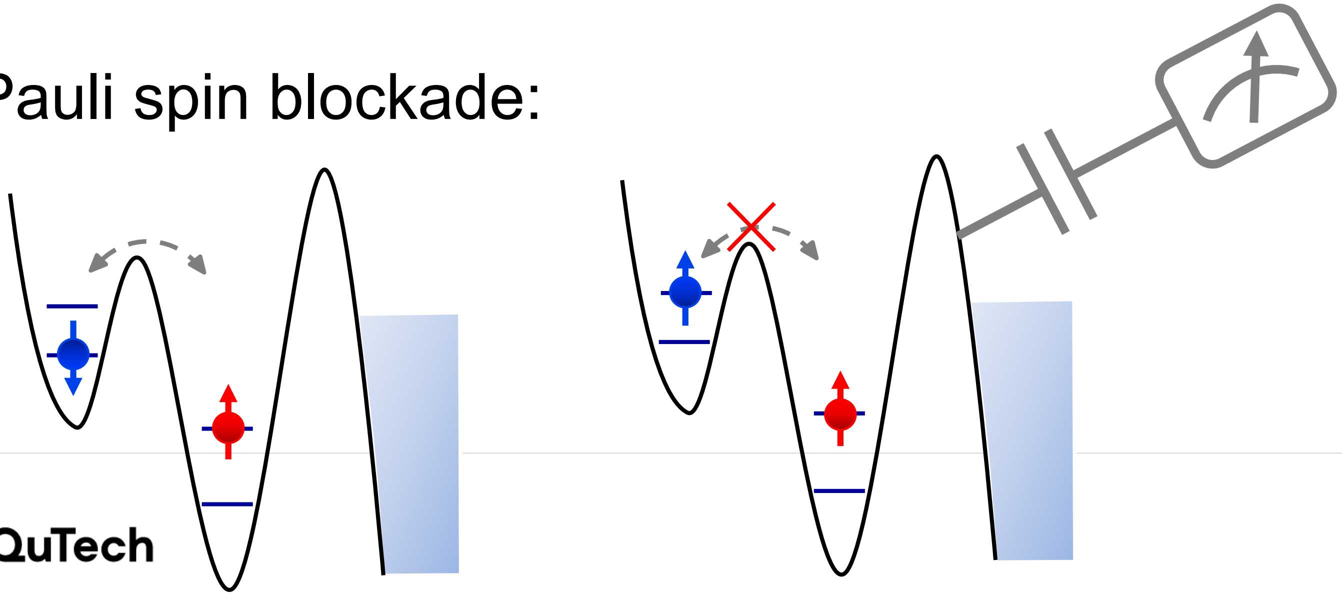

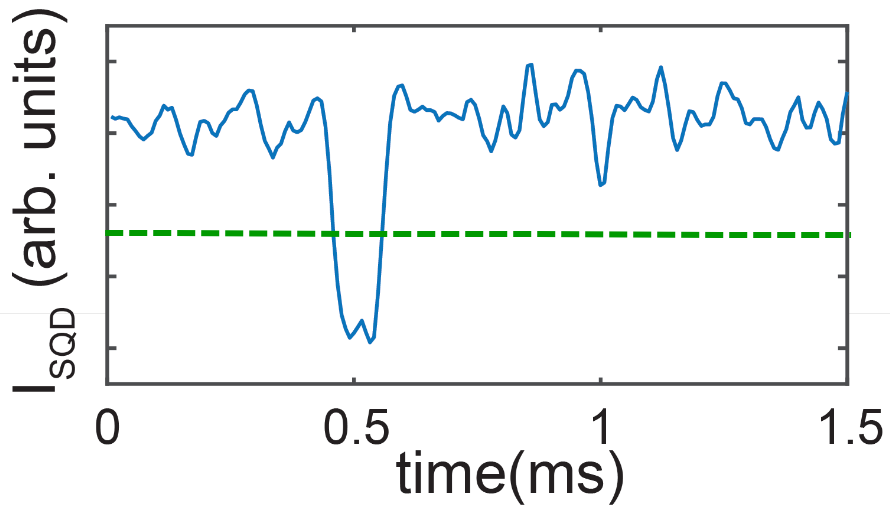

QuTech

Recap of readout

Elzerman readout:

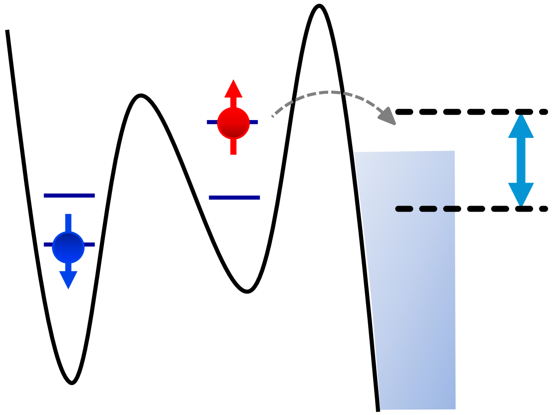

Fermi energy can be thermal-broadened

Must be operated at high field

Need an electron reservoir

Pauli spin blockade:

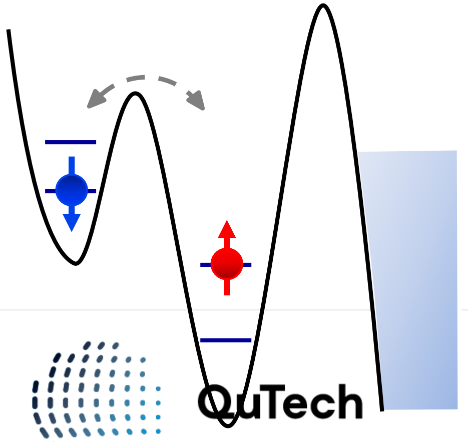

No thermal-broadening

Can be operated at low field

No need for electron reservoir

Charge stability diagram

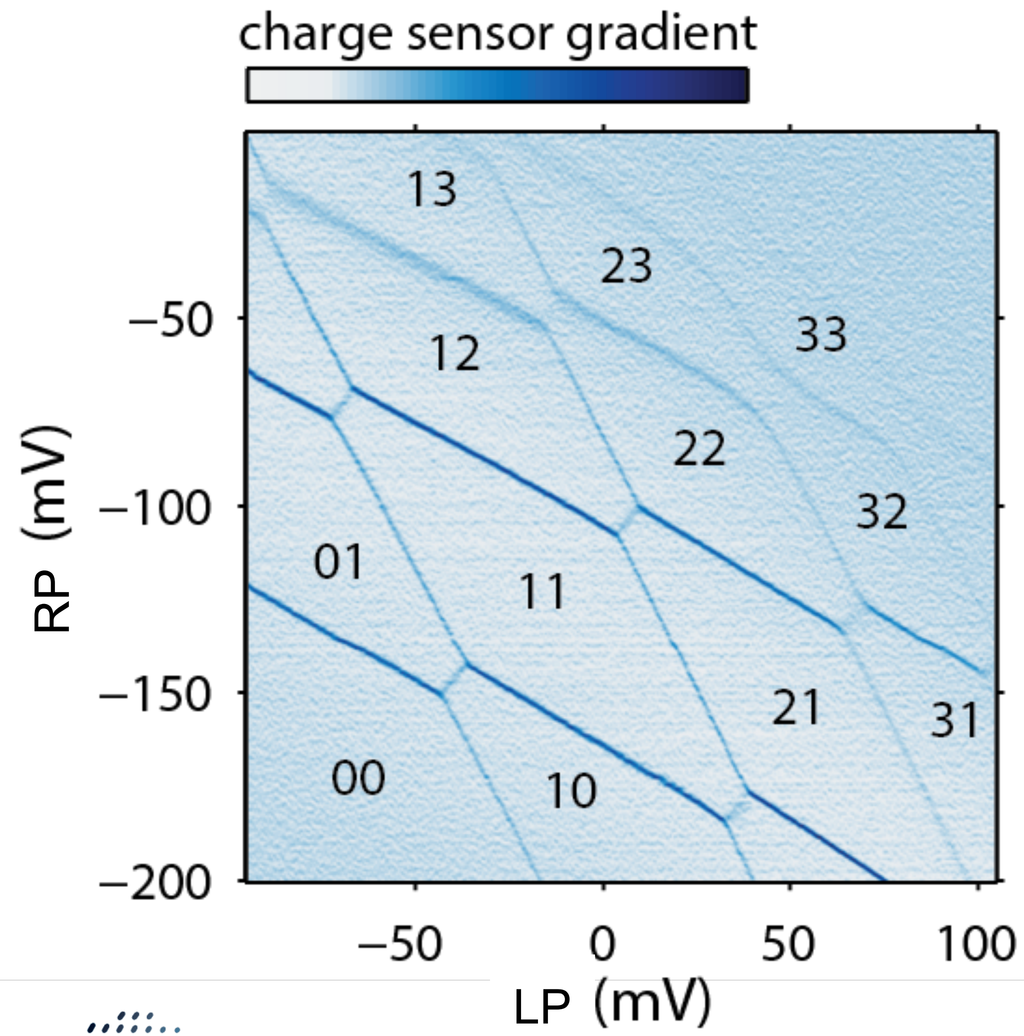

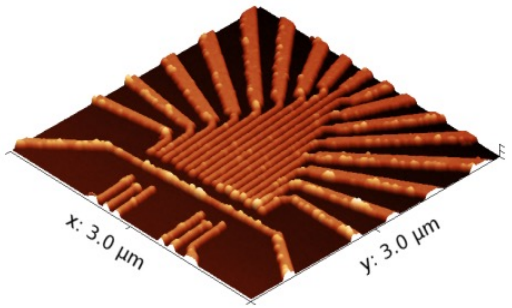

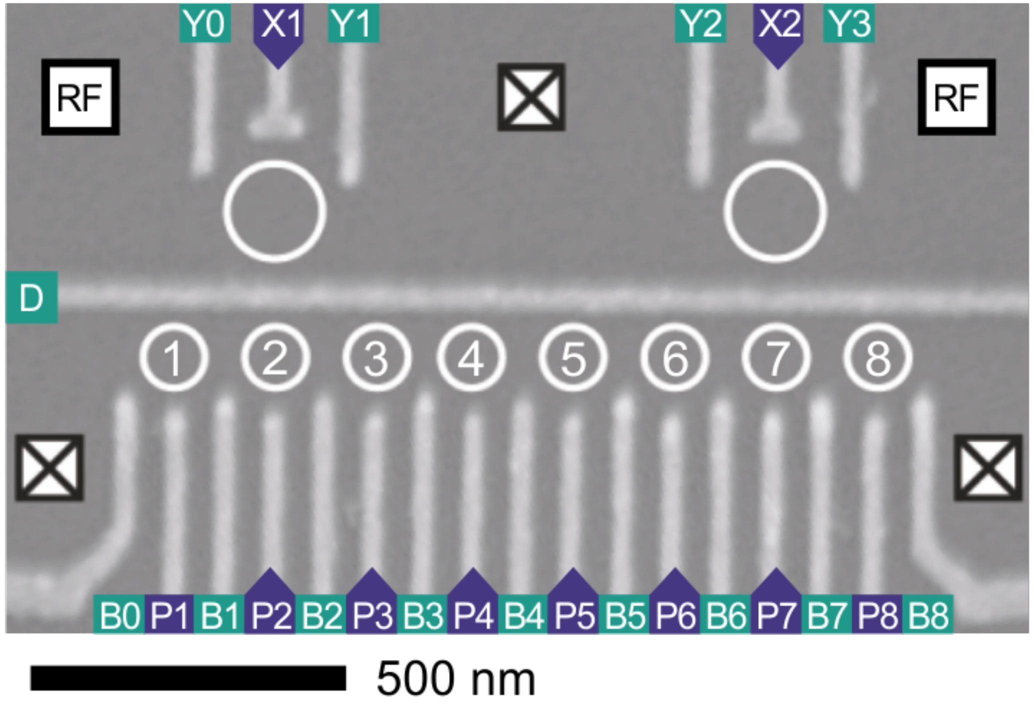

QuTech

Device fabricaton by U. Mukhopadhyay and J.P. Dehollain

Common methods are not scalable

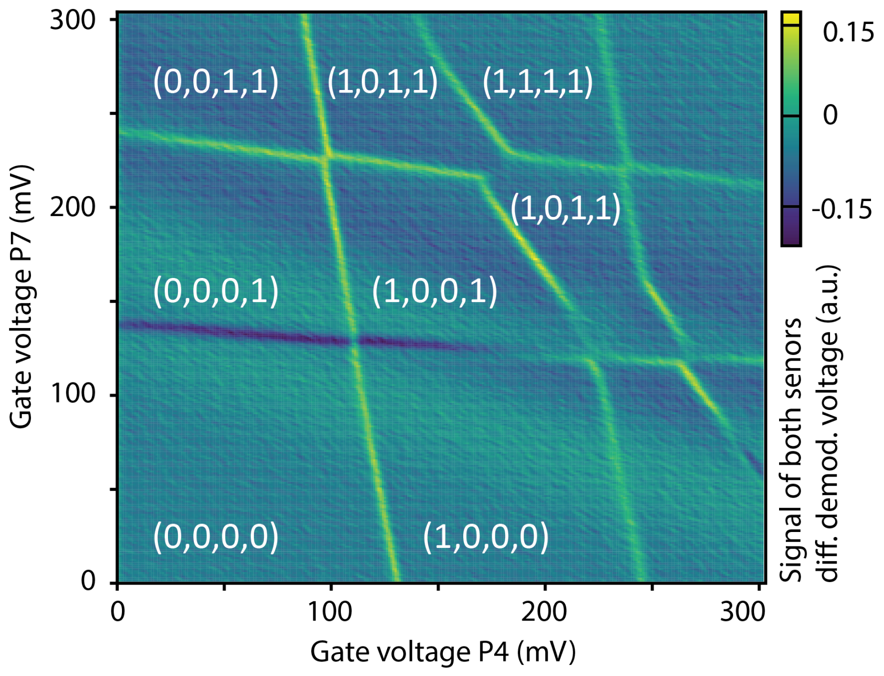

Charge stability diagram quadruple dot

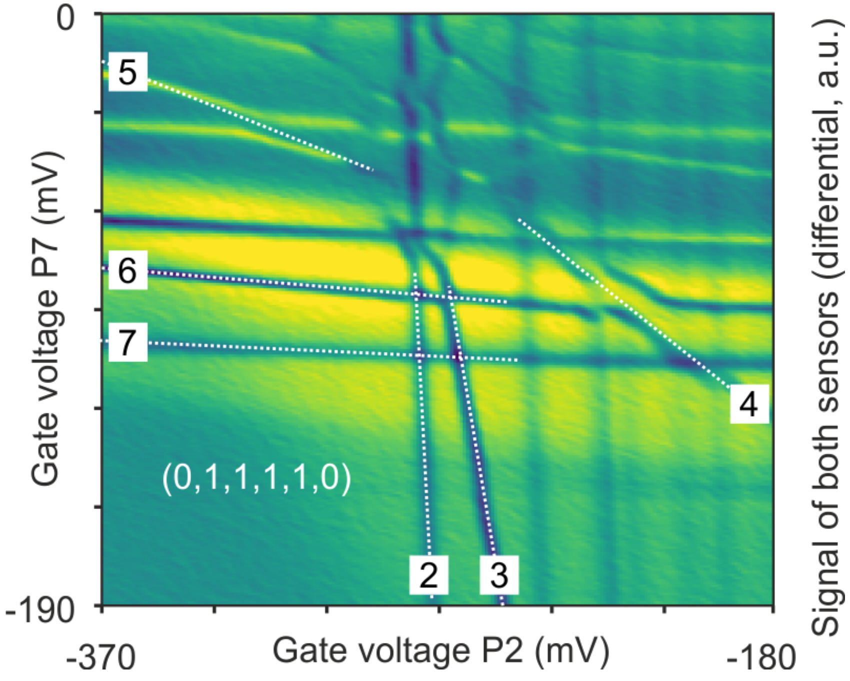

Charge stability diagram hextuple dot

Controlled filling becomes challenging due to cross-capacitances and latching effects.

QuTech

Cross capacitance

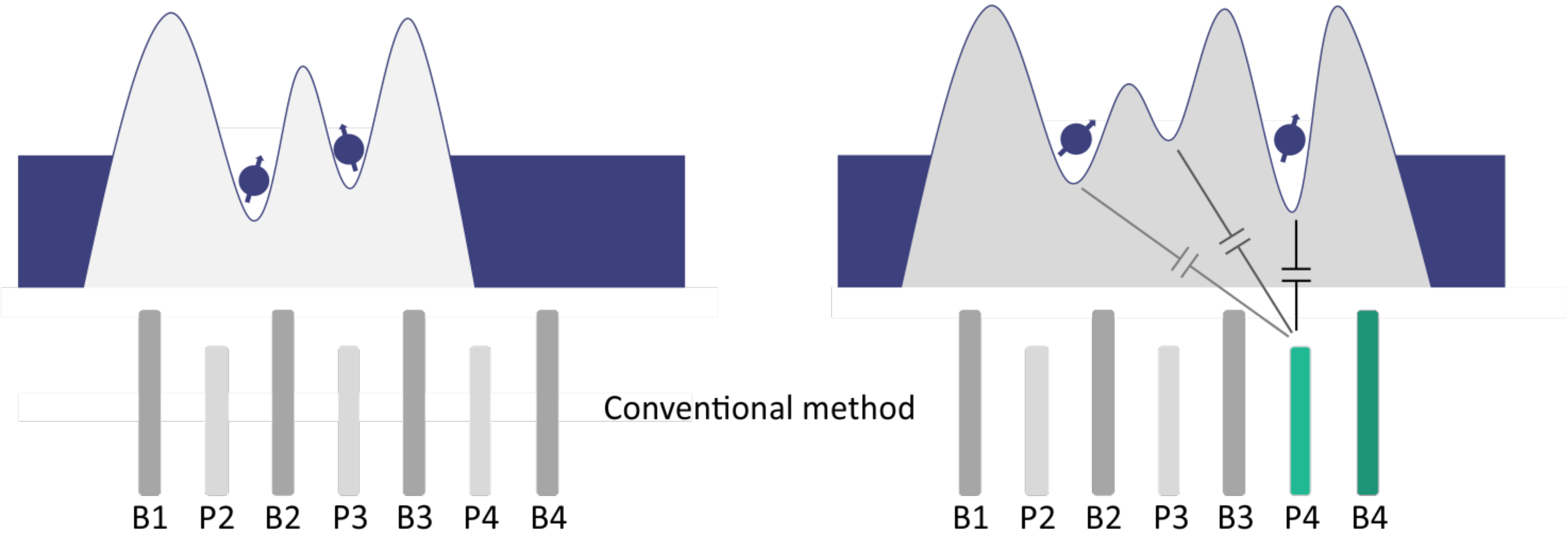

Qubit control

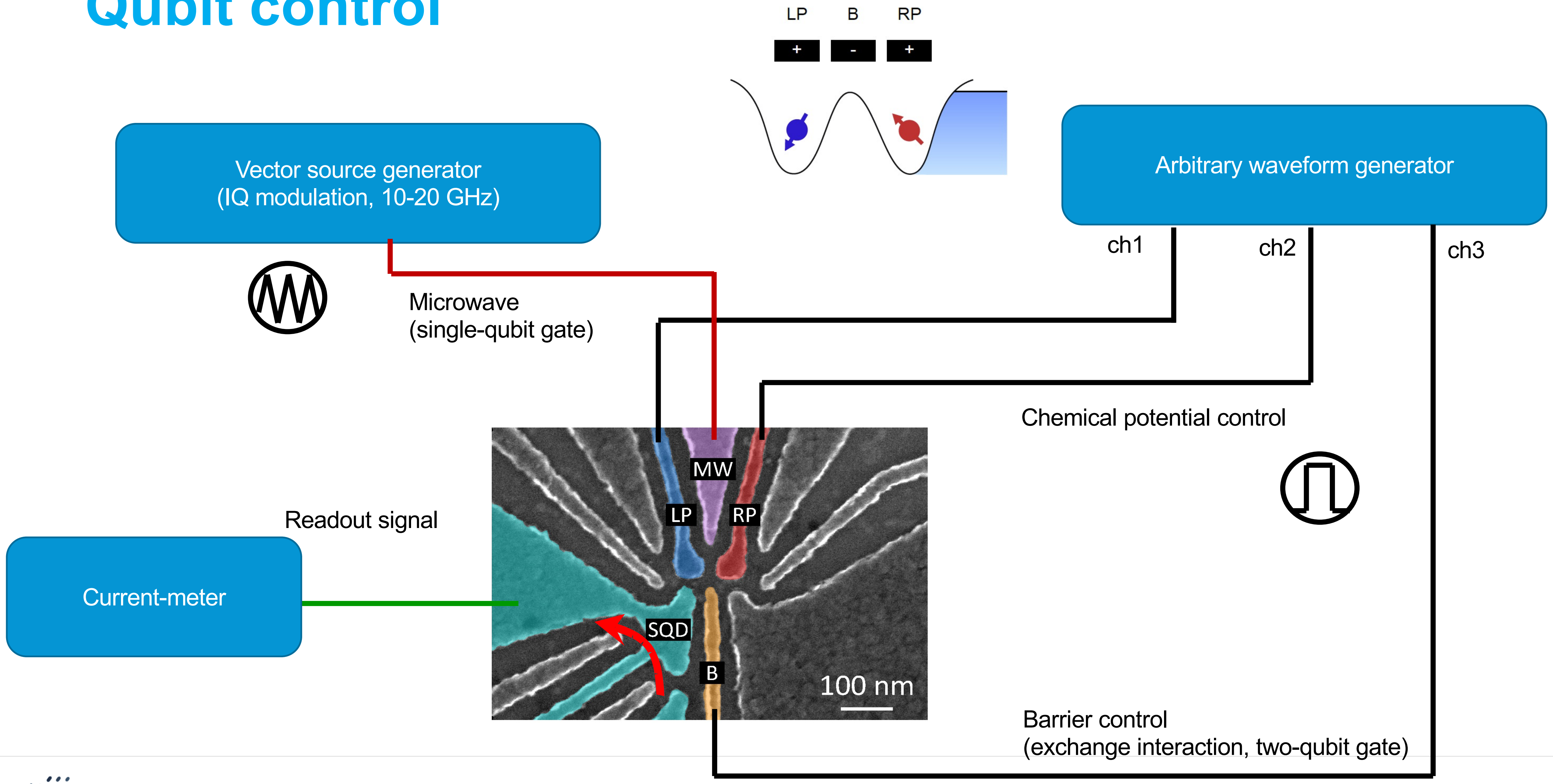

QuTech

Entering therotating frame

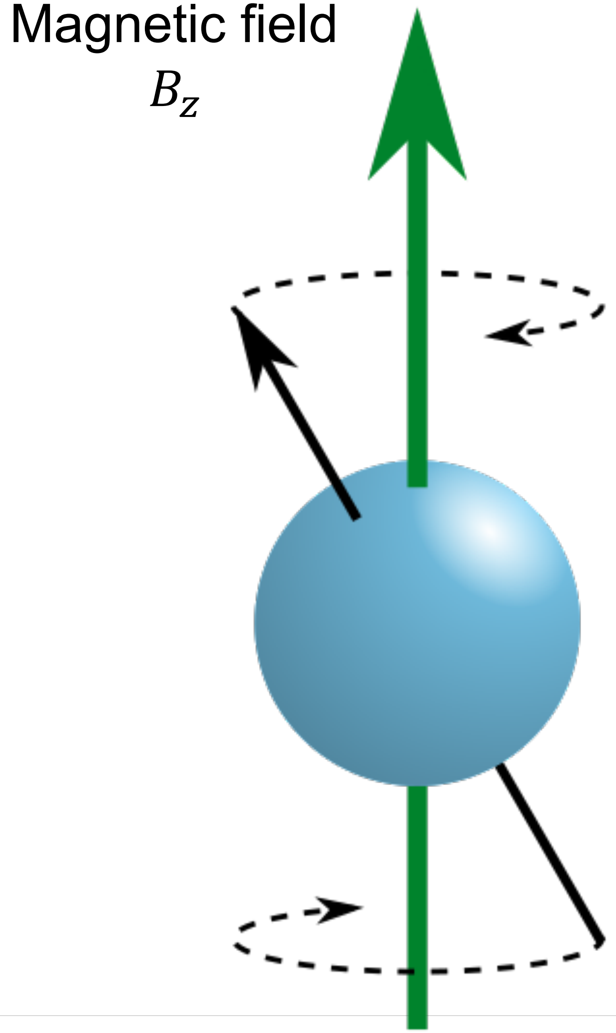

Larmor precession: electron “spins” aroud the B_z.

Q1: how to make the spin rotate around the x-axis?

A: Apply a field B_x.

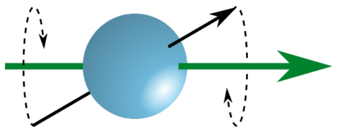

A: Simply applying a B_x field does not work.

Enter the rotating frame

$$|0(t)\rangle = e^{-iE_0 t}|0(t=0)\rangle$$

$$|1(t)\rangle = e^{-iE_1 t}|1(t=0)\rangle$$

$$= e^{-iE_0 t}e^{-i(E_1-E_0)t}|1(t=0)\rangle$$

$$= e^{-iE_0 t}e^{-ig\mu_B B_z t}|1(t=0)\rangle$$

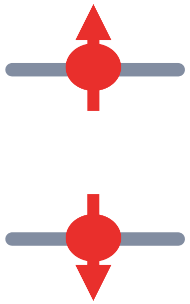

E_1

E_0

$$E_z = g\mu_B B_z$$

Step 1: ignore global phase

$$|0(t)\rangle \stackrel{\text{def}}{=} |0(t=0)\rangle$$

$$|1(t)\rangle \stackrel{\text{def}}{=} e^{-iE_z t}|1(t=0)\rangle$$

$$|0(t)\rangle + |1(t)\rangle \stackrel{\text{def}}{=} |0(t=0)\rangle + e^{-iE_z t}|1(t=0)\rangle$$

Q3: why is the qubit vector static in Bloch sphere?

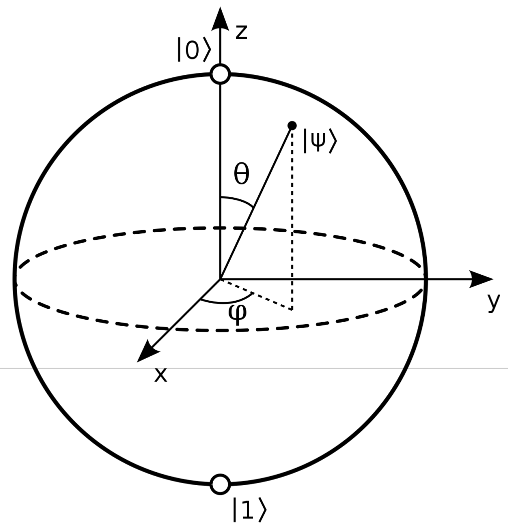

QuTech

Enter the rotating frame

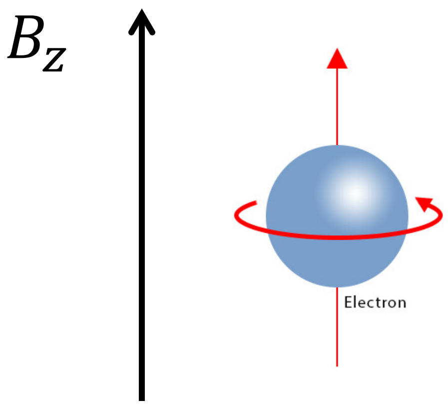

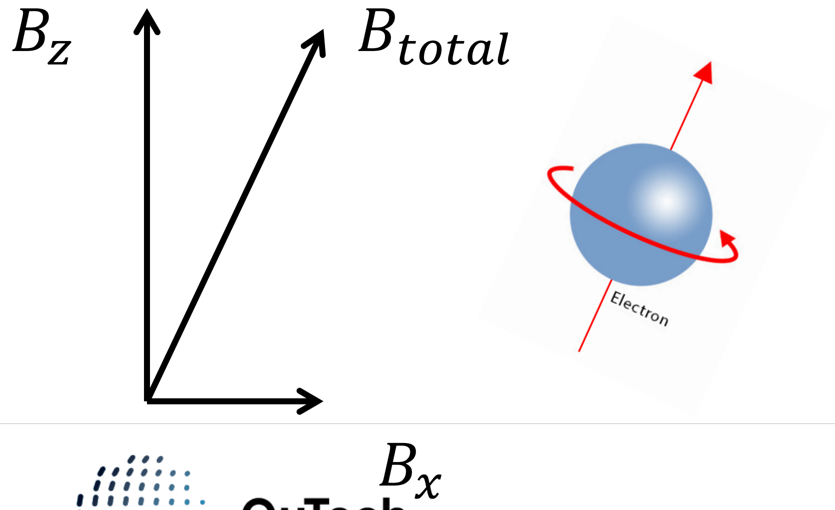

Simply applying a B_x field does not work.

For the electron, B_x is osillating.

Q2: Why do we use microwave to rotate the spin?

Hint: It’s an oscillating electro-magnetic field.

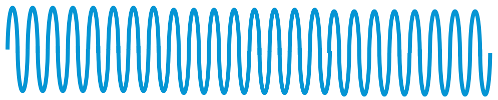

Enter the rotating frame

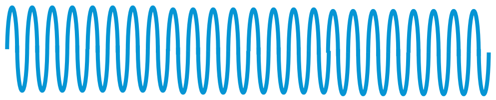

Step 2: Decompose oscillating field into two rotating fields.

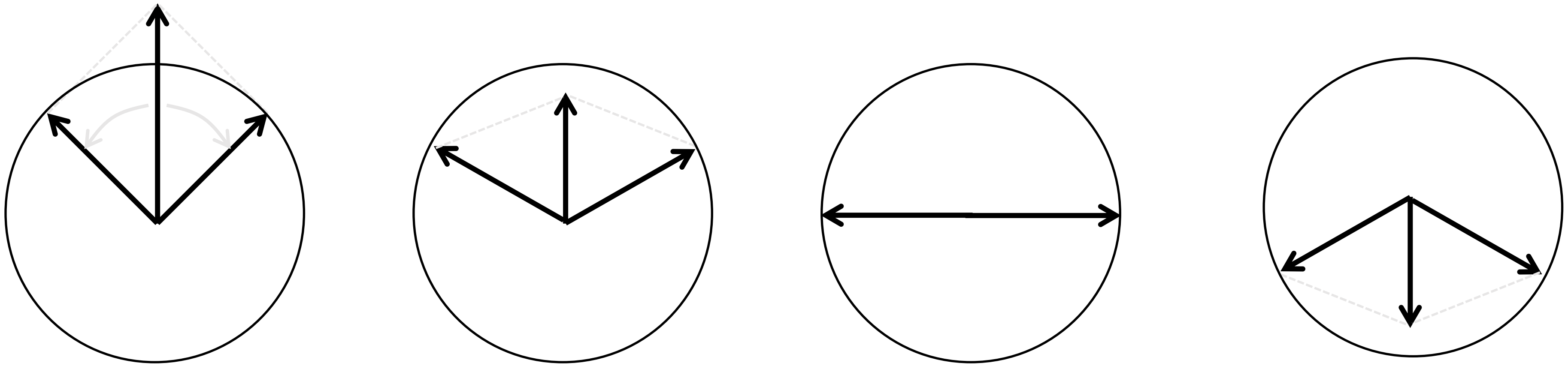

One will rotate in same direction as spins.

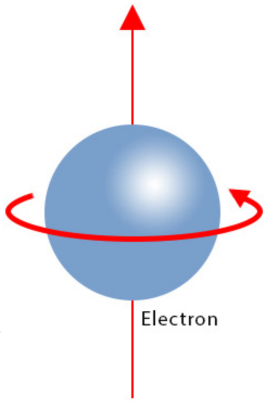

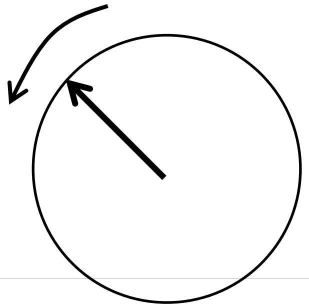

Static field in the rotating frame

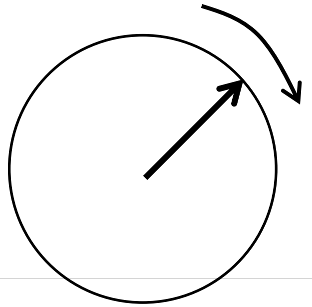

Oscillating twice as fast -> ignored

QuTech

Enter the rotating frame

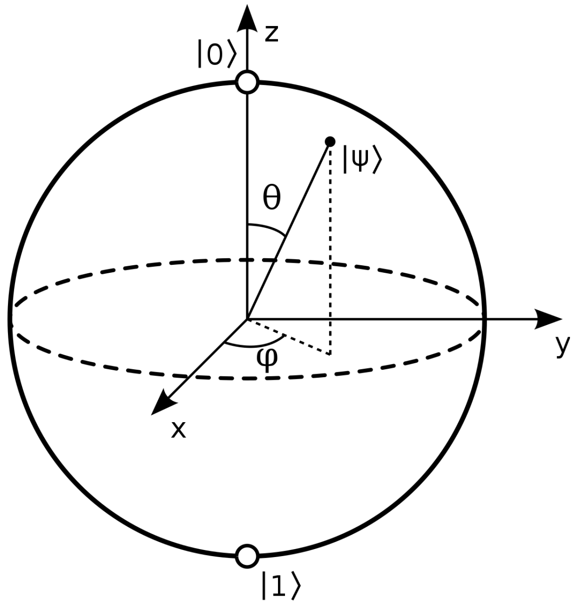

Q3: Why is the qubit vector static in Bloch sphere?

A: Bloch sphere is plotted in the rotating frame.

Rabi oscillation

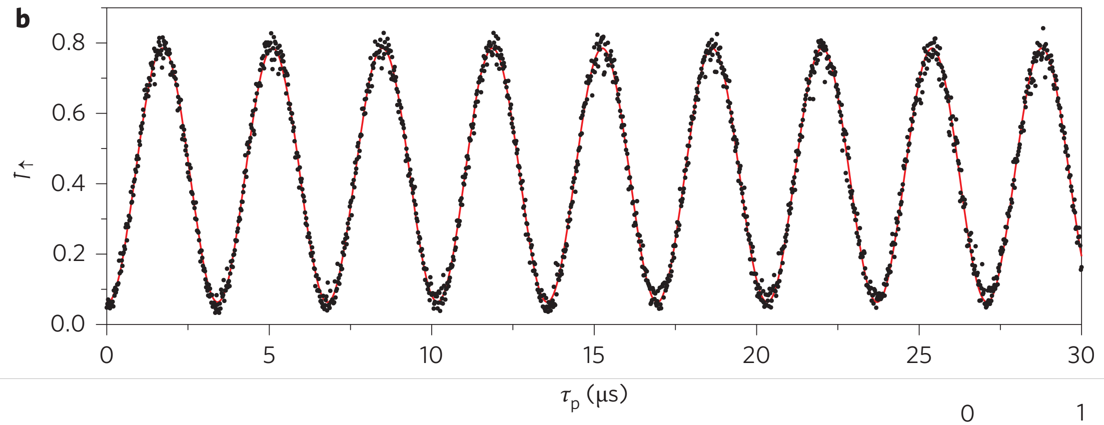

Precession

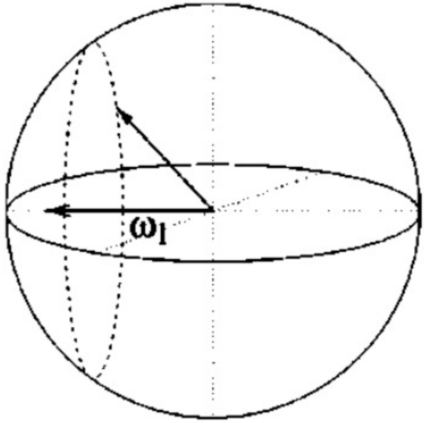

Rotating frame

Nutation

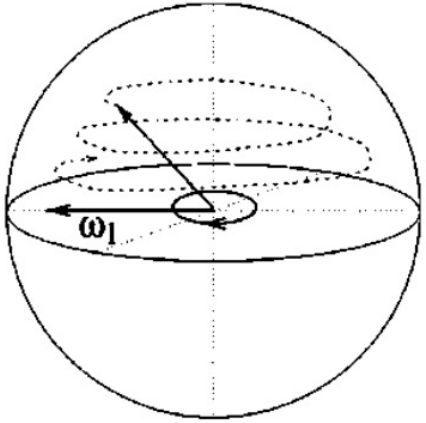

Laboratory frame

QuTech

Veldhorst et al, Nature Nano 2014

Z gate and dephasing

$$|0(t)\rangle = |0(t=0)\rangle \xrightarrow{rotating\ frame} |0\rangle$$

$$|1(t)\rangle = e^{-iE_z t}|1(t=0)\rangle \xrightarrow{rotating\ frame} |1\rangle$$

$$|0(t)\rangle + |1(t)\rangle = |0(t=0)\rangle + e^{-iE_z t}|1(t=0)\rangle \xrightarrow{rotating\ frame} |0\rangle + |1\rangle$$

A rotating frame is determined by the energy splitting (frequency) of the qubit.

Q4: What if we change the qubit energy intentionally?

A: Z gate.

$$|0(t)\rangle + |1(t)\rangle = |0(t=0)\rangle + e^{-i(E_z+\Delta E)t}|1(t=0)\rangle \xrightarrow{rotating\ frame} |0\rangle + e^{-i\Delta E t}|1\rangle$$

Q5: What if the qubit energy fluctuates under environmental noise?

A: Dephasing.

$$|0(t)\rangle + |1(t)\rangle = |0(t=0)\rangle + e^{-i(E_z+\delta E(t))t}|1(t=0)\rangle \xrightarrow{rotating\ frame} |0\rangle + e^{-i\delta E(t)t}|1\rangle$$

QuTech

Single-qubit gate: ESR and EDSR

Electron spin resonance

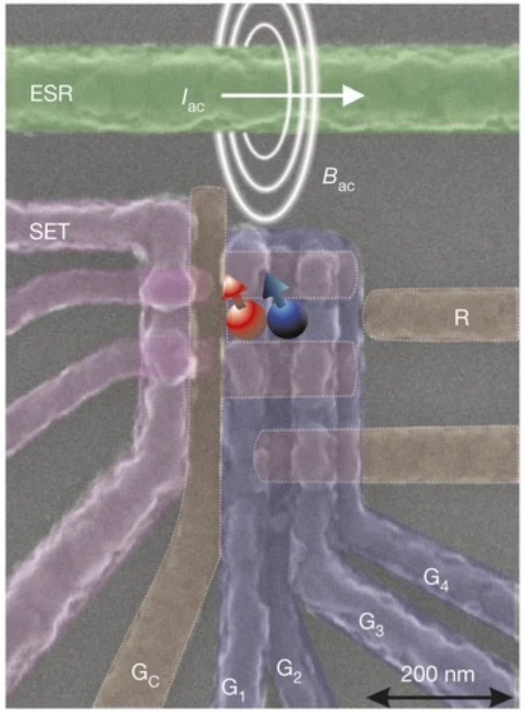

Oscillating B field

Electric dipole spin resonance

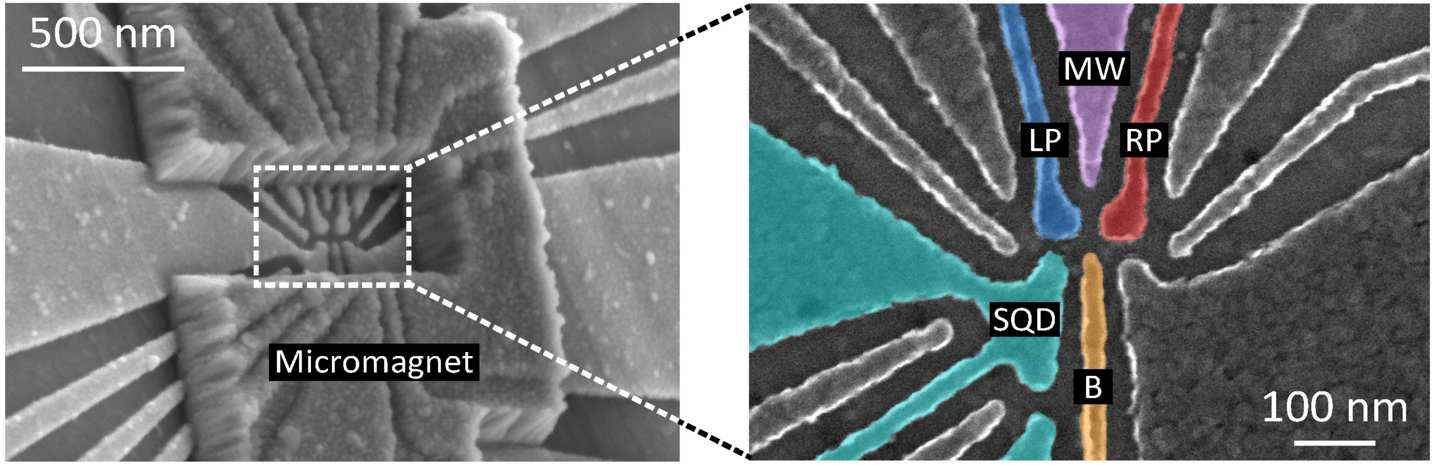

Cobalt micromagnet
enabling single-qubit gates

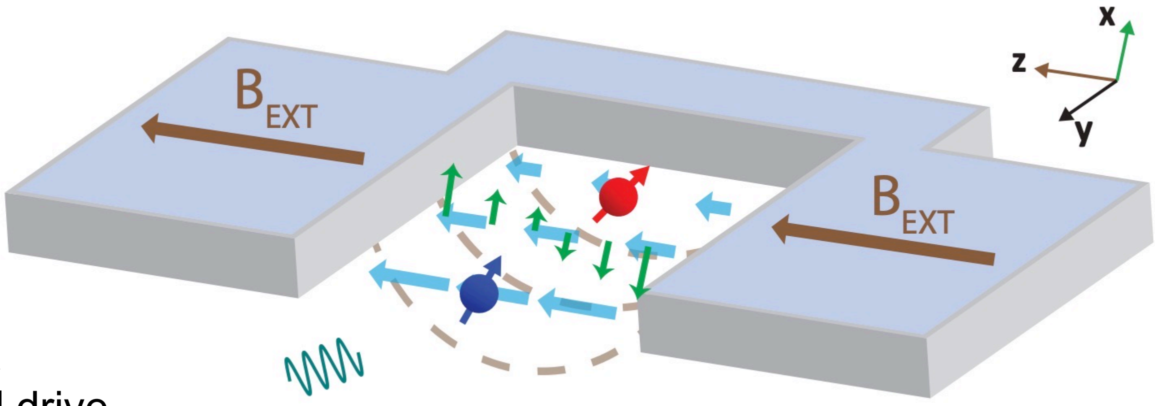

Electrical drive
-->
Effective oscillating magnetic field

QuTech

Frequency selectivity and Crosstalk

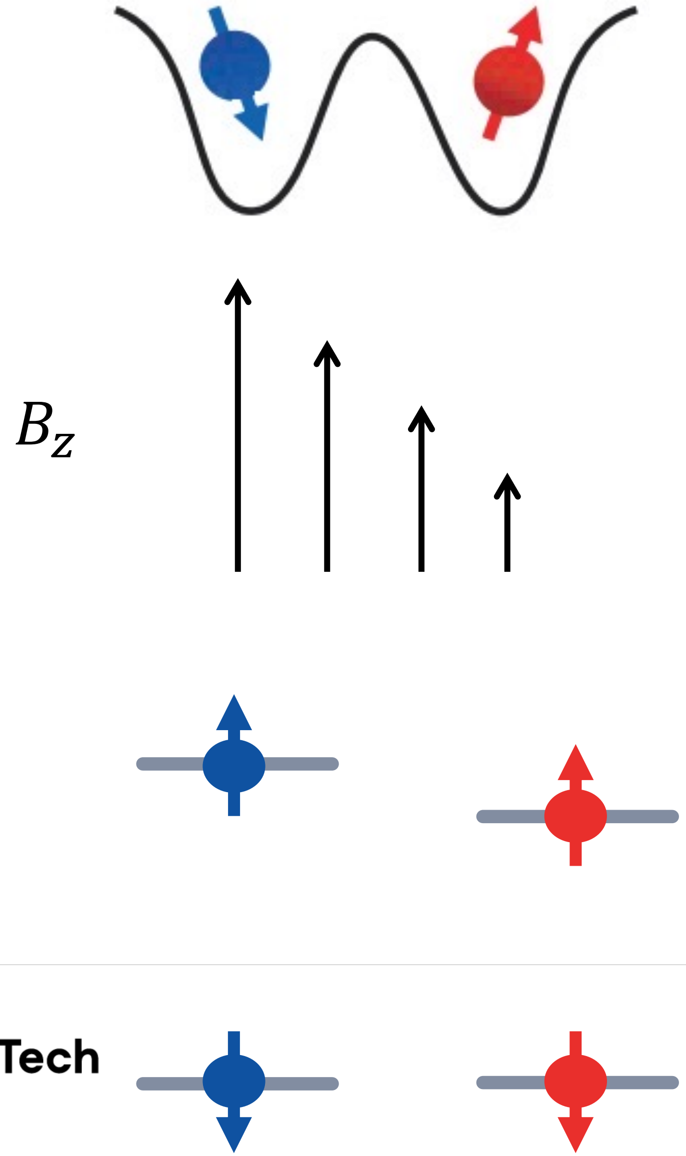

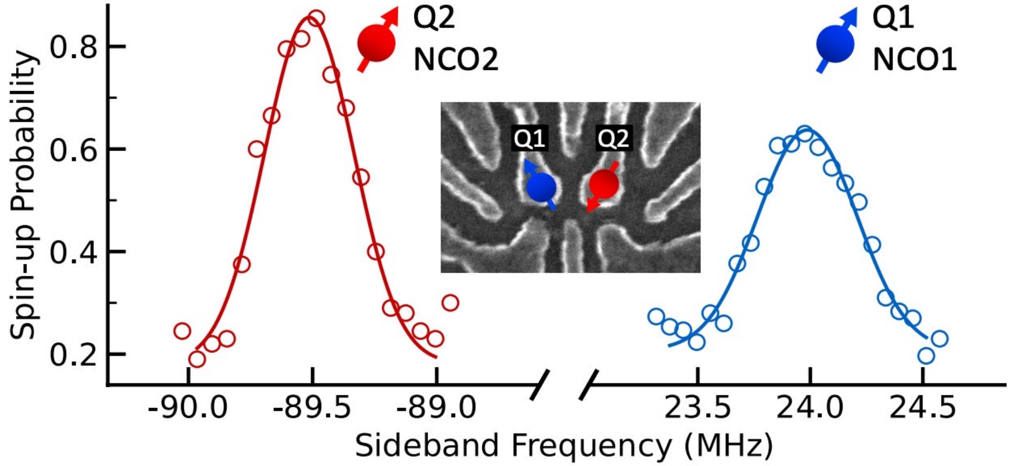

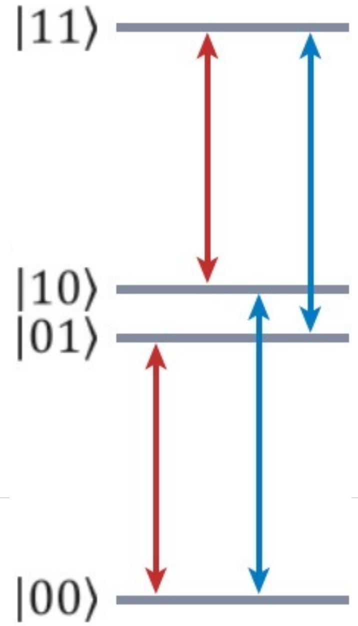

QuTech

Two-qubit gate: exchange interaction

Eigenstates (uncoupled)	Eigenstates (coupled)
$\lvert\uparrow\uparrow\rangle$	$\lvert\uparrow\uparrow\rangle$
$\lvert\downarrow\uparrow\rangle$	$(\lvert\downarrow\uparrow\rangle + \lvert\uparrow\downarrow\rangle)/\sqrt{2}$
$\lvert\uparrow\downarrow\rangle$	$(\lvert\downarrow\uparrow\rangle - \lvert\uparrow\downarrow\rangle)/\sqrt{2}$
$\lvert\downarrow\downarrow\rangle$	$\lvert\downarrow\downarrow\rangle$

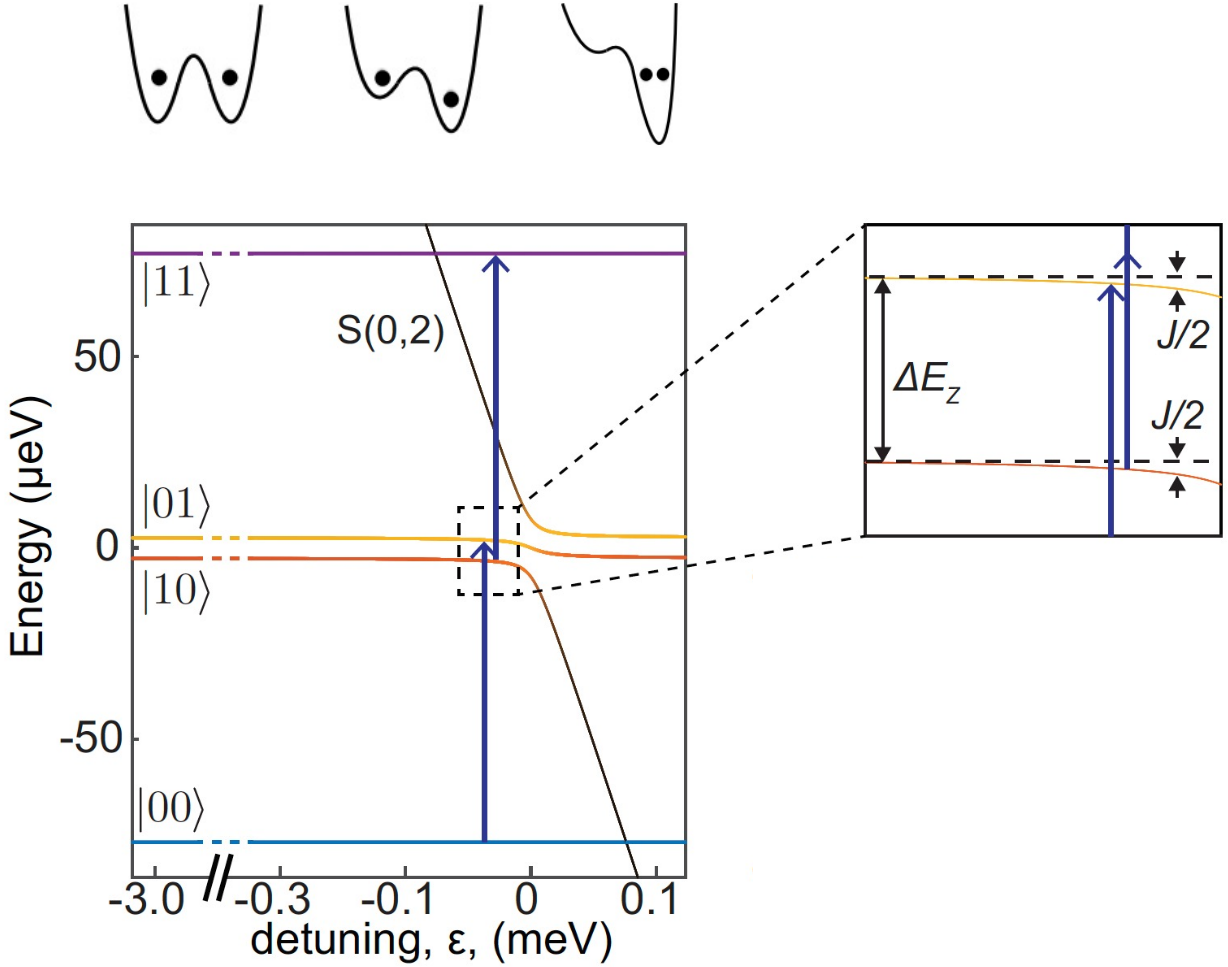

$$H_{exc} = J\vec{S_1}\cdot\vec{S_2} = J(\cancel{S_{1x}\cdot S_{2x} + S_{1y}\cdot S_{2y} +} S_{1z}\cdot S_{2z})$$

QuTech

Two-qubit gates

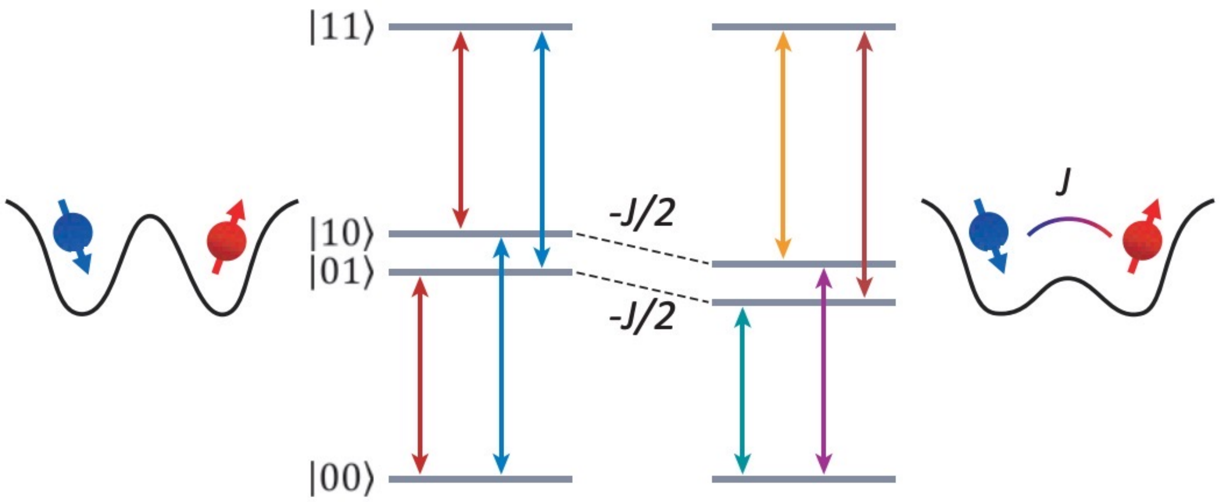

Conditional rotation:

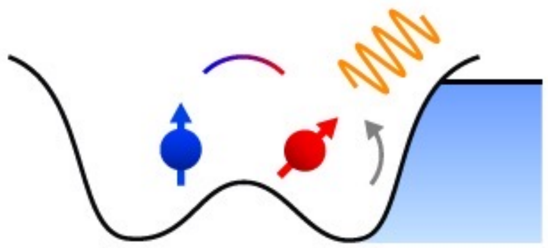

Conditional phase:

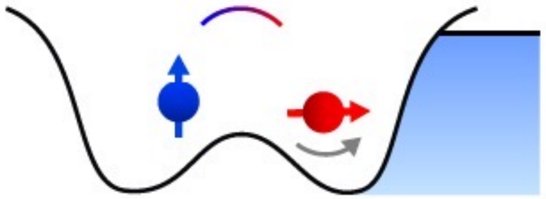

C-Phase: $$U_J(t) = \begin{pmatrix} 1 & 0 & 0 & 0 \\ 0 & e^{iJ(\epsilon)t/2\hbar} & 0 & 0 \\ 0 & 0 & e^{iJ(\epsilon)t/2\hbar} & 0 \\ 0 & 0 & 0 & 1 \end{pmatrix}$$

CZ: $$Z_1\left(-\frac{\pi}{2}\right)Z_2\left(-\frac{\pi}{2}\right)U_J\left(\frac{\pi\hbar}{J(\epsilon)}\right) = \begin{pmatrix} 1 & 0 & 0 & 0 \\ 0 & 1 & 0 & 0 \\ 0 & 0 & 1 & 0 \\ 0 & 0 & 0 & -1 \end{pmatrix}$$

Pulse sequence

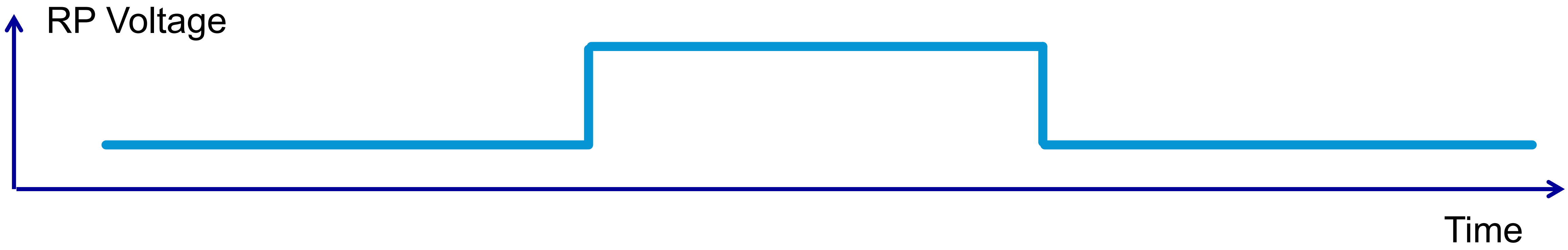

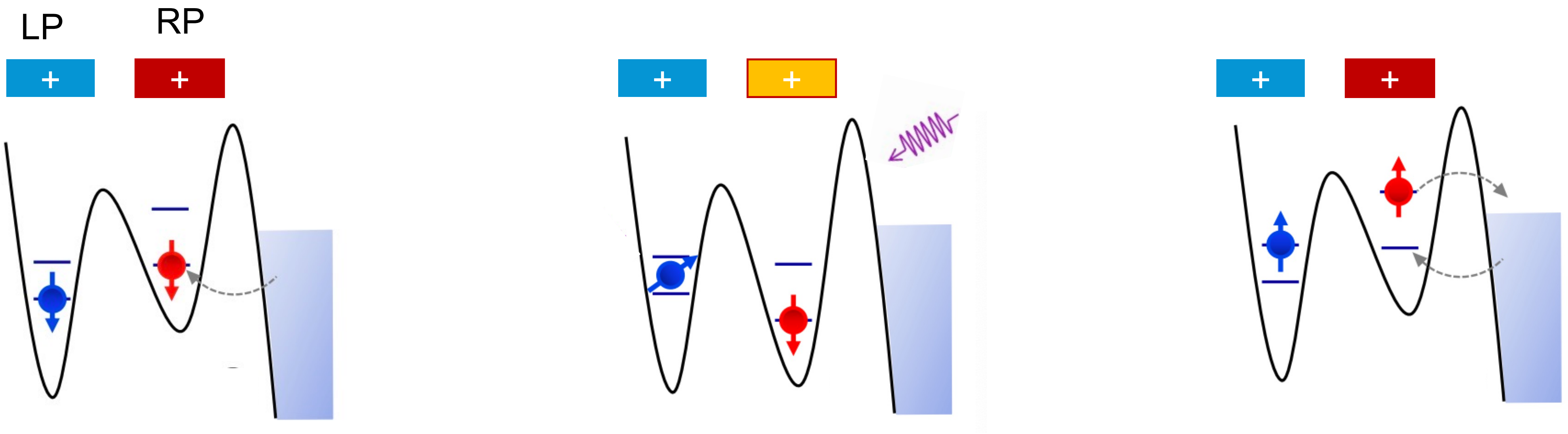

Step 1
Initialization

Step 2
Operation

Step 3
Readout

QuTech

Pulse sequence

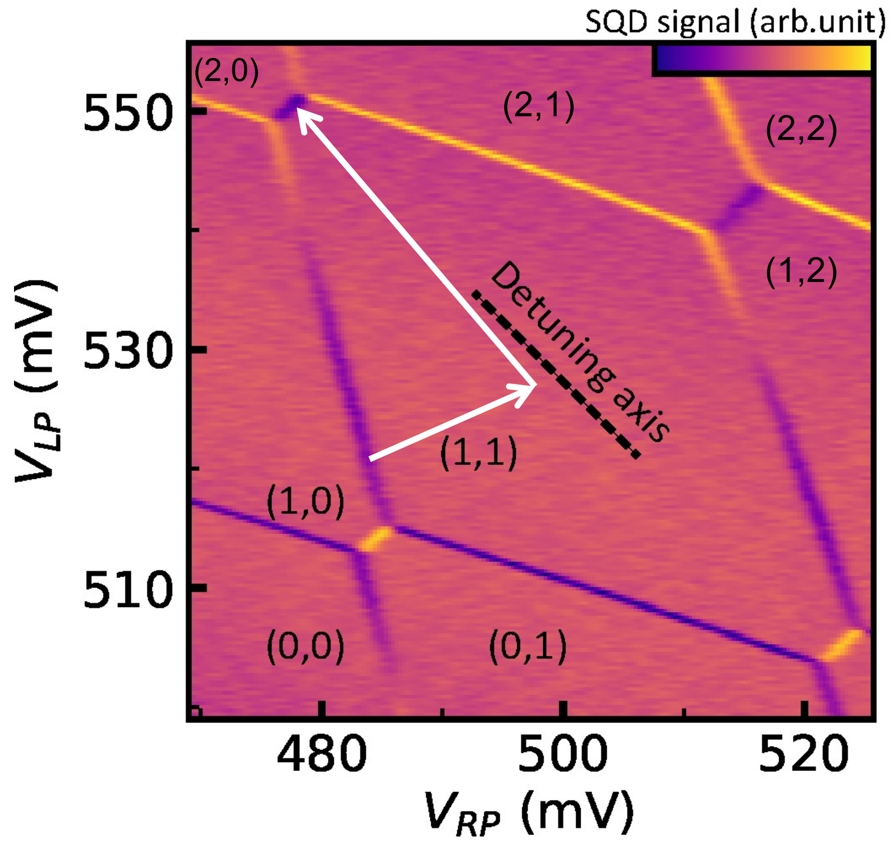

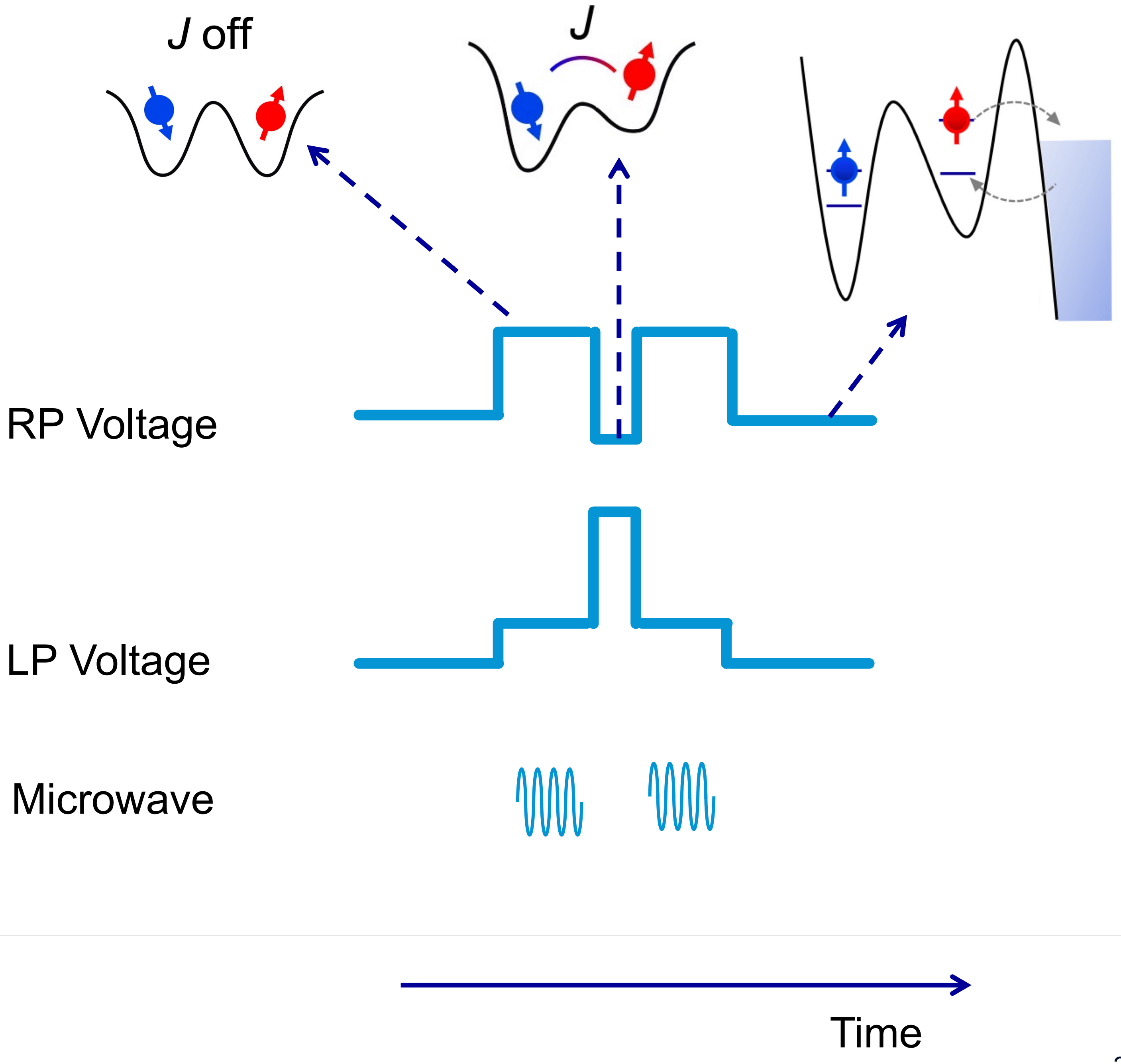

Error mechanism: Nuclear spins

$$\mathcal{H} = g\mu_B \vec{S}\,\vec{B} + \vec{S}\underbrace{\sum_i A_i \vec{I}_i}_{\text{Overhauser field } B_N}$$

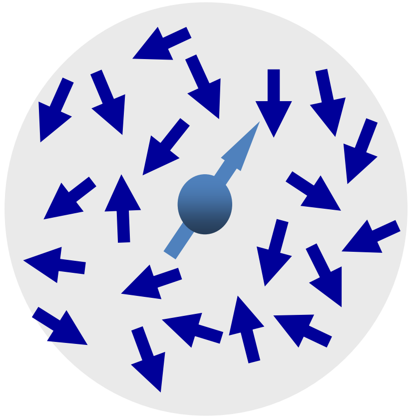

Full polarization

$\uparrow\uparrow\uparrow\uparrow\uparrow\uparrow\uparrow\uparrow\uparrow\uparrow\uparrow$

$$A = \sum_i A_i$$

GaAs: A ~ 5.5 T
Paget, 1977

Statistical polarization

$$A/\sqrt{N}$$

GaAs dot: $N \sim 10^6$
$B_N = A / N^{1/2} \sim 5$ mT

Merkulov, Efros, Rosen, PRB 2002
Khaetskii, Loss, Glazman, PRL 2002

QuTech

Error mechanism: Nuclear spins

$$\mathcal{H} = g\mu_B \vec{S}\,\vec{B} + \underbrace{\vec{S}\sum_i A_i \vec{I}_i}_{\text{Overhauser field } B_N}$$

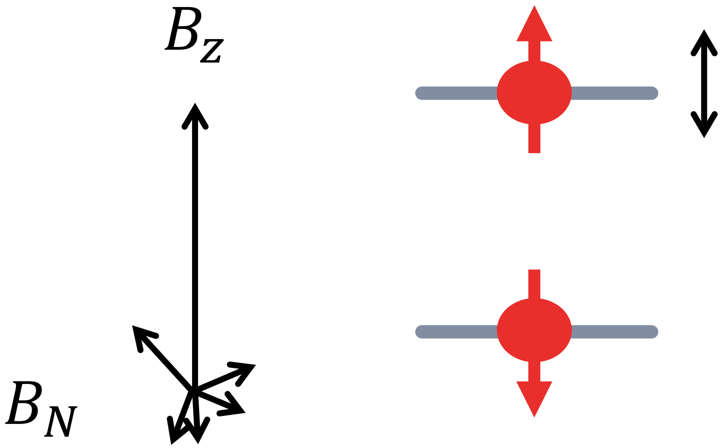

$$|0(t)\rangle + |1(t)\rangle = |0(t=0)\rangle + e^{-i(E_z+\delta E(t))t}|1(t=0)\rangle \xrightarrow{rotating\ frame} |0\rangle + e^{-i\delta E(t)t}|1\rangle$$

$$\delta E(t) = g\mu_B B_N(t)$$

Materials impact on coherence time

GaAs

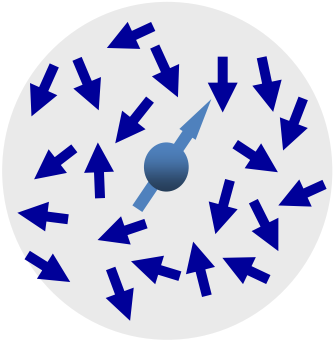

$T_2^* \sim 10$ ns

$T_2^{DD} < 0.2$ ms

Petta et al,
Science 2005

Si

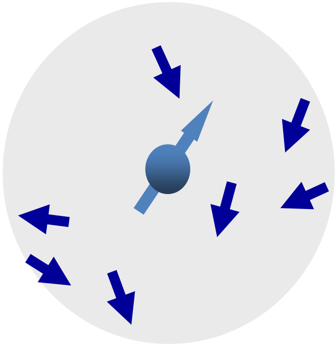

$T_2^* \sim 1\ \mu s$

$T_2^{DD} > 0.5$ ms

Kawakami, Scarlino, et al,
Nature Nano 2014

^{28}Si

$T_2^* \sim 100\ \mu s$

$T_2^{DD} \sim 28$ ms

Veldhorst, et al,
Nature Nano 2014

Error mechanism: Charge noise

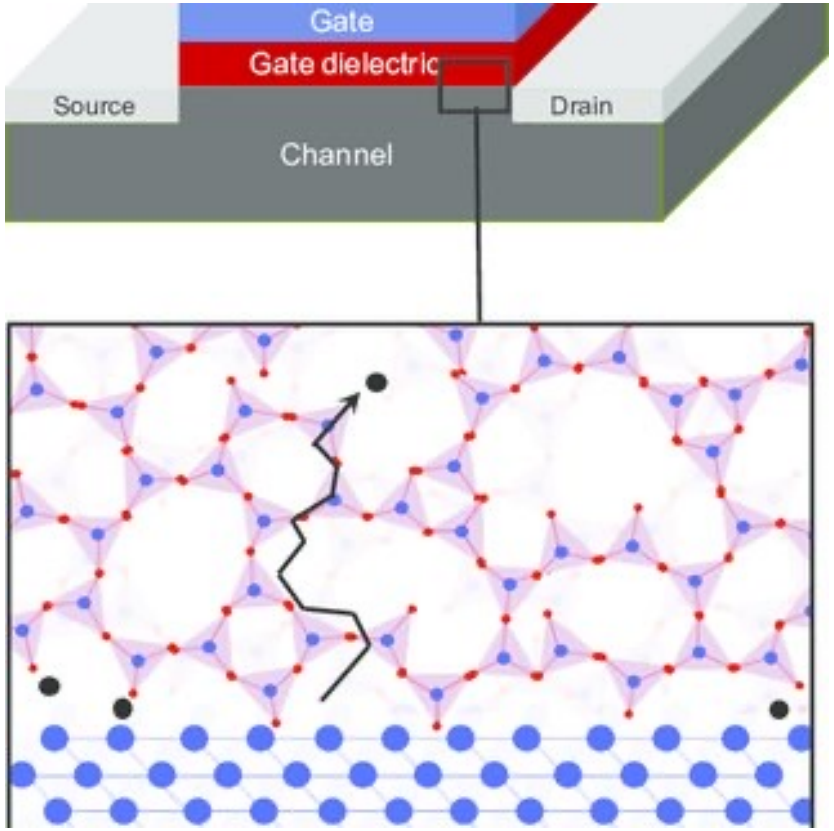

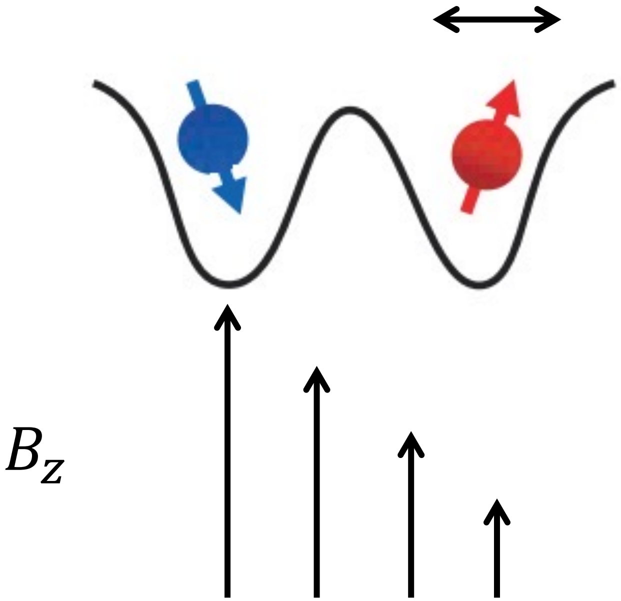

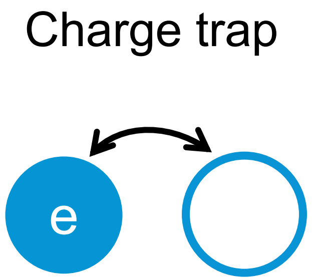

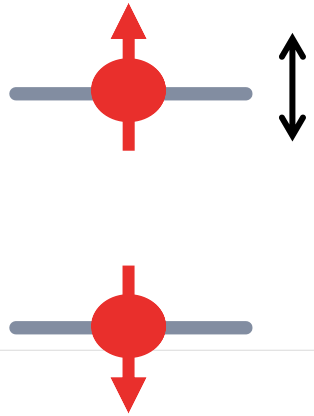

$$|0\rangle + e^{-i\delta E(x(t))t}|1\rangle$$

$$\delta E(x(t)) = g\mu_B B_z(x(t))$$

Arash Sheikholeslam et al.,
Journal of Material Chemistry C 2016

Valleys in silicon

Orbital splitting: >1 meV
Valley splitting: 0 – 300 μeV
Zeeman splitting: 30 – 80 μeV
1 GHz = 4 μeV

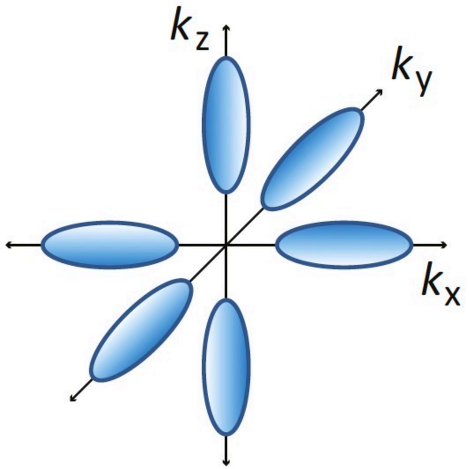

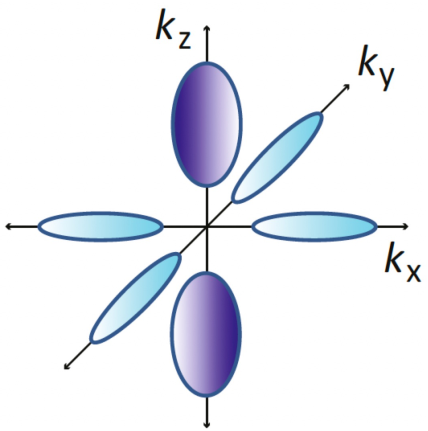

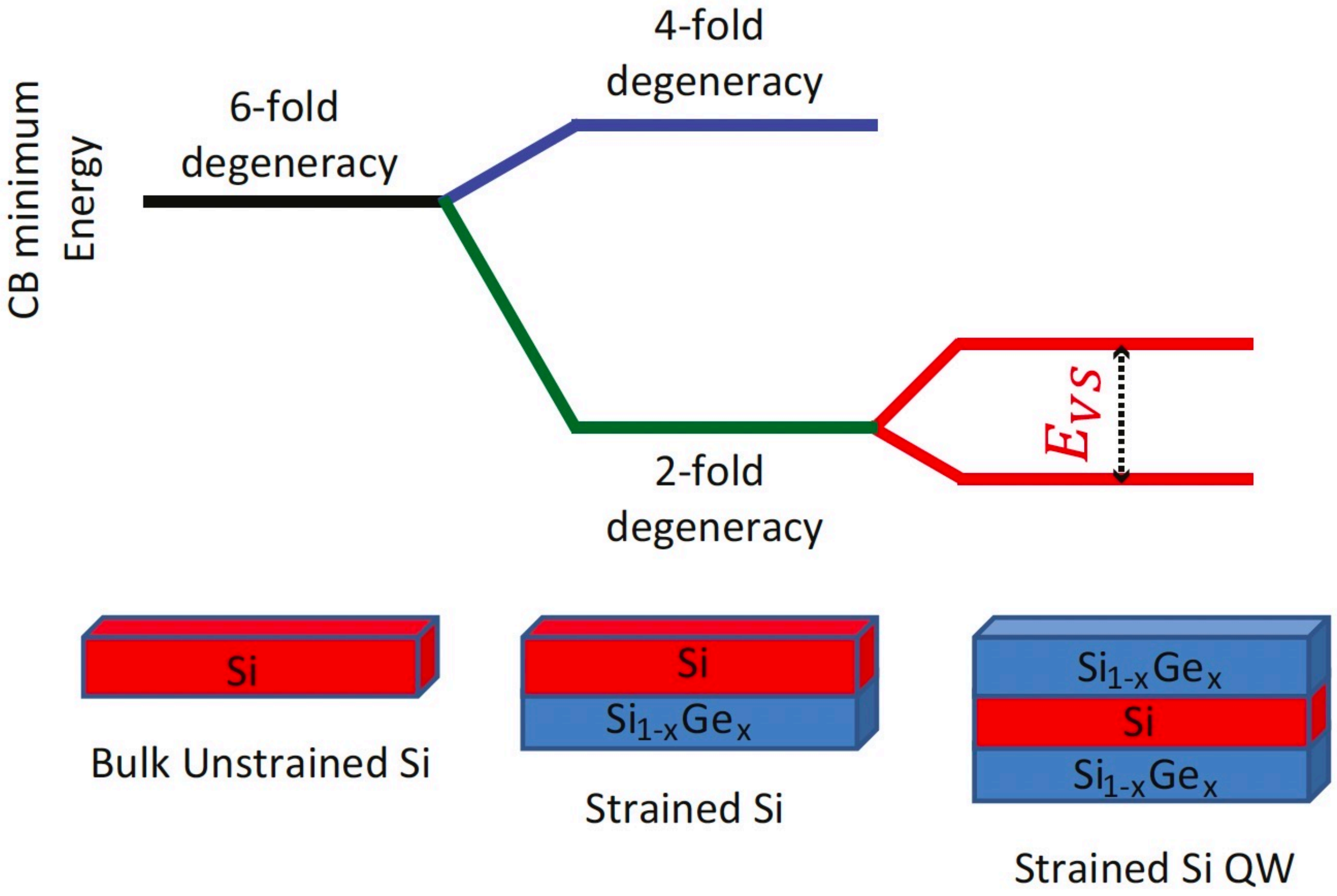

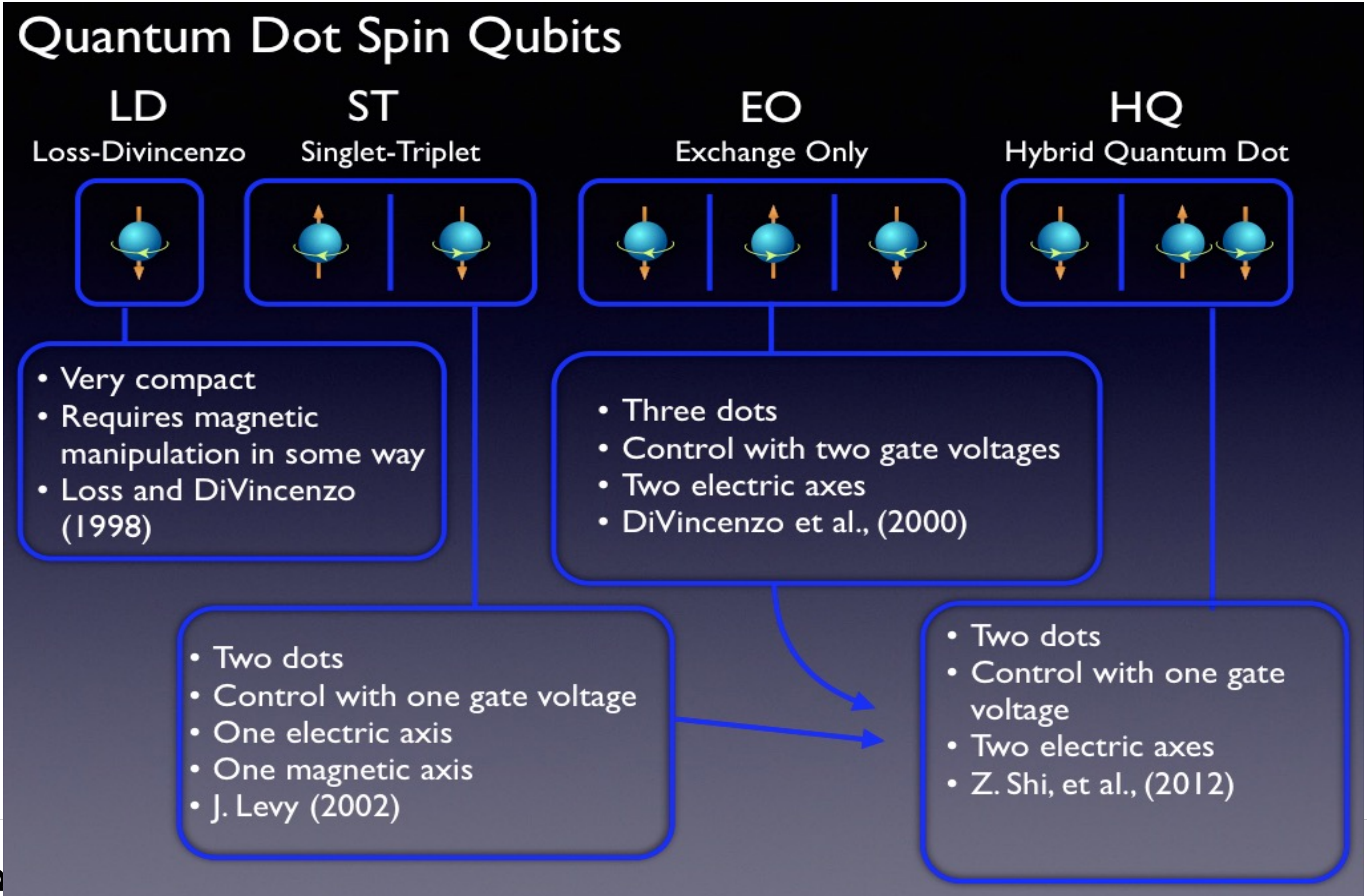

Slide courtesy Mark Eriksson

Alternative: Singlet-Triplet qubit

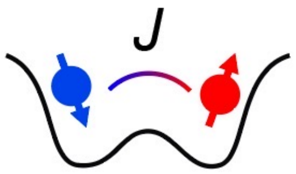

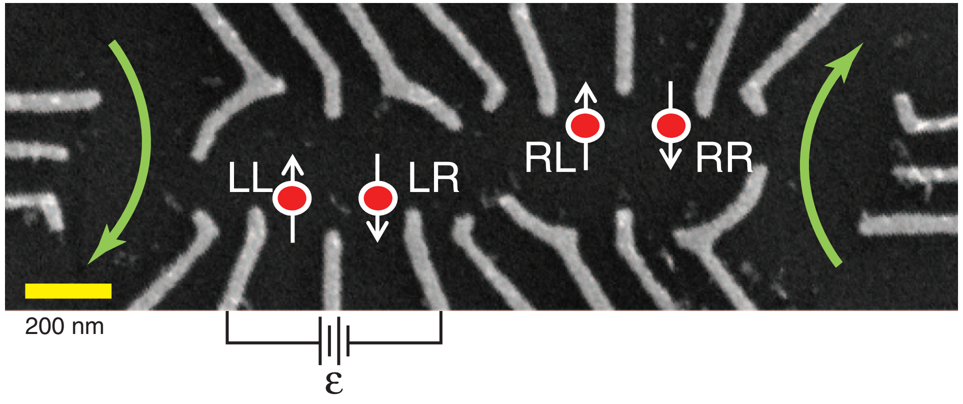

Cphase gate through capacitive coupling

Eigenstates (coupled)

$|\uparrow\uparrow\rangle$

$$(|\downarrow\uparrow\rangle + |\uparrow\downarrow\rangle)/\sqrt{2}$$

$$(|\downarrow\uparrow\rangle - |\uparrow\downarrow\rangle)/\sqrt{2}$$

Qubit space

$|\downarrow\downarrow\rangle$

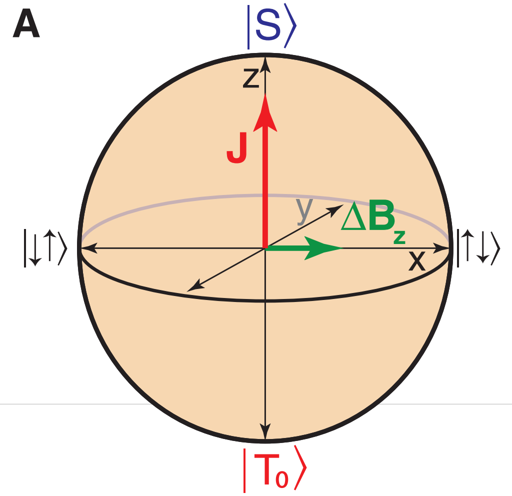

M. Shulman et al, Science 2012

QuTech

Alternative: Exchange-only qubit

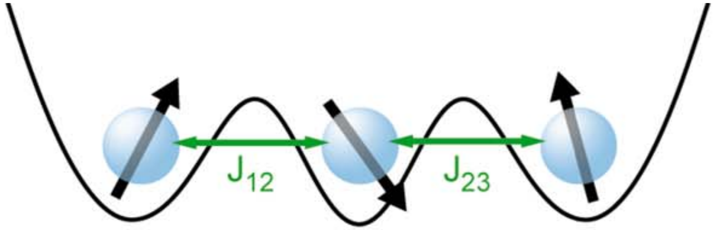

D. DiVincenzo et al, Nature 2000

$$|0_L\rangle = |S\rangle|\uparrow\rangle \qquad |1_L\rangle = (2/3)^{1/2}|T_+\rangle|\downarrow\rangle - (1/3)^{1/2}|T_0\rangle|\uparrow\rangle$$

J. Medford et al.,
Nature Nano 2013

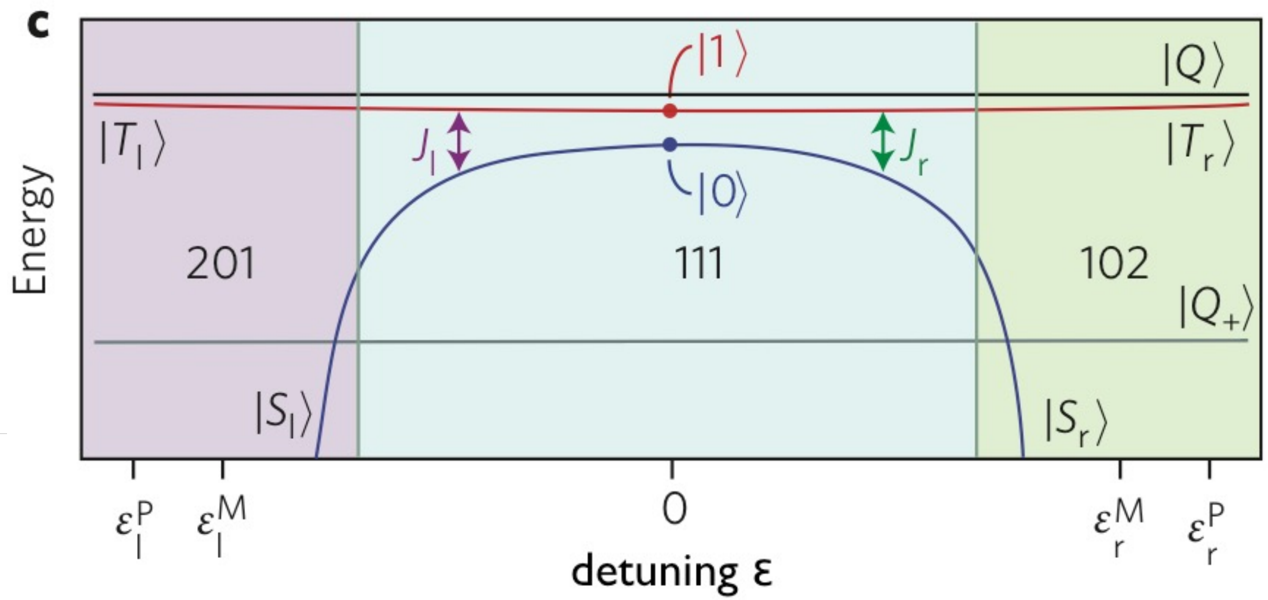

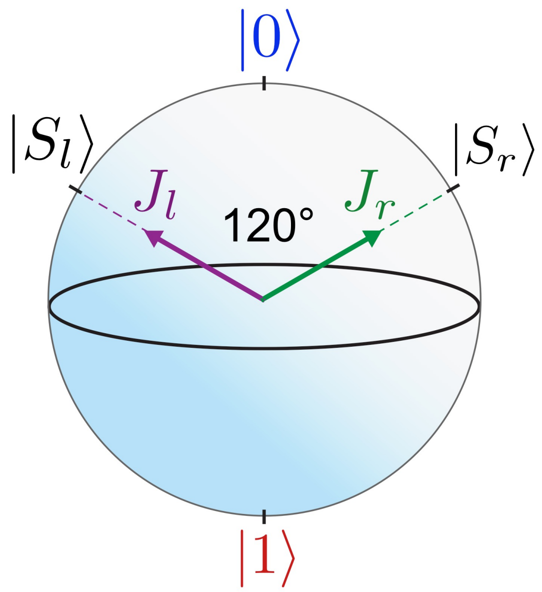

Alternative: donors

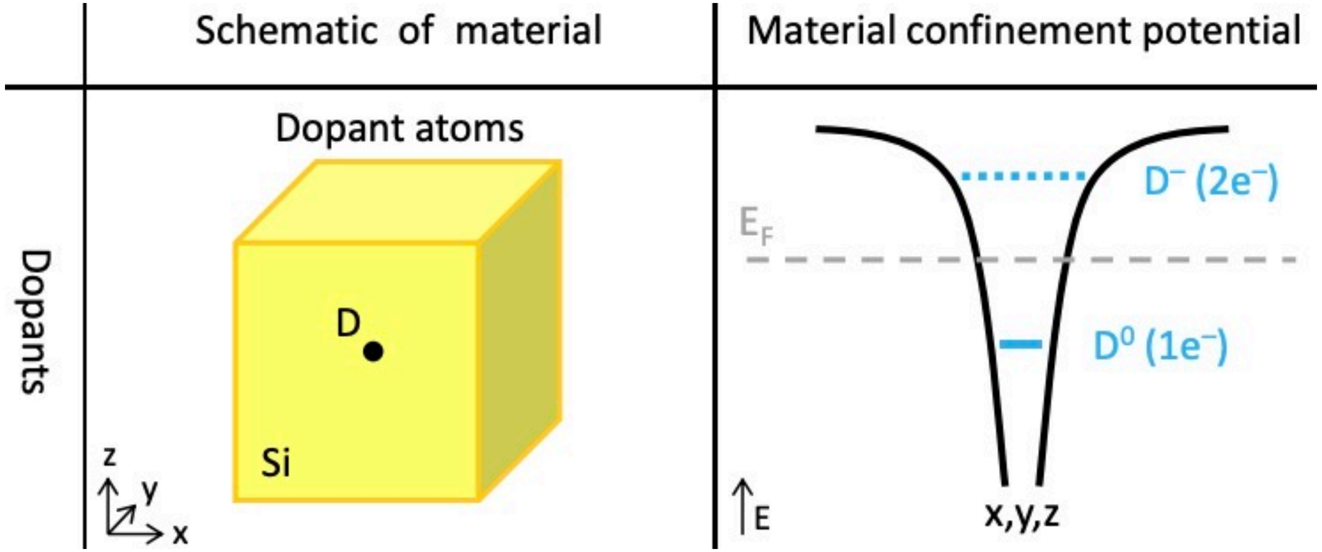

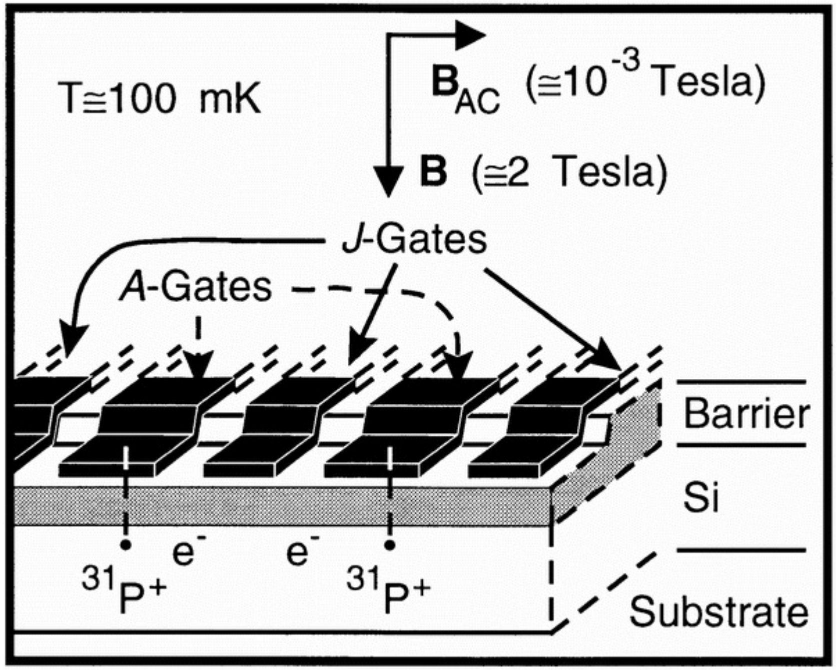

Kane, Nature 1998

Alternative: donors

Flip-flop qubit

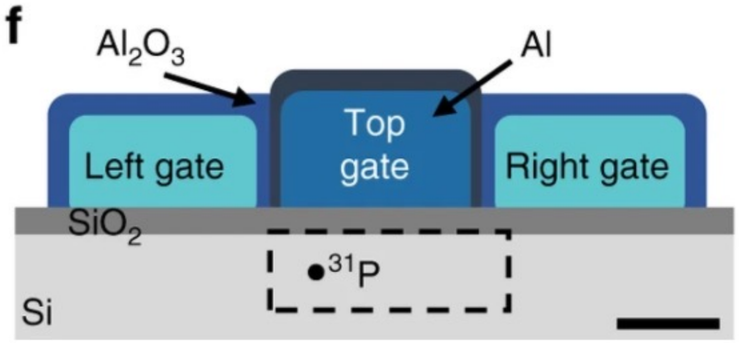

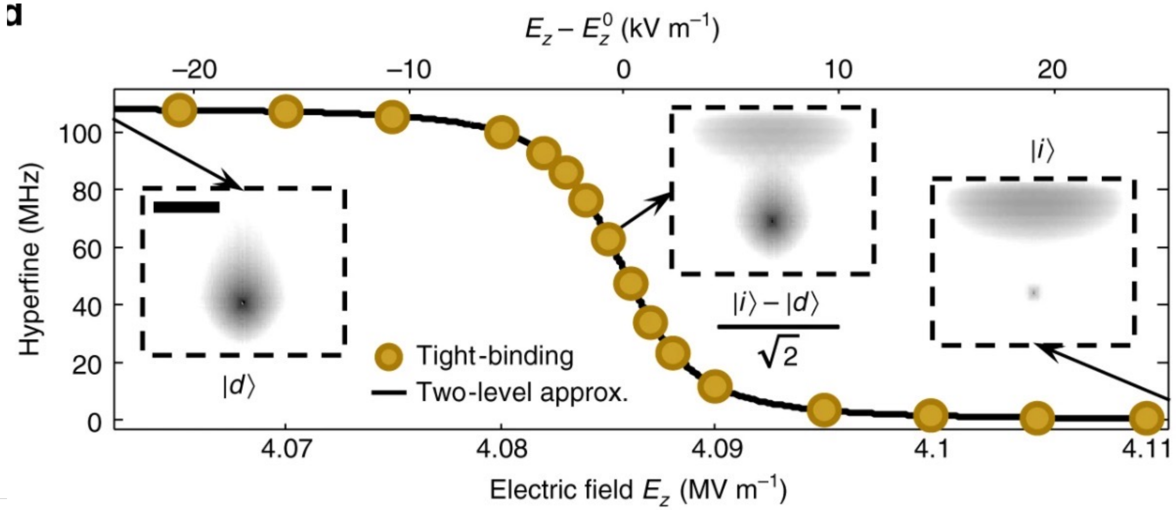

Electron spin: ~1ms
Nucler spin: ~1s

G. Tosi, et al., Nat Comm 2017

QuTech

Quantum computation with spin qubits in semiconductor

Xiao Xue

QuTech, Delft University of Technology, Lorentzweg 1, 2628 CJ Delft, Netherlands

Modular design

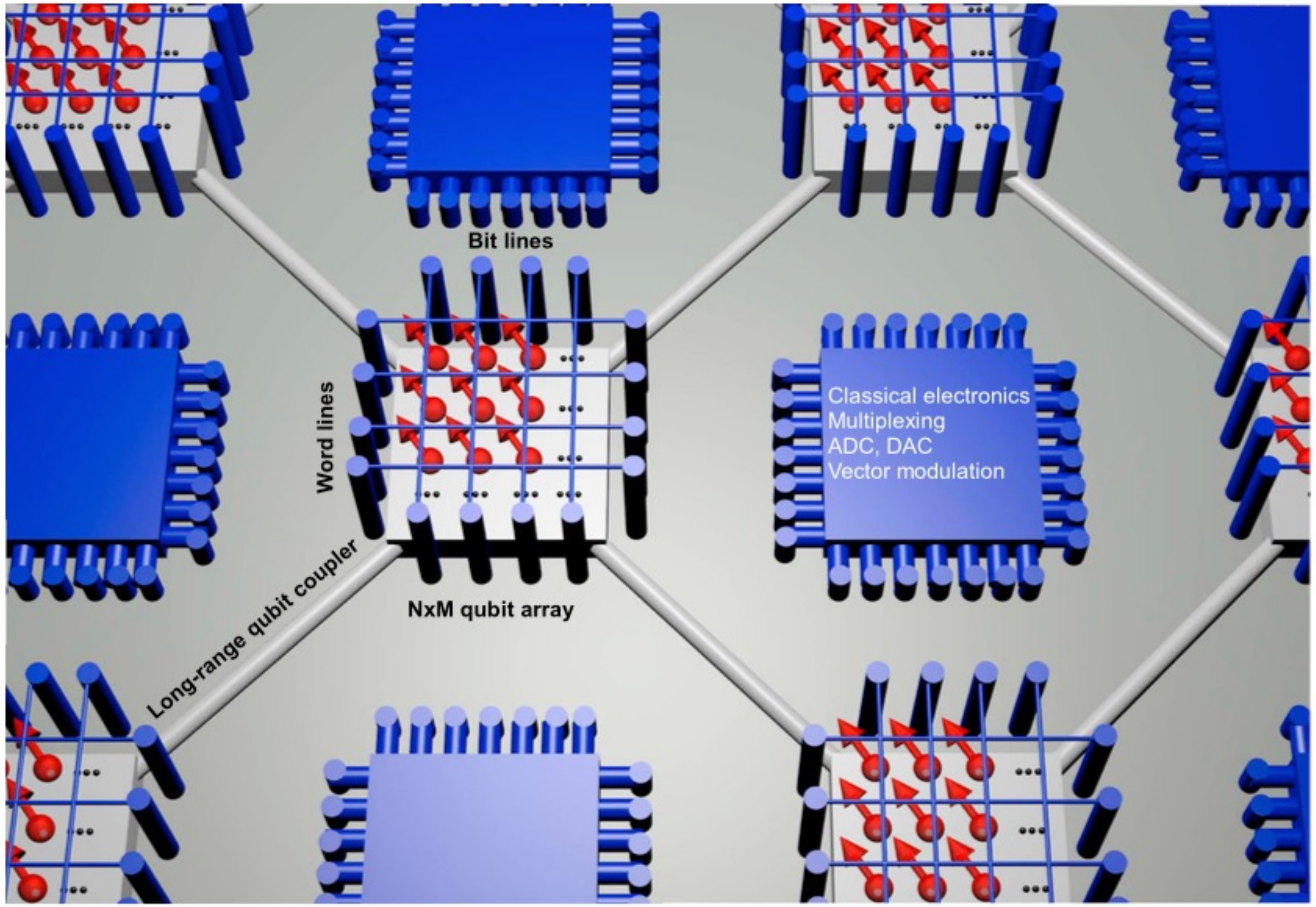

- Local operations in each module
- Remote couplers between modules
- Integrated electronics for control & readout

L. M. K. Vandersypen et al., npj Quantum Info (2017)

Modular design

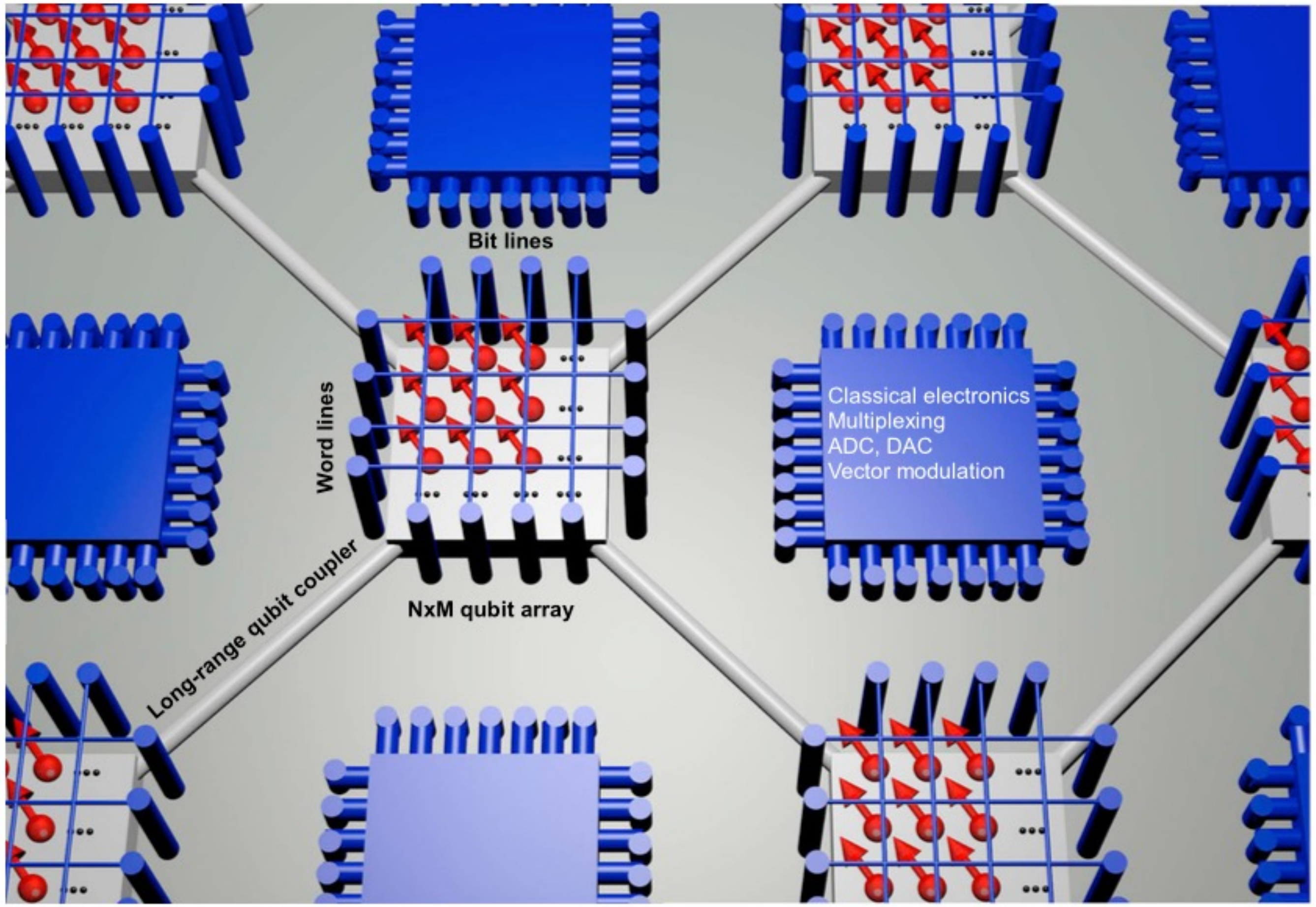

- Local operations in each module
- Remote couplers between modules
- Integrated electronics for control & readout

High-fidelity operations

L. M. K. Vandersypen et al., npj Quantum Info (2017)

QuTech

Materials impact on coherence time

GaAs	Si	^{28}Si
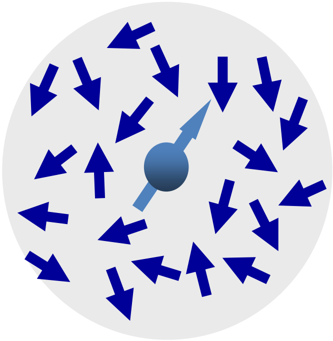	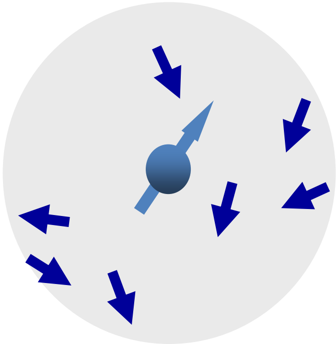	
$T_2^* \sim 10$ ns	$T_2^* \sim 1\ \mu s$	$T_2^* \sim 100\ \mu s$
$T_2^{DD} < 0.2$ ms	$T_2^{DD} > 0.5$ ms	$T_2^{DD} \sim 28$ ms
Petta et al, Science 2005	Kawakami, Scarlino, et al, Nature Nano 2014	Veldhorst, et al, Nature Nano 2014

QuTech

Materials impact on fidelities

GaAs	Si	^{28}Si
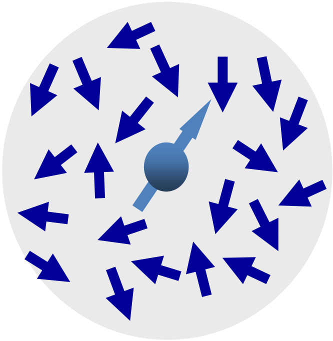	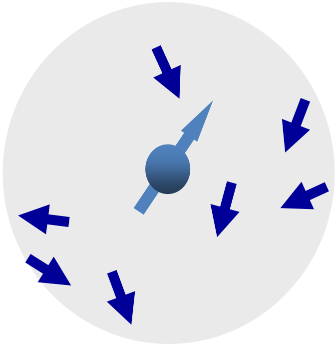	
2-spin exchange: Q > 50	1-Q gate: >99% 2-Q gate: 92.0%	1-Q gate: >99.9% 2-Q gate: 98.0%
Martins et al, PRL 2016	Reed, et al, PRL 2016 Watson, et al, Nature 2018 **X.X.**, et al, PRX 2019	Yoneda, et al, Nat Nano 2018 Huang, et al, Nature 2019

QuTech

Device

purified ^{28}Si

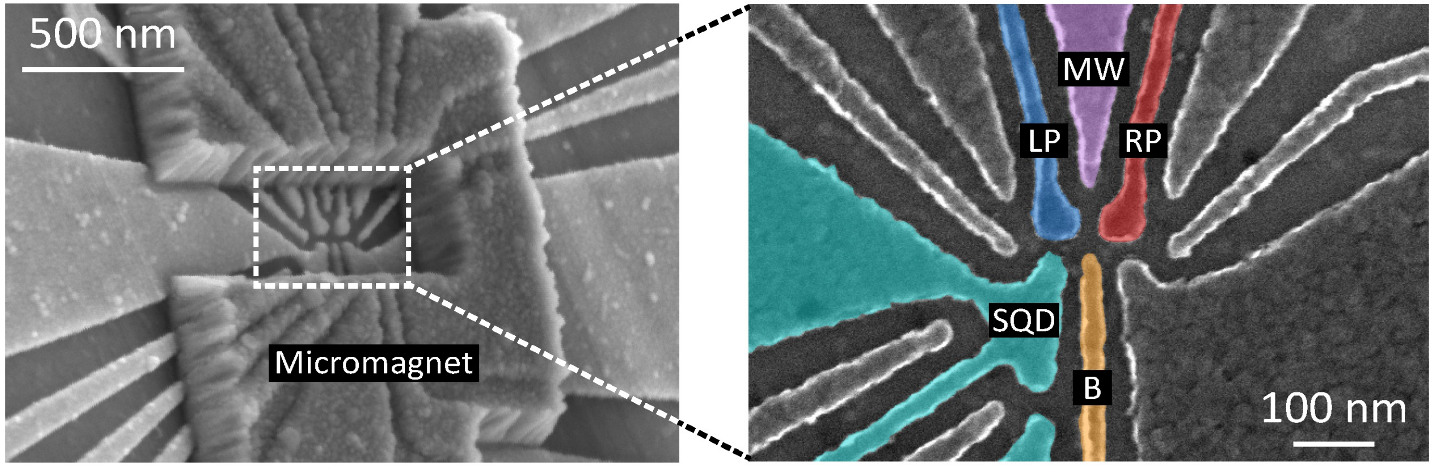

Dephasing times

T_2*: 20 μs, 10 μs (8 min avg)
Valley splitting: >140 ueV

Charge stability diagram

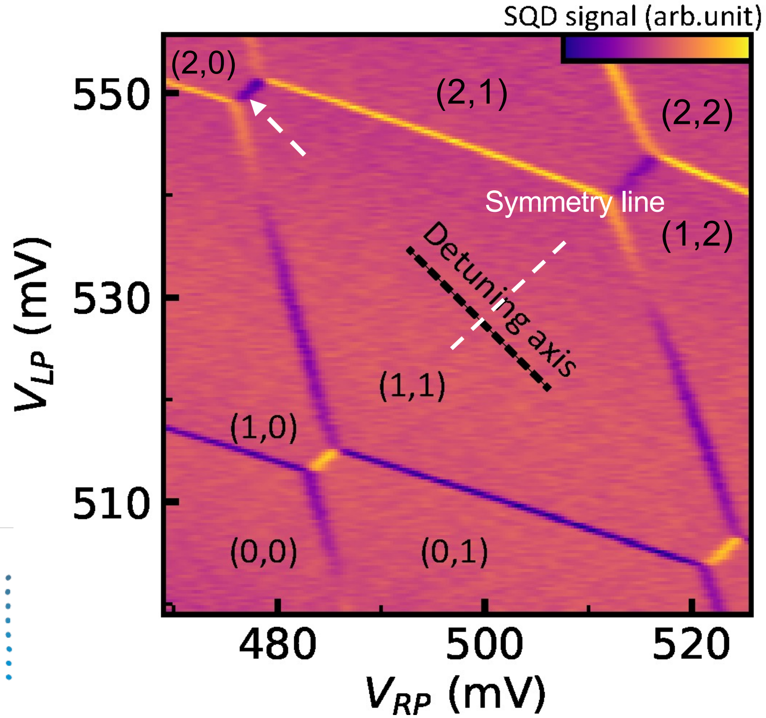

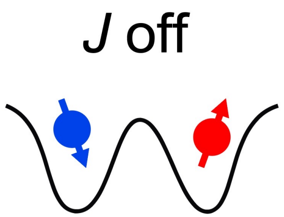

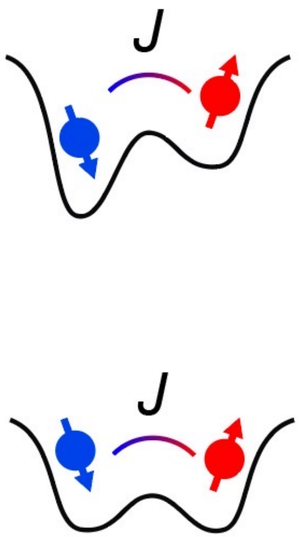

Detuning:

Couples strongly to charge noise

Barrier control at symmetry point:

Improvement of coherence by a factor of 5~6

Symmetry point: Reed et al, PRL 2016, Martins et al, PRL 2016

Symmetry operation against charge noise

Fix the barrier pulse amplitude
Sweep the detuning

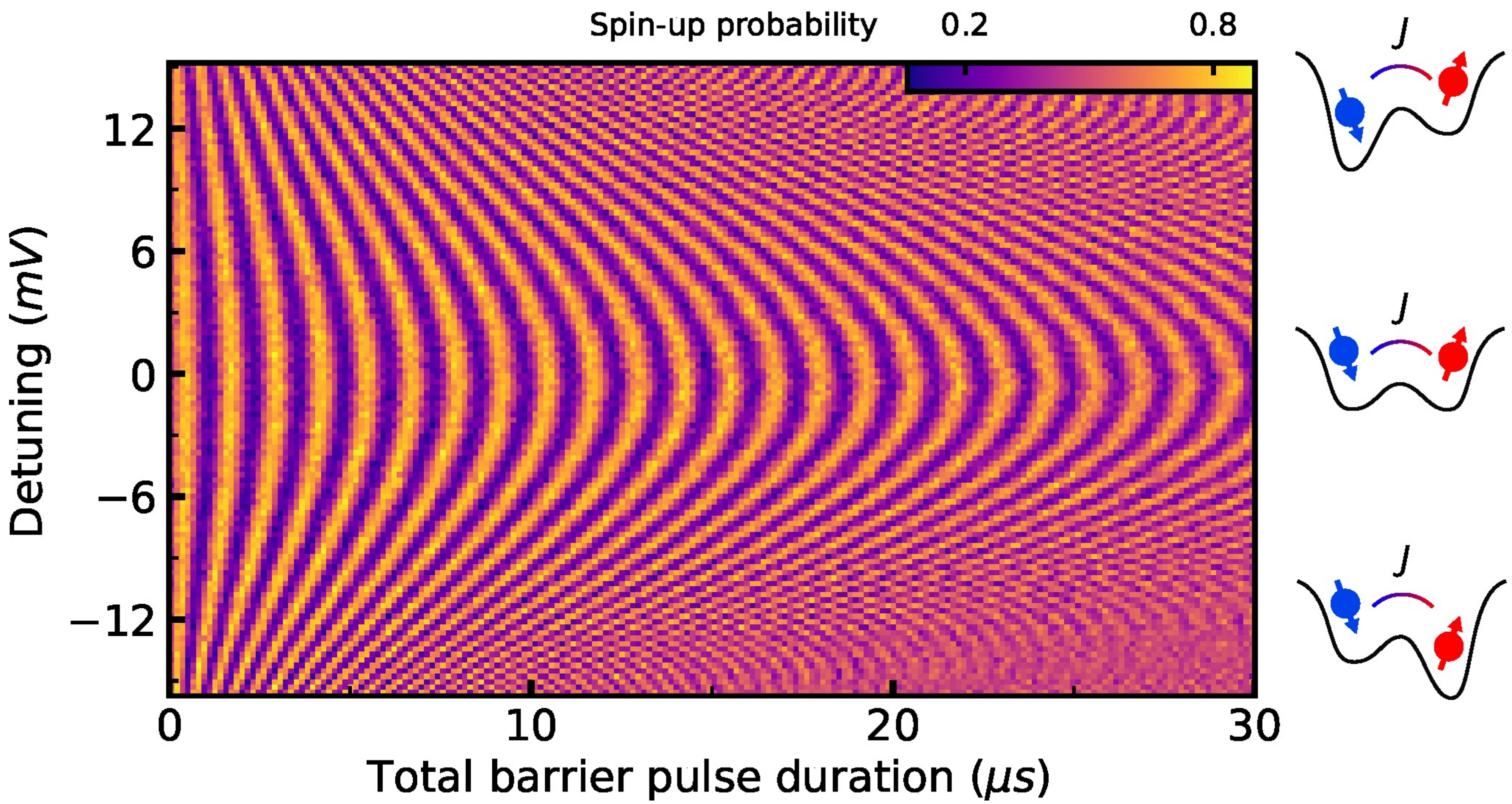

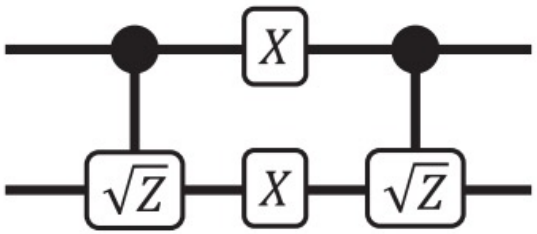

Decoupled CPhase
Watson et al, Nature 2018

Symmetry point: Reed et al, PRL 2016, Martins et al, PRL 2016

QuTech

Adiabatic CZ gate

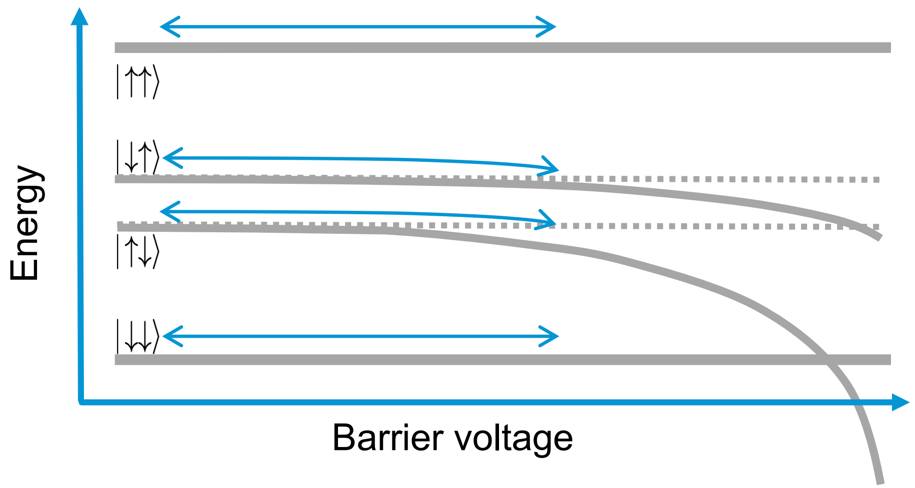

Theory:
Burkard et al., PRB 1999
Meunier et al., PRB 2010
Russ et al., PRB 2018

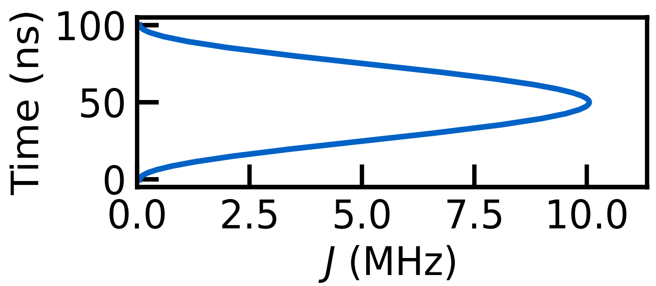

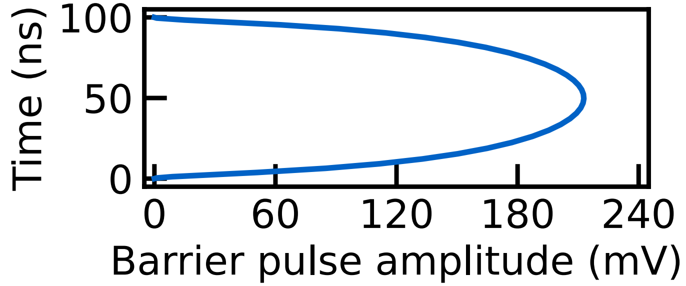

Simulated fidelity : ~99.98%

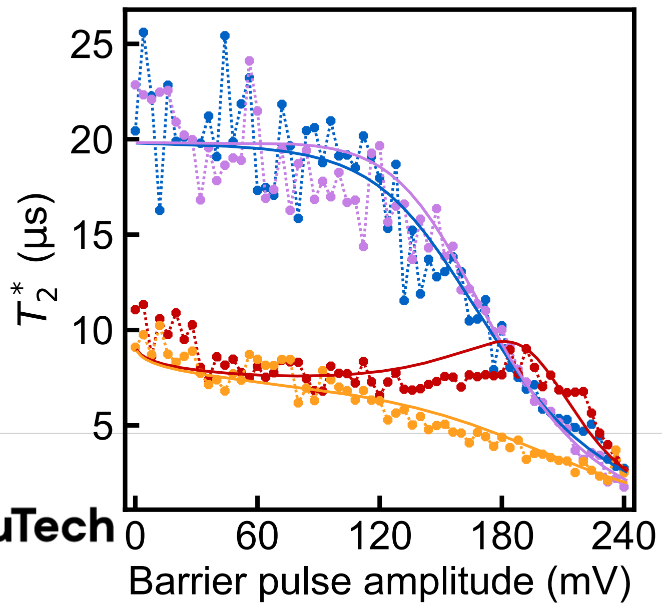

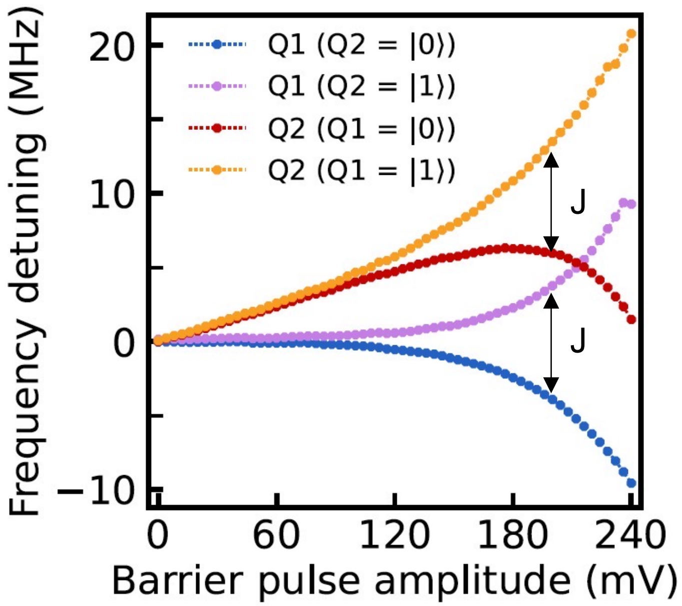

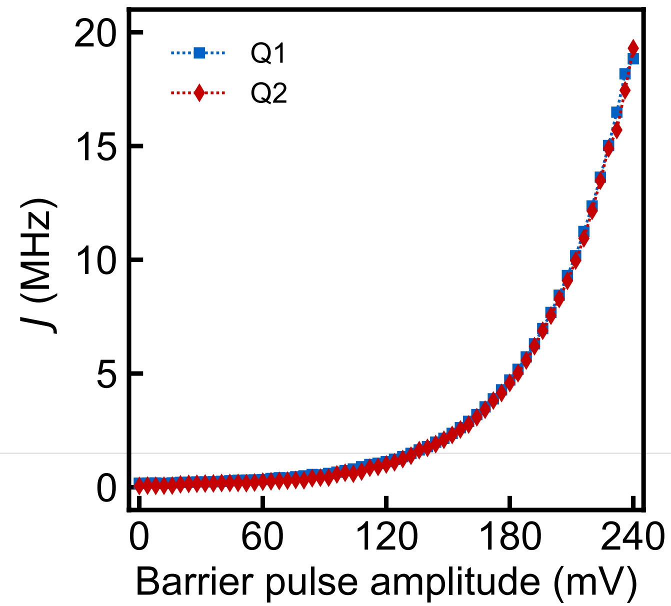

QuTech

Optimize pulse shape using Gate Set Tomography

Manual calibration (Ramsey, allXY…) → Parameter set

Parameter set:
- Qubit frequency (2x)
- 1Q gate duration (2x)
- 1Q phase shifts (1Q) (4x)
- CZ amplitude
- 1Q phase shifts (CZ) (2x)

Parameter set → Gate set tomography → Operator diagnosis

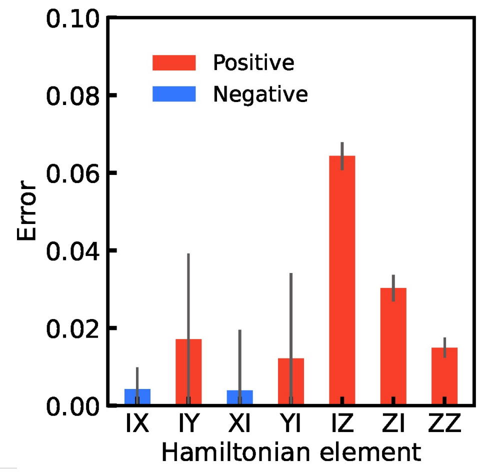

Analysis using PyGSTi (Sandia) - http://www.pigsty.info

~98% CZ gate before optimization

QuTech

Optimize pulse shape using GST

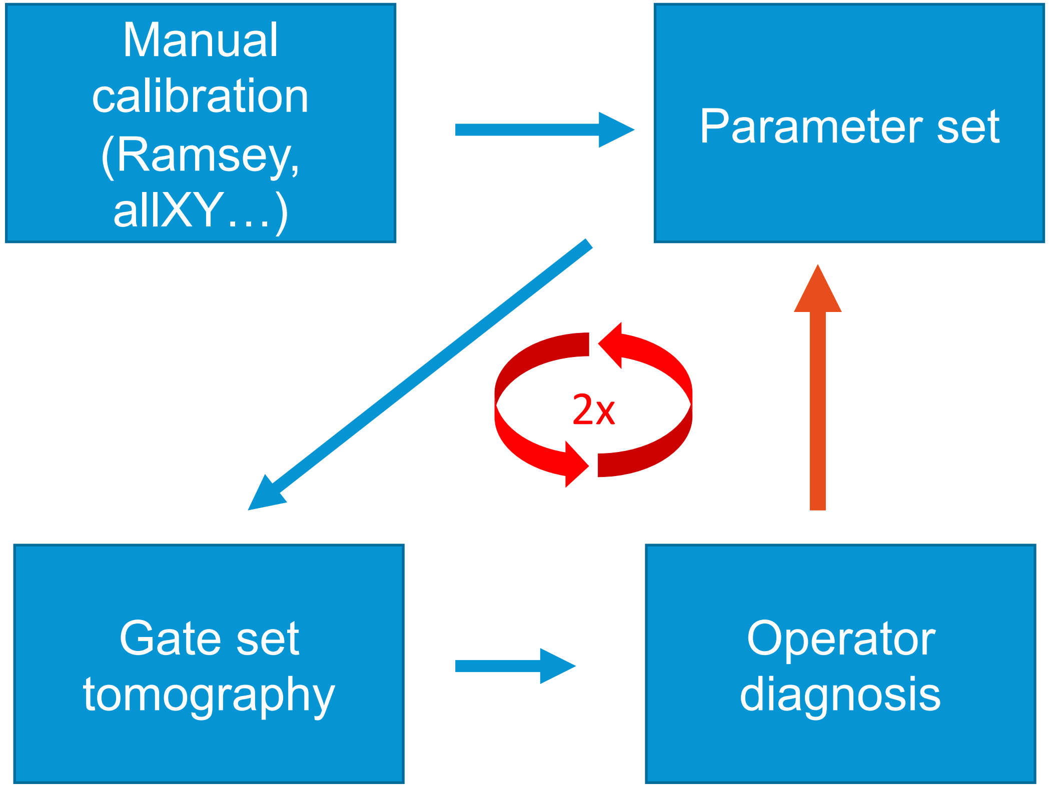

Qubit frequency (2x)
1Q gate duration (2x)
1Q phase shifts (1Q) (4x)
CZ amplitude
1Q phase shifts (CZ) (2x)

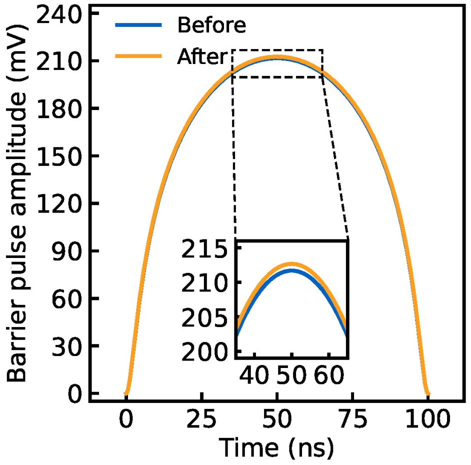

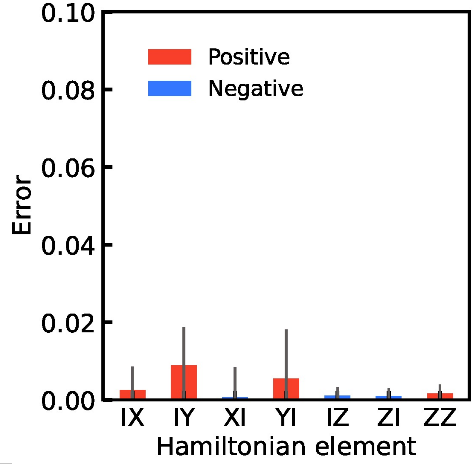

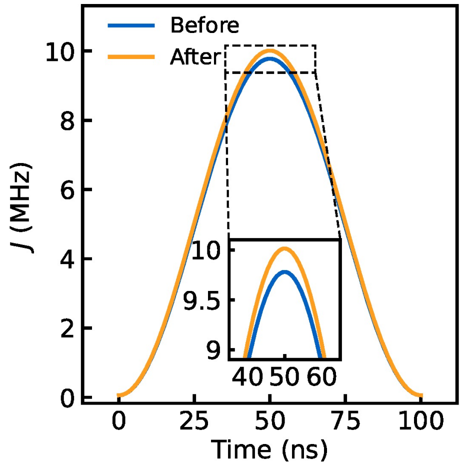

Analysis using PyGSTi (Sandia) - http://www.pigsty.info

>99.5% CZ gate after optimization

QuTech

Two-qubit CZ fidelity of 99.65% ± 0.15%

See also: ^{31}P donors: Madzik Nature 2022
and silicon (J always-on): Noiri et al., Nature 2022
and silicon (CZ): Mills et al., arxiv preprint

Measured CZ

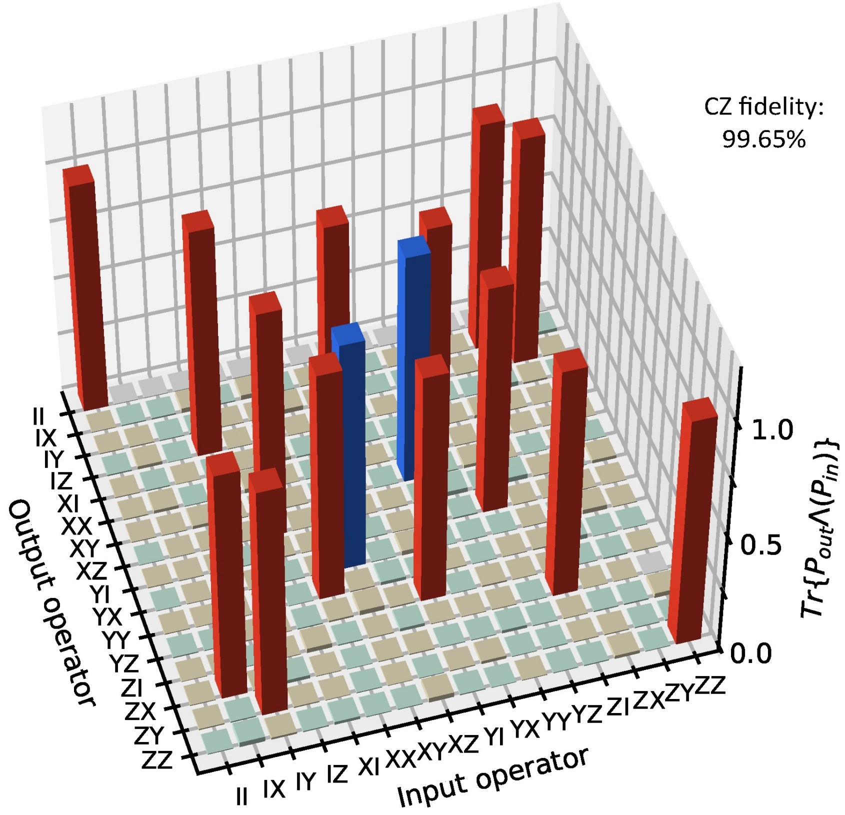

Two-qubit gate set tomography

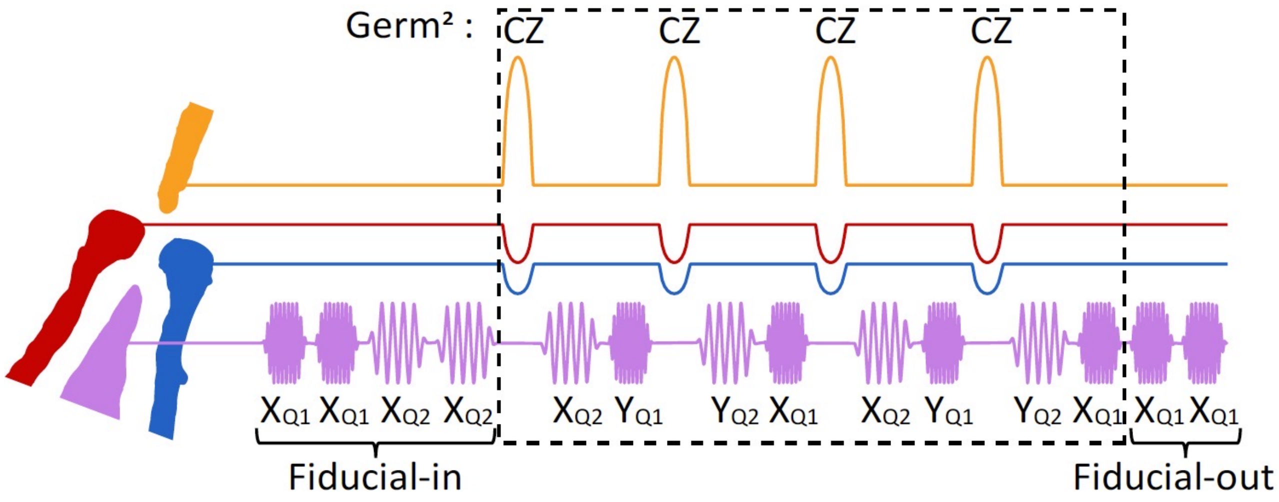

1685 such sequences in total

R. Blume-Kohout et al., PRX Quantum 2022

QuTech

Modular design

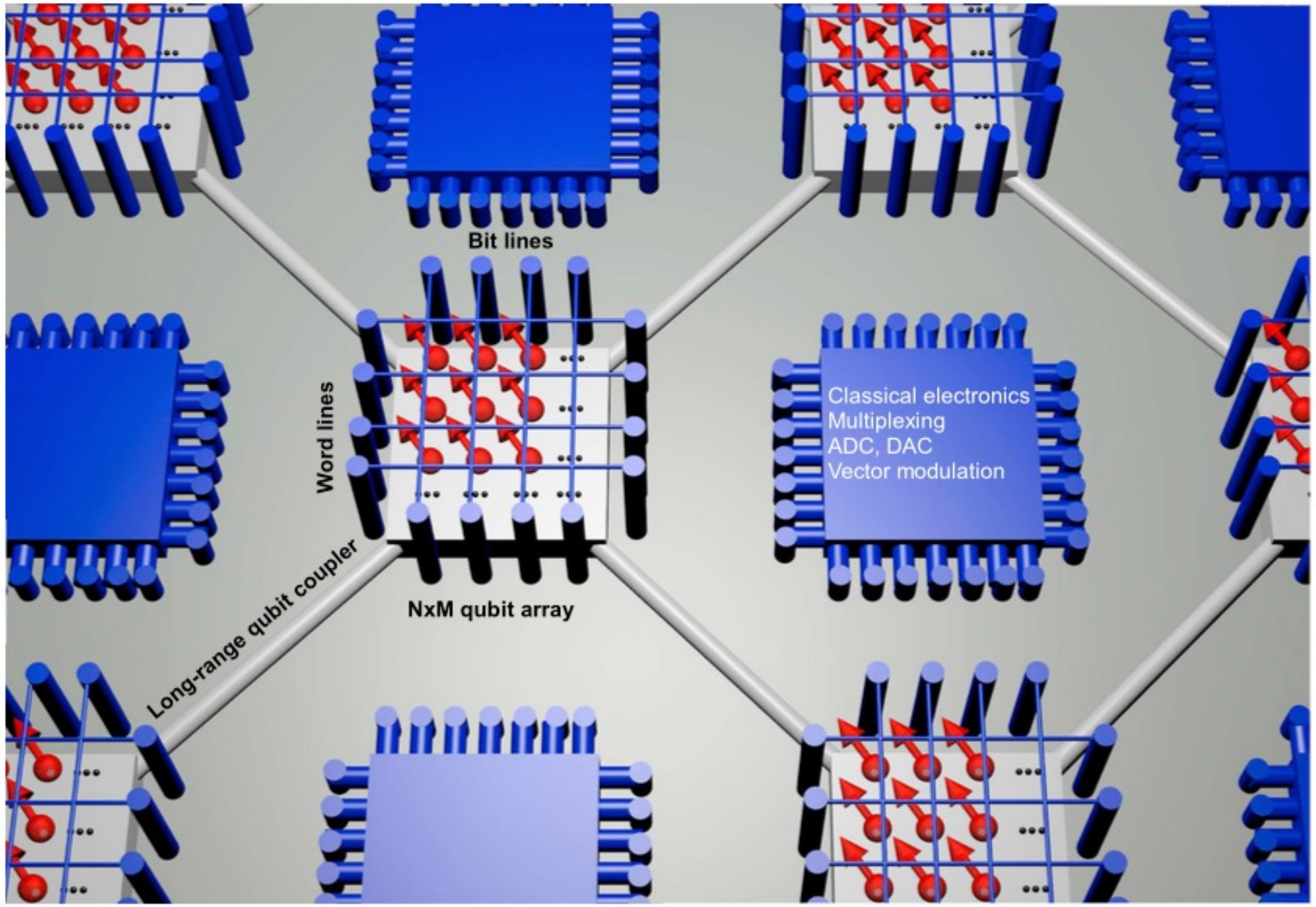

- Local operations in each module
- Remote couplers between modules
- Integrated electronics for control & readout

Multi-qubit arrays

L. M. K. Vandersypen et al., npj Quantum Info (2017)

QuTech

Building lattices from the bottom-up

Harvard 2011

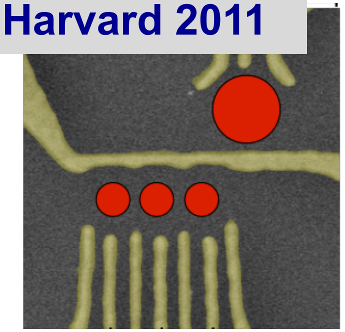

Delft 2012

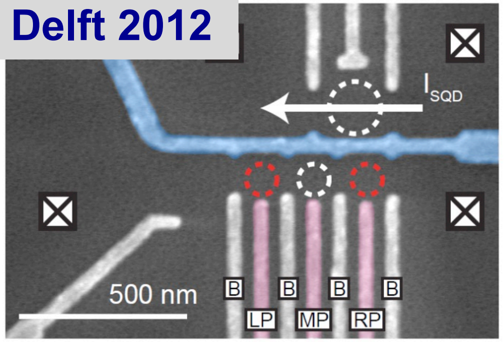

Local electrodes allow individual tunability

Delft 2013

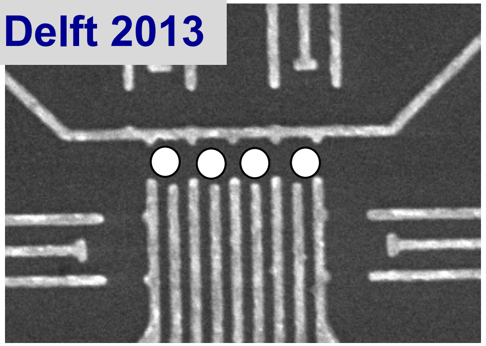

Tokyo 2014

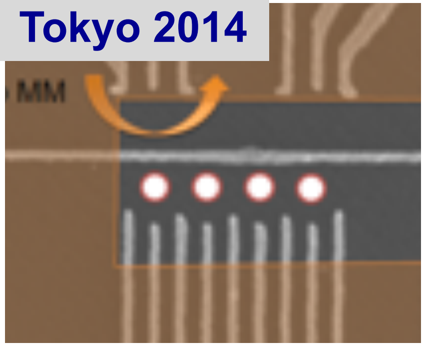

Pusan 2013

Grenoble 2012

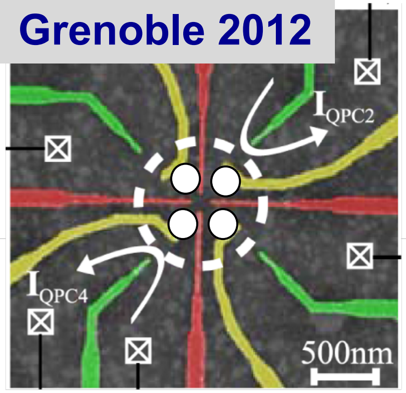

Towards larger 2D array

GaAs

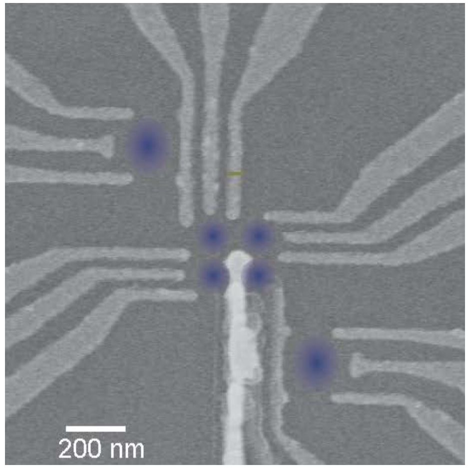

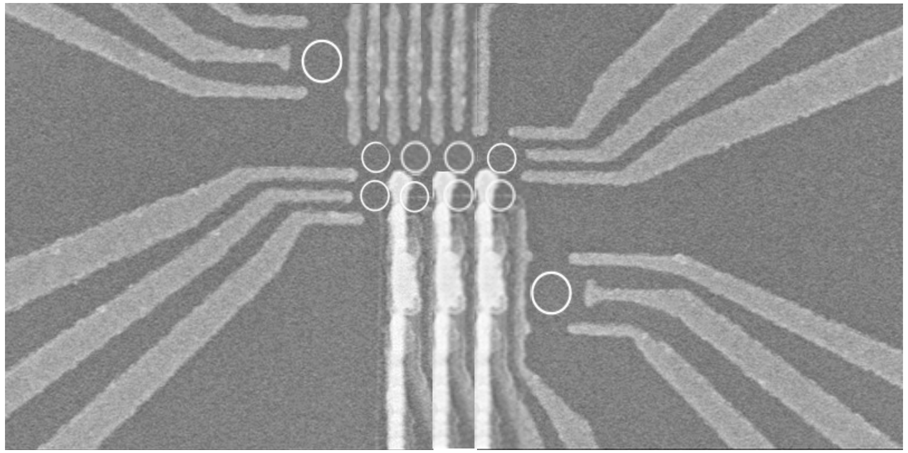

GaAs

Note: not an actual device

GaAs

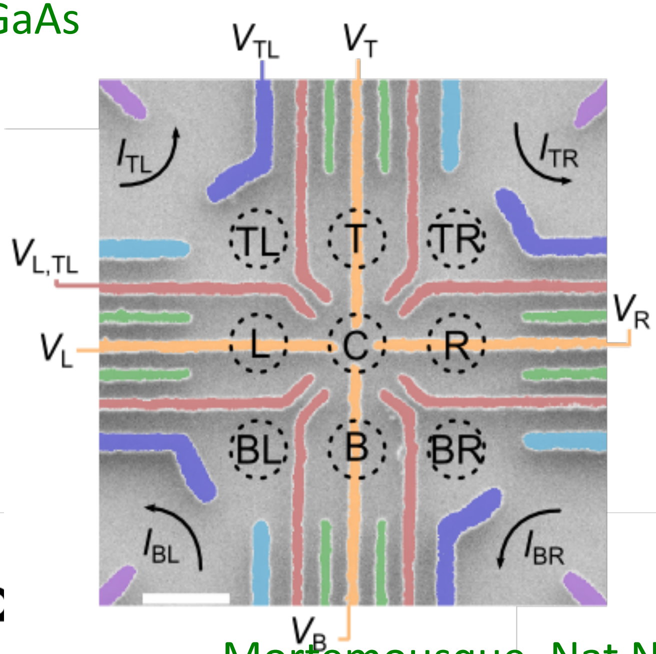

Mortemousque, Nat Nano 2021

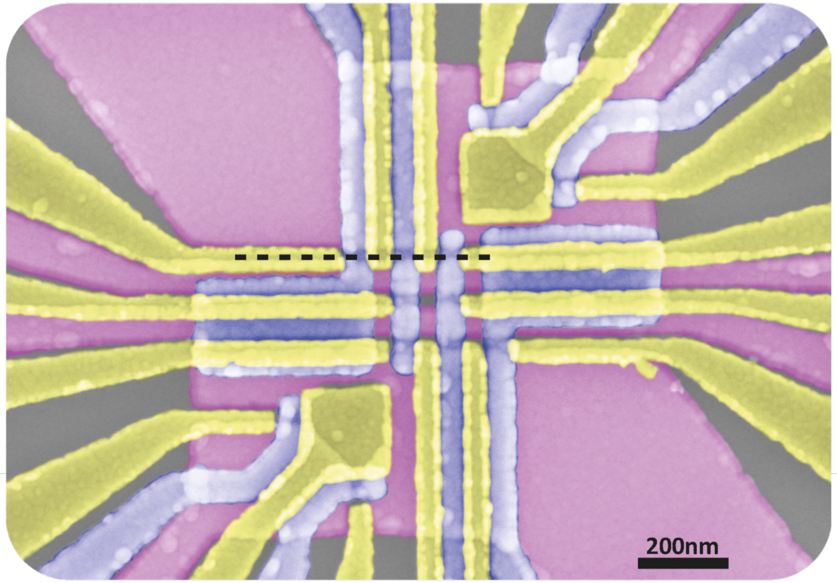

SiMOS/
SiGe

Delft
Ongoing

Qubit arrays

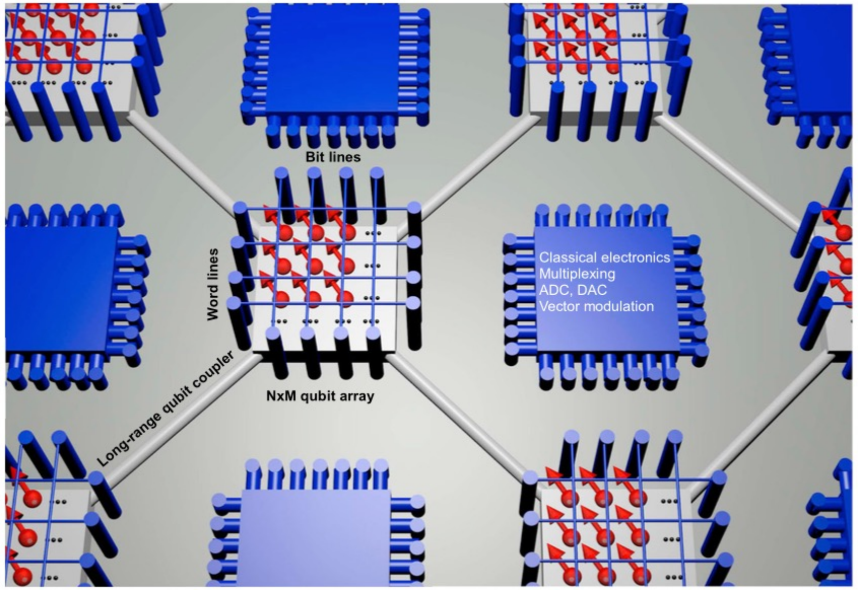

Hendrix, et al, Nature 2021

Ge/SiGe

3-qubit phase correction code

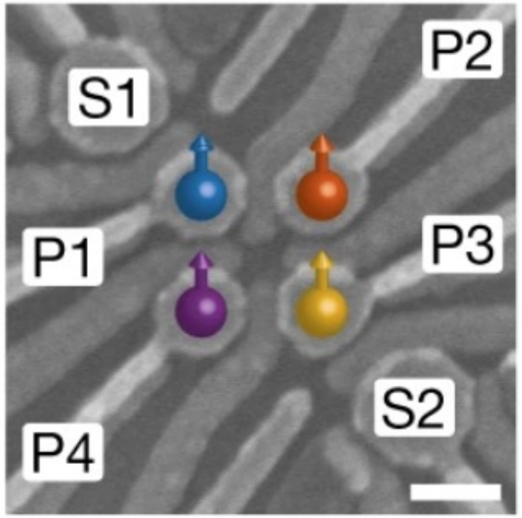

S. Philips, M. Mądzik, et al, arXiv:2202.09252

Si/SiGe

3-qubit GHZ states

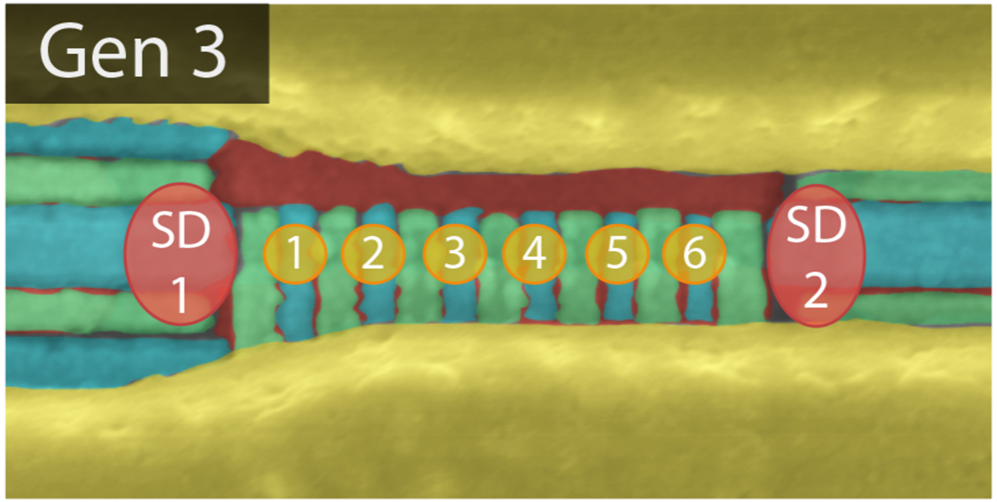

90 nm dot pitch

QuTech

Single-qubit control (EDSR)

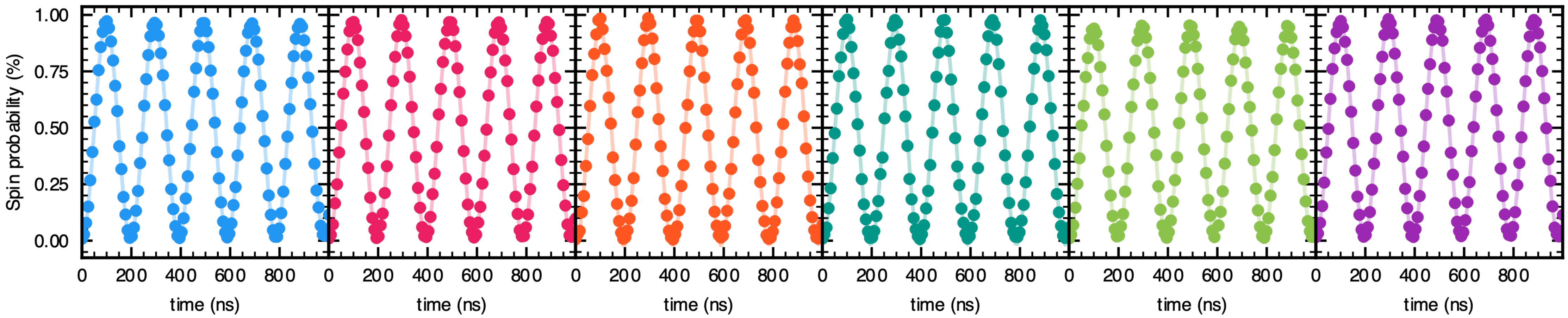

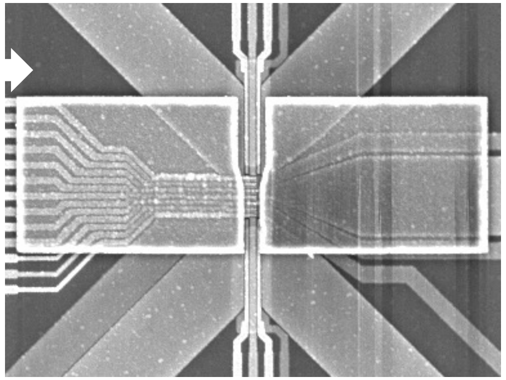

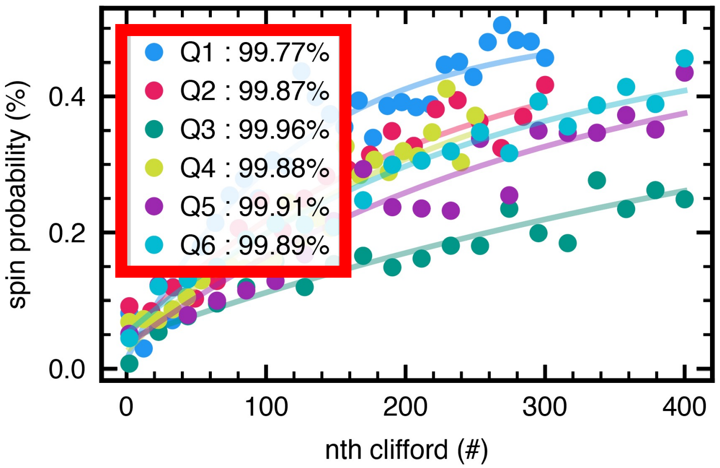

Qubit	T_2^*(us)	T_2^h(us)	Vis(%)
1	3.0	14.0	96
2	2.5	21.1	97
3	3.7	40.1	97
4	3.7	37.2	97
5	5.9	44.7	93
6	5.1	26.7	95

QuTech

Exchange control and Bell states

(MHz)	J_{12}	J_{23}	J_{34}	J_{45}	J_{56}
J_{12} on	12.1	0.023	0.018	<0.03	0.040
J_{23} on	<0.05	11.1	<0.30	<0.03	0.040
J_{34} on	0.050	<0.03	6.6	<0.07	0.042
J_{45} on	0.038	<0.03	0.031	9.8	0.250
J_{56} on	0.033	<0.03	<0.02	<0.03	5.3

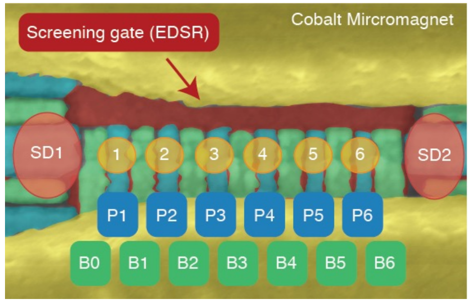

J on/off ratios $\gtrsim 100$

Qubits	Fidelity (%)	Concurence (%)
1-2	89.2 ± 2.2	86.7 ± 3.2
2-3	90.1 ± 2.2	83.9 ± 3.8
3-4	88.3 ± 3.6	87.9 ± 5.0
4-5	95.6 ± 2.0	94.9 ± 3.2
5-6	94.1 ± 1.4	90.6 ± 3.6

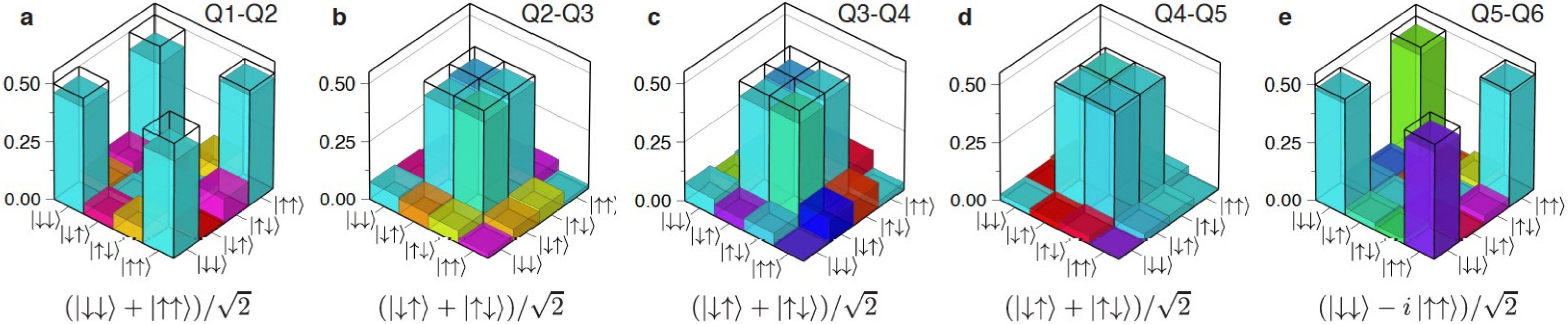

Modular design

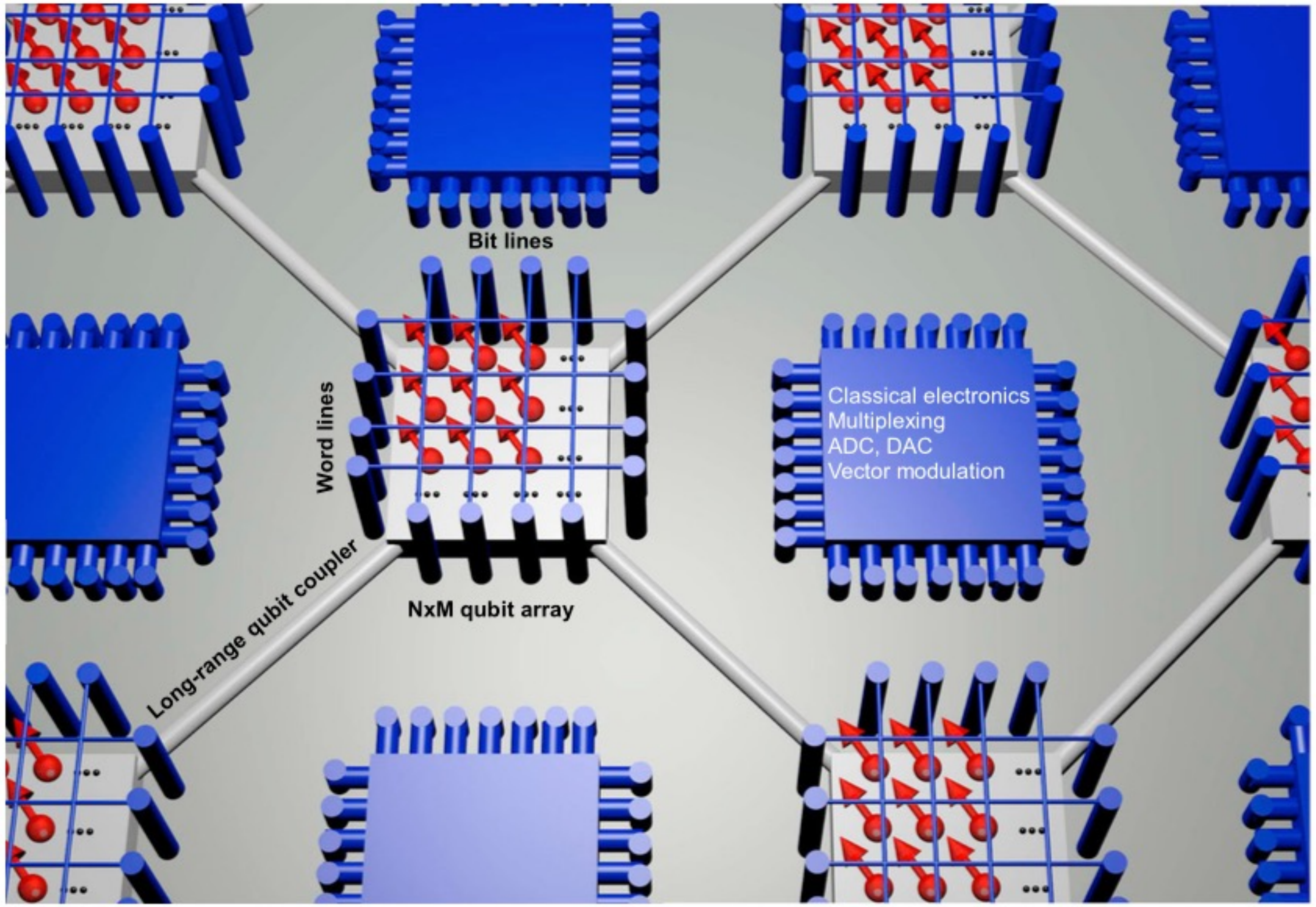

- Local operations in each module
- Remote couplers between modules
- Integrated electronics for control & readout

Spin Shuttling

L. M. K. Vandersypen et al., npj Quantum Info (2017)

QuTech

Virtual gates application: Shuttling

Material: Si/SiGe

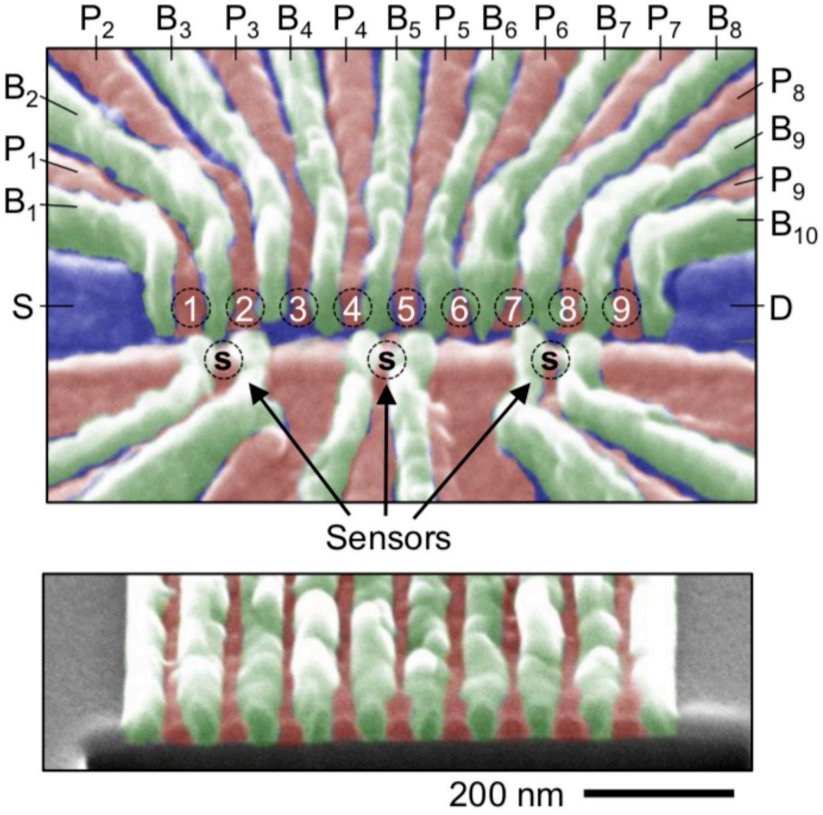

Charge shuttling

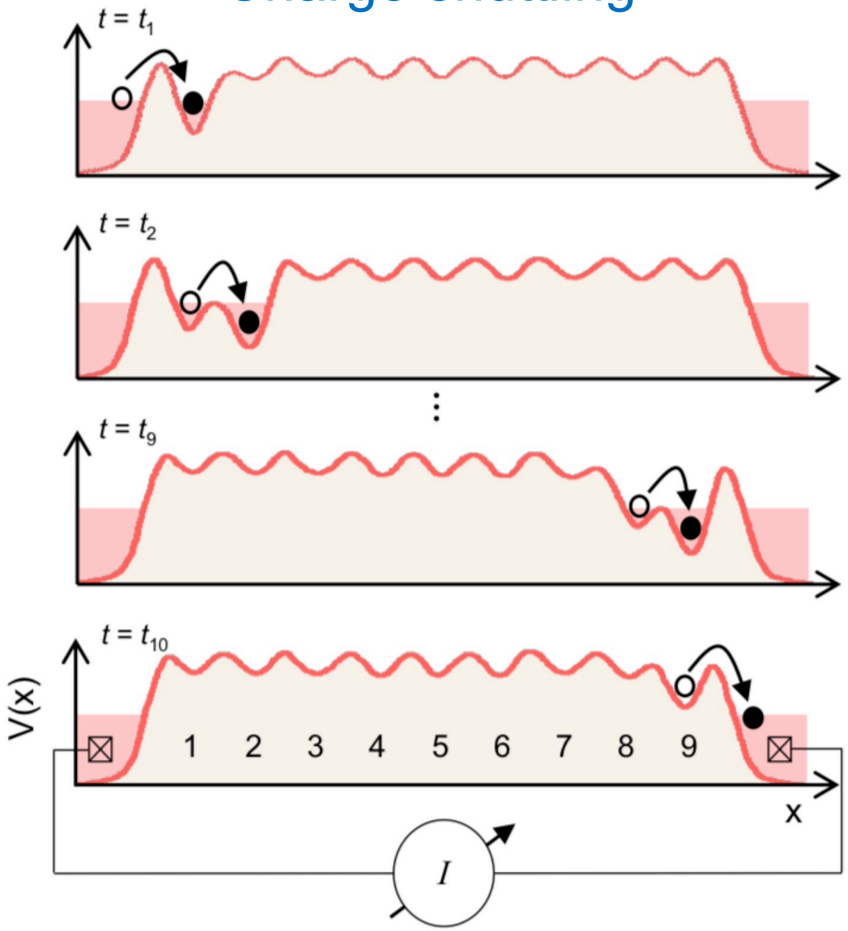

2 Electron shuttling

3 Electron shuttling

QuTech

Mills, et al, Nat Comm 2019

Conveyor mode shuttling

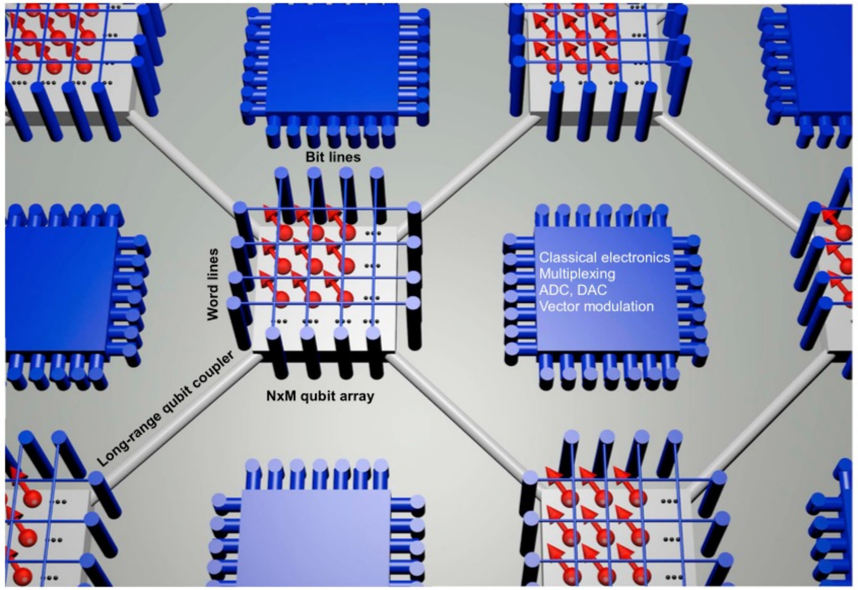

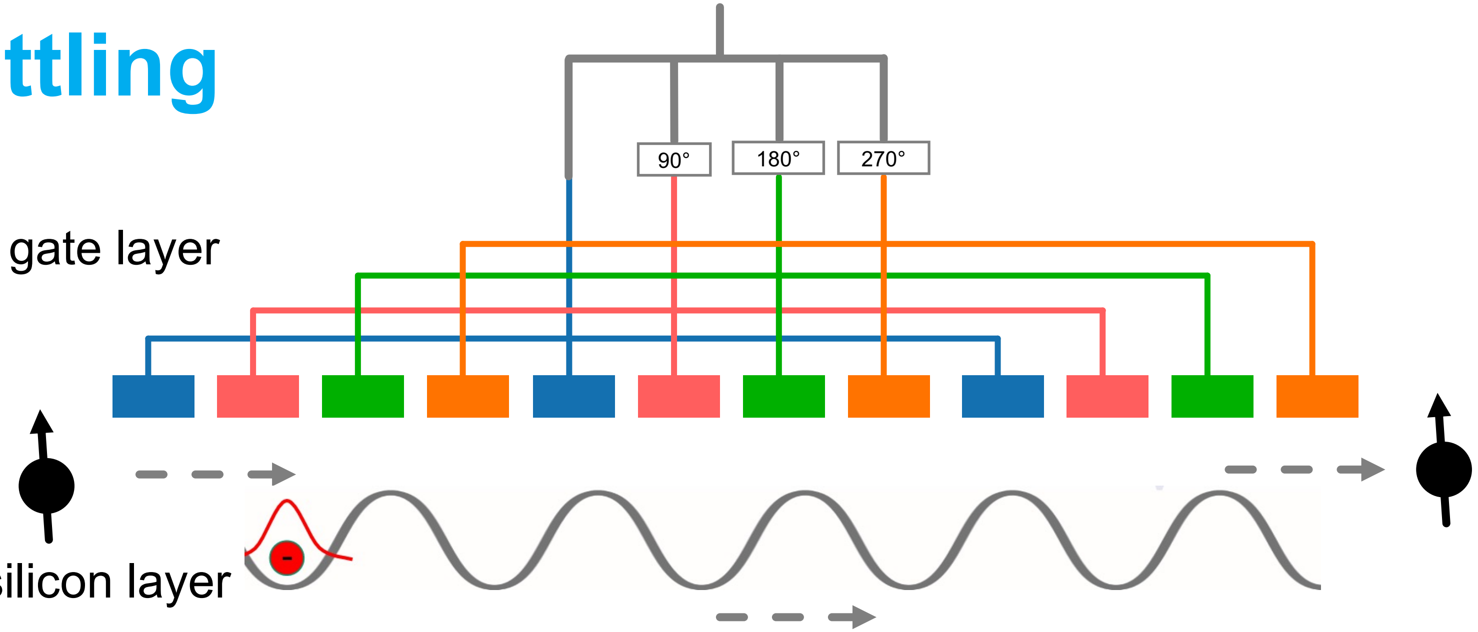

Seidler, et al., arxiv 2021

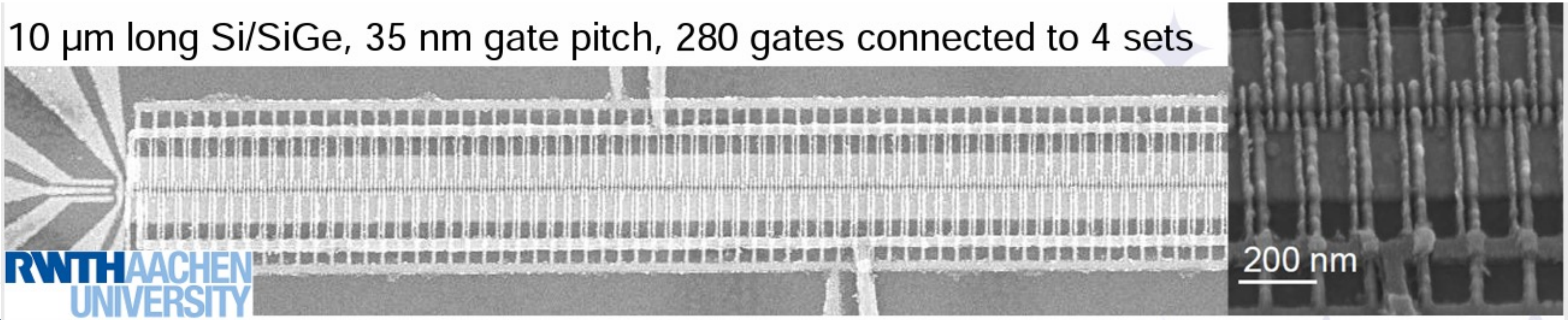

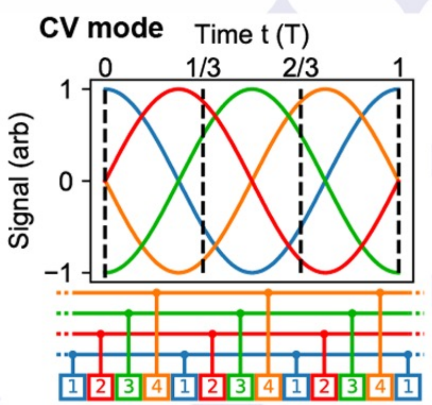

RWTH AACHEN UNIVERSITY

QuTech

Courtesy of Inga Seidler & Lars Schreiber (RWTH Aachen)

Modular design

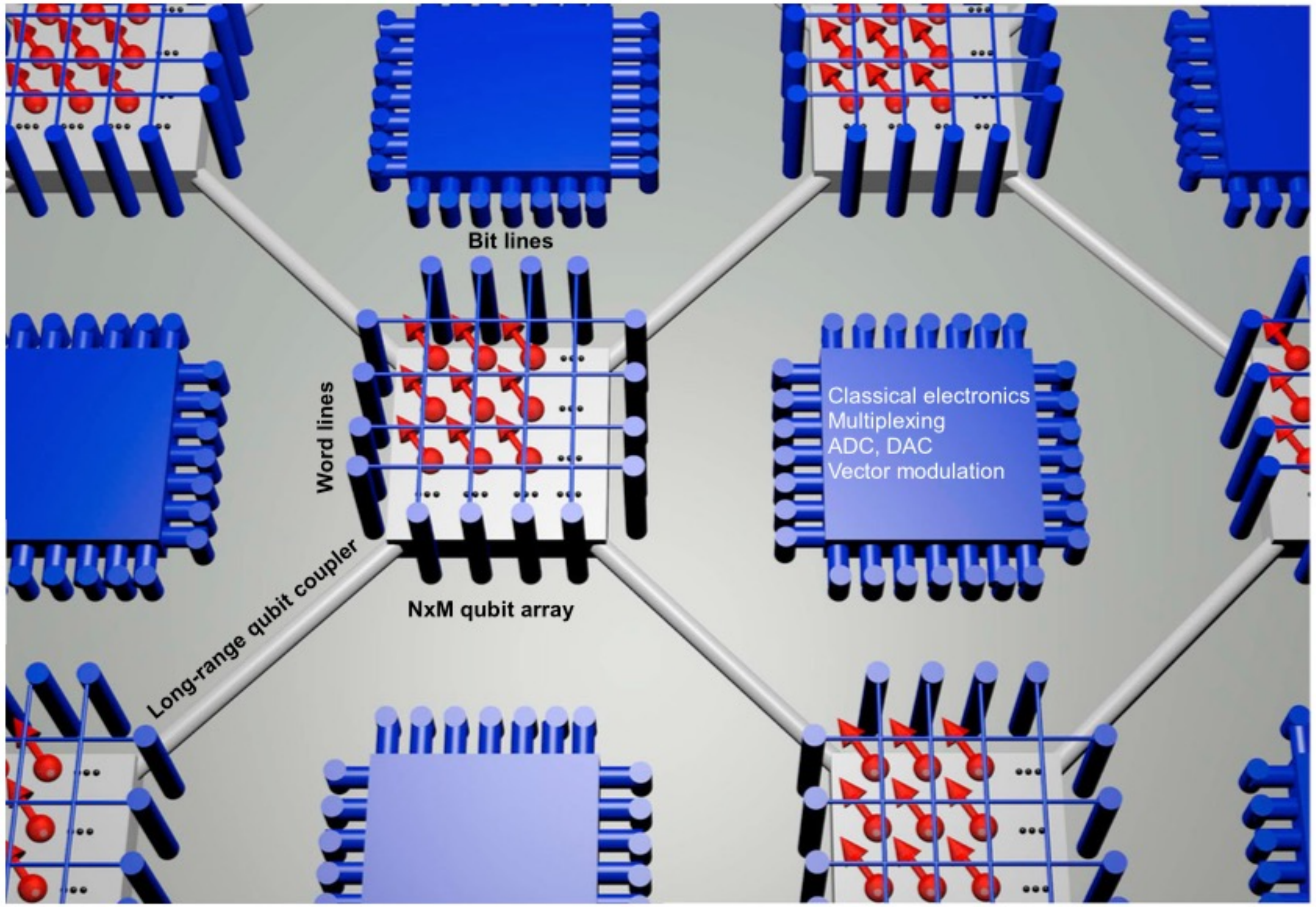

- Local operations in each module
- Remote couplers between modules
- Integrated electronics for control & readout

Spin-photon interface

L. M. K. Vandersypen et al., npj Quantum Info (2017)

QuTech

Connecting a double-dot to a resonator

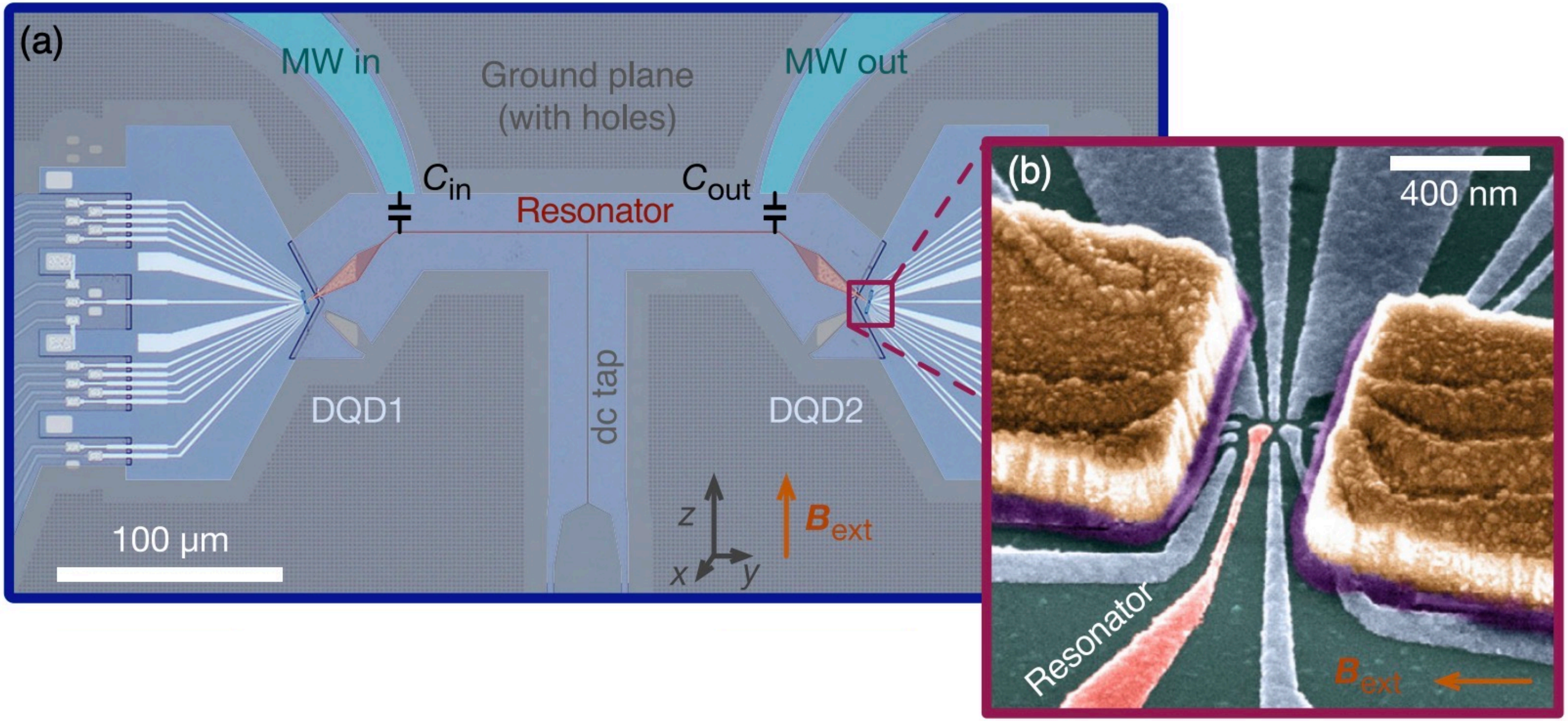

QuTech

P. Harvey-Collard et al., PRX 2022

Charge-photon admixing

Samkharadze, Zheng, et al., Science 2018

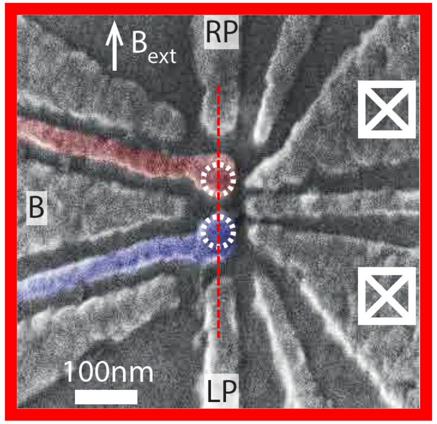

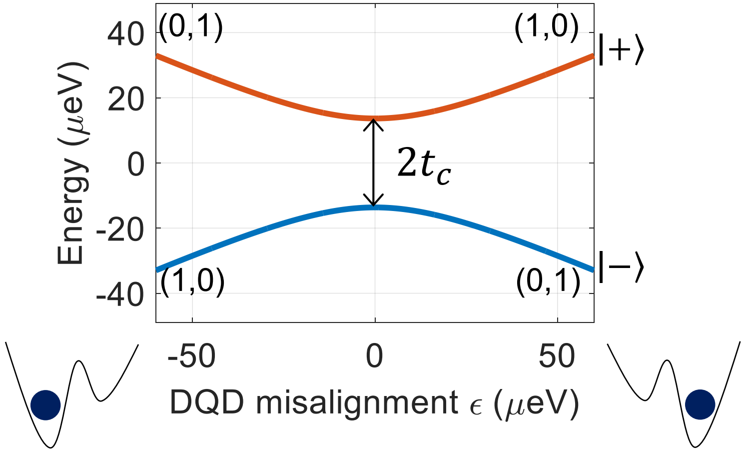

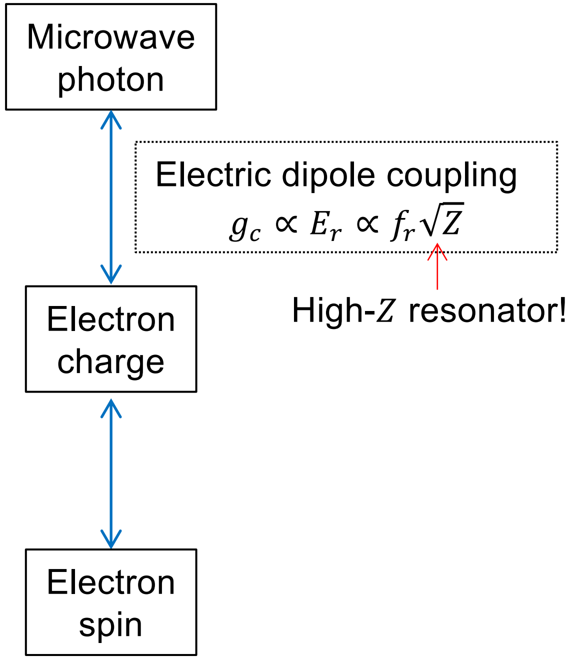

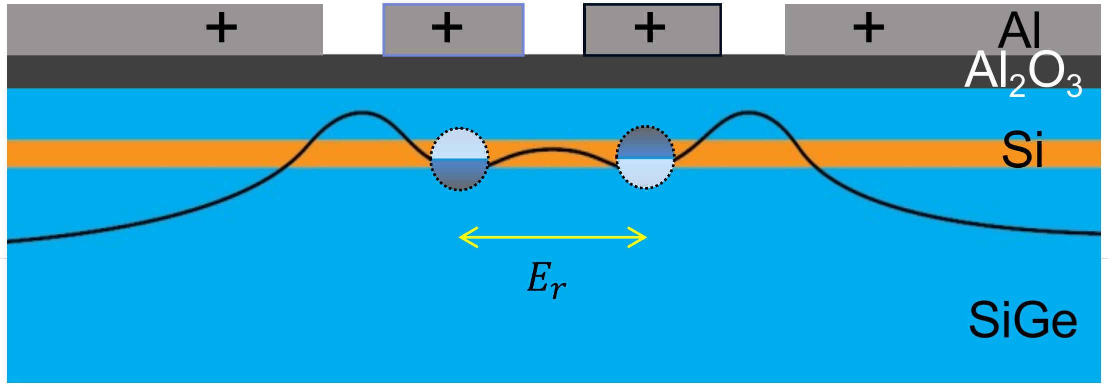

Si/SiGe growth by A. Sammak and G. Scappucci

Theory: Benito *et al.*, PRB 96 (2017)
High-Z resonator: Samkharadze *et al.*, PRApplied 5 (2016)

Spin-charge admixing

Samkharadze, Zheng, et al., Science 2018

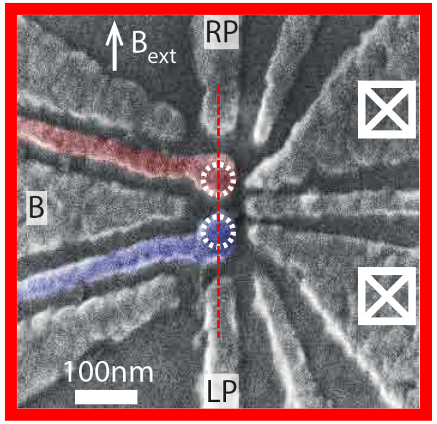

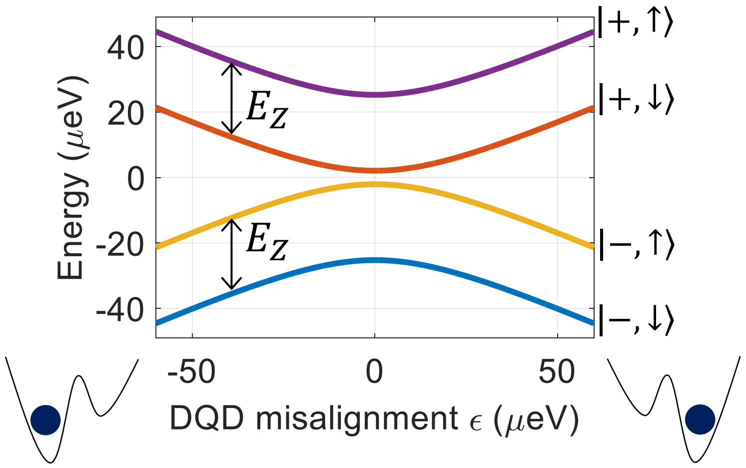

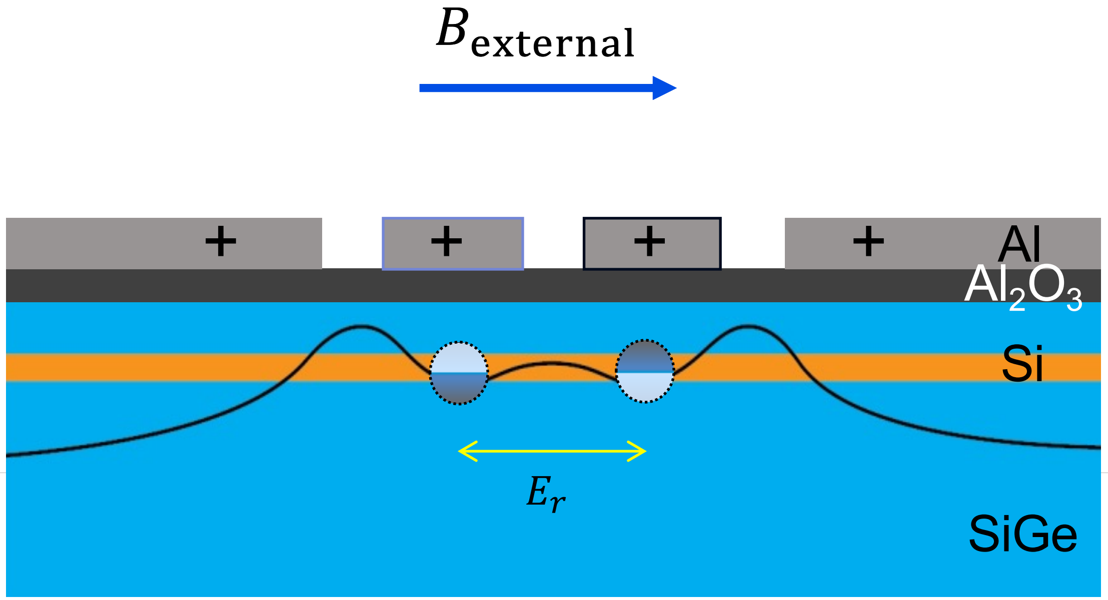

Si/SiGe growth by A. Sammak and G. Scappucci

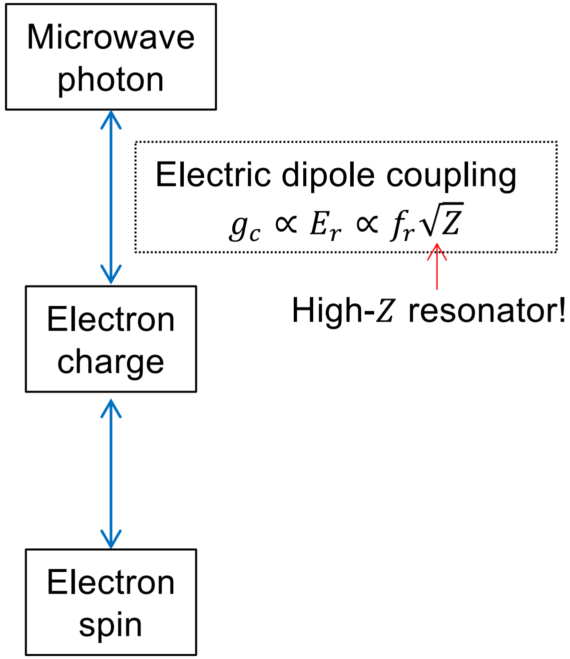

Theory: Benito *et al.*, PRB 96 (2017)
High-Z resonator: Samkharadze *et al.*, PRApplied 5 (2016)

Spin-charge admixing

Samkharadze, Zheng, et al., Science 2018

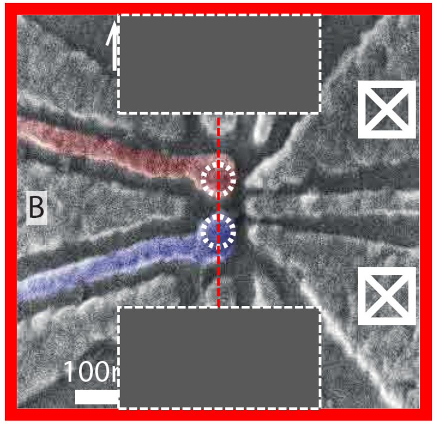

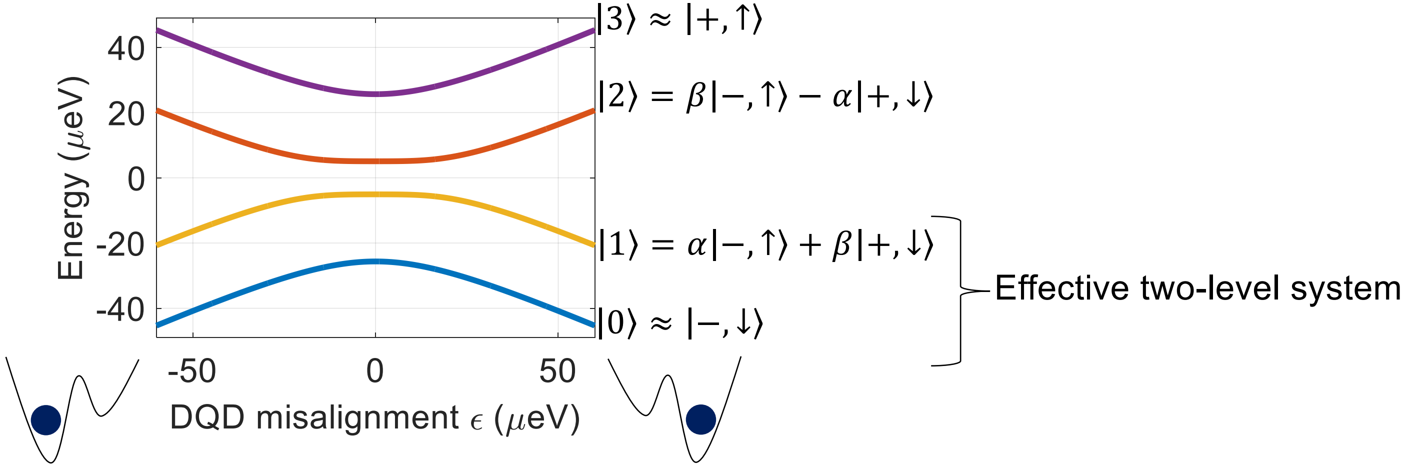

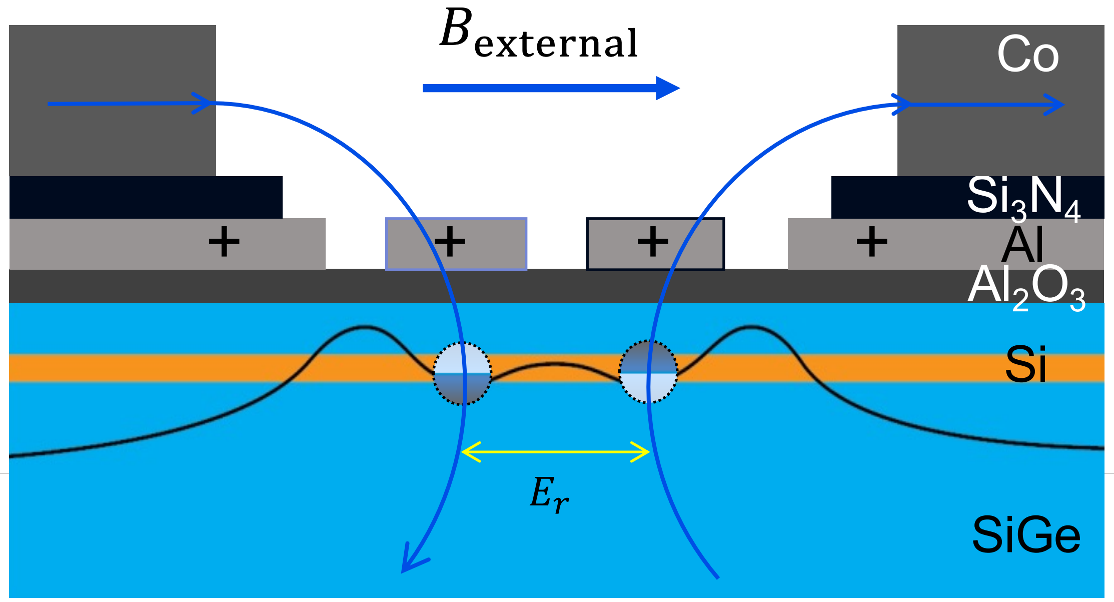

Si/SiGe growth by A. Sammak and G. Scappucci

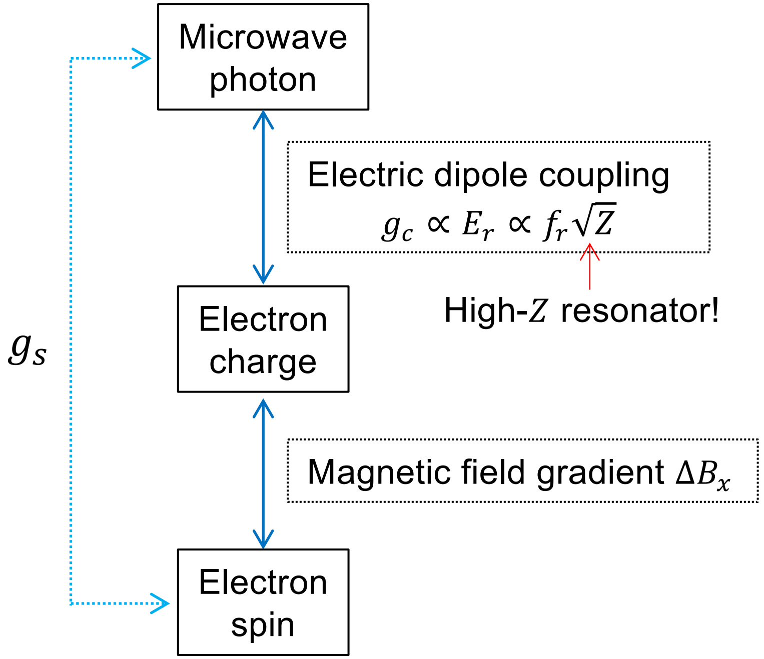

Condition for **strong coupling**

$$\boxed{g_s \propto g_c \frac{\Delta B_x}{2t_c/h - f_r}} > \kappa, \gamma_s$$

Theory: Benito *et al.*, PRB 96 (2017)
High-Z resonator: Samkharadze *et al.*, PRApplied 5 (2016)

Vacuum Rabi splitting

Samkharadze, Zheng, et al., Science 2018

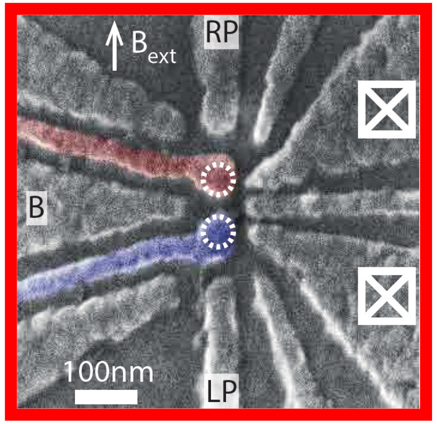

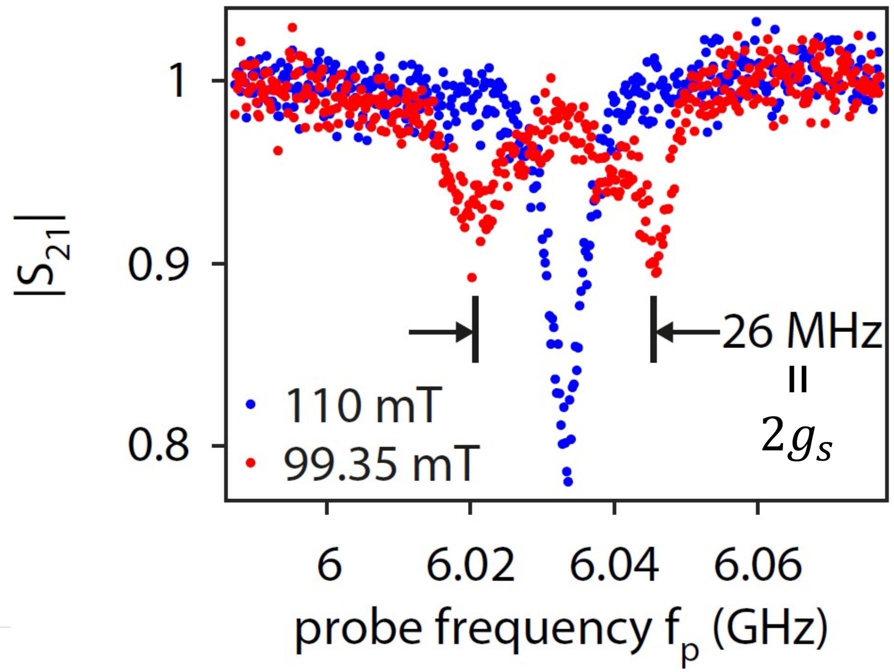

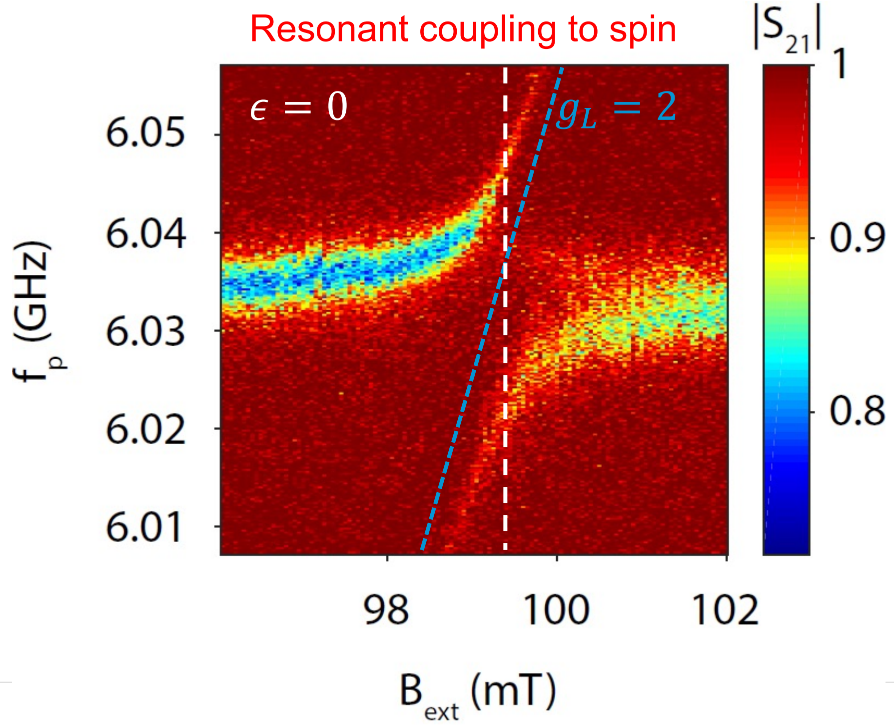

QuTech

Remote spin-spin coupling

F. Borjans et al., Nature (2020)

P. Harvey-Collard et al., PRX 2022

Spin-spin dispersive coupling

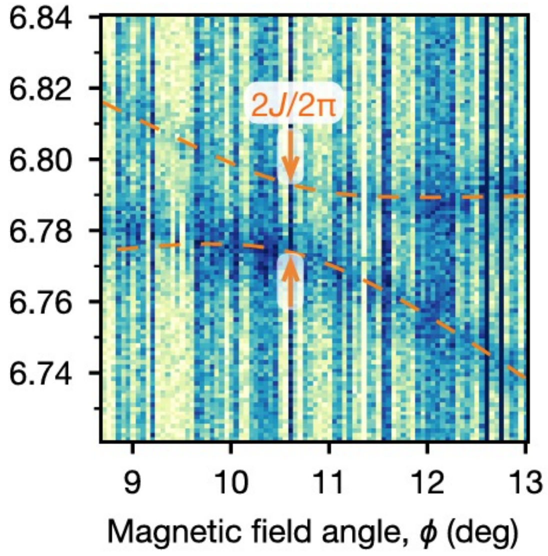

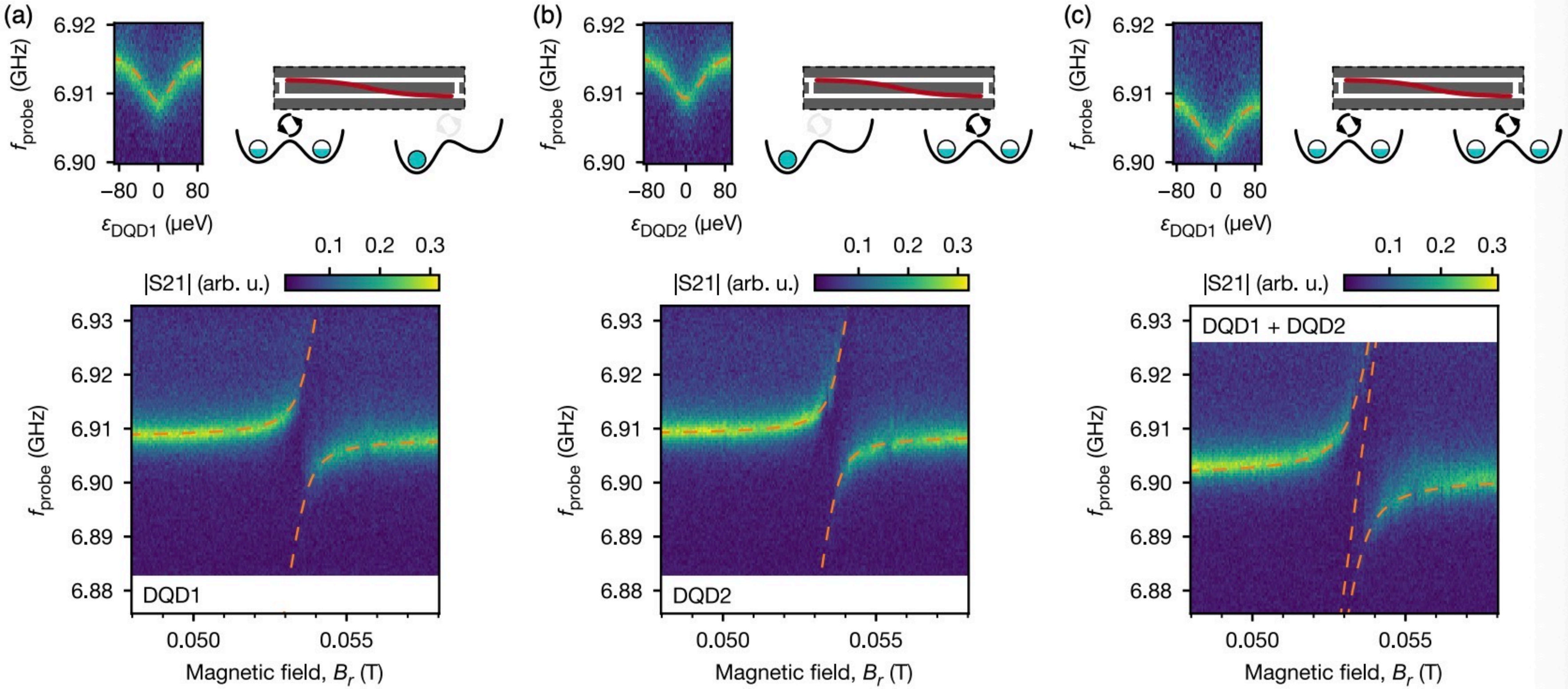

Modular design

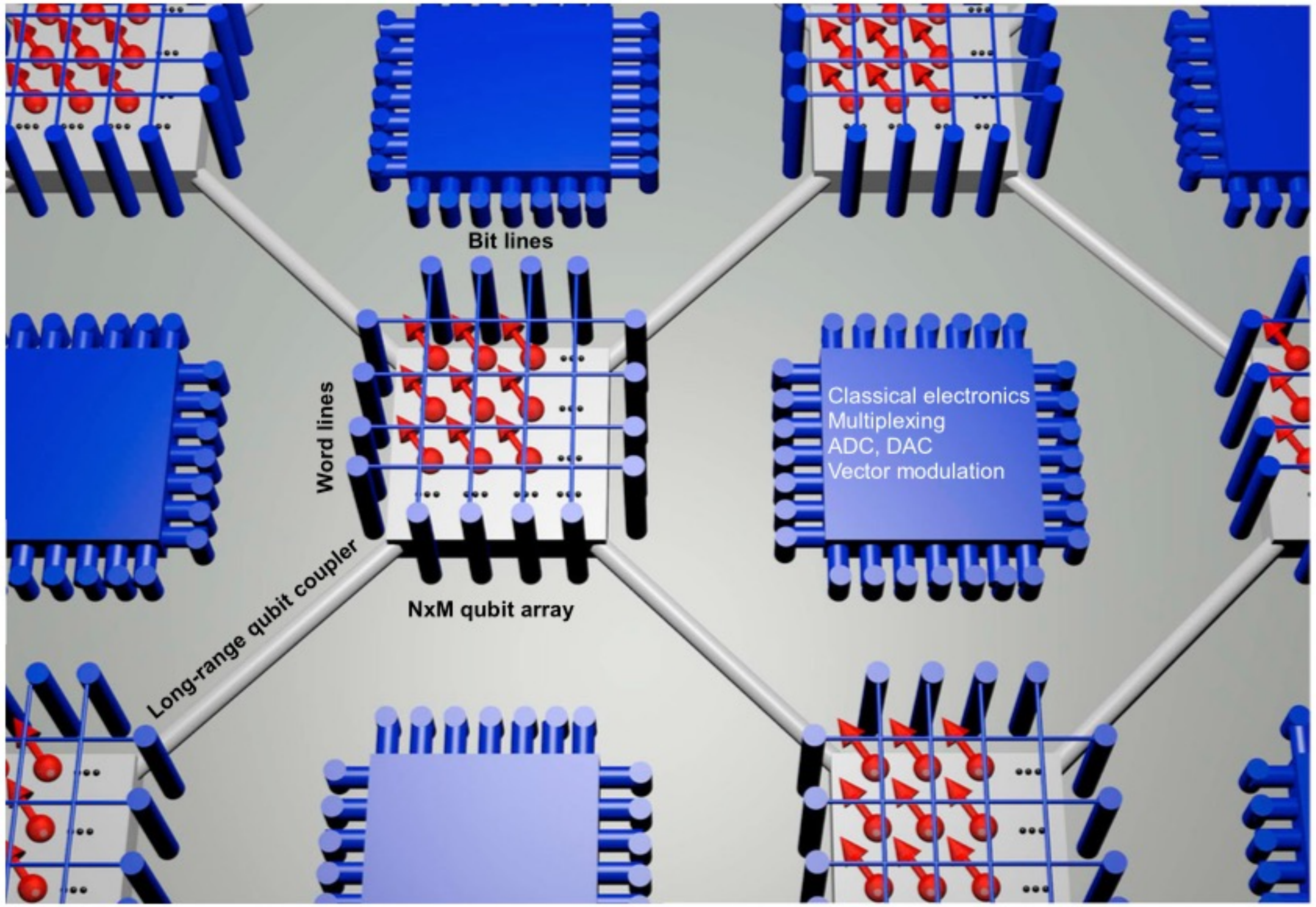

- Local operations in each module
- Remote couplers between modules
- Integrated electronics for control & readout

Quantum-classical interface

L. M. K. Vandersypen et al., npj Quantum Info (2017)

QuTech

1 billion qubits

Trapped ions

100 X 100 m^2

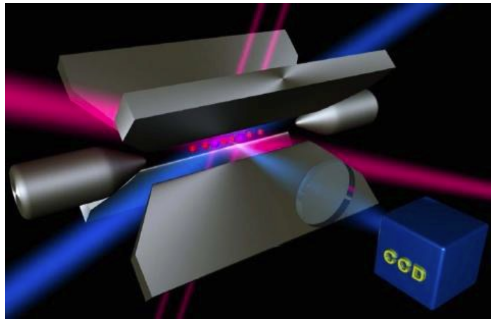

Much smaller for surface trap

Superconducting qubits

5 X 5 m^2

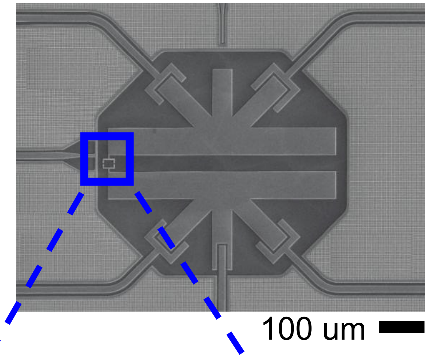

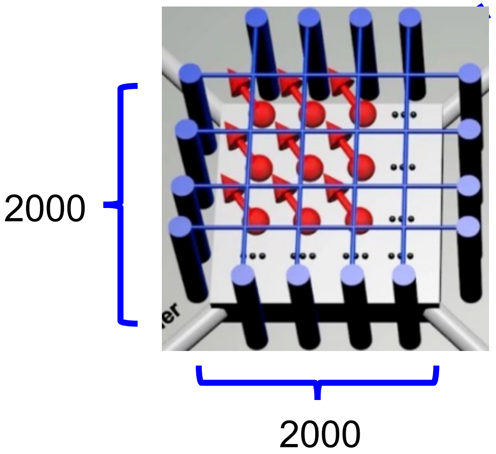

Spin qubits

5 X 5 mm^2

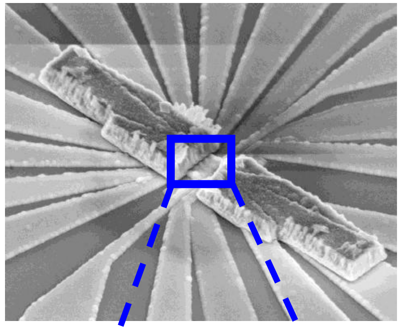

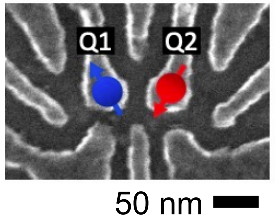

Superconducting qubits

Chip-to-chip entanglement (fidelity: 73%)

DiCarlo group (Delft)
C. Dickel, et al, PRB 2018

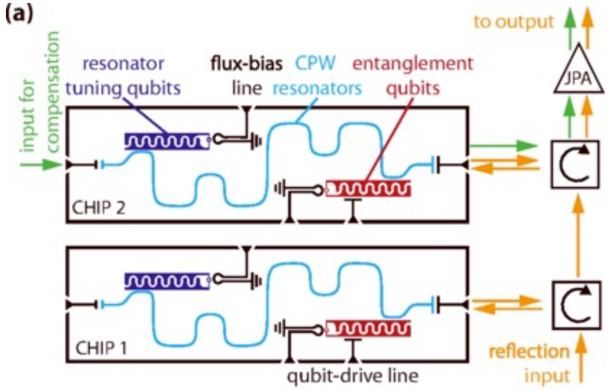

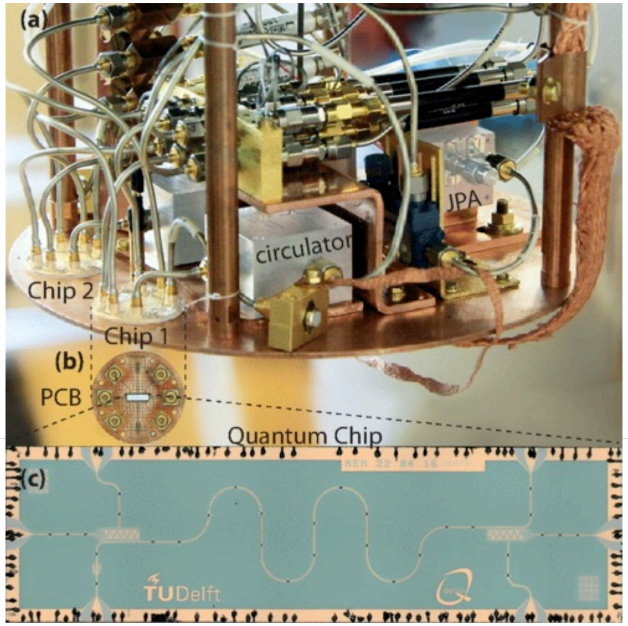

Chip-to-chip GHZ state transfer (fidelity: 65.6%)

Cleland group (U Chicago)
Y. Zhong, et al, Nature 2021

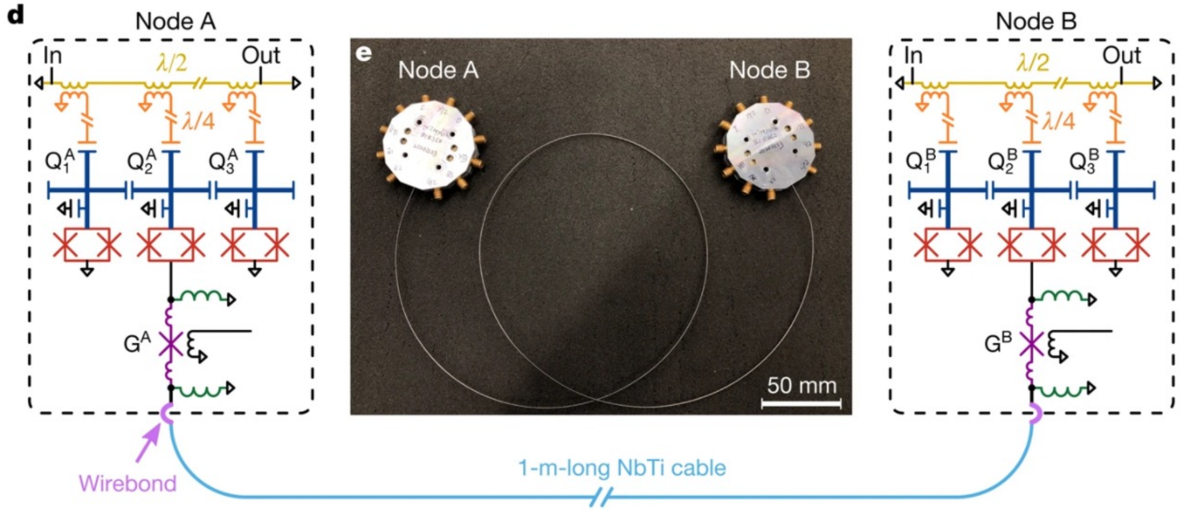

Fridge-to-fridge entanglement (fidelity: 79.5%)

Wallraff group (ETH)
P. Magnard, et al, PRL 2020

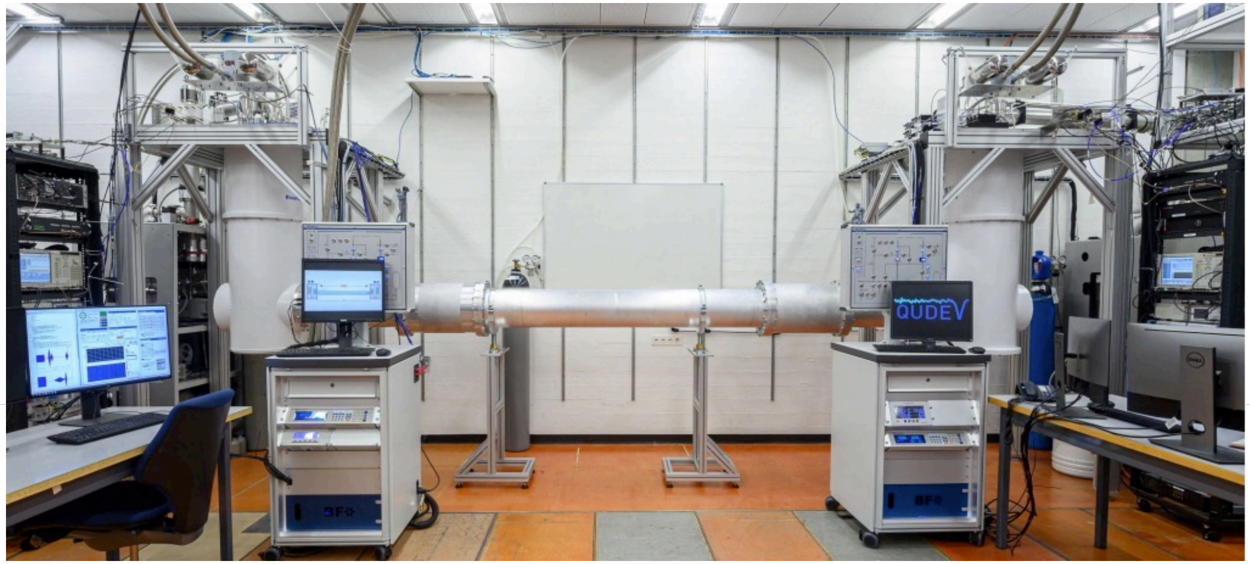

A ‘supreme’ quantum computer

Google Sycamore quantum processor

Fridge

Qubits

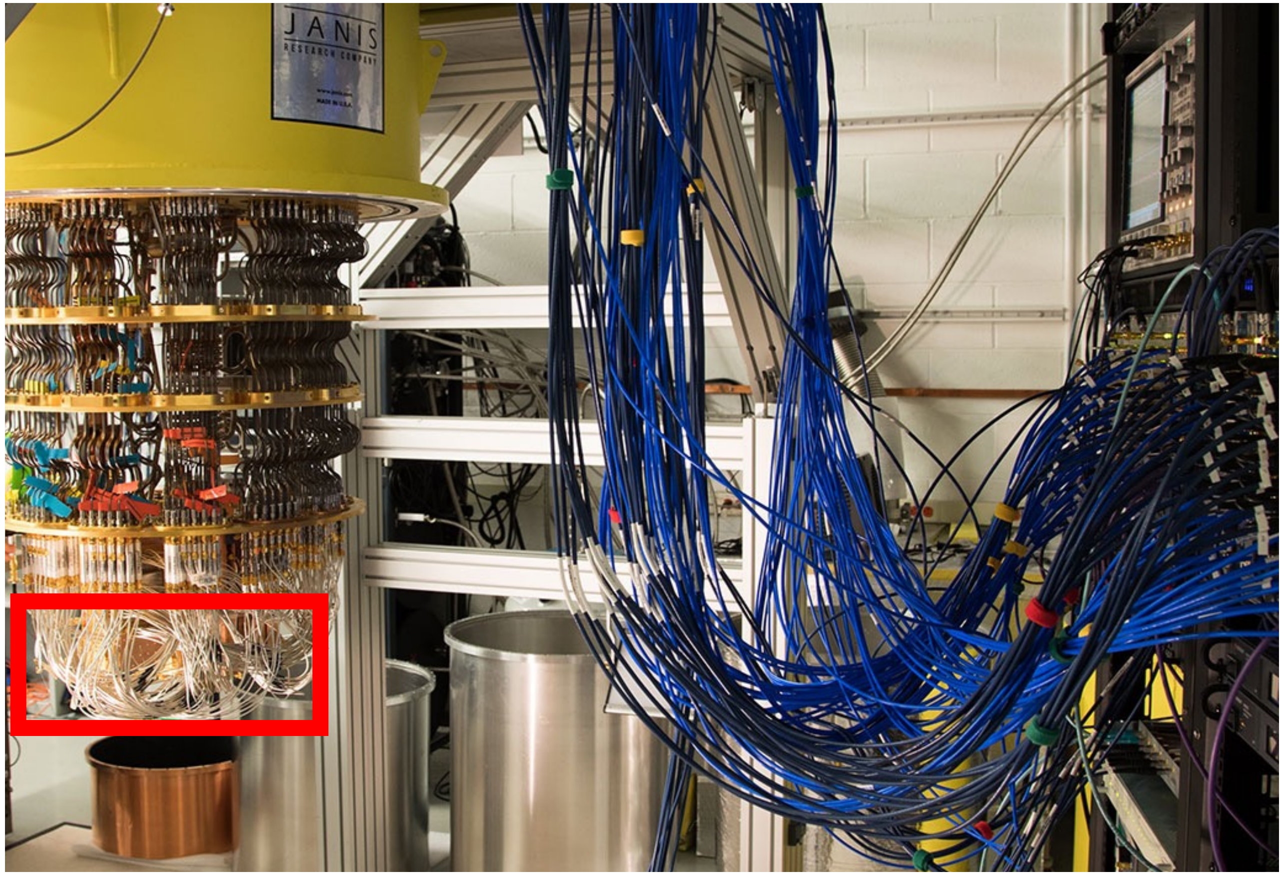

Control
&
Readout

Bardin, et al., ISSCC (2019)
Arute, et al., Nature (2019)

QuTech

Delft lab

QuTech

IQ modulation right now

Arbitrary waveform generator
(AWG, Keysight)

Vector microwave source
(Keysight)

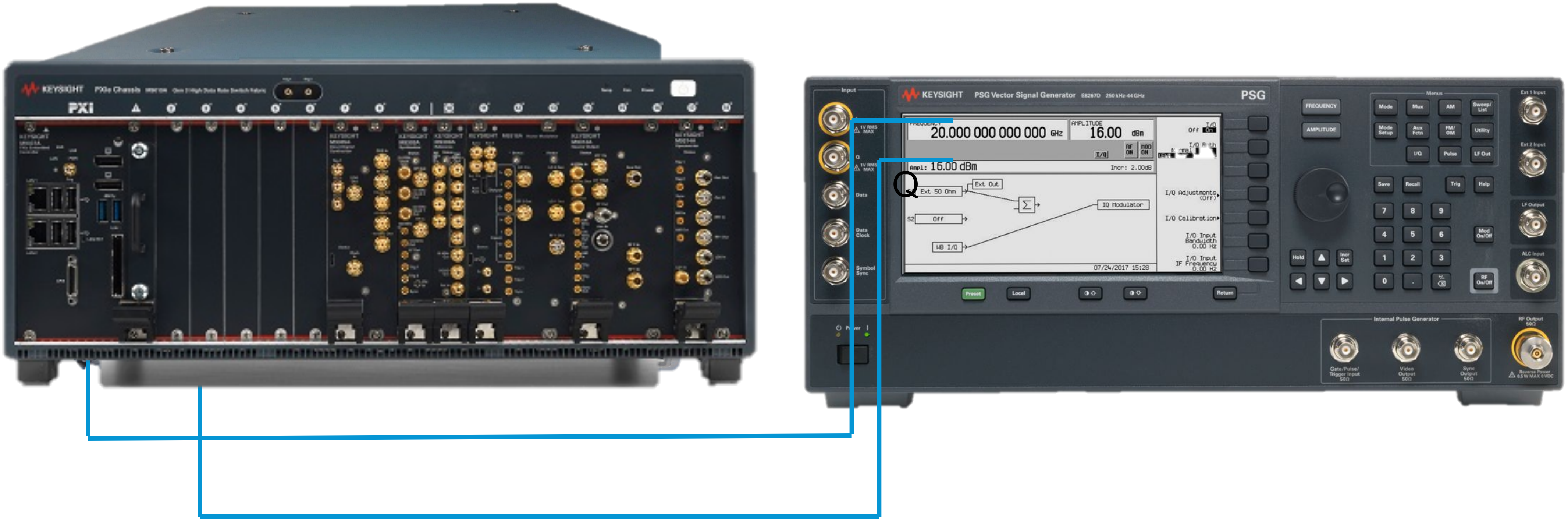

QuTech

Way forward: cryo-electronics

Integrated electronics
1% accuracy in all parameters

60 K

4 K
2 W

100 mK
0.5 mW

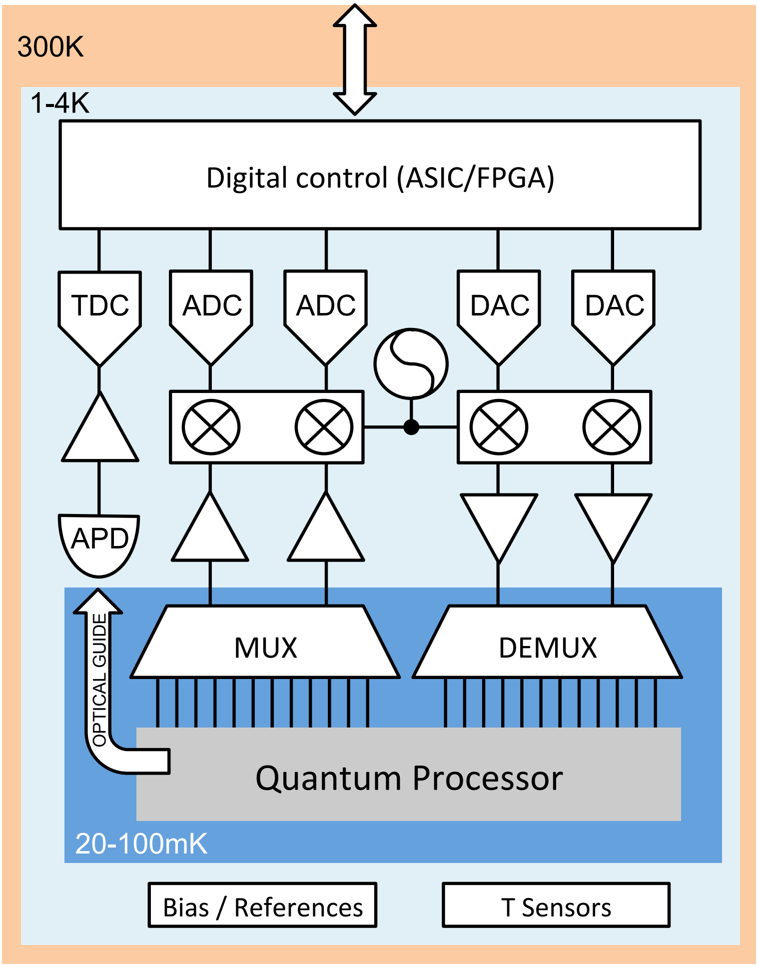

E.Charbon, et al., “Cryo-CMOS for Quantum Computing”, IEDM 2016.

Cryo-CMOS approach

Use 3K stage for qubit control using **cryo-CMOS integrated circuits**.

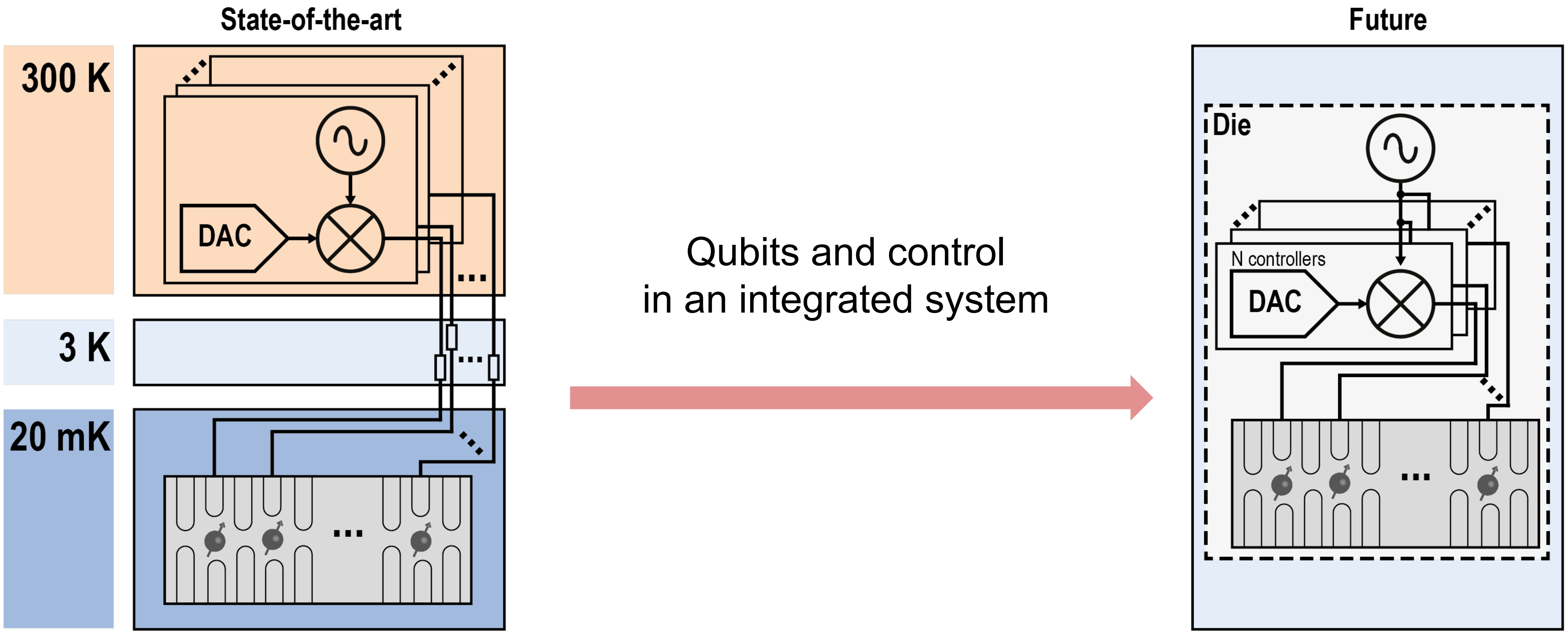

with Charbon & Sebastiano groups at QuTech
and with Pellerano et al from Intel
ISSCC 2020

Horse Ridge

Horse Ridge, Oregon
(very cold)

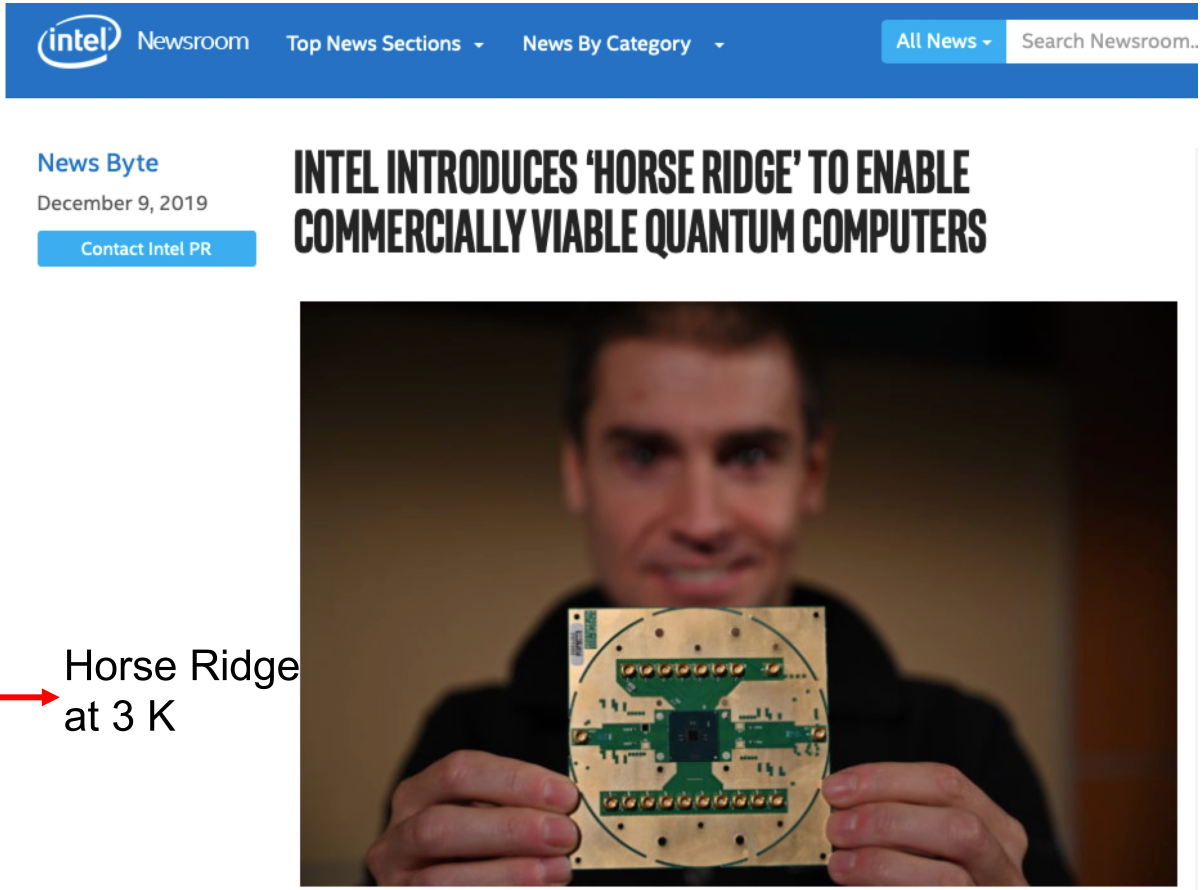

Stefano Pellerano, principal engineer at Intel Labs, holds Horse Ridge. The new cryogenic control chip will speed development of full-stack quantum computing systems, marking a milestone in the development of a commercially viable quantum computer. (Credit: Walden Kirsch/Intel Corporation)
» Click for full image

Self heating characterization

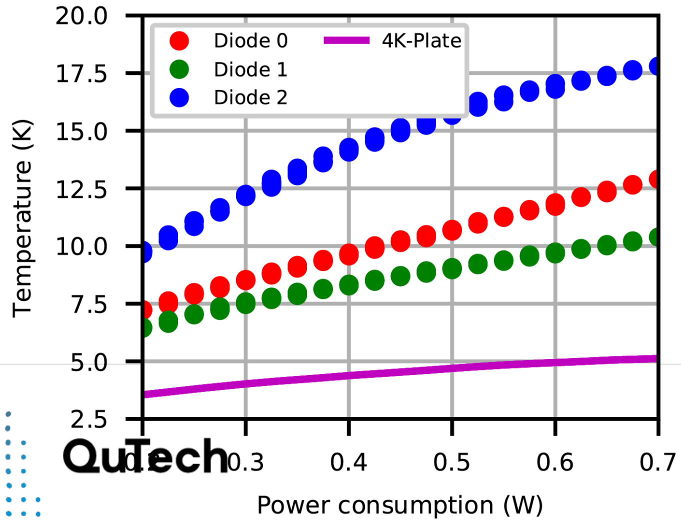

Horse Ridge
at 3 K

Qubits
at 10 mK

QuTech

with Charbon & Sebastiano groups at QuTech
and with Pellerano et al from Intel
ISSCC 2020

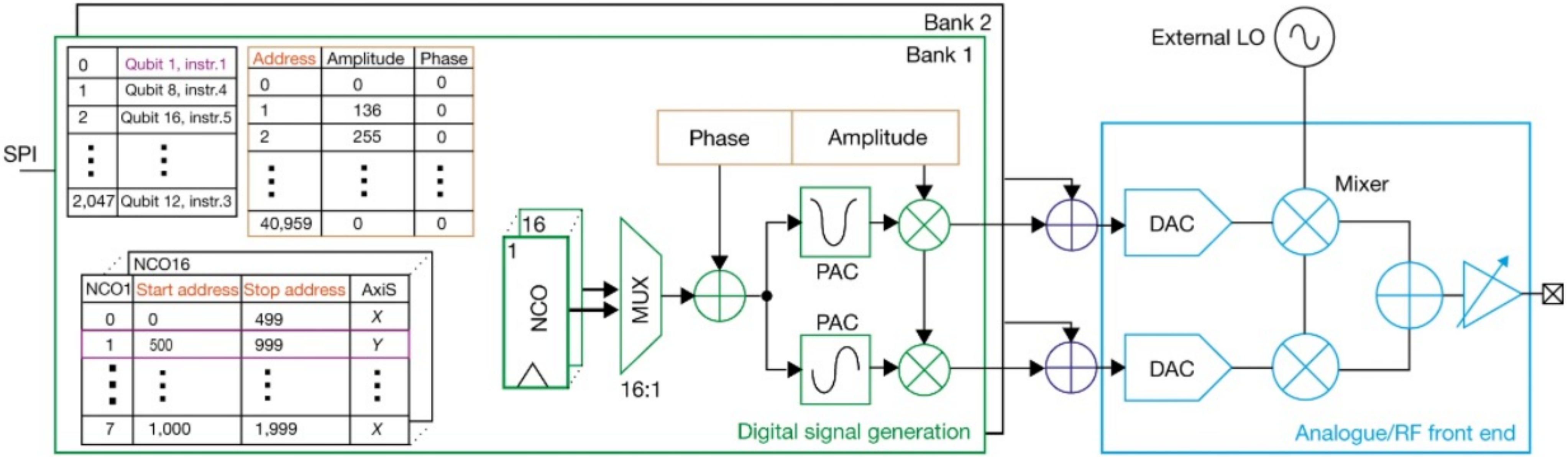

1 kHz

External trigger

Instruction list

~8 Mb/s

0	Qubit 1, instr. 1
1	Qubit 8, instr. 4
2	Qubit 20, instr. 5
3	Qubit 6, instr. 2
4	Qubit 31, instr. 7
⋮	⋮
2047	Qubit 12, instr. 3

Instruction table / qubit

~35 Mb/s

	start address	stop address	axis
0	0	999	X
1	0	999	Y
2	1000	1499	X
3	1000	1499	-Y
4	1500	1999	X
5	2000	2499	Y
6	2500	2999	X
7	3000	3125	X

Envelope memory

18 Gb/s

address	amplitude	phase
0	0	0
1	255	0
2	255	0
3	255	0
⋮	⋮	⋮
40959	0	0

Horse Ridge micrograph

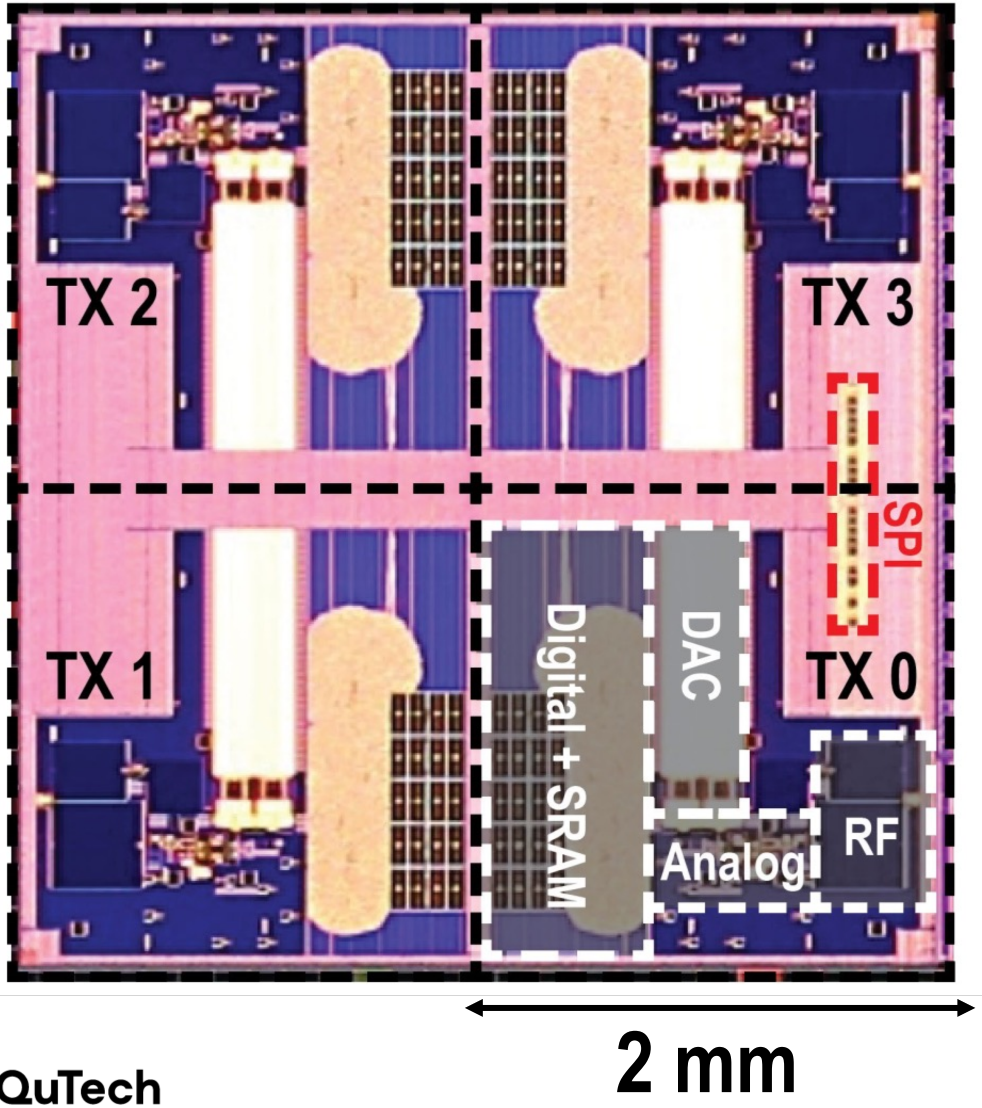

Intel 22 nm FFL Technology

- 4 Transmitters (Each with 32 Channels Multiplexed) = 128 qubits.
- Supports 2-20 GHz Microwave Output (transmons and spin qubits)
- Power Consumption = 330 mW (digital, clock, 1GHz, <u>5 times lower at 200MHz</u>), 54 mW (analog)
- SNR > 44 dB (25 MHz bandwidth)

QuTech

with Charbon & Sebastiano groups at QuTech
and with Pellerano et al from Intel
ISSCC 2020

Fidelity benchmark

AllXY

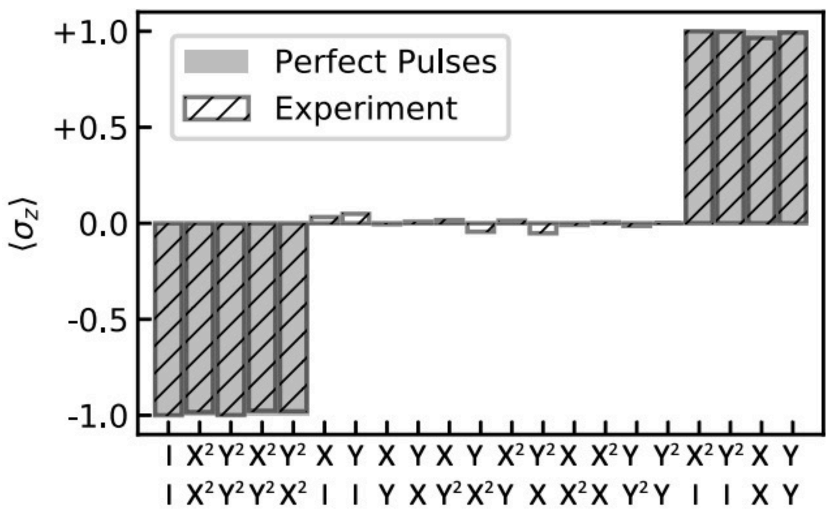

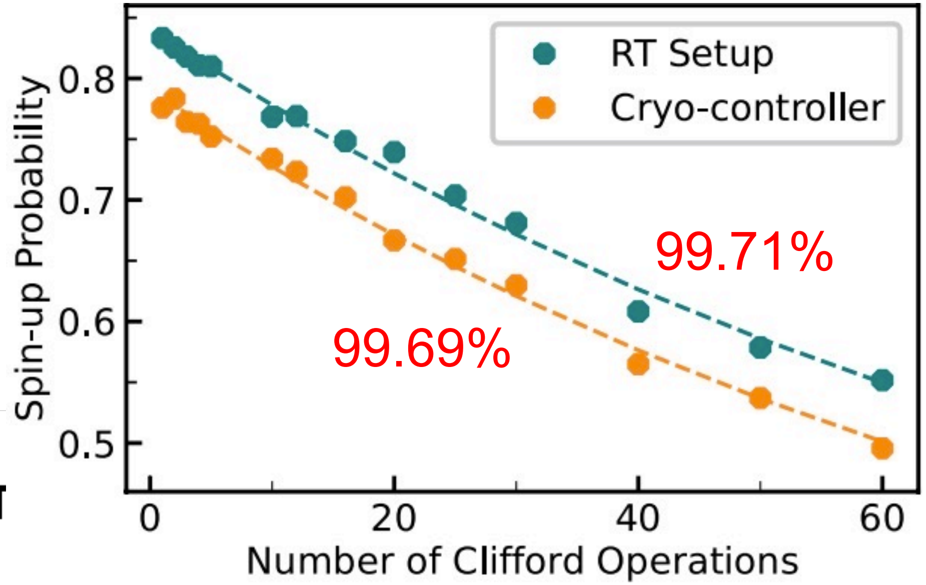

State tomography

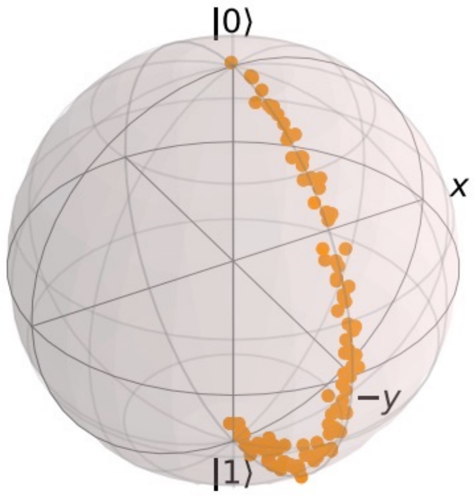

RT setup: Tektronix AWG 5014C
+ Keysight VSG E8267D

QuT

with Charbon & Sebastiano groups at QuTech
and with Pellerano et al from Intel
X. Xue, et al., Nature 2021

Cryo-CMOS: “Horse Ridge”

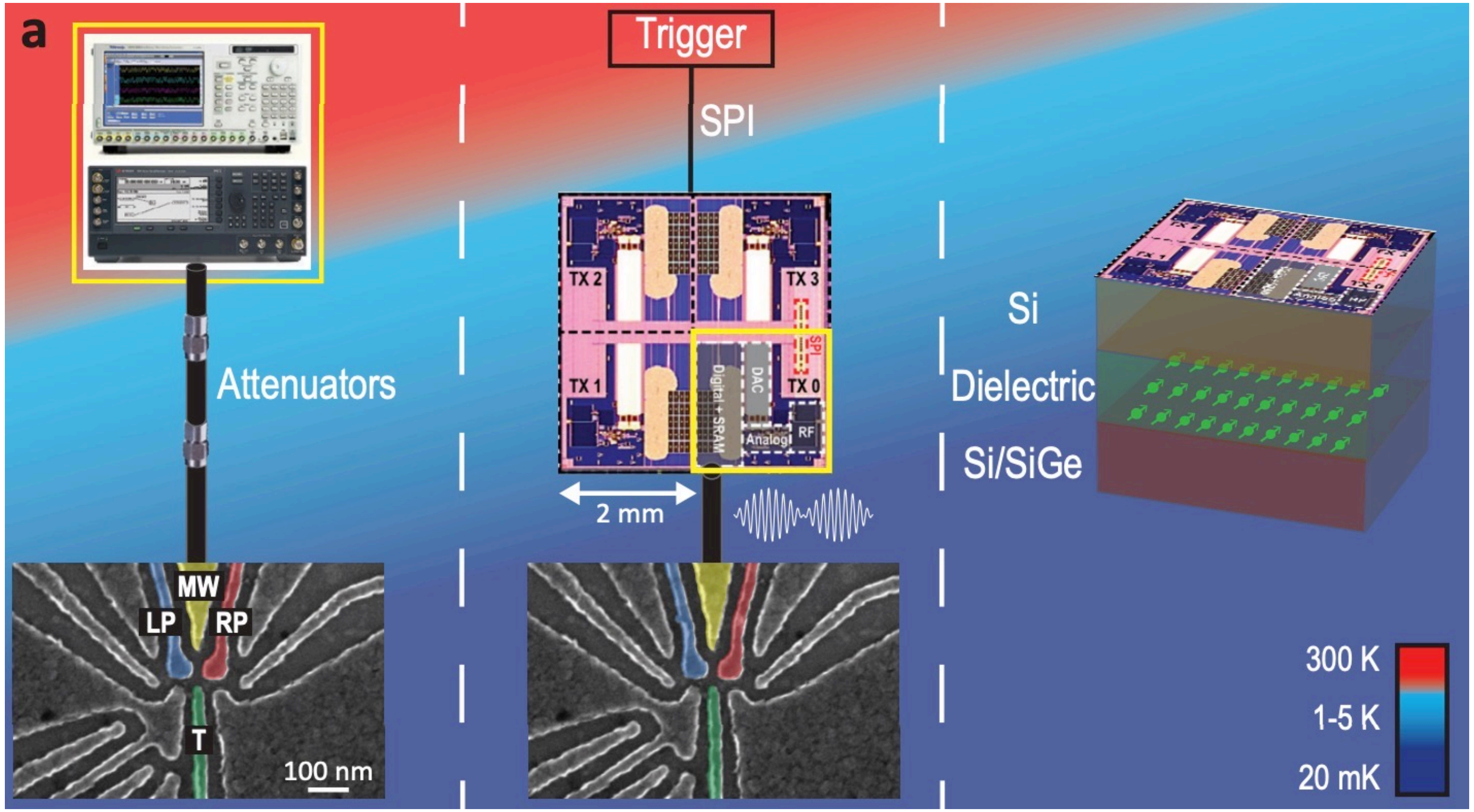

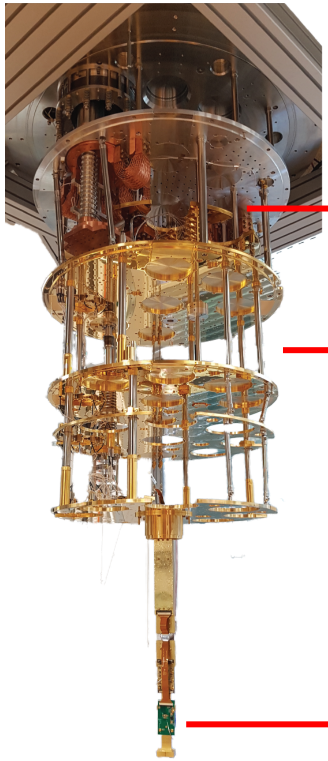

Horse Ridge
at 3 K

Qubits
at 1-4 K

Qubits
at 10 mK

X. Xue, B. Patra, et al., Nature (2021)
with Charbon & Sebastiano et al @QuTech
and Intel Quantum

“Hot” qubits

Urdampilleta, et al., Nat Nano 2019	(Grenoble)	High-fidelity readout up to 1K
Petit, et al., Nature 2020	(Delft)	Universal two-qubit operations above 1K
Yang, et al., Nature 2020	(UNSW)	Single-qubit gates above 1K
Geyer, et al., Nat Electronics 2022	(Basel)	98% single-qubit gate at 4.2K

QuTech

Modular design

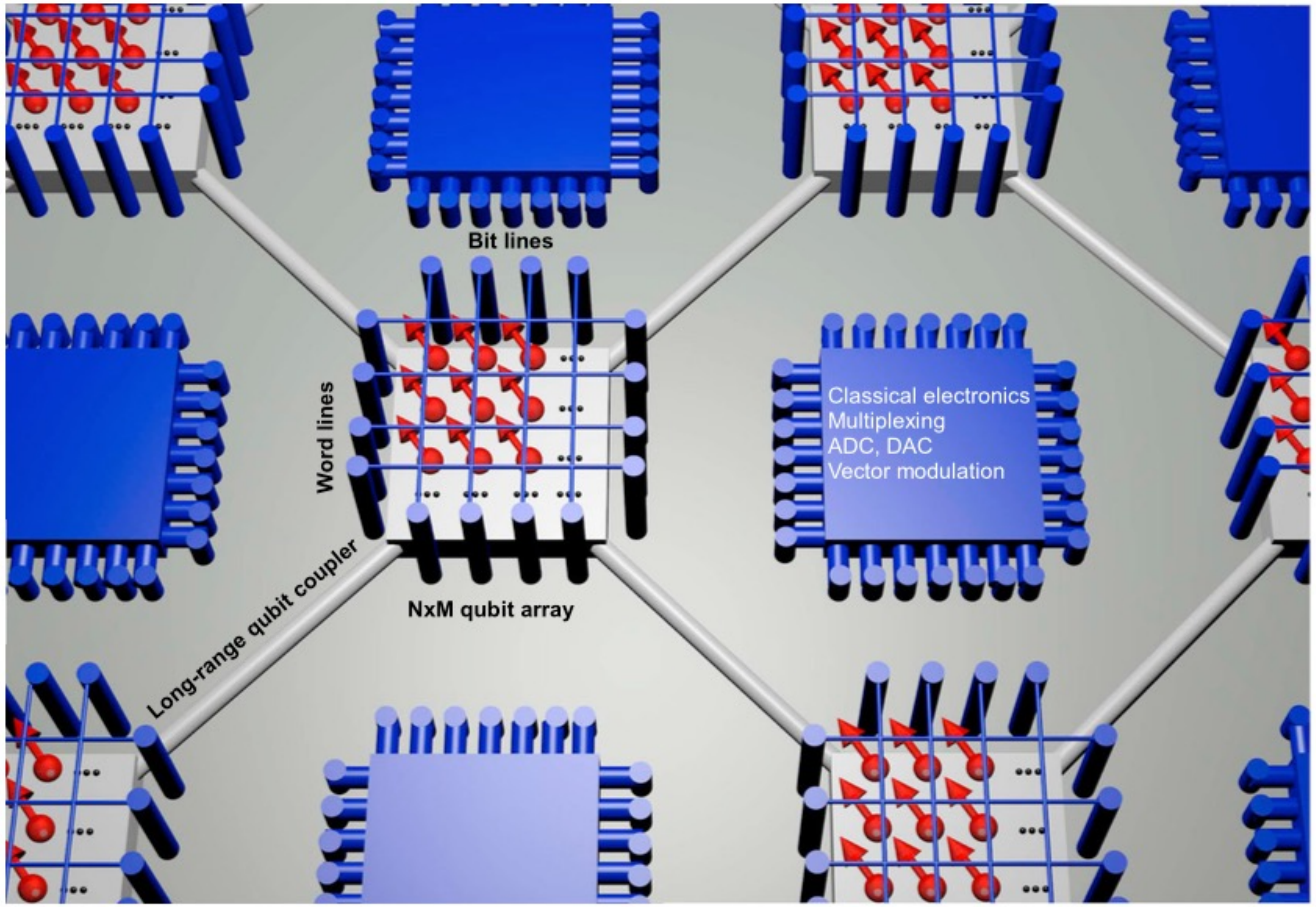

- Local operations in each module
- Remote couplers between modules
- Integrated electronics for control & readout

“Hot” qubits

L. M. K. Vandersypen et al., npj Quantum Info (2017)

QuTech

T1 and charge noise vs temperature

M. Veldhorst group @ Delft

SiMOS

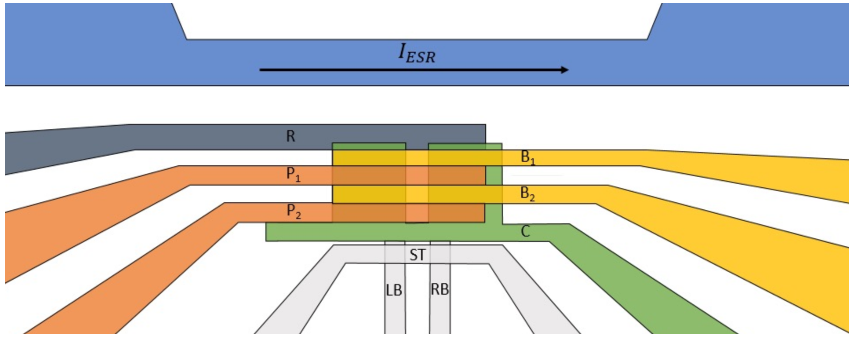

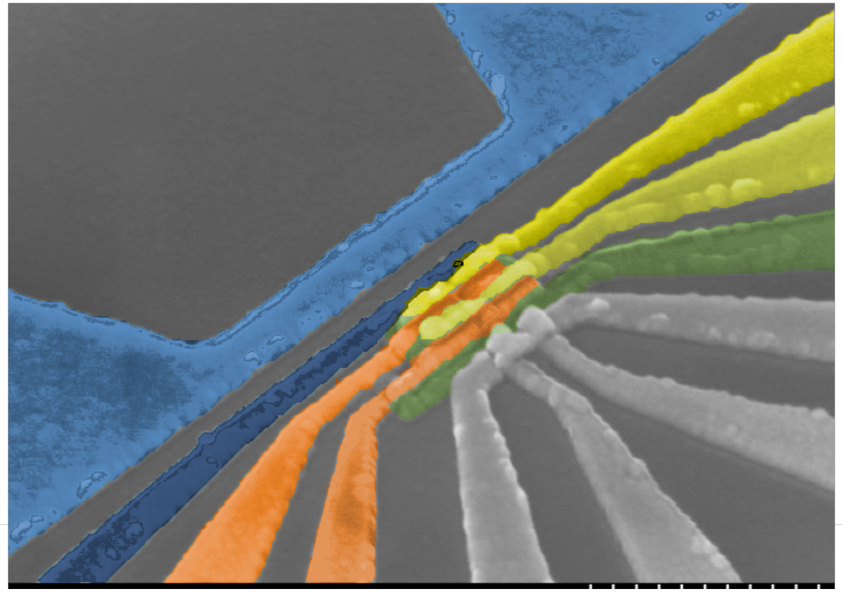

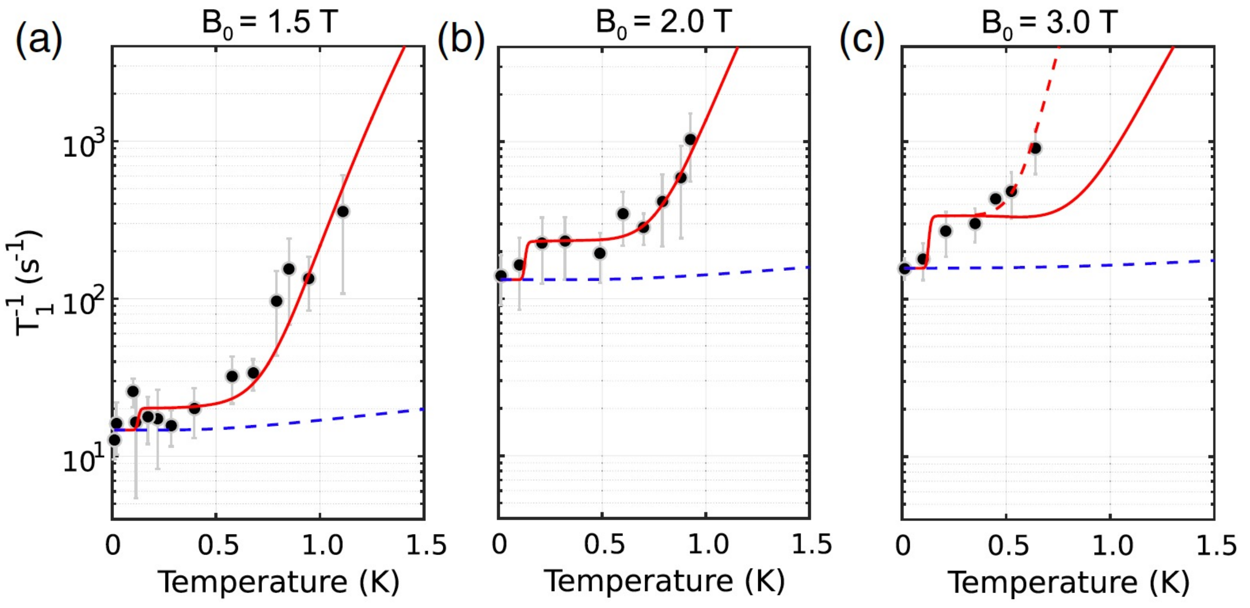

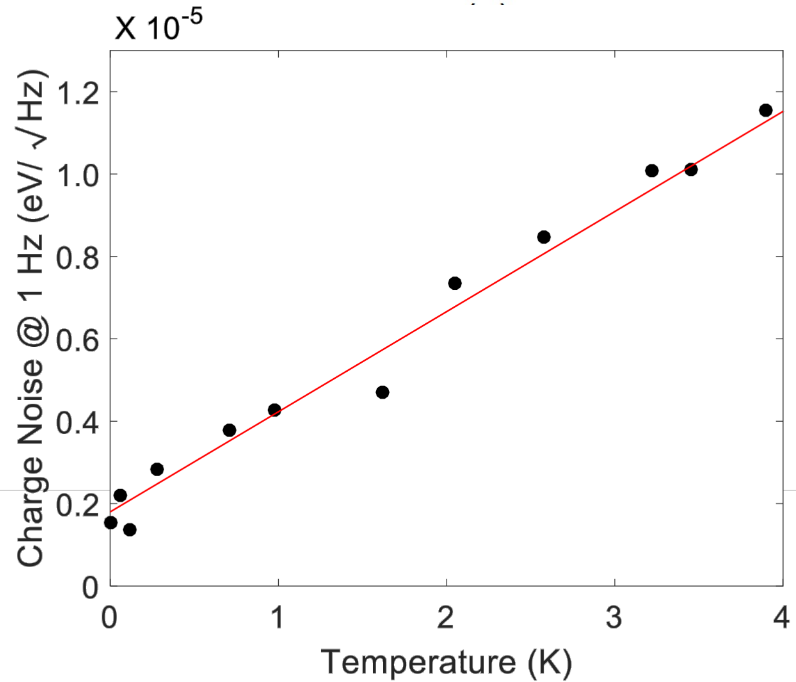

QuTech

L.Petit, et al., PRL 2018

Coherence times vs temperature

A. Dzurak group @ UNSW

SiMOS

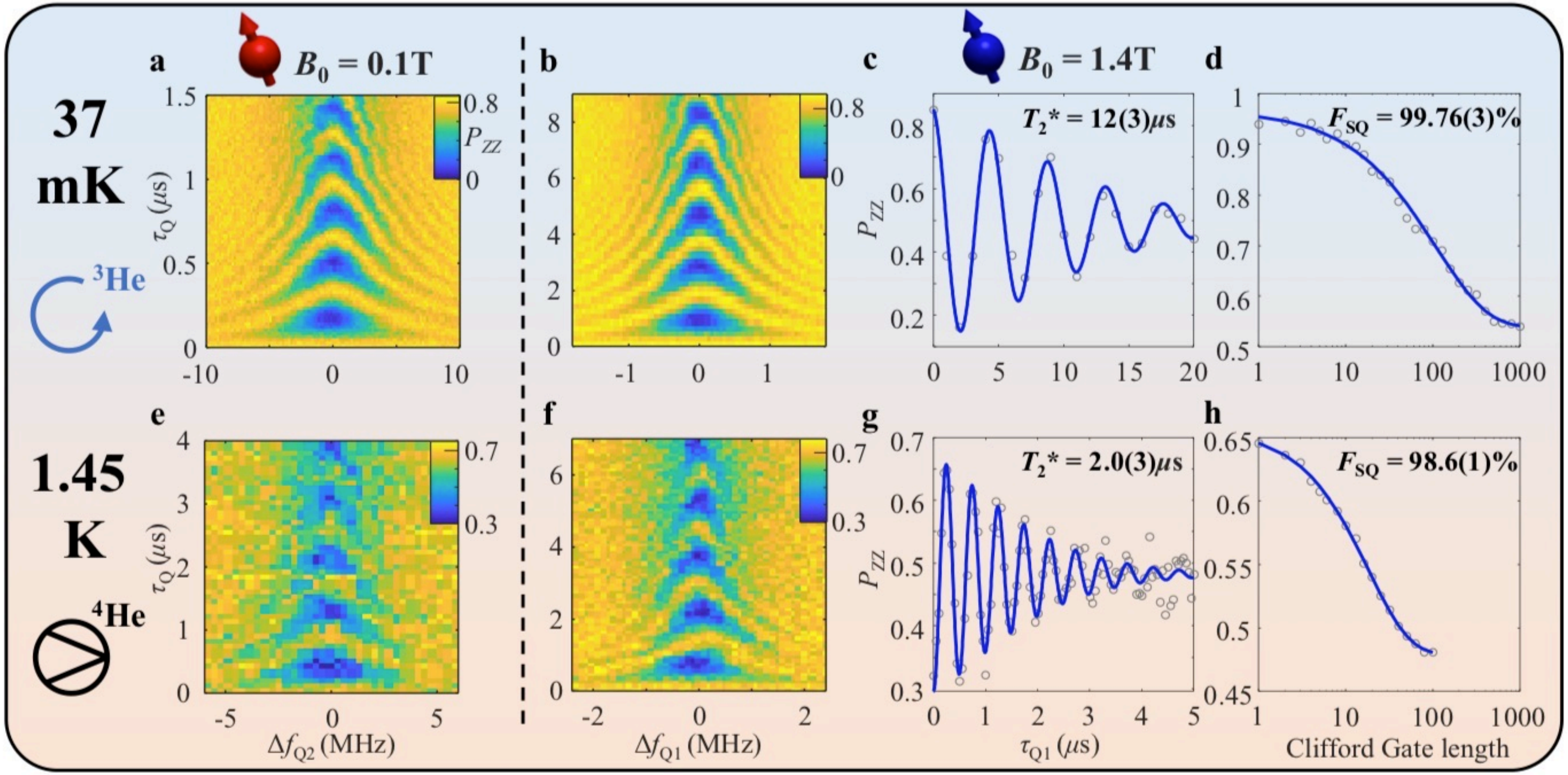

QuTech

C.H.Yang, et al., Nature 2020

Qubits at 1.1K

M. Veldhosrt group @ QuTech Delft

SiMOS

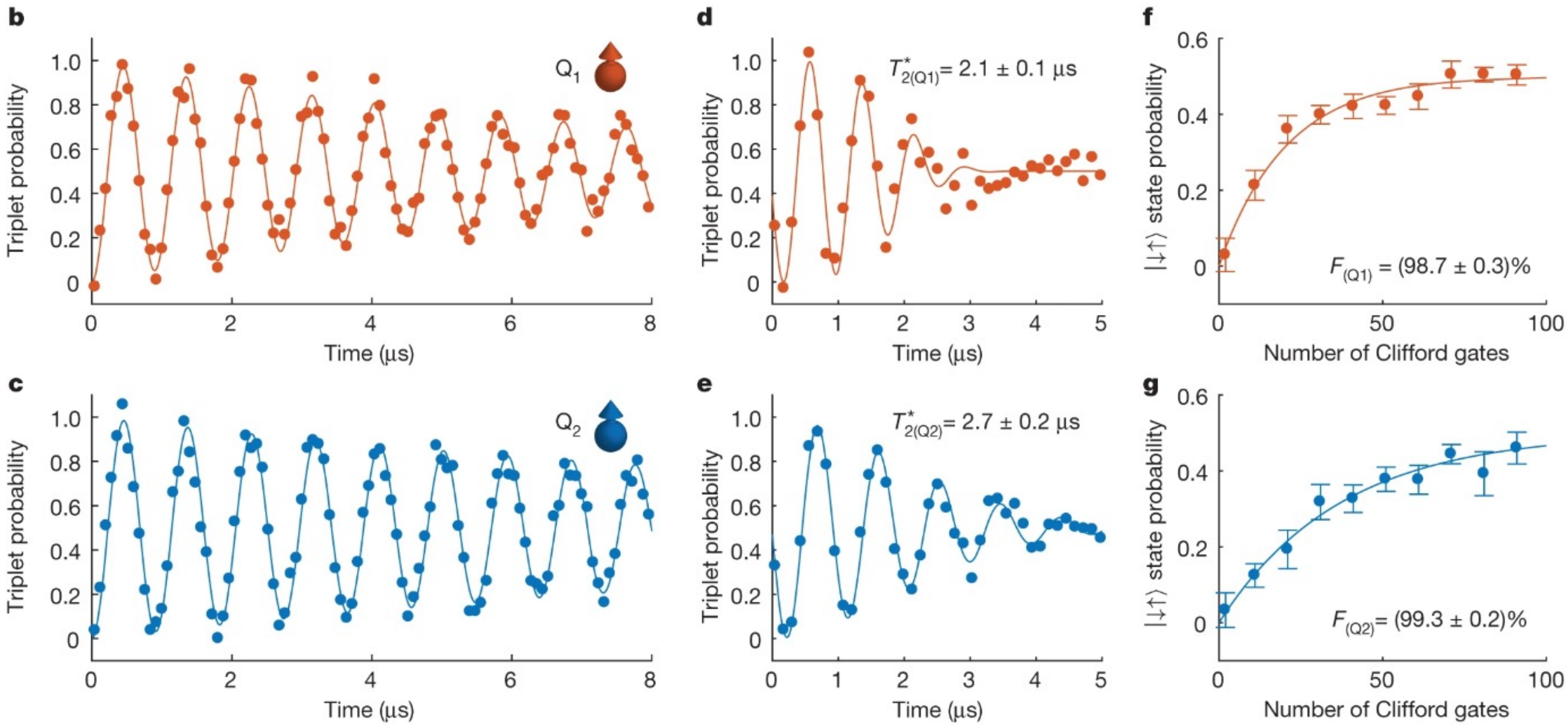

QuTech

L. Petit, et al., Nature 2020

Coherence times vs temperature

Coherence

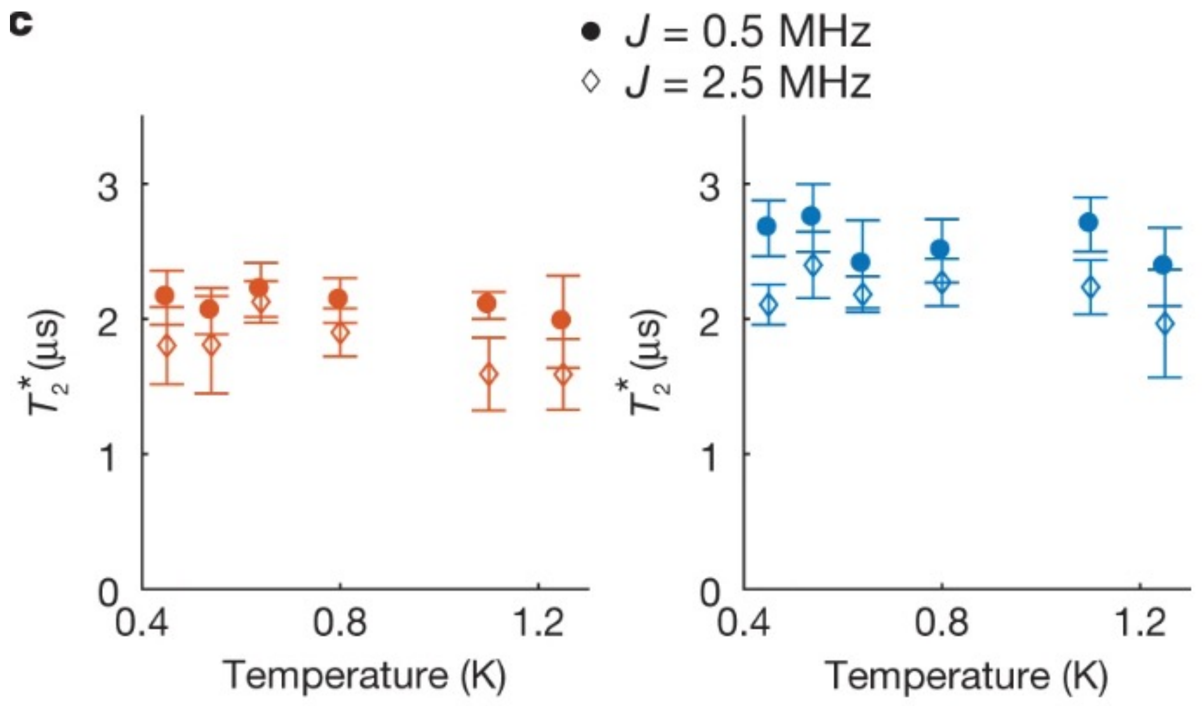

Two-qubit fidelity

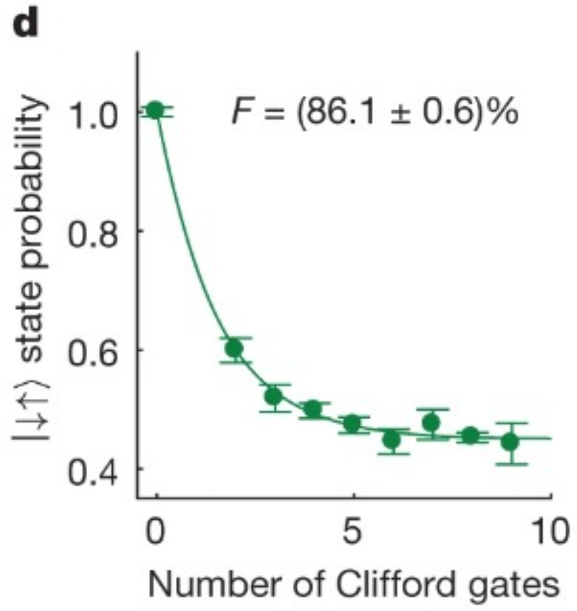

QuTech

L. Petit, et al., Nature 2020

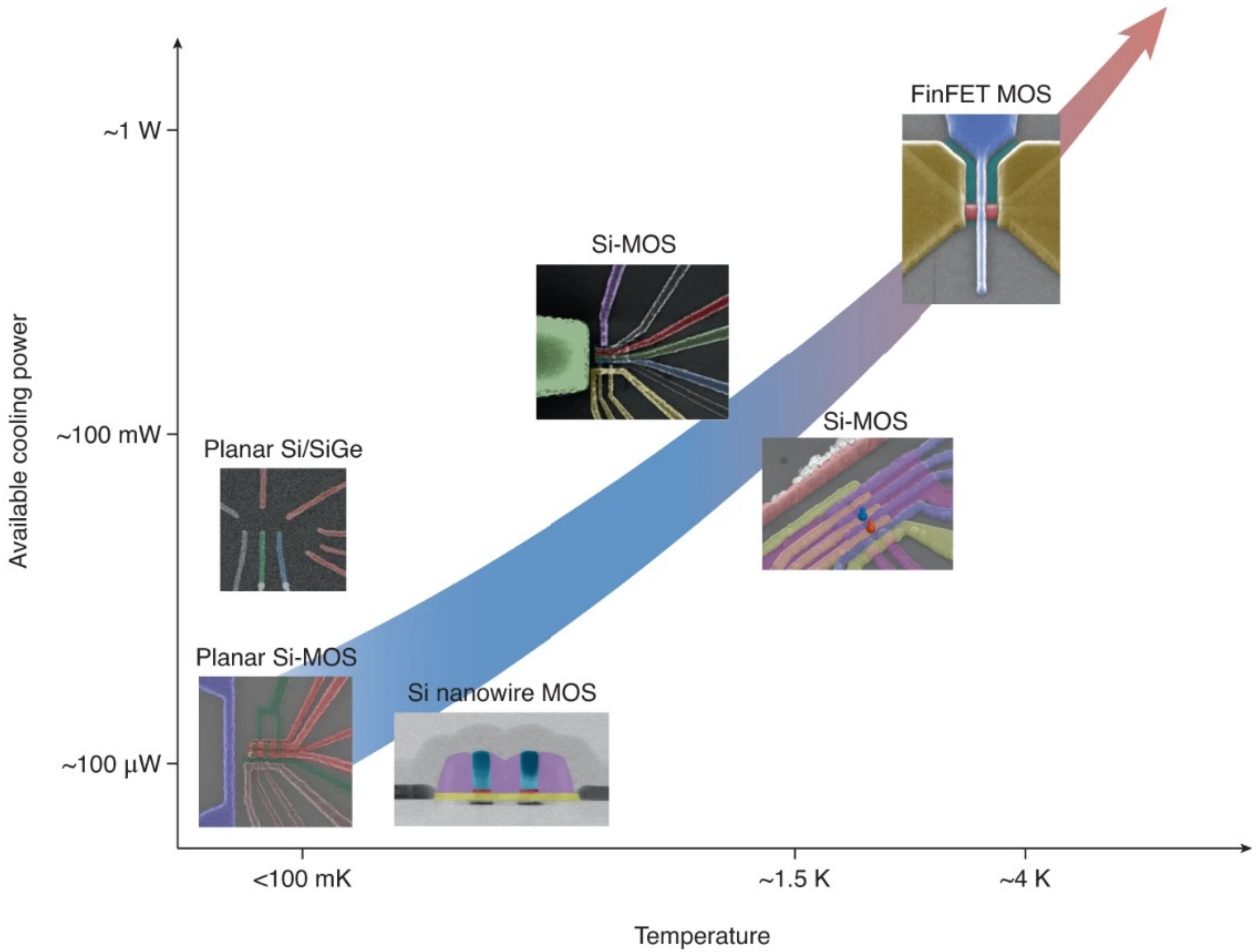

QuTech

Maurand, et al., Nature Electronics 2022

Qubits at > 4K

Coherence

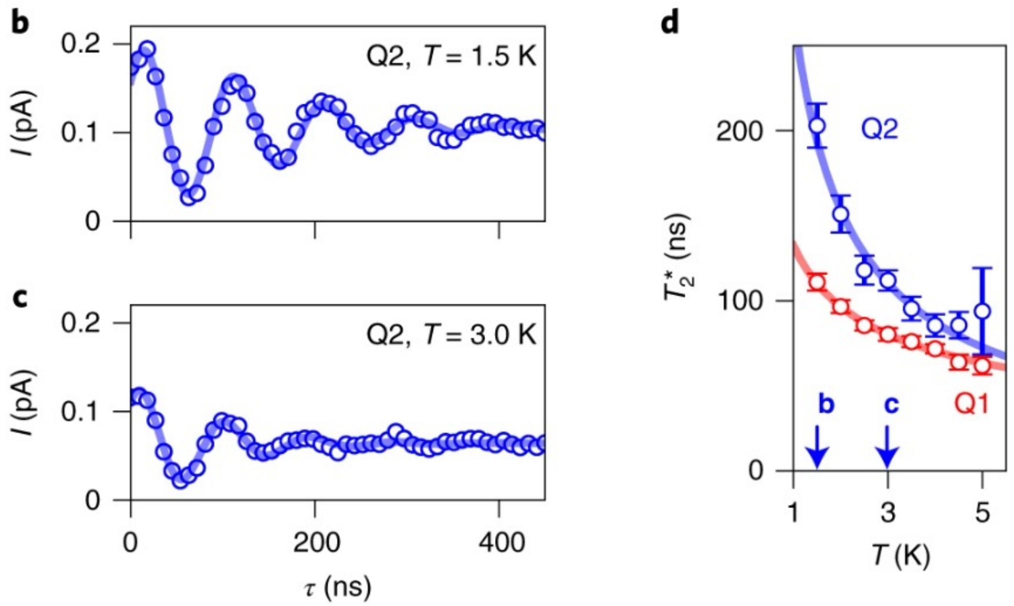

Single-qubit fidelity

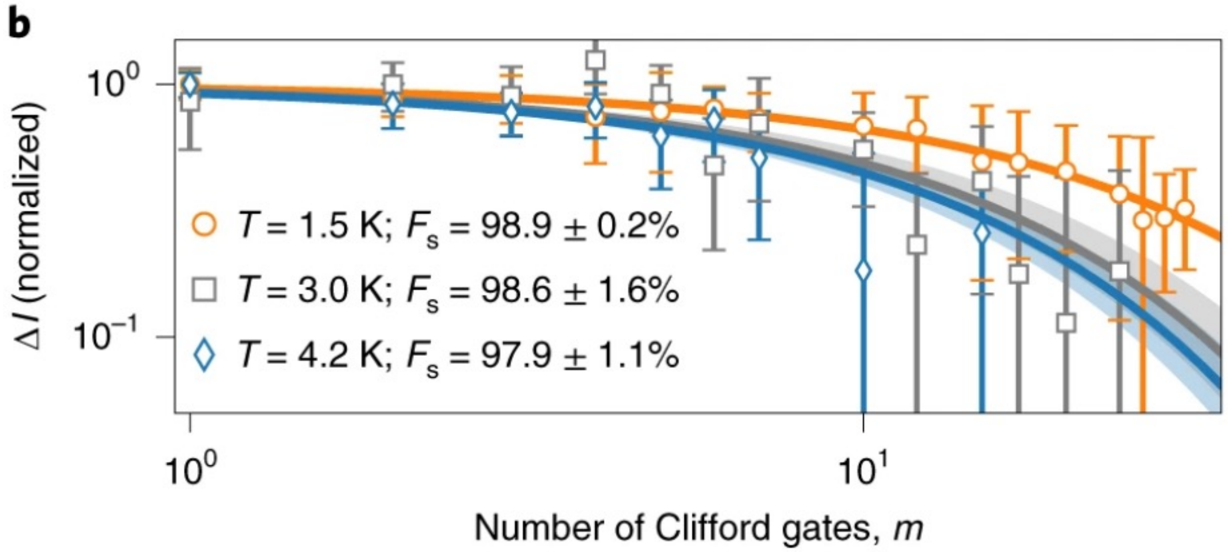

QuTech

Camenzind, et al.,
Nature Electronics 2022

Quantum simulation

A 2X2 array

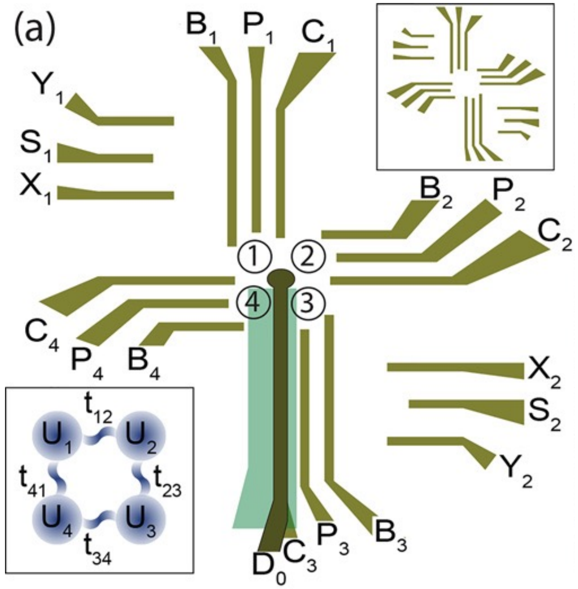

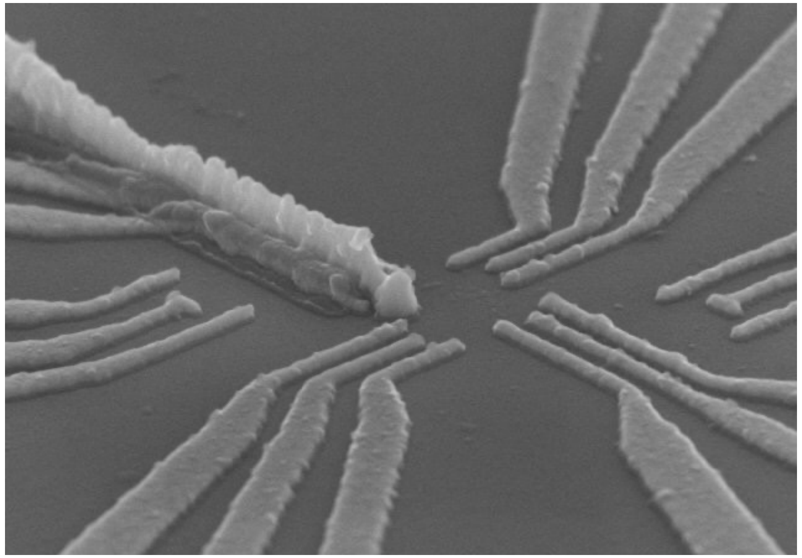

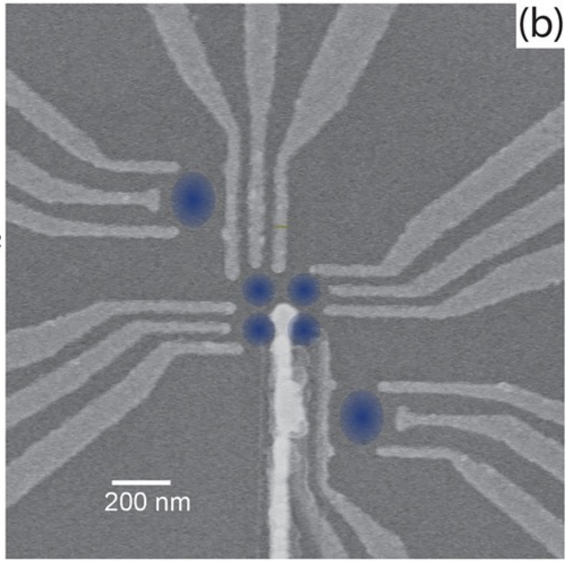

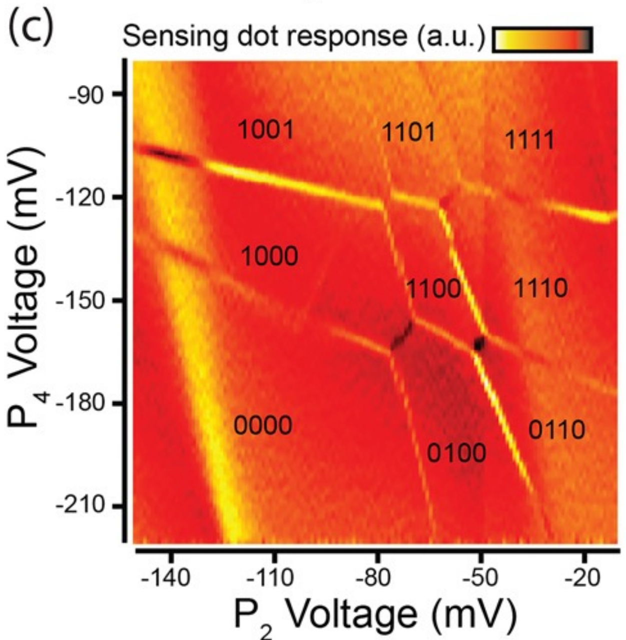

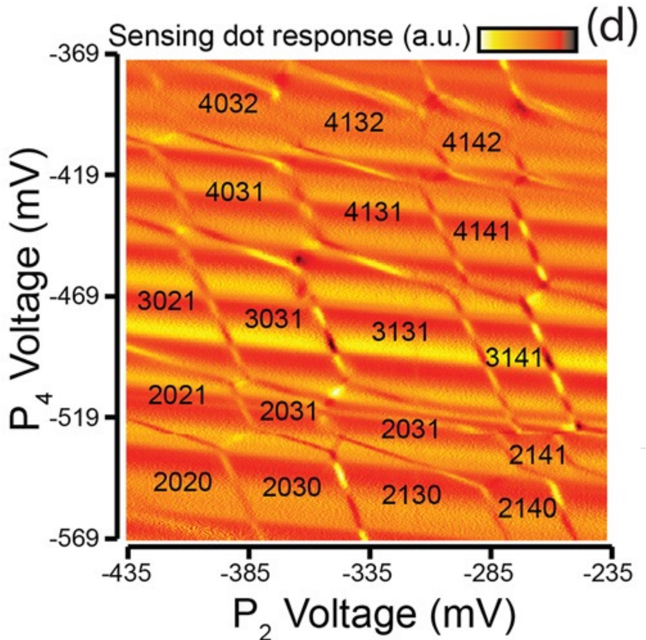

Mukhopadhyay, Dehollain et. al. APL 2018

See also Thalineau et al, APL 2013

QuTech

Controllable Tunnel Coupling

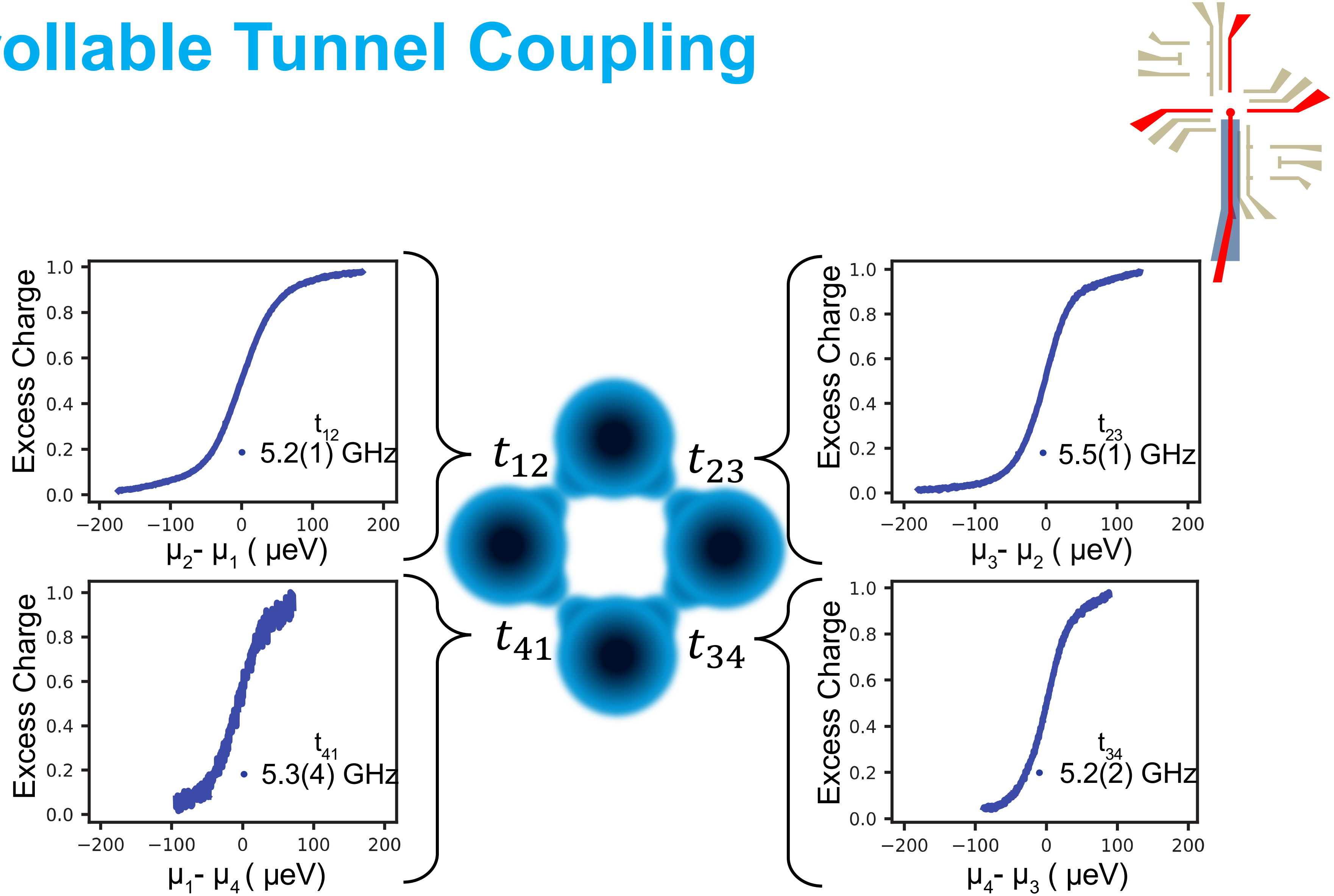

QuTech

$$5\text{ GHz} \approx 20\ \mu\text{eV}$$

Controllable Tunnel Coupling

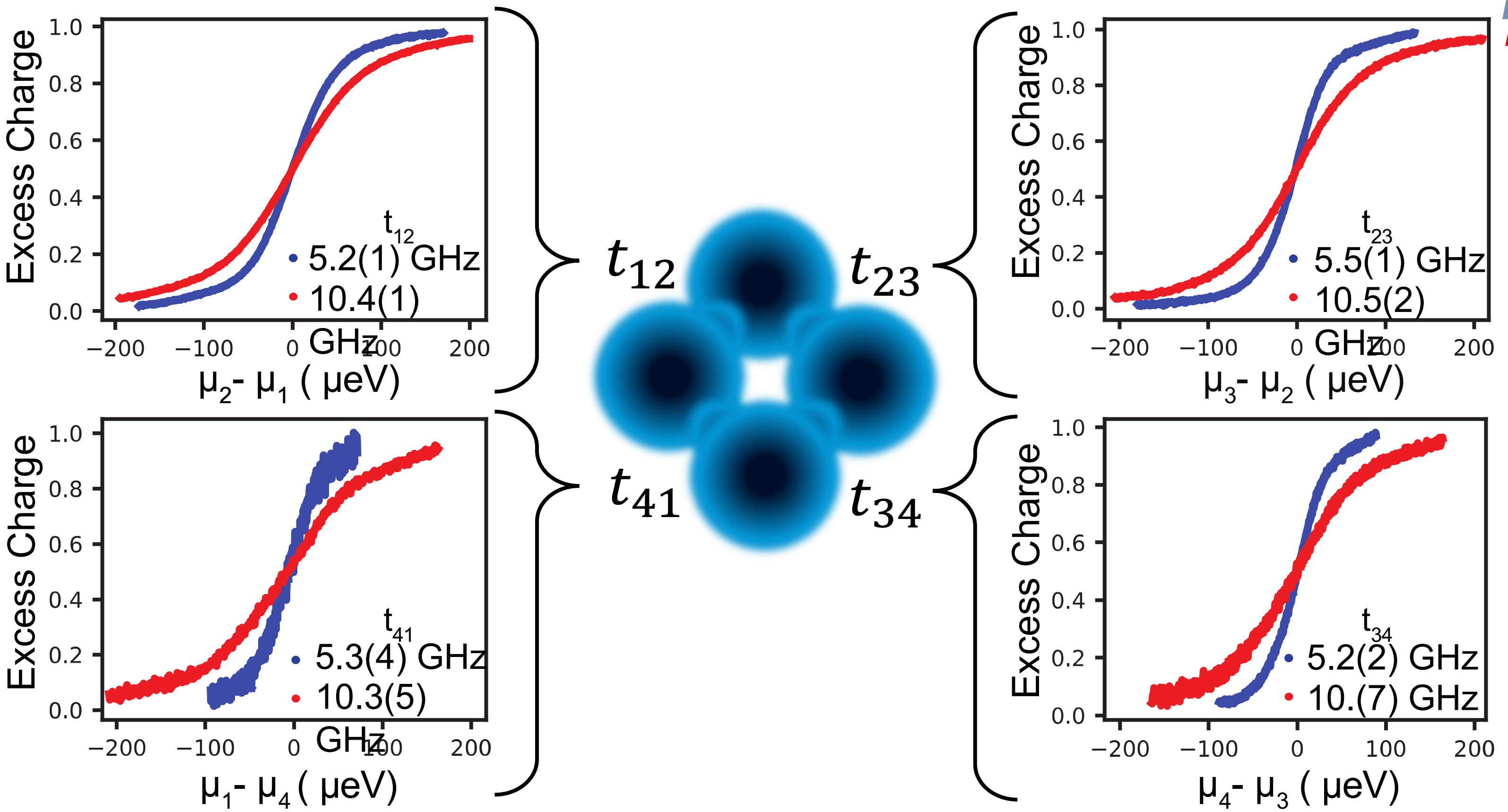

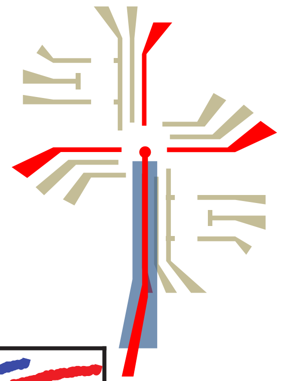

QuTech

$10\ \text{GHz} \approx 40\ \mu\text{eV}$

Quantum simulation: Nagaoka Ferromagnetism

PHYSICAL REVIEW VOLUME 147, NUMBER 1 8 JULY 1966

Ferromagnetism in a Narrow, Almost Half-Filled *s* Band*

YOSUKE NAGAOKA†
Department of Physics, University of California, San Diego, La Jolla, California
(Received 17 January 1966)

EIGENVALUES AND MAGNETISM OF ELECTRONS ON AN ARTIFICIAL MOLECULE

International Journal of Nanoscience
Vol. 2, No. 3 (2003) 165–170

D. C. MATTIS
Department of Physics, University of Utah

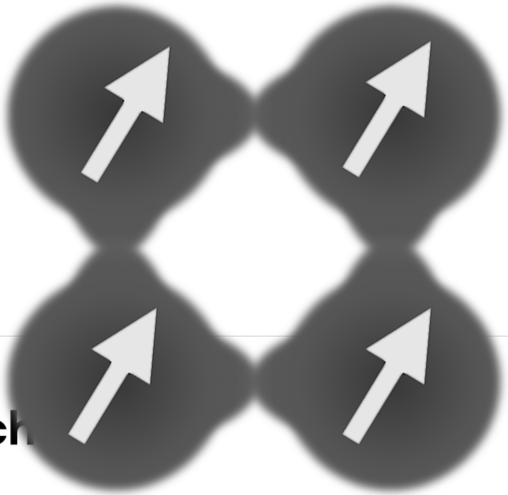

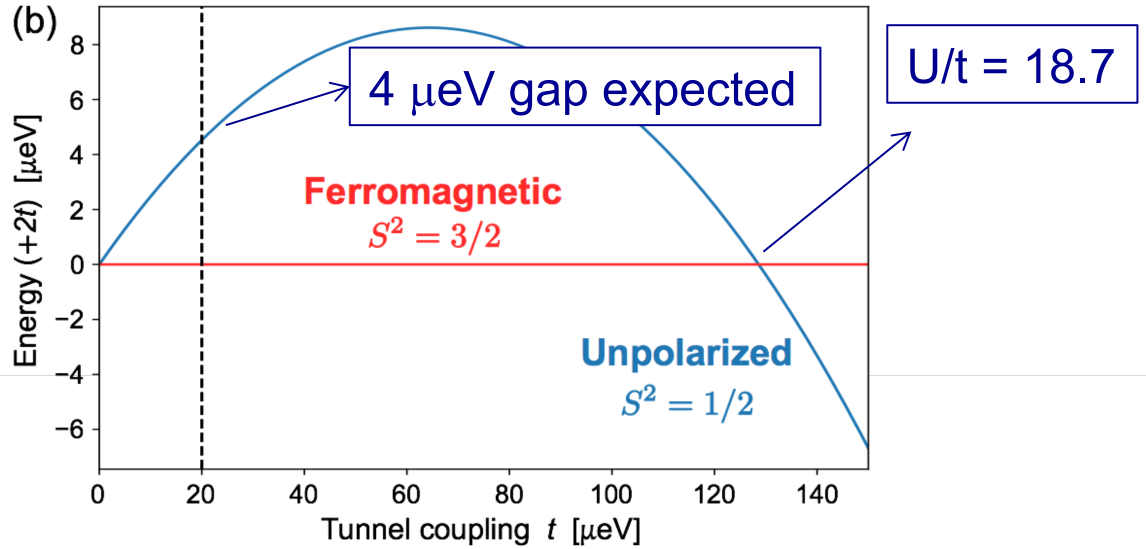

Quantum dots plaquette:
B. Wunsch,
M. Rudner,
LMKV,
E. Demler

QuTech

Nagaoka Ferromagnetism

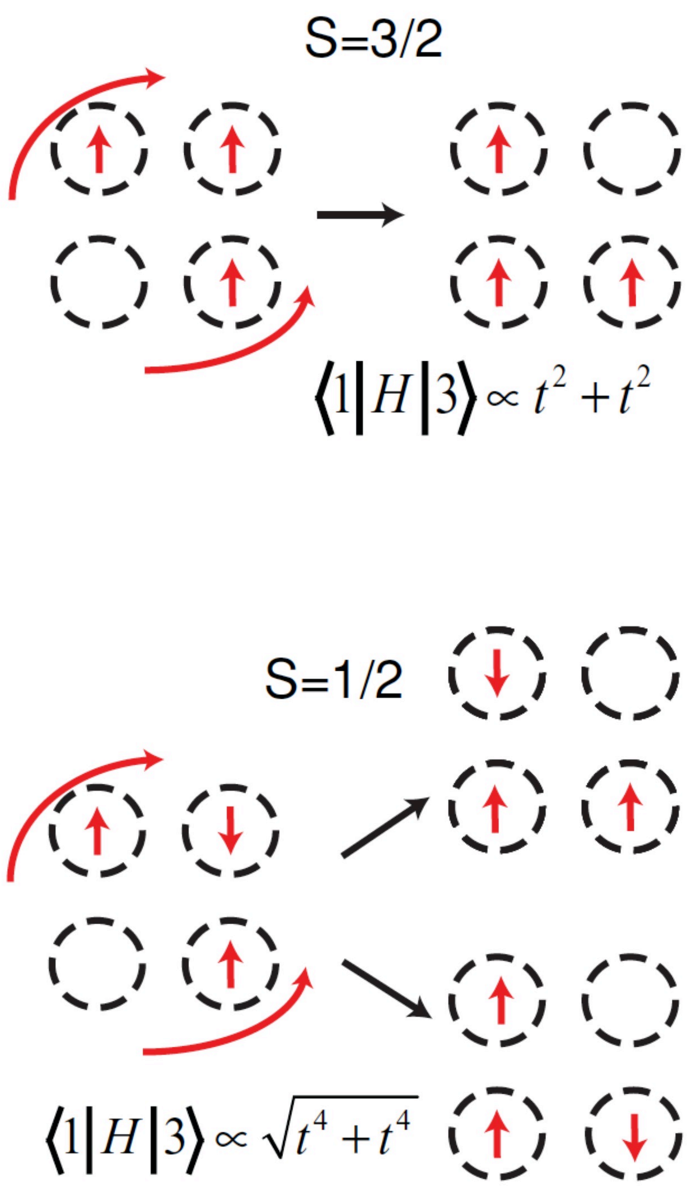

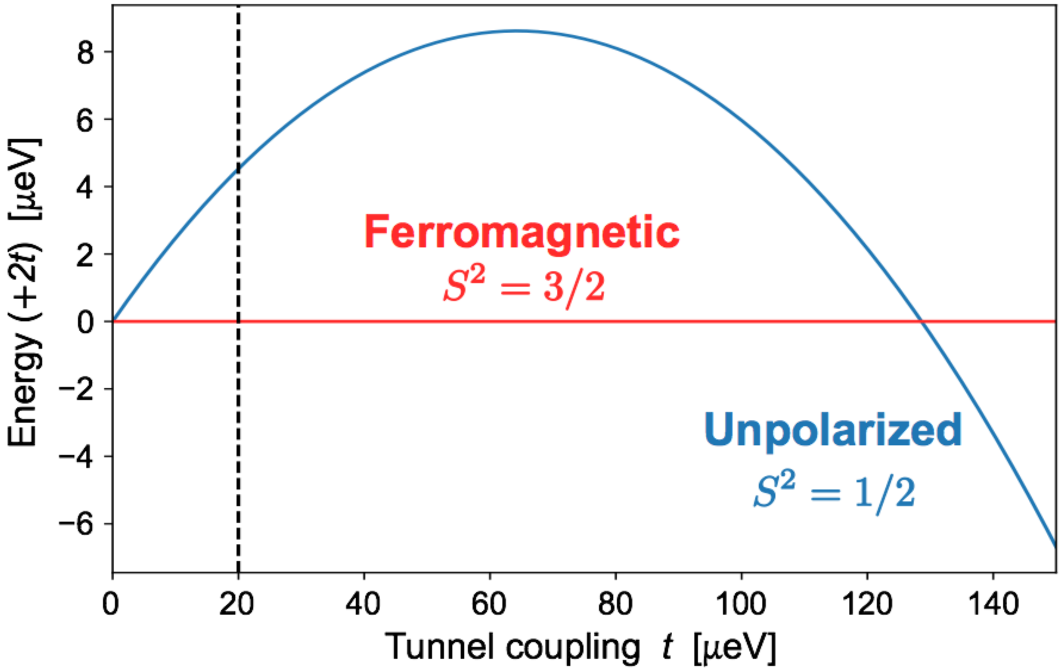

Barthelemy, Vandersypen, Ann.Phys. 2013

Experimental procedure

Dehollain, Mukhopadhyay, et. al., Nature 2020

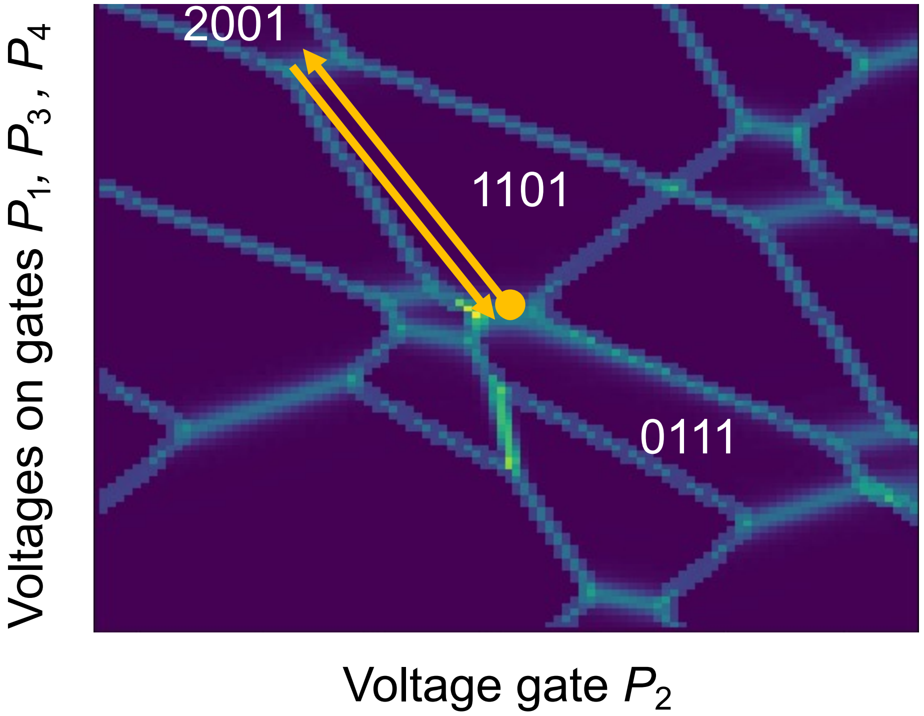

Controlled by virtual gates

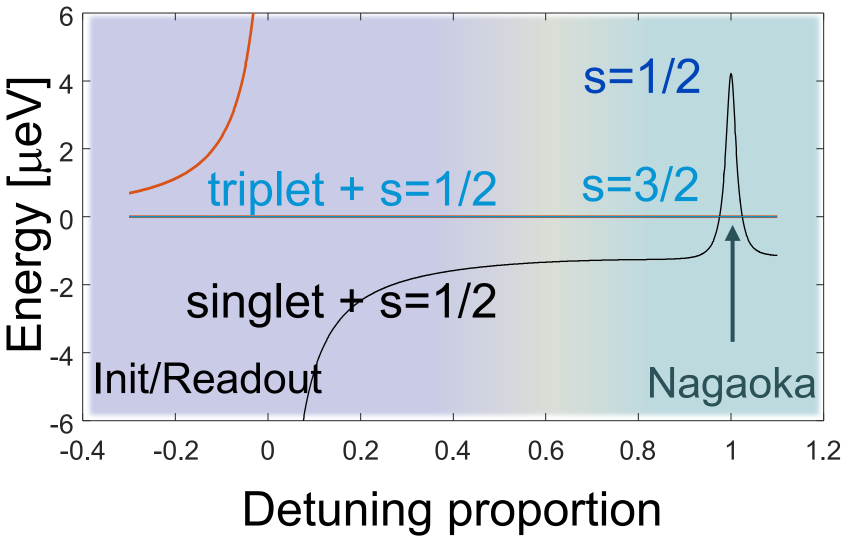

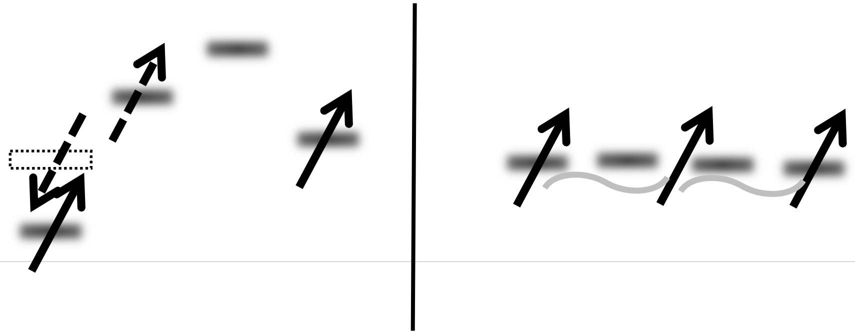

QuTech

Protocol and main observation

Dehollain, Mukhopadhyay, et. al., Nature 2020

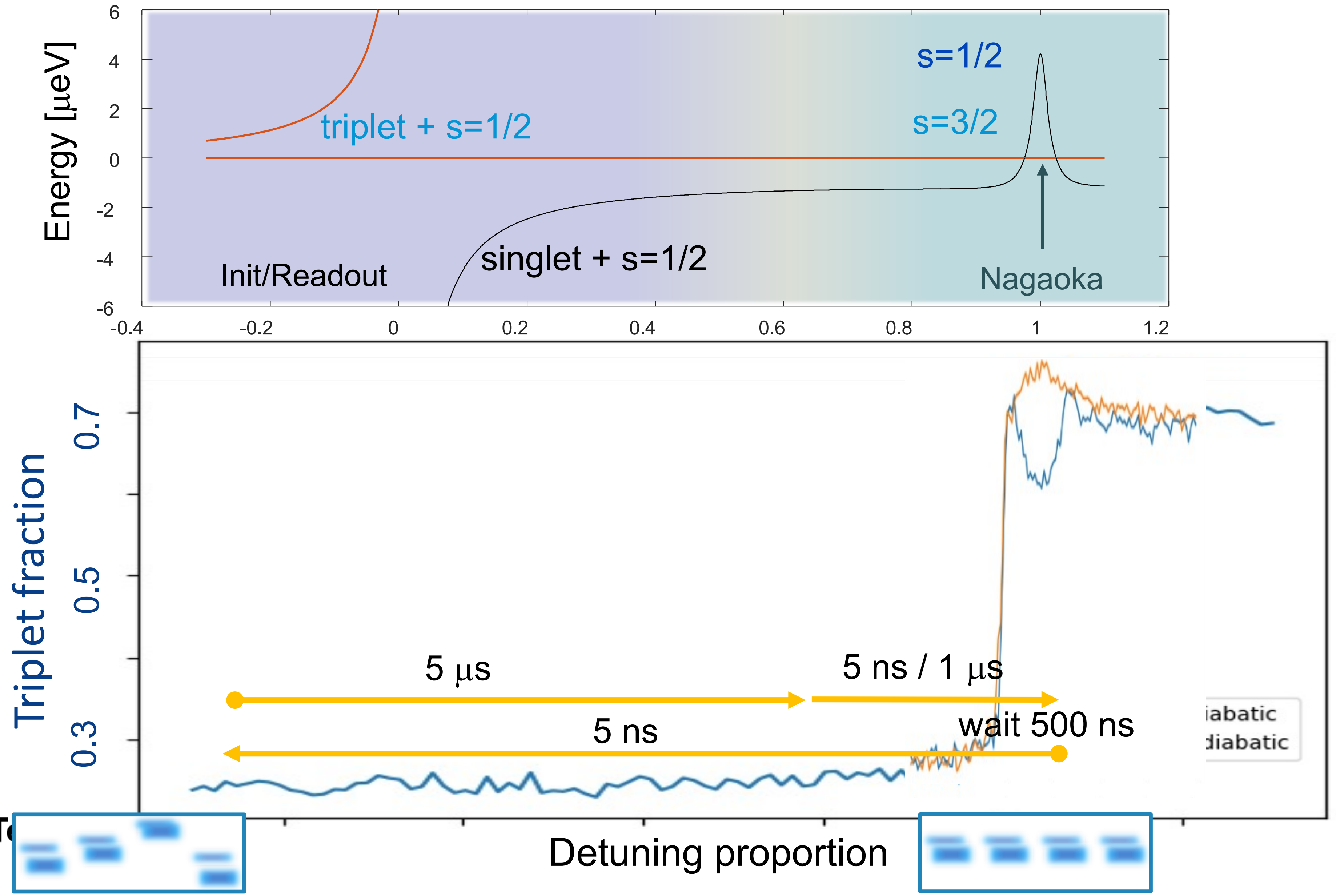

QuTe

Adiabatic to diabatic transition, and equilibration

Dehollain, Mukhopadhyay, et. al., Nature 2020

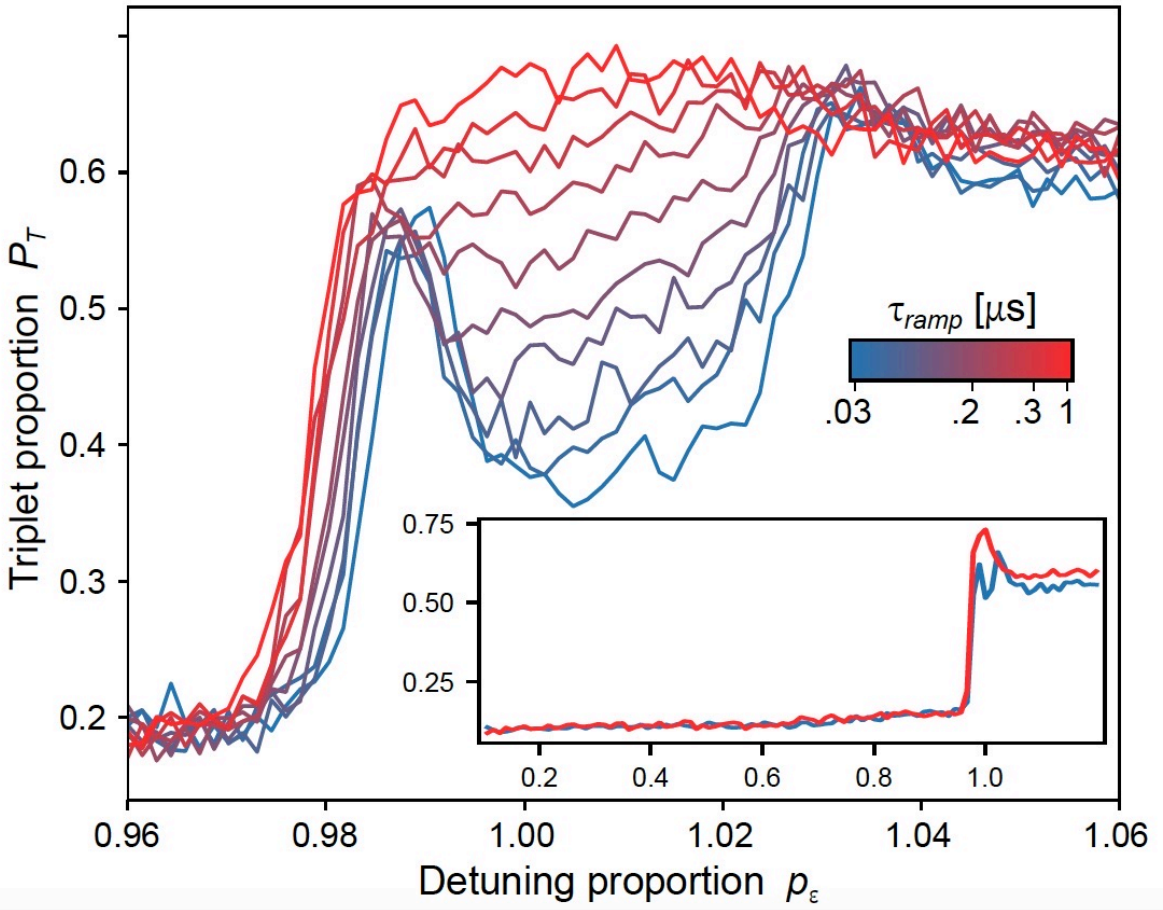

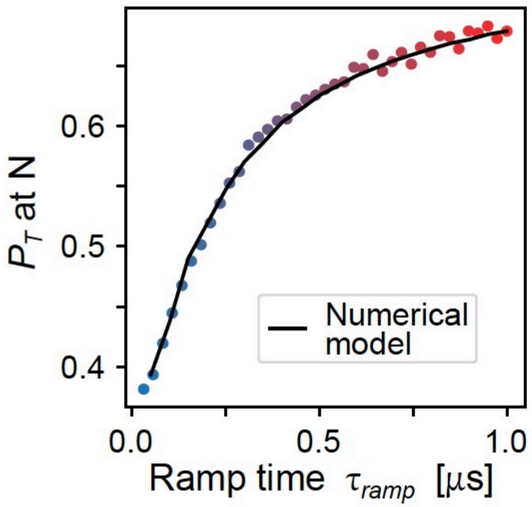

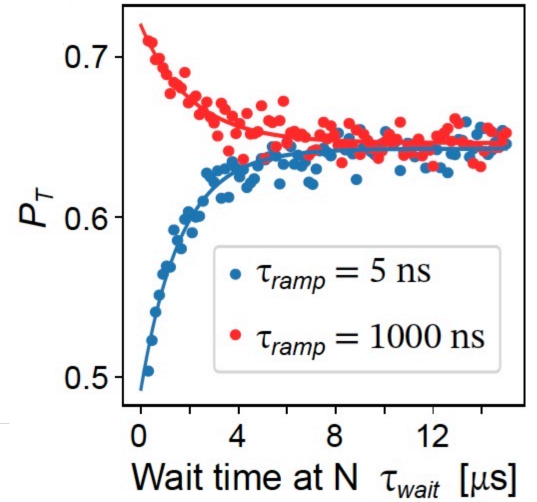

QuTech

Test 1: Change topology

Dehollain, Mukhopadhyay, et. al., Nature 2020

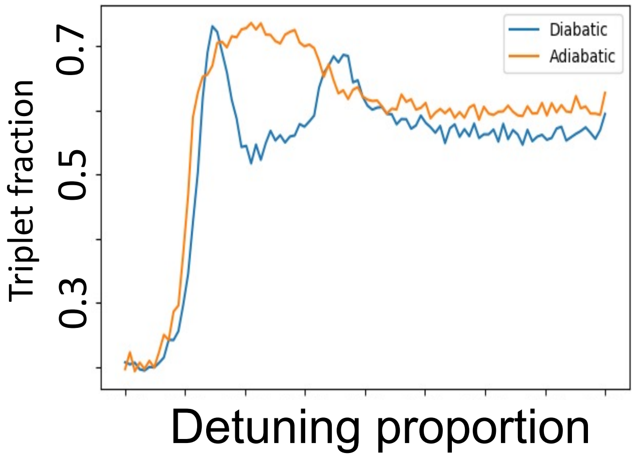

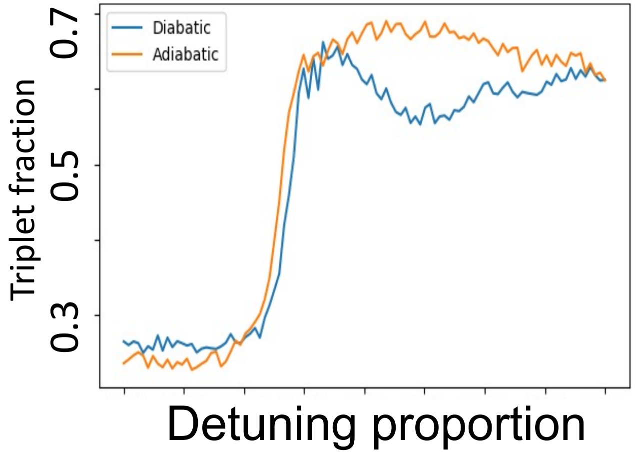

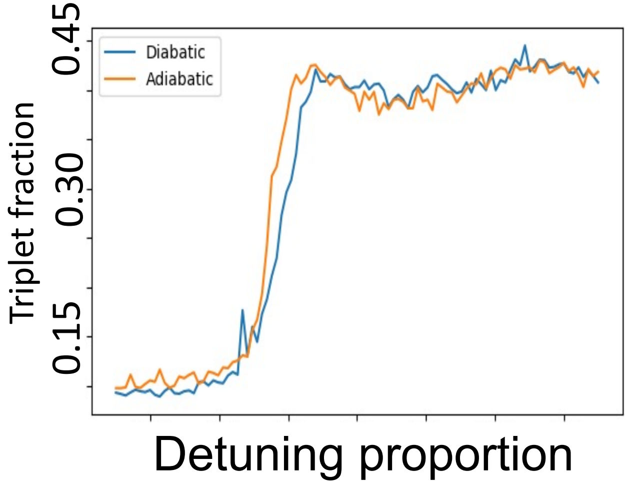

[19, 15, 17, 19] μeV

[16, 8, 20, 19] μeV

[18, 0, 21, 21] μeV

Magnetic GS disappears for a linear chain (consistent with Lieb-Mattis)

Test 2: Introduce Aharonov-Bohm phase (*B*-field)

Dehollain, Mukhopadhyay, et. al., Nature 2020

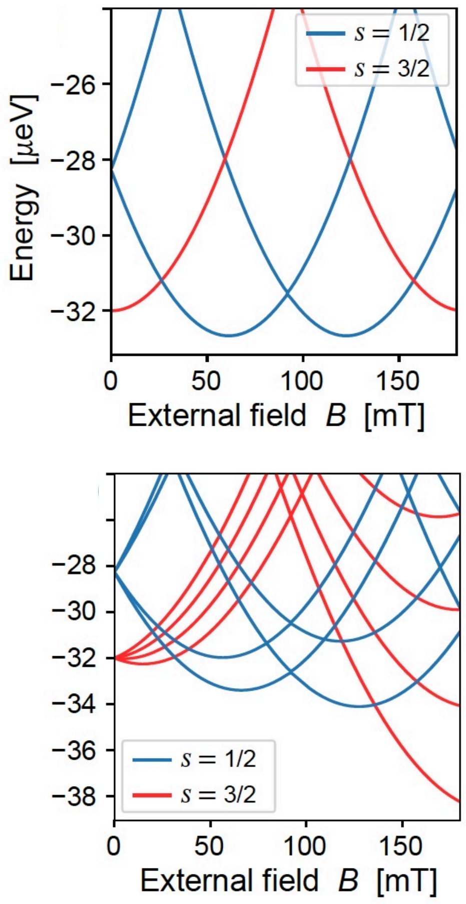

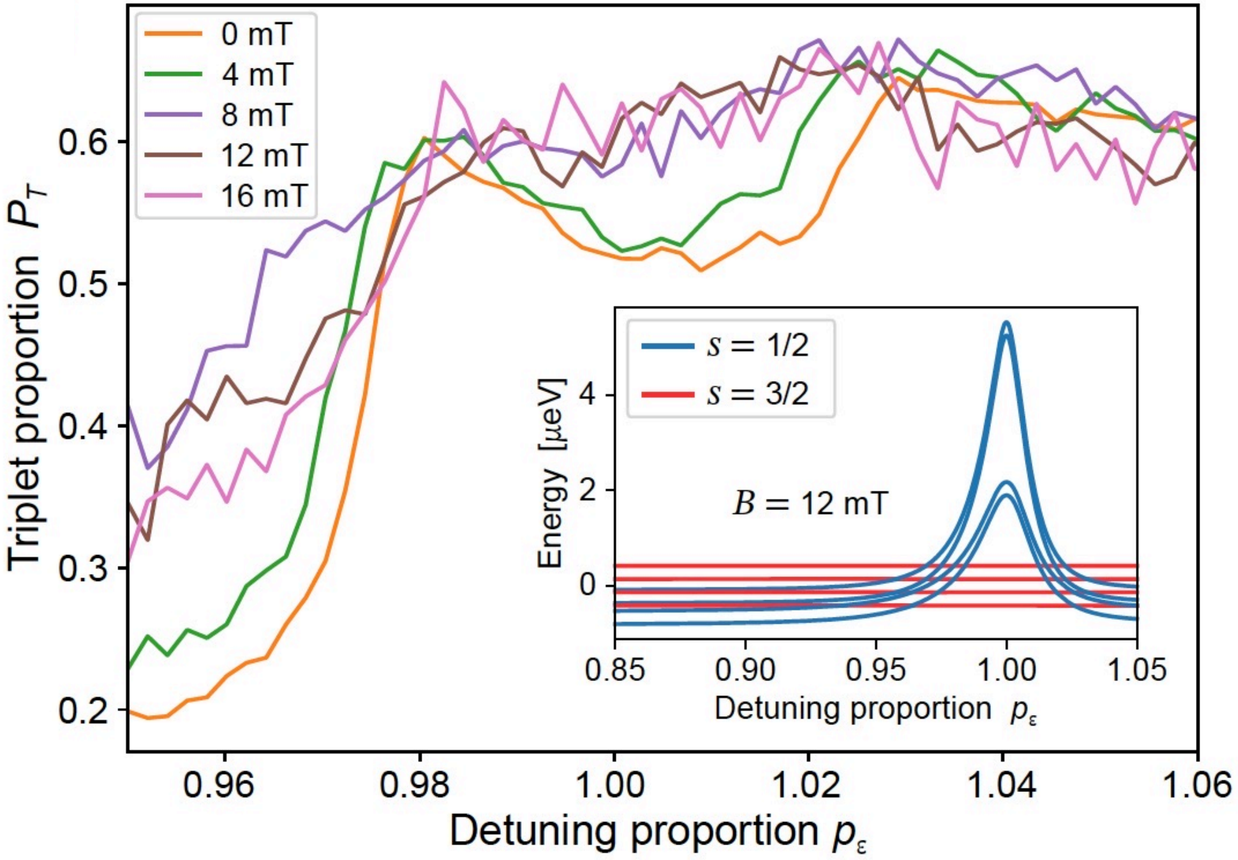

Weak B-field destroys magnetization

QuTech

Test 3: Offset local potentials

Dehollain, Mukhopadhyay, et. al., Nature 2020

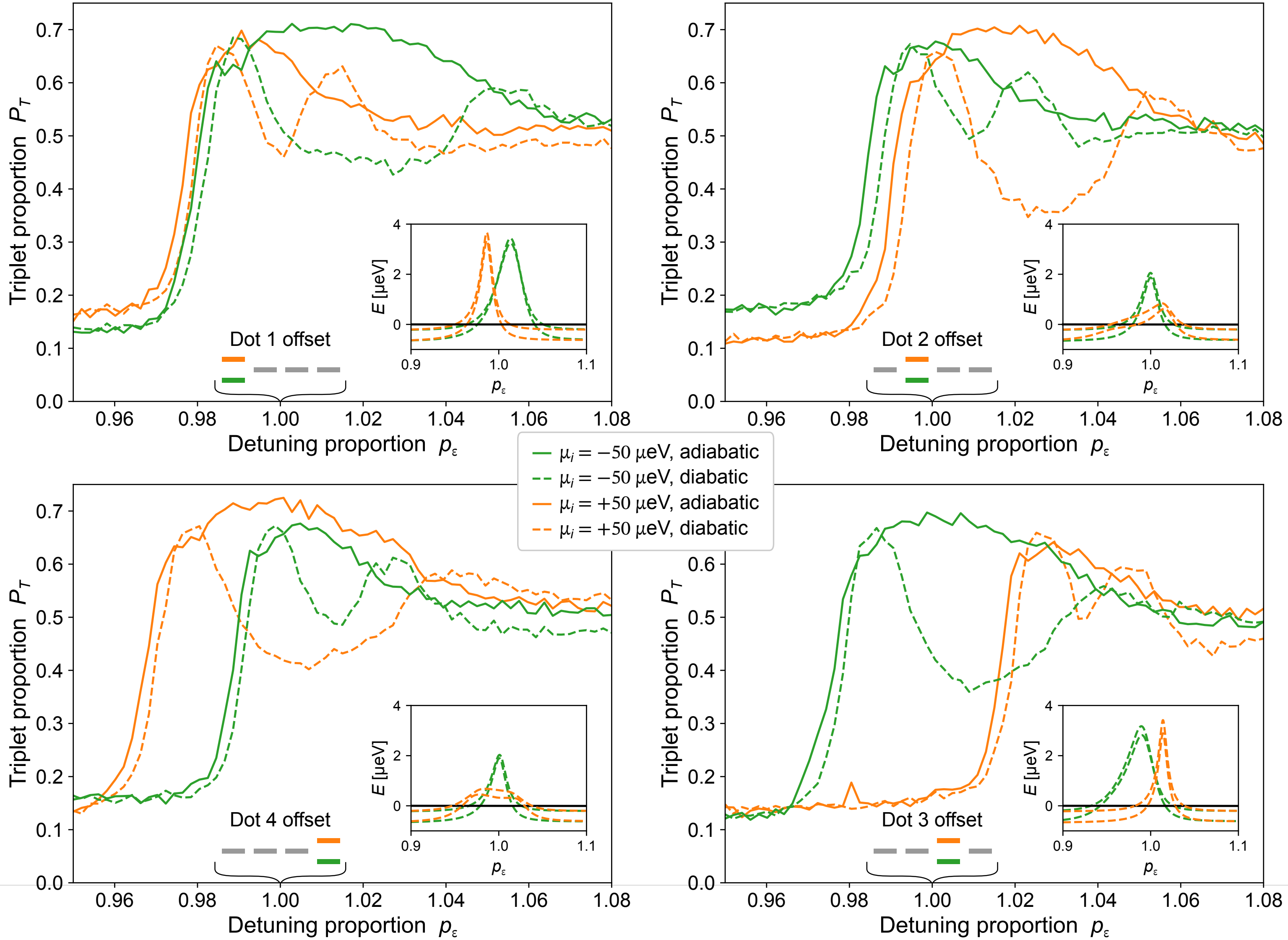

QuTech

Magnetic ground state survives potential offsets exceeding hopping